APPLICATION OF SWAT MODEL TO EVALUATE THE WATER BALANCE OF AN ARID CATCHMENT

By

ACHAMYELEH GIRMA MENGISTU

A thesis submitted in accordance with the requirements for the degree of

Doctor of Philosophy

Faculty of Natural and Agricultural Sciences

Department of Soil, Crop and Climate Sciences

University of the Free State

Bloemfontein, South Africa

Promoter (internal): **Prof. L. D. van Rensburg**

Promoter (external): **Prof. Yali E. Woyessa**

October 2019

ABSTRACT

The hydrologic processes and their behaviours in arid and semi-arid areas are poorly understood and differ highly from humid/sub-humid areas. Hydrologic models play critical roles in understanding such complex processes. However, the application of hydrologic models is limited due to the unavailability or scarcity of data for model calibration, uncertainty and validation procedures. Therefore, this study was aimed at evaluating the application of the Soil and Water Assessment Tool (SWAT model) in simulating the components of water balance in an arid and semi-arid catchment. Moreover, the spatio-temporal variabilities of the different components of the water balance were quantified and analysed. The intensity of water stress was also evaluated in the catchment.

All the components of the catchment water balance in this study were estimated using the SWAT model. The regionalization with physical similarity approach was adopted here for the calibration, uncertainty and validation processes due to the unavailability of streamflow data in the study catchment. Based on the sensitivity analysis, the top sixteen parameters were calibrated, from which the first three (the base flow alpha factor, curve number II and initial depth of water in the shallow aquifer) were found to be the most sensitive parameters, at $p < 0.01$. The result for model uncertainty also indicated acceptable values of both the R-factor (0.8) and P-factor (0.7), which is the average of the calibration and validation periods. Regarding the model performance evaluation, four statistical indicators were used, namely the Nash-Sutcliffe Coefficient (NS), the coefficient of determination (R^2), the percent bias (PBIAS), and the ratio of the root mean squared error to the standard deviation of measured data (RSR). The results showed that all the model performance indicators were in fairly acceptable ranges; taking the average of calibration and validation periods, NS was 0.76; R^2 was 0.78; and RSR was 0.49. The PBIAS indicated a slight over-estimation during calibration (by 11.8%) and under-estimation during validation periods (by 8.1%). The model performance was also verified by the comparison of the *in situ* measured and simulated soil water content outside the SWAT-CUP programmes, and showed an average R^2 of 0.71 for the verification of four hydrologic response units (HRUs).

The analyses of the model output indicated that all the components of the soil water balance exhibited a higher spatial and temporal variation in the study catchment. Hence, the long-term precipitation showed no trend on an annual time scale; however, it showed a decreasing trend (with 0.01 mm per month) on a monthly time scale. Similarly, the monthly total runoff showed a decrease of 0.002 mm per month. Evapotranspiration and revap water showed a decreasing trend in both monthly and annual time scales. Hence, evapotranspiration decreased by 0.01 and 1.25 mm, whereas revap decreased by 0.07 and 1.1 mm on monthly and annual time scales, respectively. The analyses also indicated that no significant trend was found with regard to soil water content, percolation and recharge components on both time scales. Generally, it was indicated that the variations of weather parameters were responsible for the spatio-temporal variabilities. However, topography, land use/land cover (LULC) and soil type played a role mainly for the spatial variations of water balance in the catchment.

The study also showed that the catchment under study (Soutloop Catchment) is one of the driest catchments in South Africa, with an aridity index of 0.07–0.15 (classified as arid catchment). Due to this, the area is water stress almost throughout the year. The intensity of water stress was also evaluated using available hydro-meteorological and environmental indicators, such as the standardized precipitation index (SPI), soil water anomaly (SWA), evaporative stress index (ESI), and normalized difference vegetation index (NDVI). The analyses of water stress generally revealed that the use of a satellite-based NDVI and model output-based SWA and ESI were important alternatives and/or additional indicators, other than the usual and widely applied SPI method.

The study was successful in conceptualizing the major components of the hydro-meteorological processes with a focus on the natural hydrological processes (excluding the anthropogenic impacts). However, it is understandable that the human-induced components like the LULC change and groundwater abstraction, which are related to the large-scale mining activity, could have a significant impact on the soil, water resources and the environment as a whole. Therefore, further research is recommended to investigate the impacts of human activity on the soil, water resources and environmental influences of the area.

Keywords: Arid catchments; Calibration; Hydrologic models; Regionalization; Spatial variation; SWAT model; Temporal variation; Trend analysis; Time series analysis; Water balance; Water deficit.

DECLARATION

I declare that the thesis hereby submitted by me for the degree of Doctor of Philosophy at the University of the Free State is my own independent work and has not been previously submitted by me at another University or Faculty. I furthermore cede copyright of the thesis in favour of the University of the Free State.

Achamyeleh Girma Mengistu

Signature……………………………
Date: October 2019

Place: Bloemfontein, South Africa.

ACKNOWLEDGEMENTS

First of all, I would like to thank God for giving me health, endurance, energy, the opportunity and the ability to reach the completion of this study. Without his graces and blessings, this study would not have been possible.

I would like to extend my heartfelt thanks to my promotors, Professor Leon D. van Rensburg and Professor Yali E. Woyessa, for their guidance, advice, support and encouragement during the course of this study. Your positive outlook and confidence in my research inspired me and gave me confidence.

I am also grateful to the following institutions:

- The University of the Free State, Research Development Department for awarding me a bursary to pursue this study.
- Kolomela Mine for providing research funds and the provision of field experimental sites.
- The South African Weather Services for providing me with historic daily meteorological data.
- The South African Agricultural Research Council for providing me with historic daily meteorological data and the land type data of the study area.

I would like to express my very profound gratitude to my parents and to my wife (Ayinadis T. Tadese), my son (Kidus A. Mengistu) for providing me with unfailing support and continuous encouragement throughout my years of study.

Finally, my gratitude goes to all those who helped me during this study, namely staff members of Soil, Crop and Climate Sciences, University of the Free State and from outside the university: Dr C. Tfwala, Dr Z. Bello, Mr I. Gous, I. J. Sparks-van der Linde, Hendrich Marit, Andries Burger and his family, Dr SW Mavimbela, N. Mjanyelwa, R. Masvodza, O. Chichongue, I. Gura, J. Edeh, Mrs R. van Heerden, Mrs Debre Terblanche, Dr J. van Tol, Dr J. Barnard, E. Yokwane, G. Madito, S. P. van Stade, C. C. Mc Lean, and G. S. Kotoyi. Thank you for all your encouragement!

TABLE OF CONTENTS

LIST OF TABLES

LIST OF FIGURES

LIST OF ABBREVIATIONS

95PPUs	-	Ninety-Five Percent Predictive Uncertainties
AI	-	the aridity index
ANN	-	Artificial neural network
ARC	-	Agricultural Research Institute of South Africa
ARC-ISWC	-	Agricultural Research Centre, Institute for Soil, Water and Climate
AWC	-	available water capacity
Can_{day}	-	canopy storage with in a day
CCI	-	Climate Change Initiative
CN	-	daily curve number
C_p	-	specific heat at constant pressure
CSIR	-	Council for Scientific and Industrial Research
DEA	-	Department of Environmental Affairs
DEM	-	digital elevation model
DFM	-	Dirk Friedhelm Mercker (founder of company producing DFM probes)
DOY	-	days of the year
DWA	-	Department of Water Affairs
DWAF	-	Department of Water Affairs and Forestry
E_{can}	-	evaporation from canopy
ECV	-	Essential Climate Variable
EDO	-	European Drought Observatory
EL_{band}	-	elevation from band
EL_{gauge}	-	elevation from the gauge
EMI	-	electromagnetic induction
ENSO	-	particularly variation in precipitation and El Niño–Southern Oscillation
e^o_z	-	saturated vapour pressure of air at a height of z
ERT	-	electrical resistivity tomography
ESA	-	the European Space Agency
ESI	-	evaporative stress index
ET	-	evapotranspiration

e_z	-	saturated vapour pressure of water at a height of *z*
FC	-	field capacity
fr_{bnd}	-	the fraction of the sub-catchment area within the elevation band
GCOS	-	Global Climate Observing System
GIMMS	-	Global Inventory Modelling and Mapping Studies
GIS	-	geographic information system
GLUE	-	Generalized Likelihood Uncertainty Estimation
GPR	-	ground penetrating radar
HBV	-	Hydrologiska Byrans Vattenavdelning model
HELP	-	Hydrologic Evaluation of Landfill Performance model
H_{net}	-	net radiation
HRUs	-	hydrologic response units
I_a	-	initial soil surface abstractions
IDW	-	inverse distance weighted interpolation method
K_{sat}	-	saturated hydraulic conductivity of the soil
LAI	-	leaf area index
LP DAAC	-	Land Processes Distributed Active Archive Center
LULC	-	land use and /or land cover
MCMC	-	Markov Chain Monte Carlo
MIKE-SHE	-	Integrated Hydrological Modelling System
MODFLOW	-	Modular Three-Dimensional Finite-Difference Groundwater Flow model
MODIS	-	Moderate Resolution Imaging Spectro-radiometer
MPE	-	multi-sensor precipitation estimates
NASA	-	The National Aeronautics and Space Administration
NASMID	-	North American Soil Moisture Database
NDVI	-	normalized difference vegetation index
NMM	-	the neutron moisture meter
NSE	-	Nash-Sutcliff efficiency
OAT	-	one parameter at a time (OAT)
Palps	-	precipitation lapse rate

ParaSol	-	Parameter Solution
P_{band}	-	precipitation on the elevation band
PBIAS	-	percent bias
P_{day}	-	the amount of precipitation
PET	-	potential evapotranspiration
P-P plot	-	probability-probability plot
PRMS	-	Precipitation Runoff Modelling System
PSO	-	Particle Swarm Optimization
PWC	-	Permanent Water Commission
Q_{GW}	-	the amount of return flow
Q_{lat}	-	lateral flow
Q-Q plot	-	quantile-quantile plot
Q_{surf}	-	the amount of direct runoff,
R^2	-	coefficient of determination
r_c	-	plant canopy resistance
REVAP	-	water taken up from shallow aquifer during water stress in the root zone
RMSE	-	the root mean square of errors
r_s	-	aerodynamic resistance
RSR	-	ratio of the root mean square error to the standard deviation of measured data
SA	-	South Africa
SAWS	-	South African weather service
SPI	-	standardized precipitation index
SRTM	-	Shuttle Radar Topography Mission
S	-	soil retention parameter
SUFI2	-	Sequential Uncertainty Fitting
SWA	-	soil water anomaly
SWAT-CUP	-	SWAT model calibration and uncertainty procedures
SWAT	-	the Soil and Water Assessment Tool
SWC	-	soil water content of the time scale

SW_{gains}	-	the sum of incoming water to the soil
SW_{losses}	-	the sum of outgoing water to the soil
SW_o	-	the initial soil water at a certain time scale
SW_t	-	the final soil water at a certain time scale
TDR	-	time domain reflectometry
UBeTube	-	Upwelling Bernoulli Tube
UNCCD	-	The United Nations Convention to Combat Desertification
UNEP	-	United Nations Environment Programme
UNESCO	-	The United Nations Educational, Scientific and Cultural Organization
USDA-SCS	-	United States, Department of Agriculture, Soil Conservation Service
USDA	-	United States, Department of Agriculture
USGS	-	United States geological survey
VIC-Model	-	Variable Infiltration Capacity model
WMO	-	World Meteorological Organization
W_{perc}	-	the amount of deep percolation from the root zone
WP	-	wilting point
W_{rchrg}	-	amount of recharge entering the aquifer
w_{seep}	-	amount of water exiting the bottom of the soil profile
WWF-SA	-	World Wide Fund for South Africa
γ	-	psychrometric constant
δ_{gw}	-	delay time or drainage time of the overlying geologic formations
Δ	-	slope of saturation vapour pressure-temperature curve
ΔSW	-	the change in soil water content
λE	-	latent heat flux density
ρ_{air}	-	density of air
P_{NIR}	-	the spectral reflectance at near infra-red
P_{RED}	-	the spectral reflectance at red
$e$sco	-	soil evaporation compensation factor
βrevap	-	revap coefficient

CHAPTER 1
MOTIVATION AND OBJECTIVES

1.1 Motivation

The study of the water balance is one of the basic subjects in catchment management, showing the water inflow and outflow of an area (Lvovitch, 1970; Ahmad *et al*., 2010; Entekhabi *et al*., 2014). Fresh water, including surface and ground water, is a non-renewable resource where its distribution is driven by the natural cycles of freezing and thawing, variation in precipitation, runoff pattern and evapotranspiration levels (Shams *et al*., 2013). Knowledge of the water balance enables us to quantify and evaluate the current water resources and predict their dynamics under the influence of environmental changes (Sokolov and Chapman, 1974). Due to spatial and temporal variation of these environmental factors, its distribution is of great importance in the hydrologic cycle (Ahmad *et al*., 2010).

Beyond its function in the hydrologic cycle, water has social, economic and environmental values, and is essential for development (UNESCO, 2011). However, water resources are significantly affected by the impacts of global changes. The impacts of population and economic growth, climate change, land use/cover change and environmental pollution contribute significantly to the scarcity of freshwater resources on the earth's surface (Dolman *et al*., 2003; Millennium Ecosystem Assessment, 2005; UNESCO, 2011 and UNCCD, 2017). These drivers of environmental changes could be natural or anthropogenic. Reports show that some of the drivers of environmental changes are interrelated. For example, variation in the LULC substantially contribute to climate change and this exacerbates the shortage of freshwater and ecosystem disturbances as a whole (Dolman *et al*., 2003). The impact of population and economic growth also contributes significantly to the change in land use/cover.

On the other hand, arid and semi-arid parts of the world, like South Africa, face major challenges in the availability and management of fresh water resources (Gangodagamage and Agrarwal, 2001; Wheater *et al*., 2010; Bugan *et al*., 2012). The International Water Management Institute, in its prediction, categorized South Africa as being under physical water scarcity by 2025 (Seckler and Amarasinghe, 2000). The challenges regarding the availability of freshwater resources are expected to intensify in the western part of the country, which is where this study was conducted, specifically Soutloop River Catchment. The Soutloop is one of the tributaries of the Orange River, and its catchment area is located in both the lower Orange and Lower Vaal Water Management Areas. It is a dry river throughout the year due to low precipitation and extremely high evaporation demands. The area is primarily covered by shrublands and arid grasslands. The area is also one of the regions where large-scale mining (particularly iron ore mining) activities are carried out. The iron ore mining and related activities in Sishen and Kolomela place additional pressure on water resources. Based on the environmental impact assessment report on the expansion of Kolomela Mine (Synergistics Environmental Services, 2016), the most important environmental changes identified in and around the mines over time are: lowering and contamination of groundwater levels, general land disturbance, change in the natural ecosystem and water course, and sound and air pollution. Of these impacts, the lowering of groundwater table, and air and noise pollution had already been confirmed to be prevalent by the socio-economic assessment report of the mine (Kumba Iron Ore Limited, 2014).

Research and experiences show that mining is a man-made land use that causes abrupt and extensive LULC change that are distinct from those found anywhere else (Sonter *et al*., 2014; Zhang *et al*., 2017). Apart from its direct impact on LULC, iron ore mining has a significant impact on the freshwater resources and the environment as a whole. Its impact might be experienced in both the quantity and quality of water resources. In terms of quantity, the annual reports of the mine show that a large amount of water is being used from groundwater abstraction for primary and non-primary activities of the mine. The impact of leachate from the waste rock dumps and stockpiled ore could have a negative impact on the surface and sub-surface water and the ecosystem as a whole, even though the environmental impact assessment report (Synergistics Environmental Services, 2016) shows minimum impacts. Research also shows that soil and water quantity and quality issues are interdependent. Merz (2013) reported that water quantity has a close and complex relationship with water quality. As a result, a change in water quantity immediately changes the structure and function of ecosystems (UNESCO, 2011; Merz, 2013). The change in LULC, river regulation and water abstraction affect the natural flow regimes of catchments and associated water quality characteristics, like eutrophication, contamination with toxins, salinity and pollution (Merz, 2013).

Such pressing environmental, social and economic problems of water scarcity could be addressed by using sustainable water management practices, for which a water balance study is a pre-requisite for undertaking such measures. Currently, catchment water management is a fundamental measure in South Africa (Bugan *et al*., 2012) where the optimization of water yields from catchments is an essential component of the catchment management strategy. Generally, an effective management and sustainable use of land resources will only be achieved by adopting an integrated approach to land resources (land, water, vegetation, etc.) with direct participation of the different stakeholders (Swallow *et al*., 2005). For this reason, catchment is an ideal unit for multidisciplinary resource management for the benefit of the society, while considering the benefit of future generations (Swallow *et al*., 2005; Pareta and Pareta, 2012). Moreover, water balance studies assist in integrated water resources management, planning, and ecological and environmental monitoring programmes. Policy makers can make informed decisions to develop better policies and programmes (Merz, 2013). However, detailed water balance studies have not been conducted in arid to semi-arid catchments in South Africa. Therefore, the results from such research provide baseline information of the area for future studies related to the water balance and any of its components, their distribution along the landscape patterns, and impacts of human activities, as well as long-term climate change. Therefore, this study was aimed at conceptualizing the natural hydrologic process in the catchment and evaluating the condition of water deficit using the Soil and Water Assessment Tool (SWAT model).

1.2 Objectives

The main objective of this study was to analyse the components of water balance at a catchment scale, with the intention to meet the following specific objectives: (i) evaluate the application of SWAT model to estimate water balance at catchment scale in arid climates; (ii) analyse the spatial and temporal variation of precipitation, soil water content, evapo-transpiration, direct runoff, and groundwater recharge in the catchment; and (iii) evaluate the intensity of water stress in the catchment.

1.3 Organization of the thesis

This thesis is organized into nine chapters based on the specific objectives. Chapter 1 gives the introduction of the study. In this chapter, the background, problem statement and the objectives of the study are clearly stated. This chapter also includes the scope and organization of the thesis. In Chapter 2, a general literature review is provided, covering all the components of water balance at catchment scale. In this chapter, all the theories and practical views regarding the importance, spatio-temporal variation and methods of measurements of the components of water balance are described. The gaps in knowledge are also identified in this chapter. In Chapter 3, the application of the Soil and Water Assessment Tool (SWAT) to estimate the components of soil water balance is described. In this chapter, the model setup and configuration, parameterization, sensitivity analysis, calibration and uncertainty analysis, as well as the model validation procedure, as conducted under data scarce arid catchments, are described. Therefore, in this chapter, the prediction of the spatial and temporal variation of all the components of the water balance is completed and ready for further analysis in the next consecutive chapters. Chapters 4, 5, 6, 7 and 8 deal with the spatial and temporal variation of precipitation, soil water content, evapotranspiration, direct runoff and groundwater recharge in the catchment, respectively. Chapters 3 to 8 follow an article format where each of the chapters is considered as a stand-alone chapter. The final chapter, which is Chapter 9, deals with the general discussion and recommendations for future studies. It is worthy to note that this study focuses on the natural cycles of the hydrologic processes only, i.e. the impacts of anthropogenic activities that are expected to have significant influence on water resources (such as the LULC change, groundwater abstraction, and managed groundwater recharge) are not considered in the analysis.

1.4 References

Ahmad, S., Kalra, A. and Stephen, H., 2010. Estimating soil moisture using remote sensing data: a machine learning approach. *Advances in Water Resources,* 33(1), pp. 69-80.

Bugan, R., Jovanovic, N. and De Clercq, W., 2012. The water balance of a seasonal stream in the semi-arid Western Cape (South Africa). *Water SA,* 38(2), pp. 201-212.

Dolman, A.J., Verhagen, A. and Rovers, C.A. (eds.), 2003. *Global environmental change and land use*. Springer Science and Business Media.

Entekhabi, D., Yueh, S., O'Neill, P.E., Kellogg, K.H., Allen, A., Bindlish, R., Brown, M., Chan, S., Colliander, A., Crow, W.T. and Das, N., 2014. *SMAP Handbook–Soil Moisture Active Passive: Mapping Soil Moisture and Freeze/Thaw from Space.* The National Aeronautics and Space Administration (NASA).

Gangodagamage, C. and Agrarwal, S.P., 2001. Hydrological modelling using remote sensing and GIS. *In 22nd Asian Conference on Remote Sensing*. The Singapore International Convention and Exhibition Centre, Singapore.

Lvovitch, M., 1970. *World water balance (general report).* Reading, UK, pp. 401-415.

Merz, S., 2013. *Characterizing the relationships between water quality and quantity,* Sydney, Australia: Commonwealth of Australia.

Millennium Ecosystem Assessment, 2005. *Ecosystems and Human Well-being: Synthesis*. Island Press, Washington, DC.

United Nations Convention to Combat Desertification (UNCCD), 2017. *The global land outlook, first edition*. Bonn, Germany.

Pareta, K. and Pareta, U., 2012. Integrated catchment modeling and characterization using GIS and remote sensing techniques. *Indian Journal of Engineering,* 1(1), pp. 81-91.

Seckler, D. and Amarasinghe, U., 2000. *Water supply and demand, 1995 to 2025 IWMI, annual report 1999–2000.* IWMI, Colombo, Sri Lanka.

Shams, S., Chen, D., Arevalo, J., Leone, A. and Moreno, C.C., 2013. *Water balance study: an application of WPS technologies training manual.* European Commission, Luxembourg.

Sokolov, A. and Chapman, T., 1974. *Methods for water balance computations; an international guide for research and practice-a contribution to the International Hydrological Decade.* Paris, France: the UNESCO Press.

Synergistics Environmental Services (Pty) Ltd, 2016. *Environmental impact assessment and environmental management programme report.* Kolomela Mine Amendment: expansion of activities at Kolomela Mine: Part A. SLR-Global environmental solutions.

Kumba Iron Ore Limited, 2014. Kolomela Mine SEAT report 2014. AngloAmerican.

Sonter, L.J., Moran, C.J., Barrett, D.J. and Soares-Filho, B.S., 2014. Processes of land use change in mining regions. *Journal of Cleaner Production*, 84, pp.494-501.

Zhang, J., Rao, Y., Geng, Y., Fu, M. and Prishchepov, A.V., 2017. A novel understanding of land use characteristics caused by mining activities: a case study of Wu'an, China. *Ecological Engineering*, 99, pp.54-69.

Swallow, B., Tennyson, L. and Achouri, M., 2005. *Preparing for the next generation of catchment management programmes and projects, Africa.* Food and Agriculture Organization of the United Nations, p. 282, Rome, Italy.

UNESCO, 2011. *The impact of global change on water resources: The response of UNESCO's international hydrological program.* UNESCO Paris, France.

Wheater, H., Mathias, S. and Li, X., 2010. *Groundwater modelling in arid and semi-arid areas.* Cambridge University Press, Cambridge, UK.

CHAPTER 2
GENERAL LITERATURE REVIEW

2.1 Introduction

Freshwater is one of the scarce resources on the earth's surface, yet it is vital for various aspects of life on earth. Moreover, in South Africa, water is a scarce commodity. This is mainly due to the low amounts of rainfall experienced throughout the country. Furthermore, the scarcity is worsened by the increasing demand on freshwater due to demographic pressure, rate of economic development, urbanization and water pollution (Molobela and Sinha, 2011; Du Plessis, 2017). The availability of freshwater is not evenly distributed throughout the country. Some reports (Molobela and Sinha, 2011) indicate that water scarcity will become more complex due to the increasing water uses and conflicts between the different economic sectors. Therefore, sustainable water management, which ensures the optimum and wise use of water resources without compromising the needs of future generations, should be a prerequisite for the country.

The aim of this review is to assess the freshwater resources of South Africa, their sources and sinks with predicted future trends. The trends of catchment or catchment hydrology in a South African context are also reviewed. The current theoretical knowledge of catchment hydrology, its components and methods to determine each component of the catchment water balance are reviewed. Finally, the importance of hydrologic models, setup, calibration and the uncertainty analysis is reviewed by taking The Soil and Water Assessment Tool (SWAT) as a typical example.

2.2 Hydrological cycle and review of South Africa's water resources

The hydrological cycle is the process of constant water exchange or circulation within the hydrosphere, i.e. the atmosphere, the earth's surface and the lithosphere up to a depth of 2000 m (Shiklomanov, 2009). The exchange or movement of water within the hydrosphere is derived mainly from the surplus of incoming radiation over back radiation and gravity (Dooge, 1968; Shiklomanov, 2009). When the earth's surface is heated with the sun's energy, liquid water usually evaporates and accumulates to form clouds. After the clouds become cool and denser, water comes back to the earth's surface as precipitation, thus forming the hydrologic cycle. Therefore, the water cycle is a continuous process that incorporates all three phases of water (ice, liquid water, and vapour) during the exchange between the different components of the hydrologic cycle. The primary components of the hydrologic cycle or water balance (as shown in Figure 2.1 below) are precipitation, evaporation, transpiration, runoff, percolation, soil water and groundwater.

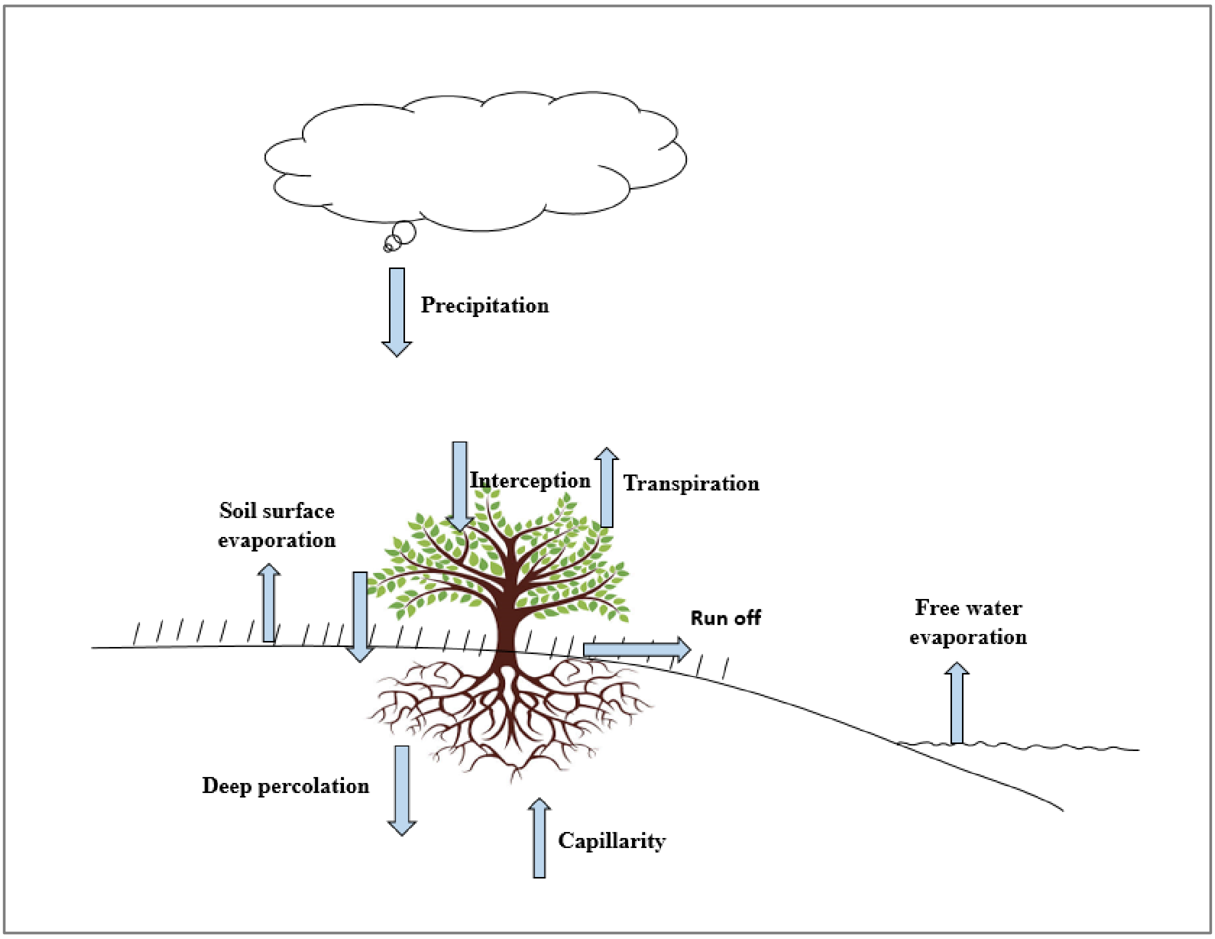

Figure 2.1: Components of the hydrologic cycle/water balance.

Although the total amount of global water content remains constant (Chow, 1988), the distribution of water is continuously changing over time on continental, regional and local drainage basin scales. Freshwater (from rivers, precipitation, soil water, groundwater, lakes, and polar ice) is particularly the most vulnerable resource for global change (Carpenter *et al.*, 2011; Dallas and Rivers-Moore, 2014; Sunardi and Wiegleb, 2016). This is due to a number of different factors that have influence individually or in an interactive way. The 5th Report by the Intergovernmental Panel for Climate Change (Porter *et al.*, 2014) shows that there are two major groups of factors that influence the distribution and availability of freshwater resources. The first group is classified as climatic drivers, in which the change in precipitation and potential evapotranspiration are the major factors. Other researchers (e.g. Carpenter *et al.*, 2011; Dallas and Rivers-Moore, 2014) include the increase of surface temperature as a major climatic factor, along with precipitation and potential evapotranspiration. The other group of factors that strongly influences future freshwater, which is termed non-climatic drivers, and includes demographic, socio-economic and technological changes.

Global freshwater use by different sectors is dominated by agriculture (which uses up to 70% of the available freshwater), followed by industrial consumption (19–20%) and direct human consumption (10–11%) (Zhuwakinyu, 2012). In South Africa, about two-thirds of freshwater is used for agriculture (CSIR, 2010; DWA, 2013; Greencape, 2017). Similarly, the industrial water use (including mining, power generation, and other industrial activities) varies from 7 to 10%. Domestic use, combining rural and urban use, constitutes 22–27% of freshwater usage. Furthermore, up to 1% of freshwater is transferred outside of South Africa. Of the total freshwater use in the country, 77% comes from surface water (rivers, dams, lakes, etc.), 9% from groundwater, and the remaining 14% from reuse of return flow (DWA, 2013).

Precipitation is the most important contributing factor for the variation of the scarcity of freshwater resources in South Africa. The mean annual precipitation ranges between 450 and 490 mm, which is half of the worldwide average (CSIR, 2010; Colvin *et al.,* 2016). Of this amount, usually 9% will be converted to runoff, 4% to groundwater recharge, and most of the remaining 87% will be lost as evapotranspiration (Colvin et al., 2016). Bennie and Hensley (2001) and Jovanovic *et al.* (2015) estimated up to 70% of precipitation would be lost as evapotranspiration every year in South Africa. Numerous sources (e.g. CSIR, 2010; DWA, 2013) report that South Africa faces a water supply crisis not only due to low rainfall and high evaporation rates, but also to an expanding economy, climate change, and water pollution, while the growing population also puts pressure on freshwater resources.

2.3 Catchment hydrology

2.3.1 Why we study according to a catchment basis?

A catchment (or watershed) is a hydrological unit that has been described and used as a physical and biological, socio-economic-political unit for planning and management of natural resources (Sheng, 1990; Wani *et al.*, 2002; Brooks *et al.*, 2013). Simply put, it is a geographic area through which water flows across the land and drains into a common body of water (stream, river, lake, or ocean). Environmental studies that are affected by the movement of water along the land surface, such as environmental pollution from point and non-point sources, soil degradation, and ecosystem functioning as a whole, should be based on a catchment approach (Browner, 1996; National Research Council, 1999). This is because the surface and sub-surface water flows in the catchment eventually pass through the same common outlet. As a result of this, any environmental, economic and social impact downstream would be linked to an upstream influence as well. We need to consider the downstream impacts since every upstream process ends up downstream. In other words, all the physical, biological and chemical processes in a catchment are highly integrated (National Research Council, 1999).

South Africa's water resources policy, law and strategies are based on the approaches of integrated catchment management (DWAF, 1997; UNEP, 2002). There are nine water management areas established in the country, each led by a decentralized Catchment Management Agency (DWA, 2013). The major role of these Catchment Management Agencies is to develop catchment management strategies that are intended to provide integrated planning, rules and regulations for managing water resources in a sustainable way. Generally, a catchment is an ideal unit for the study, management and sustainable use of land and water resources of an area.

2.3.2 Components of the catchment water balance

Quantifying the hydrological budget of catchments in arid and semi-arid climates is an important task in the process of catchment water management, since water scarcity causes conflicts regarding water use. The study of water balance is conducted with the application of the law of conservation of mass, often referred to as the continuity equation. The general water balance function could be summarized as follows:

$$\Delta SW = SW_{gains} - SW_{losses} \tag{2.1}$$

where ΔSW refers to the change in the water content in the catchment, SW_{gains} refers to the total soil water gained to the catchment, and SW_{losses} refers to the total of soil water lost from the catchment. This function could be expanded to become:

$$SW_t = SW_o + \sum_{i=1}^{t}\left(P_{day} - Q_{surf} - ET - W_{perc} - Q_{gw}\right) \tag{2.2}$$

where SW_t refers to the final soil water content (mm), SW_o is the initial soil water content on day i (mm), P_{day} is the amount of precipitation (mm), Q_{surf} is the amount of direct runoff (mm), ET is the amount of evapotranspiration (mm), W_{perc} is the amount of deep percolation below the root zone (mm), and Q_{gw} is the amount of return flow (mm) (Neitsch *et al.*, 2011).

Although some studies have been conducted on water balance on a catchment basis in South Africa (Nicholson *et al.,* 1997; Everson, 2001; Van Huyssteen *et al.,* 2009b; Van Huyssteen *et al.*, 2009a; Bugan *et al.,* 2012; Jovanovic *et al.,* 2013), most of the studies have relied on point data and do not show the spatial variability of the components of the water balance. This section reviews the theoretical concepts of the spatial and temporal distribution of the components of the water balance at a catchment scale. The functional roles of soils, landforms, land use and land cover on catchment water distribution are also reviewed.

2.3.2.1 Precipitation

Definition and importance

Precipitation is any form of condensed water in the atmosphere that falls to the land surface, including rainfall, sleet, snow and hail. Precipitation is one of the main inputs in the water balance, but is the most difficult variable to measure (Jiang, 2004; Jeniffer *et al.*, 2010; Zhang and Srinivasan, 2010). This difficulty is due to its great temporal and spatial variability in an area (Jiang, 2004; Zhang and Srinivasan, 2010; Jeniffer *et al.*, 2010). This holds especially true for arid and semi-arid ecosystems, where spatial and temporal variations in precipitation are central features influencing its functioning (Augustine, 2010). Although numerous studies have been conducted, very little is known about the spatiotemporal variation of precipitation especially in arid and semi-arid regions where a proportion of evaporation is much greater at the expense of groundwater recharge (Augustine, 2010).

Rainfall distribution

The spatial variability of rainfall has been given little attention in the study of soil surface and climate processes (Anders *et al.*, 2006). Although the sensitivity of spatial variation in precipitation seems relatively lower than other components of the water balance, rainfall can still vary significantly on a smaller scale (Kidd, 2001). Particularly, its variation in mountainous regions is inevitable. In this regard, different investigators have found variations of precipitation at different scales of study. For example, Anders *et al.* (2006) found a significant variation in rainfall within tens of kilometres. Mishra (2013) also recommended utilizing four to six rain gauges to get reasonable precipitation within a 50 km × 50 km area.

Different areas on the earth's surface receive different amounts of precipitation. Some of the factors contributing to this difference in precipitation, especially at catchment scale, include topographic properties such as altitude, aspect, direction of mountain ranges (Basist *et al.*, 1994; Daly, 2006; Cukur, 2011) and orographic enhancement which is affected by wind speed and direction (Johansson and Chen, 2003; Daly, 2006). Augustine (2010) stated that orographic variation has minimal influence on precipitation in arid and semi-arid areas, since such ecosystems are characterized by flat to gently undulating topography. Based on this statement, the source of variation in these landscapes could be local variation in intensity and path of convective thunderstorms. Moreover, the difference in surface albedo, cloud cover and general atmospheric circulation are also important factors on larger scales as in a regional climate (Türkeş, 1996).

Determining rainfall distribution

As mentioned, rainfall is one of the most challenging meteorological parameters to measure because of its spatial and temporal variability (Kidd, 2001; Kidd and Huffman, 2011). Conventional observations made through surface gauge networks provide the most valuable direct measurement of precipitation data on the earth's surface and are primarily important for catchment-wide area coverage (Kidd, 2001; New *et al.*, 2001; Kidd and Huffman 2011; Sene, 2013). However, surface gauge networks provide point data and are limited to covering only the land surface, although a few are available over oceans. Weather radar networks are also important technologies that provide data with better spatial coverage (e.g. in national weather forecasts) than surface gauges do, but are limited in extent and number due to their high cost (Kidd and Huffman, 2011; Sene, 2013). Nowadays, satellite observation systems receive great attention since these have better spatial coverage both over land surfaces and over oceans; however, these have coarser spatial and temporal resolutions (Kidd, 2001; New *et al.*, 2001; Sene, 2013). All three of these methods used to determine precipitation have their own advantages and disadvantages, depending on a number of factors. A final approach that combines all three methods is called multi-sensor precipitation estimates (MPE), combining the best features of each measurement method into a single estimate (New *et al.*, 2001; Sene, 2013).

Hydrological models often require spatially and temporally varying estimates of precipitation to be made. Precipitation data for catchments are often collected with surface rain gauges that are based on point measurements. However, the number of meteorological stations found at catchment level are very limited. Hence, other estimation methods are important to obtain spatially and temporally gridded data of precipitation, since the data estimated from satellites will be coarser for catchment level modelling (New *et al.*, 2001; Sene, 2013). Many prediction methods that can give data with acceptable error margins are available in literature. These methods are broadly categorized as interpolations and extrapolations, including methods such as inverse distance weighting, linear regression, polynomial functions (spline), artificial neural networks and kriging. A detailed review of these methods is provided in Li and Heap (2008), Yao *et al.* (2013) and Li *et al.* (2015).

2.3.2.2 Soil water content

Definition and importance

The amount of water associated with a given volume or mass of soil, which is its water content, is an essential component of the soil water balance. Many researchers (Porporato *et al.,* 2002; Western *et al.,* 2004; Endale *et al.,* 2006; Hébrard *et al.,* 2006; Mahanama *et al.,* 2008) show that soil water content influences the components of the water balance significantly. Consequently, the spatial and temporal variation of soil water content over land surfaces have received great attention (Porporato *et al.,* 2002; Western, *et al.,* 2004; Hébrard *et al.,* 2006; Endale *et al.,* 2006; Mahanama *et al.,* 2008). Although soil water has received great attention due to its influence on the land surface and the atmosphere, very little information is available on its spatial distribution (Endale *et al.,* 2006; Di Bella *et al.,* 2016).

Soil water distribution

The distribution of the soil water status in an area is the result of the interaction between the local topography and landscape, climate processes, soil properties, land use and vegetation types (Western, *et al.,* 2004; Endale *et al.,* 2006; Williams *et al.,* 2009; Zhao *et al.,* 2011). However, the level of influence of these major factors on the spatio-temporal soil water status in an area differs significantly, depending on other conditions such as the location of the area and time of measurement. For example, Williams *et al.* (2009) demonstrated that these influences are strongest during the wet period, and that rainfall and land use were the major factors in top soil water distribution (Mello *et al.,* 2011). However, the influences decline as the soil becomes dry. Research conducted at Watkinsville, Georgia, by Endale *et al.* (2006) and in Argentina by Di Bella *et al.* (2016) also showed that at their respective research sites, winters were periods of high soil water content, while summers exhibited the lowest water content, except during intense storm conditions. Regarding the times of measurement, surface water content showed lower variations in winter than in summer. Another factor influencing water distribution in landscapes is the size of the runoff contributing area above the point of interest. In principle, it is assumed that as the size of the contributing area increases, the water content will increase as the runoff outlet is approached (Zhao *et al.,* 2011). In practice, this works for wet seasons and wet areas (Hébrard *et al.,* 2006). The characteristics of topography comprise one of the major factors that play a key role in influencing the surface, sub-surface and hydraulic head flows (Western *et al.,* 2004). Even though gentle/mild slopes are assumed to have higher water content than steep slopes, this may not always be true depending on the textural differences of the soils at different slope classes (Endale *et al.*, 2006). This is because of the difference in hydraulic conductivity and water retention of soils (Western *et al.*, 2004). The aspect, as one of the characteristics of topography, also influences water distribution. Hence, research by Zhao *et al.* (2011) in the Southern Qilian Mountains of China showed that, in the Northern Hemisphere, south-facing surfaces have lower water content than north facing areas due to high insolation to the south. This is obviously dependent on the geographical location of the study area.

Determining soil water content

In recent decades, a number of methods have been developed to determine soil water content. The methods may be classified in different ways: as direct or indirect measurement methods (Cepuder *et al.*, 2008; Bittelli, 2011; Romano, 2014), or according to the spatial scale of measurement, be it a local, catchment and regional or global scale (Bittelli, 2011). In a direct measurement method, the amount of water can be measured directly, for instance measuring the mass of water as a fraction of the total weight of the soil, i.e. the gravimetric method (Cepuder *et al.*, 2008; Bittelli, 2011; Romano, 2014). With indirect methods, a variable that is significantly affected by the amount of water in a soil will be measured and the change of the variable will be related to the change in soil water content. These physically based or empirical relationships are called calibration curves. Some of the major indirect methods include the following: the neutron moisture meter (NMM), time domain reflectometry (TDR), capacitance probes, ground penetrating radar (GPR), electromagnetic induction (EMI), electrical resistivity tomography (ERT), and remote sensing techniques. A detailed description of the different types of indirect methods is given in Cepuder *et al.* (2008), Bittelli (2011), and Romano (2014).

All the methods mentioned so far have their own advantages and disadvantages. The only direct method (the gravimetric method) is advantageous since it is the most reliable and accurate method (Cepuder *et al.*, 2008; Bittelli, 2011; Romano, 2014). It is also less expensive than other methods. However, this method is sometimes not preferred because it requires destructive sampling and is also laborious and time consuming to carry out. Indirect methods allow repetitive in-field measurements and are mostly automatically recorded and non-destructive. All indirect methods require accurate calibration curves. Most importantly, all the methods mentioned above (except remote sensing techniques) share a common shortcoming, i.e. they all give point data. In other words, it is laborious, time consuming and even sometimes impractical to obtain spatial variation of soil water, especially on catchment, regional and global scales. Therefore, other more advanced methods are required to obtain continuous data describing the spatial and temporal variation of soil water on catchment, regional and global scales. In this regard, remote sensing and the different methods of interpolation described in Section 2.3.2.1 can be used here, as well.

2.3.2.3 Evapotranspiration

Definition and importance

Transpiration is the process of vaporization of water contained in plant tissues and loss to the atmosphere (Allen *et al.*, 1998), whereas evaporation is water loss from a bare soil surface or water body in the presence of heat energy. Therefore, evapotranspiration is a term describing the two processes together, since they mostly occur simultaneously and is difficult to separate them (Jovanovic and Israel, 2012). Evapotranspiration is an important component of the soil water balance and is linked to ecosystem productivity, species distribution and ecosystem health (Christensen *et al.*, 2008). Understanding the major controls and variability in catchment evapotranspiration is also important for gaining an understanding of the role of evapotranspiration in energy budgets of ecosystems (Allen *et al.*, 1998; Cooper *et al.*, 2000; Christensen *et al.*, 2008; Emanuel *et al.*, 2010). Babkin (2009) estimated that a global annual amount of 7.2×10^{13} m^3 of water is lost through evapotranspiration. Emanuel *et al.* (2010) also explained that the evapotranspiration process tells us about the hydrological controls on carbon cycling and both vegetation structure and distribution in an area. Under South African conditions, Bennie and Hensley (2001) and Jovanovic *et al.* (2015) reported that, on average, 65% of annual precipitation is lost through evapotranspiration. Evapotranspiration is not only a means of water loss, but also one of the major means of losing energy during the conversion of liquid water to vapour. As Babkin (2009) estimated, evapotranspiration uses 25% of the total energy reaching the earth's surface, which amounts to approximately 1.26×10^{24} joules. Therefore, evaporation is a very important process that influences water and energy balances between the earth's surface and the atmosphere. Hence, the accurate determination of evapotranspiration is a very important task in arid and semi-arid environments.

Factors influencing evapotranspiration

Three conditions are necessary for evapotranspiration to occur and persist (Hillel, 1977; Rasheed *et al.*, 1989; Hillel, 2004). Firstly, there should be a continual supply of heat to meet the latent heat requirement of water. Secondly, the vapour pressure in the atmosphere over the evaporating body must remain lower than the vapour pressure at the surface of that body, and thirdly, there must be a continual supply of water to the site of evaporation. The first two conditions can be considered external to the evaporating body, as they are influenced by meteorological factors such as radiation, air temperature, humidity and wind velocity, which together determine atmospheric evaporability. The third condition, however, depends upon the content and potential of water in the evaporating body and upon its conductive properties that determine the maximal rate at which the body can transmit water to the evaporation site (Hillel, 1977; Rasheed *et al.*, 1989; Hillel, 2004; Rose *et al.*, 2005).

Therefore, evapotranspiration is affected by the complex interaction between topography, soil characteristics, vegetation, and climatic factors (Mo *et al.*, 2004; Western *et al.*, 2004; Wenzhi and Xibin, 2016). These factors determine the rate of evapotranspiration by influencing the availability of water, energy and vegetation type of the area. However, their comparative influence on the spatial and temporal variation of evapotranspiration differs based on certain conditions. For example, in dry climates, water availability is a limiting factor for variation in evapotranspiration (Zhao *et al.*, 2014), distribution of the vegetation type is also a limiting factor in catchments (Western, *et al.*, 2004; Li *et al.*, 2015), while soil type (due to difference in soil water holding capacity) is another important factor in some instances (Hatfield and Prueger, 2011). Wenzhi and Xibin (2016) showed that the vapour pressure gradient and stomatal conductance are important for variations in evapotranspiration.

Determining variation in evapotranspiration

Although evapotranspiration is a key component in the soil water balance, it is one of the most difficult parameters to determine in the soil-plant-atmosphere-continuum (Jovanovic and Israel, 2012; Banimahd *et al.*, 2015) due to the complex nature of the process. A number of methods are proposed in literature either to measure or to estimate evapotranspiration from the land surface. Measurement methods include: (1) Lysimeter methods that measure evapotranspiration by the change in weight of an isolated soil sample. (2) The sap flow technique where transpiration is measured from the rate of sap flow in trees and parts of trees, such as the trunk, branches or roots, using heat as a tracer, with an estimate of the area of wood through which flow occurs. (3) The scintillometer method uses a device to measure small fluctuations of the refractive index of air caused by variations in temperature, humidity, and pressure. It measures latent and sensible heat. (4) The Eddy Covariance method determines evapotranspiration from the correlation between fluctuations in vertical wind speed and atmospheric humidity, measured at high frequency at the same location, a few meters above vegetation. (5) The Bowen Ratio method calculates evapotranspiration from the surface energy budget using the ratio of sensible to latent heat derived from the ratio of atmospheric temperature to humidity gradients. Evapotranspiration can also be determined from the soil or atmospheric water balances and remote sensing estimates. More detailed reviews of different methods to measure or estimate evapotranspiration are given by Kairu (1991), Wang and Dickinson (2012), Jovanovic and Israel (2012), Zhao *et al.* (2013), Liou and Kar (2014) and Banimahd *et al.* (2015).

2.3.2.4 Direct runoff

Definition and importance

Runoff, the natural phenomenon of free water movement under the influence of gravitational force, is an important and indispensable element of the hydrological cycle (Tarboton, 2003; Vinogradov, 2009). Four types of runoff may occur (Mockus, 2004; Wagener *et al.*, 2004) as shown in Figure 2.2 below. First, channel runoff occurs when rain falls directly on a flowing stream and appears in the hydrograph (a graph showing the rate of flow versus time) throughout the rainfall event varying with the rainfall intensity. This type of runoff is generally negligible in hydrographs except in special studies. Secondly, surface runoff occurs when the rate of water application or rainfall exceeds the soil's rate of infiltration. Surface runoff appears in the hydrograph after the demands of interception, infiltration and surface storage have been satisfied and is the major part of the rainfall-runoff process. The third type is subsurface flow that occurs when infiltrated rainfall saturates a subsurface horizon with poor drainage and travels laterally above the subsurface zone, finally reappearing as a spring. Since subsurface flow contributes to the hydrograph during, or soon after, a rainfall event, it is often called quick return flow. Lastly, base flow is a steady flow that comes from an aquifer replenished by percolation after a rainfall event. Base flow will increase the streamflow rate after a rainfall event. All these categories of runoff, excluding base flow, are called direct runoff (Mockus, 2004).

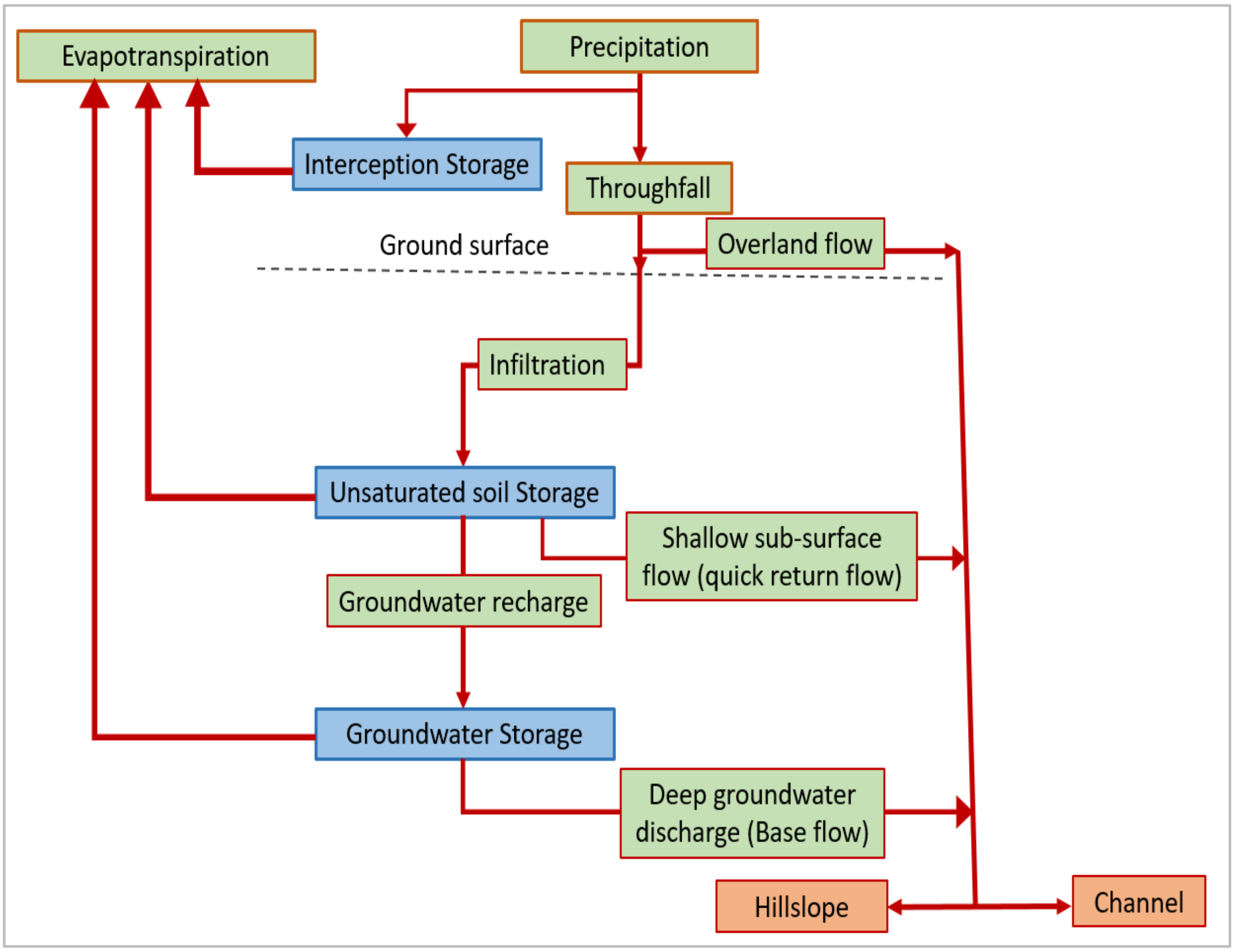

Figure 2.2: The rainfall-runoff process in a catchment

Runoff is important for many purposes in hydrological research, particularly in stream flow estimation, irrigation and flood estimation (Mdee, 2015). More especially, the significant variation of hydrological characteristics in time and space calls for the need to predict seasonal runoff fluctuations (Mdee, 2015; Rejani *et al.*, 2015). Zelelew (2012) and Rejani *et al.* (2015)

also stated that the precise estimation of runoff is essential in catchment development intervention, such as planning water harvesting and *in situ* soil water conservation structures. Particularly during the over-exploitation of groundwater in dry areas, the precise estimation of runoff is essential for planning intervention strategies (Ramakrishnan *et al.*, 2009; Zelelew, 2012; Rejani *et al.*, 2015).

Factors influencing runoff distribution

The runoff process differs from place to place and time to time, depending on a number of factors. The spatial and temporal characteristics of the runoff process are very complex since a number of factors influence them. The spatial patterns of catchment characteristics provide important information to link the runoff generation process and its controlling factors within catchments (Zelelew, 2012). The first group of factors that primarily influence surface runoff comprise the characteristics of the land surface, such as topography, land use, land cover and presence of surface sealing (Tarboton, 2003; Ramakrishnan *et al.*, 2009; Rejani *et al.*, 2015). The second group of factors is related to soil behaviour, including initial soil water content, soil type, lithology and hydraulic properties of the soil (Tarboton, 2003; Ramakrishnan *et al.*, 2009; Rejani *et al.*, 2015). Finally, climatic factors, particularly rainfall properties such as intensity, duration and frequency, are the most important for runoff processes (Tarboton, 2003; Ramakrishnan *et al.*, 2009 and Rejani *et al.*, 2015).

Determining runoff distribution

Several methods are described in the literature to determine runoff at different scales of study (catchment, regional and global scales). Mitchell *et al.* (2001) classified the methods into four classes: (i) Statistical methods that make probabilistic statements about runoff and its characteristics, assuming the measurements are representative of the population. Such methods enable the use of measured data, but are only applicable in gauged catchments. (ii) Regional methods, where the dependent variable in gauge catchments will be related to a physically based independent variable, such as catchment area. Based on this relationship (correlation or regression), the value of the dependent variable of the ungauged catchments will be estimated. These methods are easy to apply, but are only applicable to the same region where the original data was collected, and require data from gauged catchments. (iii) Transfer methods determine hydrologic characteristics of a smaller catchment from the larger catchment characteristics or vice versa. For example, a discharge transfer is made in proportion to the ratio of the tributary area and an exponent is determined from the slope of an area-flood graph. These methods require relatively little data, but are inapplicable if the two catchments are heterogeneous. (iv) Rainfall-runoff models where rainfall is considered to be an intensity, in which it varies with time over the catchment. Under this category, a number of approaches are described. Li *et al.* (2015) classified the rainfall-runoff models into three types based on their complexity and application. These are: (a) Lumped conceptual rainfall-runoff models [HBV (Hydrologiska Byrans Vattenavdelning) model and TOPMODEL]; (b) Distributed hydrological models (SWAT); and (c) Global hydrological and land surface models [VIC (Variable Infiltration Capacity) model]. Generally, rainfall-runoff models need to be simple in parameterization, but should incorporate sufficient parameters to capture the key response of the hydrological process (Wagener *et al.*, 2004), referred to as the principle of parsimony.

2.3.2.5 Deep drainage

Definition and importance

Deep drainage (or percolation) can be defined as the downward flow of water in soils below the base of rooting zones (Healy and Cook, 2002; Healy, 2010). Part of this water that infiltrates below the rooting zone follows subsurface pathways directly into streams, and is known as *interflow* or *subsurface stormflow* (Tarboton, 2003; Kumar, 2003). If this percolated water contributes to the replenishment of ground water, it is said to be *ground water recharge* (Healy and Cook, 2002; Kumar, 2003). Since ground water is a major source of fresh water, particularly in arid and semi-arid areas, the accurate estimation of groundwater recharge is extremely important for the proper management of groundwater systems (Healy and Cook, 2002; Healy, 2010; Gates *et al.,* 2014). There should be a balance between ground water depletion and recharge for the long-term sustainability of ground water resources (Kumar, 2003; Ochoa *et al.*, 2012). Hence, the determination of the spatial and temporal rates of water percolation helps to estimate the balance between ground water depletion and recharge for an area of interest.

Factors influencing deep drainage

Deep drainage of the land surface varies both spatially and temporally. Drainage from the surface of the earth occurs when the rate of the total sources of water (either precipitation or irrigation) exceeds the total rate of sinks (soil storage, evapotranspiration and runoff). Similarly, deep drainage eventually develops after the water content of the root zone exceeds its water holding capacity (Gates *et al.*, 2014). Many factors contribute to the spatial and temporal variations of deep drainage. These factors can be grouped into three categories, i.e. factors related to the water sources (precipitation and irrigation), characteristics of the infiltrating soil, and characteristics of the land surface. Literature shows that all three categories significantly affect drainage processes (e.g. Kumar, 2003; Ochoa *et al.*, 2012; Gates *et al.*, 2014). The first category, the effect of water sources, affects drainage by the intensity and duration of precipitation and/or irrigation. The second category, soil characteristics, include hydraulic properties (hydraulic conductivity and capillary pressure) of the soil horizon and the unsaturated zone as a whole. Lastly, the land surface characteristics that include topography, land use, land cover and management play a vital role.

Determining deep drainage

The determination of deep percolation or groundwater recharge is difficult to accomplish since the amount of water for recharge is smaller, compared with other components of the water balance. For example, Gieske (1992) and Sibanda *et al.* (2009) found that less than 5% of the precipitation contributes to ground water recharge. Nevertheless, there are several methods that are used to quantify deep percolation. Chung *et al.* (2016) categorized the methods into five groups: (1) Methods using groundwater data, including groundwater modelling and water table fluctuation methods. Groundwater models, such as Modular Three-Dimensional Finite-Difference Groundwater Flow Model (MODFLOW), can be used to estimate groundwater recharge. However, the water table fluctuation method can be applied to obtain point recharge data by assuming the change in water level in an aquifer is due to recharge arriving at the water table. (2) Stream flow methods include seepage meters, streamflow gain/loss measurements (seepage run), recession-curve displacement methods and catchment models. (3) Catchment hydrologic models include the use of hydrologic models like the Soil and Water Assessment Tool (SWAT) developed by Arnold *et al.* (1998) and Precipitation Runoff Modeling System (PRMS) (Leavesley *et al.*, 1983). Meteorological data, topography, soils, LULC and streamflow records comprise the basic data required to apply these models successfully. (4) Tracer methods include the use of chloride, chlorofluorocarbons, temperature and tritium as tracers to estimate ground water recharge by a mass balance equation. (5) Water budget methods include the use of the Deep Percolation and the Hydrologic Evaluation of Landfill Performance (HELP) models to compute the components of the soil water balance, including deep percolation. A detailed review and description of all the methods mentioned above can be further referred to in Adams *et al.* (2004), Risser *et al.* (2005), Sibanda *et al.* (2009), Wang *et al.* (2010), Upreti *et al.* (2015) and Chung *et al.* (2016).

2.4 Catchment hydrologic modelling

2.4.1 Importance of hydrologic models

Most hydrological systems incorporate extremely complex processes and are not easily understood (Rosenblueth and Wiener, 1945; Xu, 2002). In this regard, hydrological models play a vital role in gaining an understanding of such complex processes more easily. Hydrological models are simplified systems that characterize real hydrologic processes (Lundin *et al.*, 1999; Tessema, 2011). In this case, a system is defined as a set of interacting or interdependent components forming a complex, whole process. Therefore, models enable the users to manipulate the system's variables/parameters easily and help in understanding the interaction between variables that make up complex systems (Sokolowski and Banks, 2010; Sokolowski and Banks, 2011). Babel and Karssenberg (2013) described hydrologic models as mediators between theory and practice or the real world. Therefore, hydrologic models are important tools in the study of catchment, regional and global scales of hydrologic processes.

It is impossible in practice to measure everything that we want to know about catchments due to various reasons such as high catchment heterogeneity and limitations in measurement methods, and to the fact that the methods are laborious, time consuming and costly to implement. Due to such limitations and the need to extrapolate both spatial and temporal information on catchments, hydrologic models have a prime importance (Pechlivanidis *et al.*, 2011). Catchment hydrologic models assist in gaining a better understanding of important hydrologic processes and of how changes in the catchment affect these processes (Xu, 2002). Catchment hydrologic models also provide hydrologic data that assist in the prediction of potential future impacts of land use and climate change on water resources (Xu, 2002; Pechlivanidis *et al.*, 2011). These will again assist us during important decision regarding catchement hydrology including but not limited to water-table management, wetland restoration, irrigation water management, streamflow restoration, water quality evaluation and flood forecasting and management.

2.4.2 Types of hydrologic models

There are different approaches that are taken to build hydrologic models, which result in differences in structure and complexity, and which in turn affects the predictive performance of these models. For this reason, a general classification is important for giving an indication of model structure and complexity. Different scholars have followed different approaches to classify hydrologic models. Singh (1988) used the terms “symbolic” and “material” to classify hydrologic models (Figure 2.3 below). These two groups are sub-divided into mathematical vs. non-mathematical and laboratory vs. analogue, respectively. The mathematical group is further categorized as empirical (metric), conceptual (parametric) or theoretical (physically based or white-box) models. These three sub-groups are categorized further, as seen in Figure 2.3. Jajarmizadeh *et al.* (2012) categorized mathematical models based on four basic characteristics (criteria as shown in Figure 2.4 below), i.e. their way of simulation, spatial representation, temporal representation and method of solution. On the basis of a simulation method, hydrologic models were classified as conceptual, physically based, empirical or regression, and stochastic time series, whereas on the basis of spatial representation, models were classified as lumped, distributed and coordinate system. Based on temporal representation, models were categorized as steady state, steady state seasonal, single even, and continuous representation. Finally, models were classified as O-dimensional, formal-analytical, formal-numerical and hybrid solutions, based on the method of solution (Jajarmizadeh *et al.*, 2012).

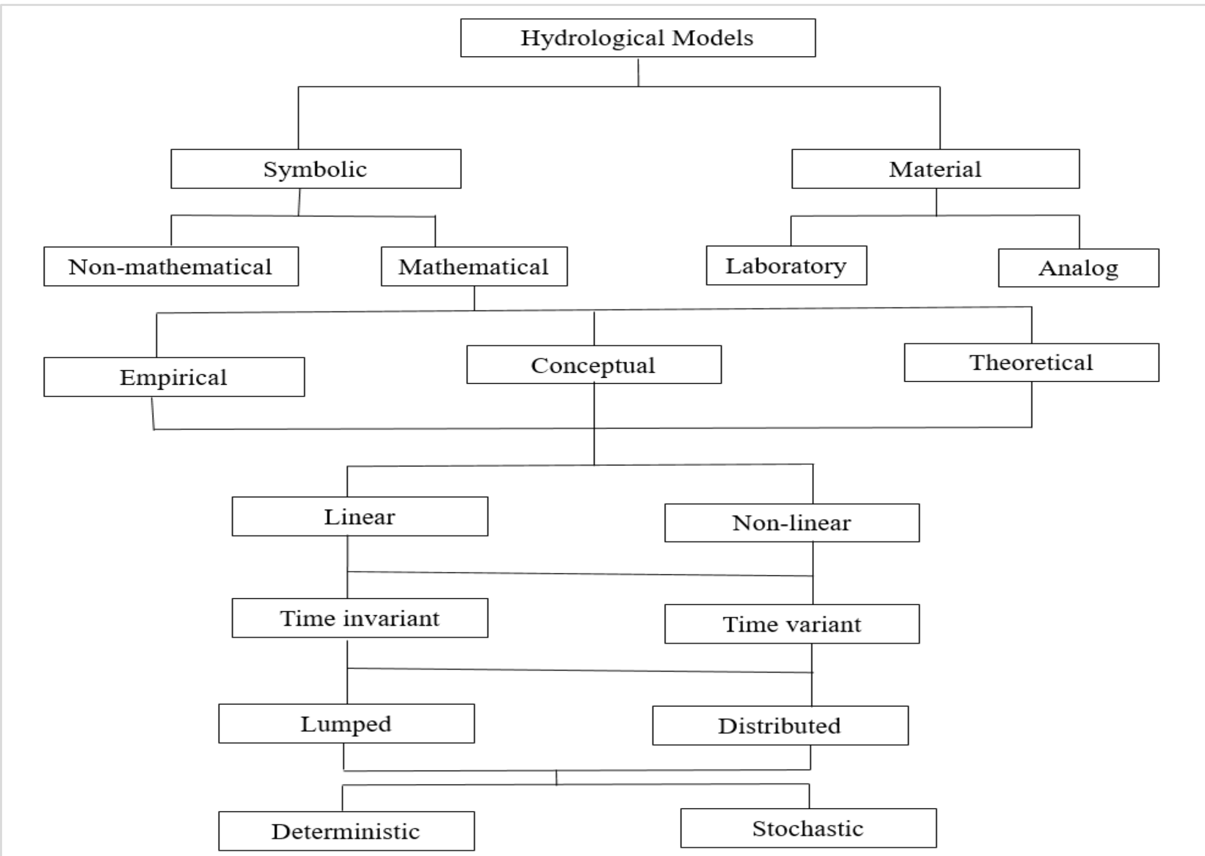

Figure 2.3: Classification of hydrological models

(Source: Singh, 1988; Xu, 2002)

Although different ways of classification have been formulated by different authors, the principles of classifying hydrological models are almost similar. Based on model structure, Pechlivanidis *et al.* (2011) also classified hydrologic models as metric, conceptual, physics-based and hybrid models. Metric or empirical models are based on simplified, experimentally derived or measured relationships such as linear regressions (Beckers *et al.*, 2009; Devia *et al.*, 2015). The mathematical equations involved are derived from concurrent input and output time series, but not from the physical catchment process. This category includes artificial neural network (ANN) and fuzzy regression. Conceptual or parametric models, on the other hand, consist of a number of interconnected physical elements in a catchment and are based on the fundamental physics and governing equations of water flow (eWater, 2012; Devia *et al.*, 2015). Conceptual models consider physical laws in a highly simplified form and are located in between empirical and theoretical models. HBV (Hydrologiska Byråns Vattenbalansavdelning) and TOPMODEL are examples. Theoretical or physics-based models are ideal to represent the real hydrological processes, since they have a logical structure similar to the real-world system (Xu, 2002; Pechlivanidis *et al.*, 2011). They use state variables that are measurable and are functions of both time and space. In this category, MIKE-SHE (Integrated Hydrological Modelling System) and SWAT (Soil and Water Assessment Tool) are good examples. Finally, hybrid models are integrated modelling structures that include more than one model and are designed to combine the strengths of the different model types in the hybrid model.

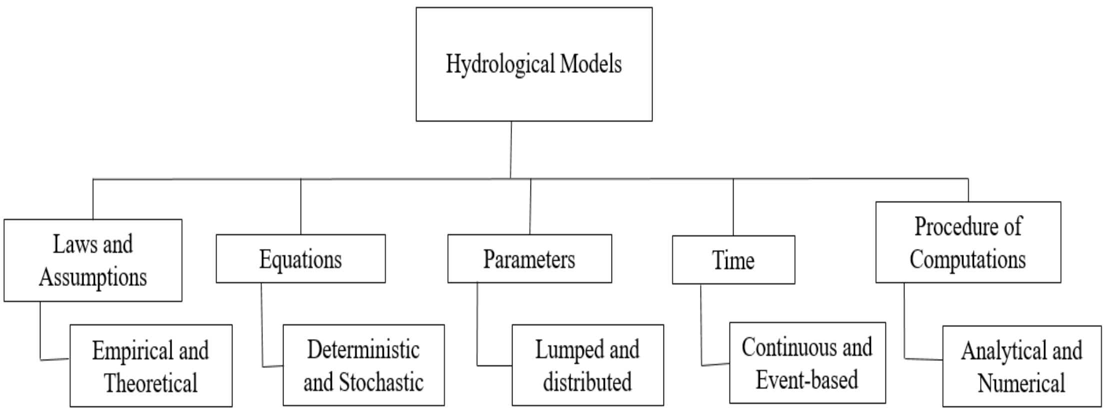

Figure 2.4: Classification of hydrological models by Jajarmizadeh *et al*. (2012)

Generally, models differ highly from one another when evaluated by different criteria. For example, they differ in spatial and temporal scales and complexity of parameters. Therefore, a suitable model should be chosen carefully. Beckers *et al.* (2009) summarized the major criteria to be considered during the model selection procedure: (1) Model functionality: the range of processes that the model will consider during simulation must be considered primarily. (2) Model complexity: the estimated data, resources (cost) and time to initialize and calibrate the model. (3) Model applicability to a particular climatic and physiographic setting, including the scale of the study. (4) The model's ability to provide the required outputs, including the spatial and temporal scale. (5) Model adaptability to represent future catchment conditions for long-term planning and climate change.

2.5 The Soil and Water Assessment Tool

2.5.1 General description of the model

The Soil and Water Assessment Tool (SWAT) is a continuous-time, semi-distributed and processed-based model developed and supported by the USDA Agricultural Research Service (Neitsch *et al.*, 2011; Arnold *et al.*, 2012). The model was originally developed to evaluate the impact of land management practices on water resources, sediment and agricultural chemical yields in large complex catchments with varying soils, land use and management conditions (Neitsch *et al.*, 2011; Daniel *et al.*, 2011). The major modules in SWAT include hydrology, erosion/sedimentation, plant growth, nutrients, pesticides, land management, stream and reservoir routing. As a result, it simulates climate changes, hydrologic processes, land use changes, water use management, water quality and water quantity assessments (Gassman *et al.*, 2007; Neitsch *et al.*, 2011; Arnold *et al.*, 2012; Parajuli & Ouyang, 2013). In SWAT, a catchment is divided into multiple sub-catchments and further sub-divided into hydrologic response units (HRUs) that comprise homogeneous land use/cover and management, topographical and soil characteristics. Therefore, HRUs are the smallest units for the simulation of different hydrologic and other processes in SWAT.

Water balance is the major driving force behind any process in SWAT since it influences plant growth and the movement of sediments, nutrients, pesticides and pathogens in a catchment (Neitsch *et al.*, 2011; Arnold *et al.*, 2012; Parajuli & Ouyang, 2013). The simulation of catchment hydrology is performed in two parts, known as the land phase and the routing phase. The land phase determines the amount of water, sediment, nutrient and pesticide loadings in the main channel in each sub-basin, while the routing phase defines the movement through the channel network to the outlet of the catchment. The model requires several data inputs to simulate the catchment hydrologic processes, and these include a digital elevation model

(DEM), land use–land cover data, soil types, and different daily weather data, including details of precipitation, maximum and minimum air temperatures, solar radiation, wind speed, and relative humidity.

SWAT has received international acceptance as a robust interdisciplinary catchment-scale modelling tool. This is evidenced by international SWAT conferences, hundreds of SWAT-related papers presented at scientific meetings, and the numbers of articles published in peer-reviewed journals (Gassman *et al.*, 2007; Gassman *et al.*, 2010; van Griensven *et al.*, 2012). For example, Gassman *et al.* (2010) reported that more than 600 peer-reviewed journal articles related to SWAT had been published up to 2010. The model has also proved to be a very flexible and adaptable tool for investigating a range of hydrologic and water quality problems. The availability of the model and its applicability through the development of geographic information system (GIS) based interfaces, together with its easy linkage to sensitivity, calibration and uncertainty analysis tools, has contributed to the popularity of SWAT in global research. Moreover, technological advancements have enabled extensive networking regarding the use of SWAT, including access to web-based documentation, user support groups, a SWAT literature database, regional and international conferences, and targeted development workshops (Gassman *et al.*, 2010; van Griensven *et al.*, 2012).

2.5.2 Model background and theories

2.5.2.1 Precipitation

The SWAT model requires weather station data, including precipitation, temperature, humidity, solar radiation, and wind speed. The model then converts the point gauge values to spatial raster values by taking the nearest gauge value to the centroid of a sub-catchment. To account for the orographic effect, SWAT also calculates elevation bands from the DEM and calculates new values based on the elevation difference from the centroid of the sub-catchment. The conversion of point precipitation data to raster values was calculated using the following formula (Neitsch *et al.*, 2011):

$$R_{band} = R_{day} + \left(EL_{band} - EL_{gauge}\right).\frac{Palps}{days_{pcp,yr}}, \text{ when } R_{day} > 0.01 \qquad (2.3)$$

where R_{band} is the precipitation in the elevation band (mm), R_{day} is the precipitation recorded at the rain gauge (mm), EL_{band} is the mean elevation at the elevation band (m), EL_{gauge} is the elevation at the recording gauge (m), *Plaps* is the precipitation lapse rate (mm km^{-1}), and $days_{pcp,year}$ is the average number of days of precipitation in the sub-catchment in a year.

Once the precipitation values have been calculated for each band, a new average sub-catchment precipitation is calculated as:

$$R_{day} = \sum_{bnd=1}^{b} R_{day} . fr_{bnd} \tag{2.4}$$

where R_{day} is the daily average precipitation adjusted for orographic effects (mm), R_{band} is the precipitation falling in each elevation band, fr_{bnd} is the fraction of the sub-catchment area within the elevation band, and b is the total number of elevation bands in the sub-catchment. Missing data from weather stations can also be estimated by the weather generator tool in SWAT. The weather generator tool needs parameters that should be calculated from long-term (up to 20 years) climate data. The list of parameters needed for simulating long-term climate data and the details of how SWAT calculates other raster weather parameters from station data can be referred to in Neitsch *et al.* (2011).

2.5.2.2 Soil water content

The fate of water that enters into a soil profile can follow one of different pathways. It may be removed by plant uptake or evaporation, it may percolate past the bottom of the root zone and recharge an aquifer, or it may move laterally in the profile and contribute to stream flow. The calculation of the root zone water content is based on the field water capacity of soils. Plants can take up soil water up to a maximum suction of 1500 kPa, which represents the lower limit (permanent wilting point) of soils. On the other hand, a fully saturated soil will lose a fraction of soil water due to gravitational force. The amount of water remaining after the release of water due to gravitational force is called the drained upper limit (field water capacity). Soils cannot store water above their field capacity. The plant-available water in soils can be calculated by:

$$AWC = FC - WP \tag{2.5}$$

where *AWC* is the plant available water, *FC* is the field water capacity, and *WP* is the permanent wilting point.

SWAT calculates the water content of a soil at a permanent wilting point for each layer as follows (Neitsch *et al.*, 2011):

$$WP_{ly} = 0.40.\frac{m_c.\rho_b}{100} \tag{2.6}$$

where WP_{ly} is the water content of a soil layer at wilting point, m_c is the percentage clay content, and ρ_b is the bulk density (Mg m^{-3}). Finally, the water content of that layer at field capacity can be calculated by:

$$FC_{ly} = WP_{ly} + AWC_{ly} \tag{2.7}$$

Lateral flow will be significant for soils that have higher hydraulic conductivity at the surface and an impermeable or semi-permeable layer in the sub-soil. SWAT uses a kinematic storage model developed by Sloan *et al.*, 1983 (cited by Neitsch *et al.*, 2011). Lateral flow starts when excess water has infiltrated to the lower horizon that is impermeable, with sloping ground. As a result, the drainable volume of water stored in the saturated zone of a hillslope per unit area can be estimated by:

$$SW_{ly,excess} = \frac{1000.H_o.\phi_d.L_{hill}}{2} \tag{2.8}$$

where $SW_{ly,excess}$ is the drainable volume of water (mm), H_o is the saturated zone thickness as a fraction (mm mm^{-1}), ϕ_d is the drainable porosity of the soil (mm mm^{-1}), and L_{hill} is the hillslope length (m). By rearranging to solve H_o:

$$H_o = \frac{2.SW_{ly,excess}}{1000.\phi_d.L_{hill}} \tag{2.9}$$

the drainable porosity of the soil layer will be calculated by:

$$\phi_d = \phi_{soil} - \phi_{fc} \tag{2.10}$$

where ϕ_d is the drainable porosity of the soil (mm mm^{-1}), ϕ_{soil} is the total porosity of the soil (mm mm^{-1}) and ϕ_{fc} is the porosity of the soil filled with water at field capacity (mm mm^{-1}). The drainable volume of water from a saturated layer is:

$$SW_{ly,excess} = SW_{ly} - FC_{ly} \tag{2.11}$$

where SW_{ly} is the water content of a layer at a given day (mm), and FC_{ly} is the water content of the layer at field capacity (mm). The net discharge for that specific hillslope can be estimated by:

$$Q_{lat} = 24.\mathrm{H}_o - v_{lat} \qquad (2.12)$$

where Q_{lat} is the discharge from the hillslope (mm) and v_{lat} is the velocity of flow at the outlet of the hillslope (mm h^{-1}).

2.5.2.3 Evapotranspiration

Evapotranspiration is the primary mechanism of water removal from a catchment. There are three options for calculating the potential evapotranspiration (PET) in SWAT, i.e. the Penman-Monteith equation, and the Priestley-Taylor and Hargreaves methods. After calculating PET, SWAT calculates the actual evapotranspiration with four components, i.e. evaporation from the canopy, transpiration, soil surface evaporation, and groundwater revap (water extracted from shallow groundwater by deep-rooted vegetation, plus the water moved upwards to the root zone as a result of soil water deficit due to evapotranspiration) in areas where the groundwater is closer to the root zone.

In the SWAT model, canopy evaporation is the first of all the factors to be calculated. To calculate the amount of rain trapped by the canopy during a day:

$$can_{day} = can_{mx} \cdot \frac{LAI}{LAI_{mx}} \qquad (2.13)$$

where can_{day} is the amount of water trapped by the canopy for that day (mm), can_{mx} is the maximum amount of water that can be trapped by the canopy during full development of the vegetation (mm), LAI is the leaf area index for that day, and LAI_{mx} is the maximum leaf area index of the vegetation.

$$R_{INT(f)} = R_{INT(i)} + R'_{day} \text{ and } R_{day} = 0, \text{ When } R'_{day} \le can_{day} - R_{INT(i)} \qquad (2.14)$$

$$R_{INT(f)} = can_{day} \text{ and } R_{day} = R'_{day} - (can_{day} - R_{INT(i)}), \text{ when } R'_{day} > can_{day} - R_{INT(i)} \qquad (2.15)$$

where $R_{INT(i)}$ is the initial amount of free water held on the canopy on that day (mm), $R_{INT(f)}$ is the final amount of free water held on the canopy on that day (mm), R'_{day} is the amount of precipitation before the canopy interception is removed (mm), R_{day} is the amount of precipitation after the canopy interception is removed (mm), and can_{day} is the maximum amount of water that can be trapped by the canopy for that day (mm). Finally, if potential evapotranspiration (E_o) is less than the amount of free water held in the canopy:

$$E_a = E_{can} = E_o \text{, and } R_{INT(f)} = R_{INT(i)} = E_{can} \tag{2.16}$$

And if the amount of free water in the canopy is greater than the potential evaporation:

$$E_{can} = R_{INT(i)} \text{, and } R_{INT(f)} = 0 \tag{2.17}$$

where E_a is the actual amount of evapotranspiration for the day (mm), E_{can} is the amount of evaporation from free water in the canopy (mm), and E_o is the potential evapotranspiration of the catchment for that day (mm).

The next component of evapotranspiration to be calculated is transpiration. In this study, the Penman-Monteith method has been selected to calculate the potential evapotranspiration, and given in the following equations (Neitsch *et al.*, 2011):

$$\lambda E = \frac{\Delta.(H_{net} - G) + \rho_{air}.c_p.\left[e^o - e^z\right]/r_a}{\Delta + \gamma.(1 + r_c / r_a)} \tag{2.18}$$

where λE is the latent heat flux density (MJ m^{-2} d^{-1}), E is the depth rate of evaporation (mm d^{-1}), Δ is the slope of saturation vapour pressure-temperature curve, *de/dt* (kPa $^oC^{-1}$), H_{net} is the net radiation (MJ m^{-2} d^{-1}), G is the heat flux density to the ground (MJ m^{-2} d^{-1}), ρ_{air} is the density of air (kg m^{-3}), C_p is the specific heat at constant pressure (MJ kg^{-1} $^oC^{-1}$), e^o_z is the saturated vapour pressure of air at a height of *z* (kPa), e_z is the saturated vapour pressure of water at a height of *z* (kPa), γ is the psychrometric constant (kPa $^oC^{-1}$), r_c is the plant canopy resistance (s m^{-1}), and r_s is the aerodynamic resistance (s m^{-1}). For the details regarding the calculation of all the parameters in the above equation (Equation 2.18 above), see Allen *et al.* (1998) and Neitsch *et al.* (2011).

The third component of evapotranspiration, which is the soil evaporation on a given day, is a function of the transpiration, degree of shading, and potential evapotranspiration adjusted for canopy evaporation (Abiodun *et al.*, 2018). The maximum soil evaporation for a given day is calculated as:

$$E_s = E'_o \operatorname{cov}_{sol} \tag{2.19}$$

$$\operatorname{cov}_{sol} = e^{(-5.0\times10^{-5}\times cv)} \tag{2.20}$$

where cov_{sol} is the soil cover index (-) and cv is the aboveground biomass for the day (kg ha^{-1}). The maximum possible soil evaporation in a day is then subsequently adjusted for plant water use ($E's$) (mm d^{-1}):

$$E'_s = \min\left(E_s, \frac{E_s.E'_o}{E_s + E_t} \right) \quad (2.21)$$

where E'_s is the maximum soil evaporation adjusted for plant water use in a given day (mm), E_s is the maximum evaporation for a given day (mm), E'_o is the potential evapotranspiration adjusted for evaporation from the canopy (mm), and E_t is the transpiration on a given day (mm). During evaporation from soil, SWAT partitions the evaporation demand between soil layers. Equation 2.22 below is used to determine the maximum amount of evaporation for a given depth. Similarly, Equation 2.23 below is used to calculate evaporation for different soil layers.

$$E_{soil,z} = E''.\left(\frac{z}{z + \exp(2.374 - 0.00713.z)} \right) \quad (2.22)$$

$$E_{soil,1} = E_{soil,zl} - E_{soil,zu}.esco \quad (2.23)$$

where $E_{soil,z}$ is the water demand for evaporation at depth z (mm), $E''s$ is the maximum possible water to be evaporated in a day (mm), e_{sco} is the soil evaporation compensation factor, $E_{soil,zl}$ is the water demand for evaporation in layer l (mm), $E_{soil,zl}$ is the evaporative demand at the lower boundary of the soil layer (mm), $E_{soil,zu}$ is the evaporative demand at the upper boundary of the soil layer (mm), F_{cl} is the water content of the soil layer l at field capacity (mm), $E''_{soil,l}$ is the volume of water evaporated from soil layer l (mm d^{-1}), and E_{soil} is the total volume of water evaporated from soil on a given day (mm d^{-1}). Details can be referred to in Neitsch *et al.* (2011) and Abiodun *et al.* (2018).

Finally, the groundwater revap is calculated if there is an evapotranspiration demand in the root zone. Revap is estimated as a fraction of potential evapotranspiration and it is primarily a function of depth of water table to the root zone. The amount of evaporation from revap is calculated by SWAT as follows:

$$W_{revap,mx} = \beta_{revap}.E_o \quad (2.24)$$

$$W_{revap} = 0 \text{ if } aq_{sh} \le aq_{shthr,rvp} \quad (2.25)$$

$$W_{revap} = W_{revap,mx} - aq_{shthr,rvp} \text{, if } aq_{shthr,rvp} < aq_{sh} < (aq_{shthr,rvp} + W_{revap,mx}) \quad (2.26)$$

$$W_{revap} = W_{revap,mx} \text{, If } aq_{sh} \ge (aq_{shthr,rvp} + W_{revap,mx}) \quad (2.27)$$

where $w_{revap,mx}$ is the maximum volume of water transferred to the unsaturated zone in response to water shortages for the day (mm), β_{revap} is the revap coefficient (-), w_{revap} is the actual volume of water transferred to the unsaturated zone to supplement water shortage for the day (mm), a_{sh} is the water volume stored in the shallow aquifer at the beginning of the day (mm) and a_{thr} is the threshold water level in the shallow aquifer required for revap to occur (mm) (Neitsch *et al.*, 2011; Abiodun *et al.* (2018).

2.5.2.4 Direct runoff

Direct runoff in SWAT (excluding base flow, as it is defined in Section 2.3.2.4) can be estimated by two options, i.e. the Green and Ampt (1911) or the USDA-SCS curve number method (USDA-SCS, 1972). In this review, the focus will be on the SCS curve number method. The equation used to estimate direct runoff by the SCS curve number method is (USDA-SCS, 1972):

$$Q_{surf} = \frac{(R_{day} - I_a)}{(R_{day} - I_a + S)} \qquad (2.28)$$

where Q_{surf} is the accumulated runoff (mm), R_{day} is the rainfall depth for the day (mm), I_a is the initial abstractions (including surface storage, interception and infiltration prior to runoff (mm)), and S is the retention parameter (mm), which differs spatially, based on the soil, land use, management and slope, and can be estimated by:

$$S = 25.4\left(\frac{1000}{CN} - 10\right) \qquad (2.29)$$

where CN is the curve number for the day. The initial abstraction, I_a, is commonly approximated as $0.2S$, and Equation 2.28 becomes:

$$Q_{surf} = \frac{(R_{day} - 0.2S)^2}{(R_{day} + 0.8S)} \qquad (2.30)$$

The SCS curve number is a function of the soil's permeability, land use and land cover, and the antecedent soil water. Therefore, it depends on the soil's hydrologic group, soil water conditions, and even needs adjustment for different slope classes. For the detailed procedure for determining SCS curve number, refer to USDA-SCS (1972) and Neitsch *et al.* (2011).

2.5.2.5 Deep drainage

The excess water that passes the deeper horizon by percolation, or sometimes bypass-flows through the vadose zone, contributes to shallow or deep aquifer recharge. The time it takes for the recharge water to enter the shallow aquifer depends primarily on the depth of the water table and the hydraulic properties of the vadose and groundwater zones (Neitsch *et al.*, 2011). The recharge amount to both the shallow and deep aquifers can be calculated as:

$$W_{rchrg,i} = \left(1 - \exp\left[-1/\delta_{gw}\right]\right).W_{seep} + \exp\left[-1/\delta_{gw}\right].W_{rchrg,i-1} \qquad (2.31)$$

where $W_{rchrg,i}$ is the amount of recharge entering the aquifer on day i (mm), δ_{gw} is the delay time or drainage time of the overlying geologic formations (days), W_{seep} is the total amount of water exiting the bottom of the soil profile on day i (mm), and $W_{rchrg,i-1}$ is the amount of recharge entering the aquifer on day $i-1$ (mm).

The total amount of water exiting the bottom of the soil profile on day i is calculated as:

$$W_{seep} = W_{perc,ly=n} + W_{crk,,btm} \qquad (2.32)$$

where $W_{perc,ly=n}$ is the amount of water percolating out of the lowest layer, n is the soil profile on day i (mm), and $W_{crk,btm}$ is the amount of water flow going past the lower boundary of the soil profile due to bypass-flow on day i (mm).

2.6 Model calibration and uncertainty analysis

Catchment modelling plays an important part in developing a water management plan and environmental monitoring in arid and semi-arid environments. Due to the high spatial and temporal variability of the hydrologic system, model calibration is a prerequisite, especially for physics-based, as well as distributed and semi-distributed models. Catchments with available observed data, including but not limited to discharge data, rainfall and profile water content, can be modelled with reasonable accuracy. On the other hand, the unavailability or insufficiency of observed data due to the high cost of spatial hydrological data acquisition makes the calibration of physics based models challenging (Bárdossy, 2007; Bekele and Nicklow, 2007).

Calibration is a process of adjusting model parameters in such a way that the differences between observed and simulated values of variables are kept at a minimum. It is one of the key procedures in catchment modelling. Several methods have been proposed to calibrate hydrologic models for ungauged catchments. These include: (1) The regionalization approach where a similar but gauged catchment will be parameterized, and the model parameters transferred to the ungauged catchment (Bárdossy, 2007; Bekele and Nicklow, 2007; Emam *et al.*, 2017). (2) Calibration based on crop yield where the calibration of a crop yield gives confidence on the evapotranspiration and simulates other hydrologic components better (Emam *et al.*, 2015; Emam *et al.*, 2017). (3) Calibration based on data retrieved from remote sensing, where remote sensing enables the acquisition of important spatial data, such as evapotranspiration and soil water content. Hydrologic models can be calibrated using spatial data, such as MODIS products (Jajarmizadeh *et al.*, 2012; Emam *et al.*, 2017).

Generally, two approaches are available for model calibration in the literature, i.e. deterministic and stochastic. Deterministic calibration involves the adjustment of model parameters manually by trial and error until a reasonable match between measured and observed values is obtained. This is an outdated approach, as explained by Abbaspour (2015). The stochastic approach involves the automatic calibration of models by using software such as SWAT-CUP (SWAT Calibration and Uncertainty Programs) (Abbaspour, 2015). SWAT-CUP, developed by Abbaspour *et al.* (2007), is a specialized computer program primarily developed for SWAT calibration and uncertainty analysis. It comprises five algorithms for calibration and uncertainty analysis, i.e. SUFI2 (Sequential Uncertainty Fitting v. 2), PSO (Particle Swarm Optimization), GLUE (Generalized Likelihood Uncertainty Estimation), ParaSol (Parameter Solution), and MCMC (Markov Chain Monte Carlo).

In SUFI2, uncertainty in parameters accounts for all sources of uncertainties such as uncertainties from driving variables, model parameters and measured data (Abbaspour, 2015). The propagation of all these model uncertainties also leads to uncertainties in the model output variables, which are expressed as 95PPUs (95 Percent Predictive Uncertainties), and are usually expressed in ranges calculated at 2.5% and 97.5% levels of the cumulative distribution of an output, using Latin hypercube sampling. In SUFI2, the degree of uncertainty is measured by two factors: the P-factor which is the percentage of observed data enveloped by the modelling result (95PPU), and the R-factor which is the ratio of average width of 95PPU (Abbaspour, 2015; Emam *et al.*, 2017). It is attempted to find the reasonable values of these factors. For example, Abbaspour (2015) has suggested a higher P-factor (towards 100%) and a lower R-factor (towards 0) for the calibration of SWAT. Details of the calibration and uncertainty analysis of SWAT encountered with the SWAT-CUP program can be found in Abbaspour *et al.* (2007), Yang *et al.* (2008) and Abbaspour (2015).

Some of the objective functions that may be applied during model calibration and validation include the root mean squared of errors (RMSE), coefficient of determination (R^2), and Nash-Sutcliff efficiency (NSE). Moreover, some of the model parameters can be found by direct measurement of physical characteristics, whereas others cannot. Parameters that are measured are difficult to use directly due to a difference in the measurement scale (Ajami *et al.*, 2004; Bekele and Nicklow, 2007). Therefore, in ungauged catchments, the literature recommends the transfer of parameters from homogeneous catchments that have sufficient observed data for the calibration and validation process.

2.7 Concluding remarks

In this section, a general review of the literature has been undertaken to assess the catchment scale hydrologic cycles and processes, and their determination with hydrologic models (emphasizing the SWAT model). The review showed that freshwater scarcity is a global problem, and that South Africa is one of the countries where fresh water is a scarce commodity. This is mainly attributable to the insufficiency of precipitation in the country. Therefore, water management is an important task for South Africa to undertake in monitoring the different uses of freshwater.

Hydrologic models are crucial in the assessment of freshwater resources. This is because the hydrologic cycle is a complex process that is influenced by inter-linked environmental factors. In this regard, the soil and water assessment tool (SWAT) is a semi-distributed model that can simulate continuous time impacts of complex environmental factors on fresh water at different scales of study (catchment or river basin scales).

The application of SWAT model requires different types and spatially explicit data where unavailability or insufficiency of the data leads to difficulty or poor performance of the model. These include weather parameters, soil data, land use and land cover, and topographic parameters. Moreover, SWAT requires time series data of stream flow, erosion, and chemical loadings, from point and non-point sources, for the purposes of model calibration, validation, and uncertainty analysis. However, ungauged catchments in arid and semi-arid areas usually lack such time series data. In such instances, the regionalization approach plays a critical role for the assessment of water resources.

2.8 References

Abbaspour, K., Vejdani, M., Haghighat, S. and Yang, J., 2007. SWAT-CUP: calibration and uncertainty programs for SWAT. In *Oxley, L. and Kulasiri, D. (eds) MODSIM 2007 International Congress on Modelling and Simulation*. Modeling and Simulation Society of Australia and New Zealand, December 2007, pp. 1596-1602. ISBN: 978-0-9758400-4-7.

Abbaspour, K.C., 2015. SWAT-CUP 2012: *SWAT calibration and uncertainty programs: a user manual*. Eawag (Swiss Federal Institute of Aquatic Science and Technology). Zurich, Switzerland.

Abiodun, O.O., Guan, H., Post, V.E. and Batelaan, O., 2018. Comparison of MODIS and SWAT evapotranspiration over a complex terrain at different spatial scales. *Hydrology and Earth System Sciences*, 22(5), pp.2775-2794.

Adams, S., Titus, R. and Xu, Y., 2004. *Groundwater recharge assessment of the basement aquifers of central Namaqualand.* South African Water Research Commission. Bellville, South Africa.

Ajami, N., Gupta, H., Wagener, T. and Sorooshian, S., 2004. Calibration of a semi-distributed hydrologic model for streamflow estimation along a river system. *Journal of Hydrology,* 298(1), pp. 112-135.

Allen, R. G., Pereira, L. S., Raes, D. and Smith, M., 1998. *Crop evapotranspiration - guidelines for computing crop water requirements.* FAO Irrigation and drainage paper 56. Rome, Italy.

Anders, A.M., Roe, G.H., Hallet, B., Montgomery, D.R., Finnegan, N.J. and Putkonen, J., 2006. Spatial patterns of precipitation and topography in the Himalaya. *Geological Society of America Special Papers,* Volume 398, pp. 39-53.

Arnold, J., Srinivasan, R., Muttiah, R. and Williams, J., 1998. Large area hydrologic modeling and assessment part I: Model development. *Journal of the American Water Resources Association,* 34(1), pp. 73-89.

Arnold, J.G., Moriasi, D.N., Gassman, P.W., Abbaspour, K.C., White, M.J., Srinivasan, R., Santhi, C., Harmel, R.D., van Griensven, A., Van Liew, M.W. and Kannan, N., 2012. SWAT: model use, calibration, and validation. *Transactions of the ASABE,* 55(4), pp. 1491-1508.

Augustine, D., 2010. Spatial versus temporal variation in precipitation in a semiarid ecosystem. *Landscape Ecology,* 25(6), pp. 913-925.

Babel, L. and Karssenberg, D., 2013. Hydrological models are mediating models. *Hydrology and Earth System Sciences Discussions,* 10(8), pp. 10535-10563.

Babkin, V., 2009. Evaporation from the surface of the globe. In: *Hydrological Cycle Volume II.* Encyclopedia of Life Support Systems (EOLSS), p. 48 Paris, France.

Banimahd, S., Khalili, D., Kamgar-Haghighi, A. and Zand-Parsa, S., 2015. Evapotranspiration model selection for estimation of actual evaporation from bare soil, as required in annual potential groundwater recharge studies of a semi-arid foothill regions. *Archives of Agronomy and Soil Science,* 61(10), pp. 1455-1472.

Bárdossy, A., 2007. Calibration of hydrological model parameters for ungauged catchments. *Hydrology and Earth System Sciences Discussions,* 11(2), pp. 703-710.

Basist, A., Bell, G. and Meentemeyer, V., 1994. Statistical relationships between topography and precipitation patterns. *Journal of Climate,* 7(9), pp. 1305-1315.

Beckers, J., Smerdon, B. and Wilson, M., 2009. *Review of hydrologic models for forest management and climate change applications in British Columbia and Alberta.* Forrex Forum for Research and Extension in Natural Resources, FORREX Series 25th ed. Kamloops, BC, Canada.

Bekele, E. and Nicklow, J., 2007. Multi-objective automatic calibration of SWAT using NSGA-II. *Journal of Hydrology,* 341(3), pp. 165-176.

Bennie, A.T.P. and Hensley, M., 2001. Maximizing precipitation utilization in dryland agriculture in South Africa-a review. *Journal of Hydrology*, 241 (1), 124-139.

Bittelli, M., 2011. Measuring soil water content: a review. *HortTechnology,* 21(3), pp. 293-300.

Brooks, K.N., Ffolliott, P.F. and Magner, J.A., 2013. *Hydrology and the management of catchments*. John Wiley & Sons.

Browner, C.M., 1996. *Catchment approach framework*. US Environmental Protection Agency. Washington, USA.

Bugan, R., Jovanovic, N. and De Clercq, W., 2012. The water balance of a seasonal stream in the semi-arid Western Cape (South Africa). *Water SA,* 38(2), pp. 201-212.

Carpenter, S.R., Stanley, E.H. and Vander Zanden, M.J., 2011. State of the world's freshwater ecosystems: physical, chemical, and biological changes. *Annual Review of Environment and Resources,* 36, pp.75-99.

Cepuder, P., Evett, S., Heng, L. K., Hignett, C., Laurent, J.P. and Ruelle, P., 2008. *Field estimation of soil water content: A practical guide to methods, instrumentation and sensor technology.* International Atomic Energy Agency. Vienna, Austria.

Chow, Y.S., 1988. On the rate of moment convergence of sample sums and extremes. *Bulletin of the Institute of Mathematics*. 16(3), pp.177-201.

Christensen, L., Tague, C.L. and Baron, J.S., 2008. Spatial patterns of simulated transpiration response to climate variability in a snow dominated mountain ecosystem. *Hydrological Processes,* 22(18), pp.3576-3588.

Chung, I., Sophocleous, M., Mitiku, D. and Kim, N., 2016. Estimating groundwater recharge in the humid and semi-arid African regions: review. *Geosciences Journal,* 20(5), pp. 731-744.

Cooper, D.I., Eichinger, W.E., Kao, J., Hipps, L., Reisner, J., Smith, S., Schaeffer, S.M. and Williams, D.G., 2000. Spatial and temporal properties of water vapor and latent energy flux over a riparian canopy. *Agricultural and Forest Meteorology,* 105(1), pp. 161–183.

Council for Scientific and Industrial Research (CSIR), 2010. *A CSIR perspective on water in South Africa-2010.* CSIR Report No. CSIR/NRE/PW/IR/2011/0012/A ISBN: 978-0-7988-5595-2.

Cukur, H., 2011. Daily precipitation variations of selected meteorological stations in Turkey. *Procedia-Social and Behavioral Sciences,* Volume 19, pp. 617-626.

Dallas, H.F. and Rivers-Moore, N., 2014. Ecological consequences of global climate change for freshwater ecosystems in South Africa. *South African Journal of Science*, 110(5-6), pp.01-11.

Daly, C., 2006. Guidelines for assessing the suitability of spatial climate data sets. *International journal of climatology,* 26(6), pp. 707-721.

Daniel, E.B., Camp, J.V., LeBoeuf, E.J., Penrod, J.R., Dobbins, J.P. and Abkowitz, M.D., 2011. Catchment modeling and its applications: a state-of-the-art review. *The Open Hydrology Journal,* 5(1), pp. 26-50.

Department of Water Affairs (DWA), 2013. *Strategic overview of the water sector in South Africa- 2013*. Pretoria, South Africa.

Department of Water Affairs and Forestry (DWAF), 1997. *White paper on a national water policy for South Africa*. Pretoria, South Africa.

Devia, G., Ganasri, B. and Dwarakish, G., 2015. A review on hydrological models. *Aquatic Procedia,* Volume 4, pp. 1001-1007.

Di Bella, C.E., Striker, G.G., Loreti, J., Cosentino, D.J. and Grimoldi, A.A., 2016. Soil water regime of grassland communities along subtle topographic gradient in the Flooding Pampa (Argentina). *Soil & Water Research,* 11(2), pp. 90-96.

Dooge, J.C., 1968. The hydrologic cycle as a closed system. *Hydrological Sciences Journal*, 13(1), pp. 58-68.

Du Plessis, A., 2017. *Freshwater Challenges of South Africa and its Upper Vaal River*. Springer.

Emam, A. R., Kappas, M., Nguyen, L. H. K. and Renchin, T., 2017. Hydrological modeling and runoff mitigation in an ungauged basin of Central Vietnam using SWAT model. *Hydrology,* 4(1), p. 16.

Emam, A.R., Kappas, M., Akhavan, S., Hosseini, S.Z. and Abbaspour, K.C., 2015. Estimation of groundwater recharge and its relation to land degradation: Case study of a semi-arid river basin in Iran. *Environmental Earth Sciences,* Volume 74, p. 6791–6803.

Emanuel, R.E., Epstein, H.E., McGlynn, B.L., Welsch, D.L., Muth, D.J. and D'Odorico, P., 2010. Spatial and temporal controls on catchment ecohydrology in the northern Rocky Mountains. *Water Resources Research,* 46(11), pp. 1-14.

Endale, D., Fisher, D. and Schomberg, H., 2006. Soil water regime in space and time in a small Georgia Piedmont catchment under pasture. *Soil Science Society of America Journal,* 70(1), pp. 1-13.

Everson, C., 2001. The water balance of a first order catchment in the montane grasslands of South Africa. *Journal of Hydrology,* 241(1), pp. 110-123.

eWater Ltd, 2012. *General approaches to modelling and practical issues of model choice: a series on model choice.* eWater Ltd. Accessed on 18/08/2017 on the following url: https://toolkit.ewater.org.au/tools/ModelChoice/MC-1.pdf.

Gassman, P. W., Reyes, M. R., Green, C. H. and Arnold, J. G., 2007. The soil and water assessment tool: historical development, applications, and future research directions. *American Society of Agricultural and Biological Engineers,* 50(4), pp. 1211-1250.

Gassman, P., Arnold, J., Srinivasan, R. and Reyes, M., 2010. The worldwide use of the SWAT model: technological drivers, networking impacts, and simulation trends. *American Society of Agricultural and Biological Engineers*, pp. 21-24.

Gates, J., Steele, G., Nasta, P. and Szilagyi, J., 2014. Lithologic influences on groundwater recharge through incised glacial till from profile to regional scales: evidence from glaciated Eastern Nebraska. *Water Resources Research,* 50(1), pp. 466-481.

Gieske, A.S.M., 1992. Dynamics of groundwater recharge: a case study in semi-arid eastern Botswana (a PhD Thesis). University of Twente, Enschede, Netherlands.

Greencape, 2017. Water: market intelligence report-2017 (Eds: Bronkhorst, S., Pengelly, C. and Seyler, H.). Internet source that is accessed on September 28, 2018 from: https://www.greencape.co.za/assets/Uploads/GreenCape-Water-MIR-2017-electronic-FINAL-v1.pdf.

Green, W.H. and G. Ampt, 1911. Studies of soil physics, part I: the flow of air and water through soils. *Journal of Agriculture Science*, 4, pp. 1-24.

Hatfield, J. and Prueger, J., 2011. Agroecology: implications for plant response to climate change. *In: Yadav, S.S, Redden, R.J., Hatfield, J.L., Lotze-Campen and Hall, A.E., ed. Crop adaptation to climate change.* Wiley-Blackwell, pp. 27-43. West Sussex, UK.

Healy, R., 2010. *Estimating groundwater recharge.* Cambridge, UK: Cambridge University Press.

Healy, R.W. and Cook, P.G., 2002. Using groundwater levels to estimate recharge. *Hydrogeology journal*, 10(1), pp.91-109.

Hébrard, O., Voltz, M., Andrieux, P. and Moussa, R., 2006. Spatio-temporal distribution of soil surface moisture in a heterogeneously farmed mediterranean catchment. *Journal of Hydrology,* 329(1), pp. 110-121.

Hillel, D., 1977. *Computer simulation of soil-water dynamics: a compendium of recent work.* IDRC, Ottawa, Canada.

Hillel, D., 2004. *Introduction to environmental soil physics.* Academic Press, 1st edn. New York, USA.

Jajarmizadeh, M., Harun, S. and Salarpour, M., 2012. A review on theoretical consideration and types of models in hydrology. *Journal of Environmental Science and Technology,* 5(5), p. 249-261.

Jeniffer, K., Su, Z., Woldai, T. and Maathuis, B., 2010. Estimation of spatial-temporal rainfall distribution using remote sensing techniques: a case study of Makanya Catchment, Tanzania. *International Journal of Applied Earth Observation and Geoinformation,* 12, pp. 590-599.

Jiang, H., 2004. *Quantitative precipitation and hydrometeor content estimation in tropical cyclones from remote sensing observations.* University of Utah, Salt Lake City, USA.

Johansson, B. and Chen, D., 2003. The influence of wind and topography on precipitation distribution in Sweden: Statistical analysis and modelling. *International Journal of Climatology,* 23(12), pp. 1523-1535.

Jovanovic, N. and Israel, S., 2012. Critical review of methods for the estimation of actual evapotranspiration in hydrological models. *In: Irmak, D.A., ed. Evapotranspiration – remote sensing and modeling.* InTechOpen, pp. 329-350.

Jovanovic, N., Bugan, R. and Israel, S., 2013. Rainfall, soil water content, and groundwater levels at the Riverlands Nature Reserve (South Africa). *Dataset Papers in Science,* 2013 p. 14.

Jovanovic, N., Mu, Q., Bugan, R. and Zhao, M., 2015. Dynamics of MODIS evapotranspiration in South Africa. *Water SA,* 41(1), pp. 79-90.

Kairu, E., 1991. A review of methods for estimating evapotranspiration. *GeoJournal,* 25(4), pp. 371-376.

Kidd, C. and Huffman, G., 2011. Global precipitation measurement. *Meteorological Applications,* 18(3), pp. 334-353.

Kidd, C., 2001. Satellite rainfall climatology: a review. *International Journal of Climatology,* 21(9), pp. 1041-1066.

Kumar, C., 2003. Estimation of groundwater recharge using soil moisture balance approach. *Journal of Soil and Water Conservation,* 2(1-2), pp. 53-58.

Leavesley, G., Lichty, R., Thoutman, B. and Saindon, L., 1983. *Precipitation-runoff modeling system: User's manual.* US Geological Survey, Washington, DC, USA.

Li, H., Zhang, Y. and Zhou, X., 2015. Predicting surface runoff from catchment to large region. *Advances in Meteorology,* 2015 p. 13.

Li, J. and Heap, A., 2008. *A review of spatial interpolation methods for environmental scientists.* Geoscience Australia, Canberra, Australia.

Liou, Y. and Kar, S., 2014. Evapotranspiration estimation with remote sensing and various surface energy balance algorithms-a review. *Energies,* 7(5), pp. 2821-2849.

Lundin, L.-C., Bergström, S., Eriksson, E. and Seibert, J., 1999. Hydrological models and modelling. *In: Lundin, L., ed. Sustainable water management in the Baltic Sea Basin.* Uppsala, Sweden: The Baltic University Program, pp. 129-140.

Mahanama, S., Koster, R., Reichle, R. and Zubair, L., 2008. The role of soil moisture initialization in subseasonal and seasonal streamflow prediction-a case study in Sri Lanka. *Advances in Water Resources,* 31(10), pp. 1333-1343.

Mdee, O. J., 2015. Spatial distribution of runoff in ungauged catchments in Tanzania. *Water Utility Journal,* 9, pp. 61-70.

Mello, C.R.D., Ávila, L.F., Norton, L.D., Silva, A.M.D., Mello, J.M.D. and Beskow, S., 2011. Spatial distribution of top soil water content in an experimental catchment of Southeast Brazil. Scientia Agricola, 68(3), pp.285-294.

Mitchell, J.K., Banasik, K., Hirschi, M.C., Cooke, R.A.C. and Kalita, P., 2001, January. There is not always surface runoff and sediment transport. In Soil Erosion Research for the 21st Century. Proc. Int. Symp. Eds JC Ascough, DC Flanagan. St. Joseph, MI, USA, ASAE (pp. 676-678).

Mishra, A., 2013. Effect of rain gauge density over the accuracy of rainfall: a case study over Bangalore, India. *SpringerPlus,* 2(1), p. 311.

Mo, X., Liu, S., Lin, Z. and Zhao, W., 2004. Simulating temporal and spatial variation of evapotranspiration over the Lushi basin. *Journal of Hydrology,* 285(1), pp. 125-142.

Mockus, V., 2004. Estimation of direct runoff from storm rainfall (Chapter 10). *In: National Engineering Handbook, Part 630-Hydrology.* USDA Soil Conservation Service, pp. 10.1-10.22 Washington, DC, USA.

Molobela, I.P. and Sinha, P., 2011. Management of water resources in South Africa: a review. *African Journal of Environmental Science and Technology*, 5(12), pp.993-1002.

National Research Council, 1999. *New strategies for America's catchments*. National Academies Press, Washington, D.C., USA.

Neitsch, S.L., Arnold, J.G., Kiniry, J.R. and Williams, J.R., 2011. *Soil and water assessment tool: theoretical documentation, Version 2009.* Texas Water Resources Institute Technical Report No. 406. Texas A&M University, Texas, USA.

New, M., Todd, M., Hulme, M. and Jones, P., 2001. Precipitation measurements and trends in the twentieth century. *International Journal of Climatology,* 21(15), pp. 1889-1922.

Nicholson, S., Kim, J., Ba, M. and Lare, A., 1997. The mean surface water balance over Africa and its interannual variability. *Journal of Climate,* 10(12), pp. 2981-3002.

Ochoa, C.G., Fernald, A.G., Guldan, S.J., Tidwell, V.C. and Shukla, M.K., 2012. Shallow aquifer recharge from irrigation in a semiarid agricultural valley in New Mexico. *Journal of Hydrologic Engineering,* 18(10), pp. 1219-1230.

Parajuli, P. and Ouyang, Y., 2013. Catchment-scale hydrological modeling methods and applications. *In: Bradley, P., ed. Current perspectives in contaminant hydrology and water resources sustainability.* Intech Open Sciences, pp. 57-80.

Pechlivanidis, I., Jackson, B., McIntyre, N. and Wheater, H., 2011. Catchment scale hydrological modelling: a review of model types, calibration approaches and uncertainty analysis methods in the context of recent developments in technology and applications. *Global NEST Journal,* 13(3), pp. 193-214.

Porporato, A., D'odorico, P., Laio, F., Ridolfi, L. and Rodriguez-Iturbe, I., 2002. Ecohydrology of water-controlled ecosystems. *Advances in Water Resources,* 25(8), pp. 1335-1348.

Porter, J.R., Xie, L., Challinor, A.J., Cochrane, K., Howden, S.M., Iqbal, M.M., Lobell, D.B., Travasso, M.I., Field, C.B., Barros, V.R. and Dokken, D.J., 2014. *Climate change 2014: impacts, adaptation, and vulnerability. Part A: global and sectoral aspects*. Contribution of Working Group II to the Fifth Assessment Report of the Intergovernmental Panel on Climate Change. Food security and food production systems, pp.485-533.

Ramakrishnan, D., Bandyopadhyay, A. and Kusuma, K., 2009. SCS-CN and GIS-based approach for identifying potential water harvesting sites in the Kali Catchment, Mahi River Basin, India. *Journal of Earth System Science,* 118(4), pp. 355-368.

Rasheed, H., Al-Anaz, H. and Abid, K., 1989. *Evaporation from soil surface in presence of shallow water tables.* IAHS Publishing, Baltimore, Maryland, USA.

Rejani, R., Rao, K.V., Osman, M., Chary, G.R., Reddy, K.S. and Rao, C.S., 2015. Spatial and temporal estimation of runoff in a semi-arid microcatchment of Southern India. *Environmental Monitoring and Assessment,* 187(8), pp. 1-16.

Risser, D., Gburek, W. and Folmar, G., 2005. *Comparison of methods for estimating ground-water recharge and base flow at a small catchment underlain by fractured bedrock in the eastern United States,* U.S. Geological Survey, Reston, Virginia, USA.

Romano, N., 2014. Soil moisture at local scale: Measurements and simulations. *Journal of Hydrology,* 516, pp. 6-20.

Rose, D., Konukcu, F. and Gowing, J., 2005. Effect of watertable depth on evaporation and salt accumulation from saline groundwater. *Soil Research,* 43(5), pp. 565-573.

Rosenblueth, A. and Wiener, N., 1945. The role of models in science. *Philosophy of Science,* 12(4), pp. 316-321.

Sene, K., 2013. *Flash floods: forecasting and warning.* Springer Science & Business Media, 1st edn. Dordrecht, The Netherlands.

Sheng, T.C., 1990. *Catchment management field manual*: catchment *survey and planning.* FAO conservation guide, 13(6), Rome, Italy.

Shiklomanov, I.A., 2009. *Hydrological cycle-vol. I-the hydrological cycle.* Encyclopaedia of Life Support Systems (EOLSS), p. 348.

Sibanda, T., Nonner, J. and Uhlenbrook, S., 2009. Comparison of groundwater recharge estimation methods for the semi-arid Nyamandhlovu area, Zimbabwe. *Hydrogeology Journal,* 17(6), pp. 1427-1441.

Singh, V., 1988. *Hydrologic systems. v. 1. rainfall-runoff modeling.* Prentice Hall, Inc. New Jersey, USA.

Sokolowski, J. and Banks, C., 2010. *Modeling and simulation fundamentals: theoretical underpinnings and practical domains.* John Wiley and Sons, Hoboken, New Jersey, USA.

Sokolowski, J. and Banks, C., 2011. *Principles of modeling and simulation: a multidisciplinary approach.* John Wiley and Sons, Hoboken, New Jersey, USA.

Sunardi, S. and Wiegleb, G., 2016. Climate-induced hydrological changes and the ecology of tropical freshwater biota. *Biodiversitas-Journal of Biological Diversity*, 17(1).

Tarboton, D., 2003. *Rainfall-runoff processes.* Utah State University, Logan, Utah, USA.

Tessema, S., 2011. *Hydrological modeling as a tool for sustainable water resources management: a case study of the Awash River Basin (Doctoral dissertation),* KTH Royal Institute of Technology, Stockholm, Sweden.

Türkeş, M., 1996. Spatial and temporal analysis of annual rainfall variations in Turkey. *International Journal of Climatology,* 16(9), pp. 1057-1076.

United Nations Environment Program (UNEP), 2002. *World summit on sustainable development: Country Profiles Series-South Africa*. Johannesburg, South Africa.

Upreti, H., Ojha, C.S.P. and Hari Prasad, K.S., 2015. Estimation of deep percolation in sandy-loam soil using water-balance approach. *Irrigation and Drainage Systems Engineering*, 4(S1), p.002.

United States Department of Agriculture-Soil Conservation Service (USDA-SCS), 1972. *National Engineering Handbook, Section 4: Hydrology*. Washington, DC, USA.

Van Griensven, A., Ndomba, P., Yalew, S. and Kilonzo, F., 2012. Critical review of SWAT applications in the upper Nile basin countries. *Hydrology and Earth System Sciences,* 16(9), pp. 3371-3381.

Van Huyssteen, C., Zere, T. and Hensley, M., 2009[a]. Soil water variability in the Weatherley Grassland Catchment, South Africa: I. evapotranspiration. *South African Journal of Plant and Soil,* 26(3), pp. 170-178.

Van Huyssteen, C., Zere, T. and Hensley, M., 2009[b]. Soil water variability in the Weatherley Grassland Catchment, South Africa: II. Soil water content. *South African Journal of Plant and Soil,* 26(3), pp. 179-185.

Vinogradov, Y., 2009. Surface water runoff. *In: Hydrological cycle.* Encyclopedia of Life Support Systems (EOLSS), p. 35.

Wagener, T., Wheater, H. and Gupta, H., 2004. *Rainfall-runoff modelling in gauged and ungauged catchments.* 1st edn. Imperial College Press, London, UK.

Wang, K. and Dickinson, R., 2012. A review of global terrestrial evapotranspiration: Observation, modeling, climatology and climatic variability. *Reviews of Geophysics,* 50(2).

Wang, L., Dochartaigh, B.O. and Macdonald, D., 2010. *A literature review of recharge estimation and groundwater resource assessment in Africa.* British Geological Survey, Groundwater Resources Programme, Nottingham, UK.

Wani, S.P., Pathak, P. and Rego, T.J. (eds.), 2002. *A training manual on integrated management of catchments.* International Crops Research Institute for the Semi-Arid Tropics, p. 44. Patancheru, 502 324, Andhra, Pradesh, India.

Wenzhi, Z. and Xibin, J., 2016. Spatio-temporal variation in transpiration responses of maize plants to vapour pressure deficit under an arid climatic condition. *Journal of Arid Land*, 8(3), pp.409-421.

Western, A.W., Zhou, S.L., Grayson, R.B., McMahon, T.A., Blöschl, G. and Wilson, D.J., 2004. Spatial correlation of soil moisture in small catchments and its relationship to dominant spatial hydrological processes. *Journal of Hydrology,* 286(1), pp. 113-134.

Williams, C., McNamara, J. and Chandler, D., 2009. Controls on the temporal and spatial variability of soil moisture in a mountainous landscape: the signature of snow and complex terrain. *Hydrology and Earth System Sciences,* 13(7), pp. 1325-1336.

World Wide Fund for Nature-South Africa, 2016. Water: Facts and Futures, 2016 Report.

Xu, C.Y., 2002. *Hydrologic models.* Uppsala University, Department of Earth Science. Uppsala, Sweden.

Yang, J., Reichert, P., Abbaspour, K.C., Xia, J. and Yang, H., 2008. Comparing uncertainty analysis techniques for a SWAT application to the Chaohe Basin in China. *Journal of Hydrology,* 358(1), pp. 1-23.

Yao, X., Fu, B., Lü, Y., Sun, F., Wang, S. and Liu, M., 2013. Comparison of four spatial interpolation methods for estimating soil moisture in a complex terrain catchment. *PloS one,* 8(1), p. e54660.

Zelelew, M., 2012. *Improving runoff estimation at ungauged catchments (Doctoral Dissertation),* Norwegian University of Science and Technology. Trondheim, Norway.

Zhang, X. and Srinivasan, R., 2010. GIS-based spatial precipitation estimation using next generation radar and raingauge data. *Environmental Modelling and Software,* 25(12), pp. 1781-1788.

Zhao, C., Peng, S. and Feng, Z., 2011. Spatial Modelling of the Variability of the Soil Moisture Regime at the landscape scale in the Southern Qilian Mountains, China. *Journal of Ecosystem and Ecography,* 1(1), pp. 102-110.

Zhao, L., Xia, J., Xu, C.Y., Wang, Z., Sobkowiak, L. and Long, C., 2013. Evapotranspiration estimation methods in hydrological models. *Journal of Geographical Sciences,* 23(2), pp. 359-369.

Zhao, W., Li, A. and Deng, W., 2014. *Spatial and temporal variation of evapotranspiration estimated by MODIS data over South Asia.* Institute of Electrical and Electronics Engineers (IEEE), pp. 3049-3052. Quebec City, Canada.

Zhuwakinyu, 2012. Water 2012: *A review of South Africa's water sector*. Creamer Media (Pty) Ltd, Johannesburg, South Africa.

CHAPTER 3
SWAT MODEL SETUP, CALIBRATION, UNCERTAINTY AND VALIDATION USING THE REGIONALIZATION APPROACH

3.1 Introduction

Most hydrological systems incorporate extremely complex processes and are not easily understood (Xu, 2002). It is also impractical to measure every data about hydrologic systems and processes due to various reasons. This could be due to higher spatial and temporal heterogeneity of the systems, limitations in measurement methods and to the fact that measurement methods are usually laborious, time taking and costly to implement. Therefore, hydrological models enable users to manipulate the system's variables/parameters easily and help in understanding the interaction between variables that make up complex systems (Sokolowski and Banks, 2010; Sokolowski and Banks, 2011). Hydrological models also enable the users to extrapolate both spatial and temporal information on the area of interest (Pechlivanidis et al., 2011). It is assumed that hydrological models are simplified systems that represent the real hydrologic processes (Lundin et al., 1999; Tessema, 2011). Hence, Babel and Karssenberg (2013) described hydrologic models are mediators between theory and practice or the real world. Therefore, hydrologic models are important tools in the study of hydrologic processes at catchment, regional and global scales.

Even though it is an essential task, hydrologic modelling is challenging in arid and semi-arid environments because most catchments in this environments are ungauged. It is obvious that the calibration and validation processes are integral part of catchment hydrologic modelling due to the higher spatial and temporal variability of the hydrologic system. This is particularly important for physics-based models. Catchments with available observed data, including but not limited to discharge data, evapotranspiration, profile water content, can be modelled with reasonable accuracies. On the other hand, the unavailability or the presence of limited observed data due to the high cost of spatial hydrological data acquisition makes the use of physics-based models challenging (Ajami et al., 2004; Bekele and Nicklow, 2007; Bárdossy, 2007). Moreover, hydrological modelling in arid and semi-arid catchments is challenging due to the distinctive feature of the hydro-climatological variables in those regions (Pilgrim et al., 1988; Kan et al., 2017). Reports (e.g., Wheater, 2005; Li et al., 2015) indicate that most models are also developed for humid and sub-humid areas where their performance in arid/semi-arid areas vary considerably.

The Soil and Water Assessment Tool (SWAT) is a continuous-time, semi-distributed and processed-based model developed and supported by the USDA Agricultural Research Service (Neitsch et al., 2011; Arnold et al., 2012). The model was originally developed to evaluate the impact of land management practices on water resources, sediment and agricultural chemical yields in large complex catchments with varying soils, land use and management conditions (Neitsch et al., 2011; Daniel et al., 2011). Water balance is the major driving force behind any process in SWAT. Hence, besides the different components of water balance, SWAT is being used to model plant growth and the movement of sediments, nutrients, pesticides and pathogens in a catchment (Neitsch et al., 2011; Arnold et al., 2012; Parajuli & Ouyang, 2013). The model requires several input data to simulate catchment hydrologic processes, and these include a digital elevation model (DEM), land use–land cover data, soil types, and different daily weather data, including details of precipitation, maximum and minimum air temperatures, solar radiation, wind speed, and relative humidity. SWAT has received international acceptance as a robust interdisciplinary catchment-scale modelling tool. However, its application in arid and semi-arid areas is still challenging due to the unavailability of flow data for model calibration and validation procedures.

Even though the calibration of hydrologic models is challenging for data scarce catchments, some methods have been proposed in literature. These include: (i) the regionalization approach, in which a similar, but gauged, catchment will be parametrized and calibrated. The model parameters will then be transferred to the ungauged catchment. It is one of the most widely used method in the prediction of hydrologic variables in ungauged basins (Merz and Blo¨schl, 2004; Bárdossy, 2007; Bekele and Nicklow, 2007; Reichl et al., 2009; Gitau and Chaubey, 2010; Farsadnia et al., 2014; Swain and Patra, 2017; Emam et al., 2017). (ii) Calibration based on crop yield: this gives confidence on the evapotranspiration and simulates other hydrologic components better. Many researchers (e.g., Nair et al., 2011; Emam et al., 2015; Sinnathamby et al., 2017; Emam et al., 2017) used this method of calibration (calibration based on crop yield). (iii) Calibration based on data retrieved from remote sensing: this method enables the acquisition of important spatio-temporal data like the soil water content and evapotranspiration. Hydrologic models could be calibrated using such data, like the Moderate Resolution Imaging Spectro-radiometer (MODIS) and other satellite products (Jajarmizadeh et al., 2012, Zhang et al., 2017; Tobin and Bennett, 2017; Emam et al., 2017; Rajib et al., 2018; Odusanya et al., 2019).

The first and widely implemented method (regionalization approach) has many types. Generally, this approach could be further classified by three. These are regionalization by spatial proximity, physical similarity and regression methods. In the spatial proximity approach, it is usually assumed that neighbouring catchments have homogenous physical and climatic characteristics and hence, have similar hydrological responses (Blöschl et al., 2013; Emam et al., 2017). As a result of this, calibrated parameters could be transferred from gauged to ungauged neighbouring catchments. Calibration with regression methods consist of developing some empirical relationships between catchment descriptors (both physical and climatic) and model parameter values calibrated on gauged catchments (Bastola et al., 2008; Emam et al., 2017). Once these relationships have been established, one determines the parameters of an ungagged basin using its physical and climatic attributes. The regionalization with physical similarity is based on the similarity between an ungagged catchment and one or more gauged donor catchments (Blöschl et al., 2013; Emam et al., 2017).

Focussing on the regionalization by physical similarity approach, catchments are evaluated and grouped based on their similarity in selected physical variables (physiography, geology and soils, climate and potential natural vegetation). In this approach, catchments categorized under similar regions or groups are assumed to have a similar hydrologic response. Hence, during catchment modelling, parameters could be transferred from a gauged and calibrated catchment to ungauged catchments. The regionalization approach has enabled researchers to exploit the potentials of hydrologic models in data scarce catchments. However, it is also believed that the procedure is exposed to higher uncertainty of model outputs since the calibration and validation processes are usually conducted outside the target catchment. Therefore, the aim of this paper was to calibrate and validate SWAT model in an arid and ungauged catchment by the regionalization with physical similarity approach for further analysis of the components of the catchment water balance that is continued in the next consecutive chapters. Some best practices valuable to minimise model uncertainty in SWAT modelling were also suggested.

3.2 Materials and methods

3.2.1 The study area

3.2.1.1 Location of the study area

The study area is located in the Northern Cape Province of South Africa. It is a catchment that includes Kolomela Mine, with a geographic location of between 22°11’00” and 23°28”00” E longitudes and between 28°03’00” and 29°06’00” S latitudes. The catchment is a combination of two quaternary catchments (D73A and D73B), according to the referencing system of the South African Department of Water and Sanitation Affairs. The location and some hydrologic features of the study catchment (Soutloop Catchment) are depicted in Figure 3.1.

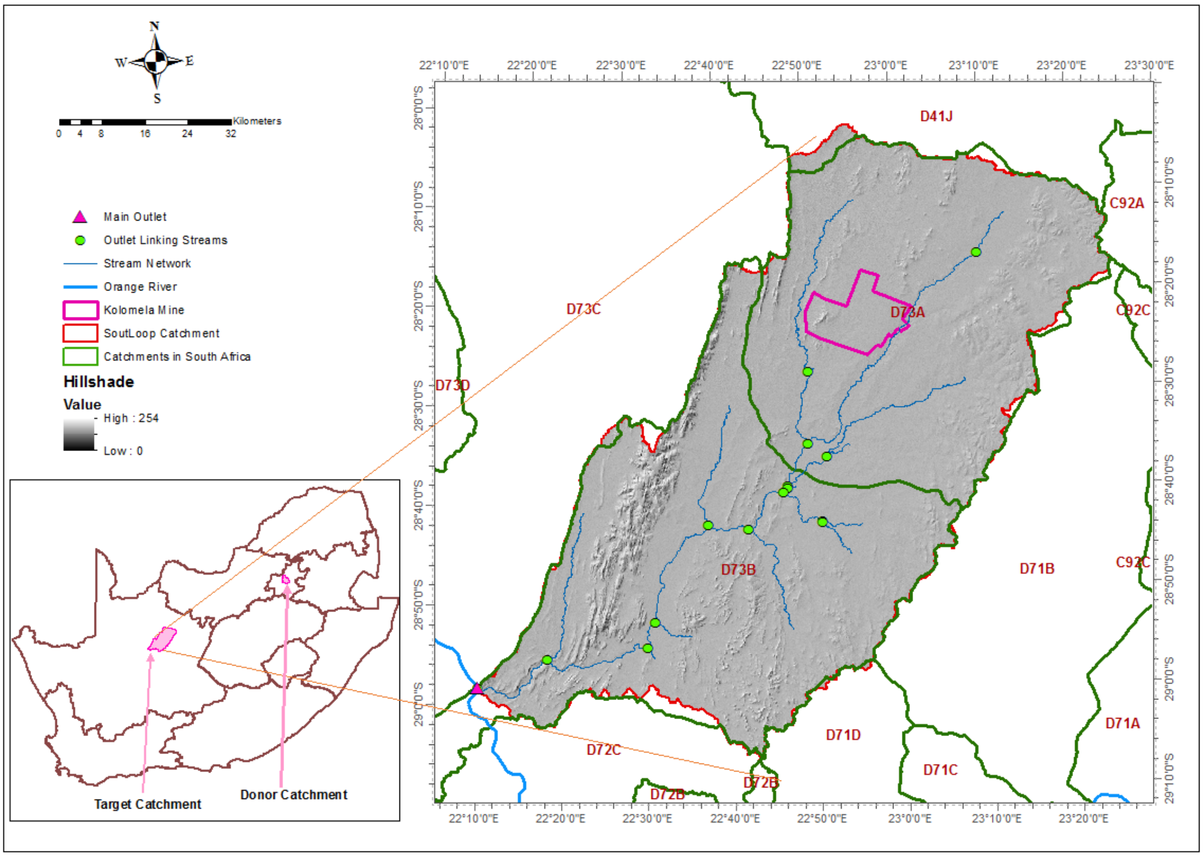

Figure 3.1: Location of the donor catchment (A21C Quaternary Catchment) study area (Soutloop Catchment, about 6770 km^2) with its important hydrologic features.

3.2.1.2 Description of the study area

The total area of the study catchment is 6769.7 km^2, with an altitudinal range from 871 up to 1687 masl. Nearly 68% of the catchment has a slope of less than 5%, while the remaining 32% of the area is above a 5% slope. Figure 3.2 depicts the spatial distributions of the slope classes in the catchment. The soil type in the area is dominated by Oxidic soils (59%, which includes Hutton and Clovelly soil forms), followed by Lithic origins (21%, including Mispah and rock surfaces). Other soil groups include Calcic (12%, which includes Coega soil form), Duplex soils (6% – Valsrivier soil form), Gleyic groups (1.6% – Katspruit and Kroonstad) and a very small amount of Cumulic soil groups (Dundee and Fernwood). The spatial distribution of the soil groups is shown in Figure 3.3. According to the South African LULC classification of

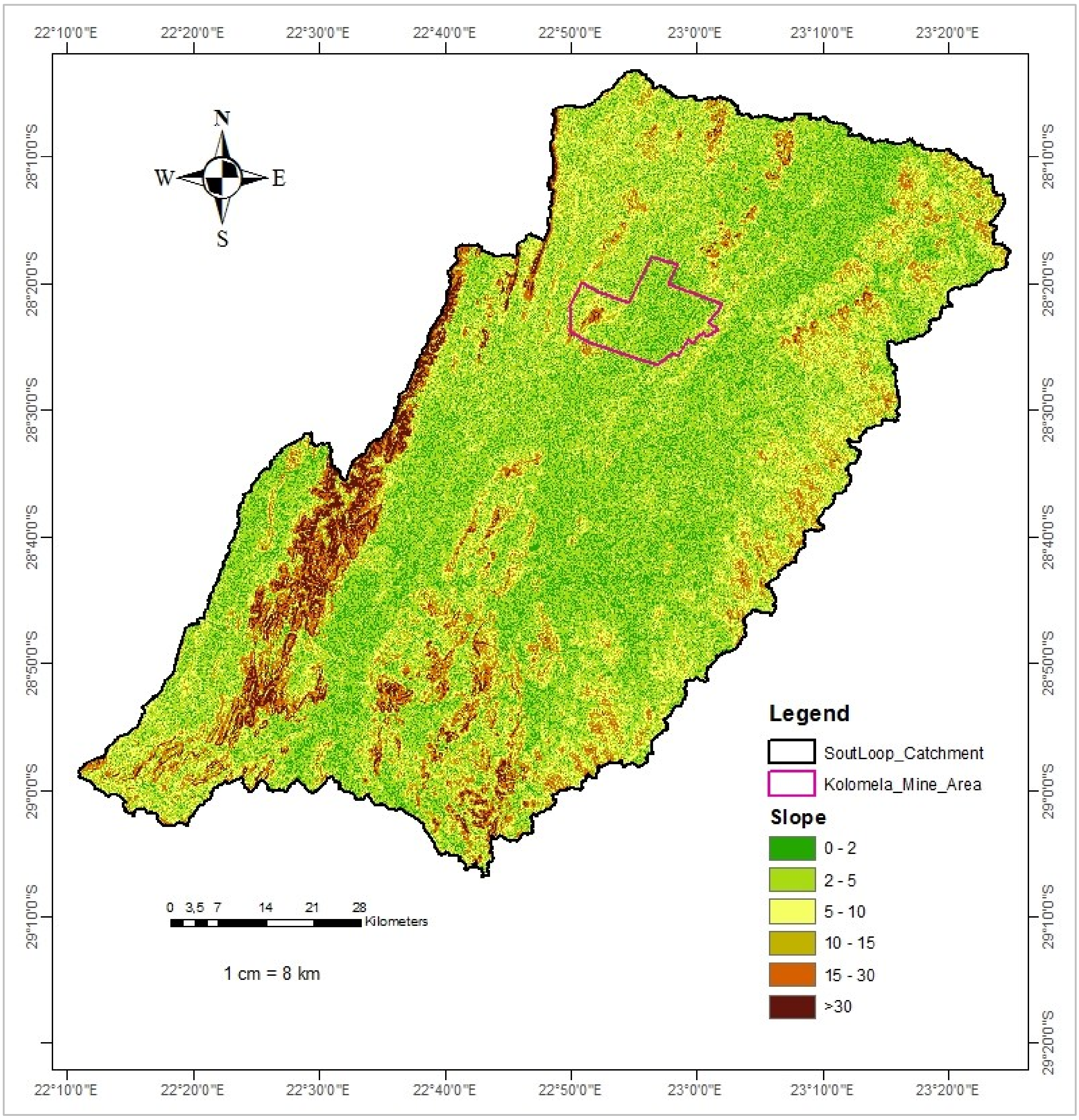

Figure 3.2: The spatial variation of the slope classes in the catchment.

2013/2014 (GEOTERRAIMAGE, 2015), land cover within the catchment is dominated by low shrublands (80%), which is classified as range-brush in the SWAT database, followed by grassland (11%, range grass in SWAT), and bushland (7%, classified as forest-mixed), while the remaining 2% of the study area is covered with other land cover classes. Figure 3.4 shows the spatial variations of LULC classes in the study catchment. The area is also known for its arid climate. Hence, mean annual precipitation varies from 214 to 365mm whereas the mean annual air temperature varies from 17.7ºC to 19.7ºC spatially in the study catchment.

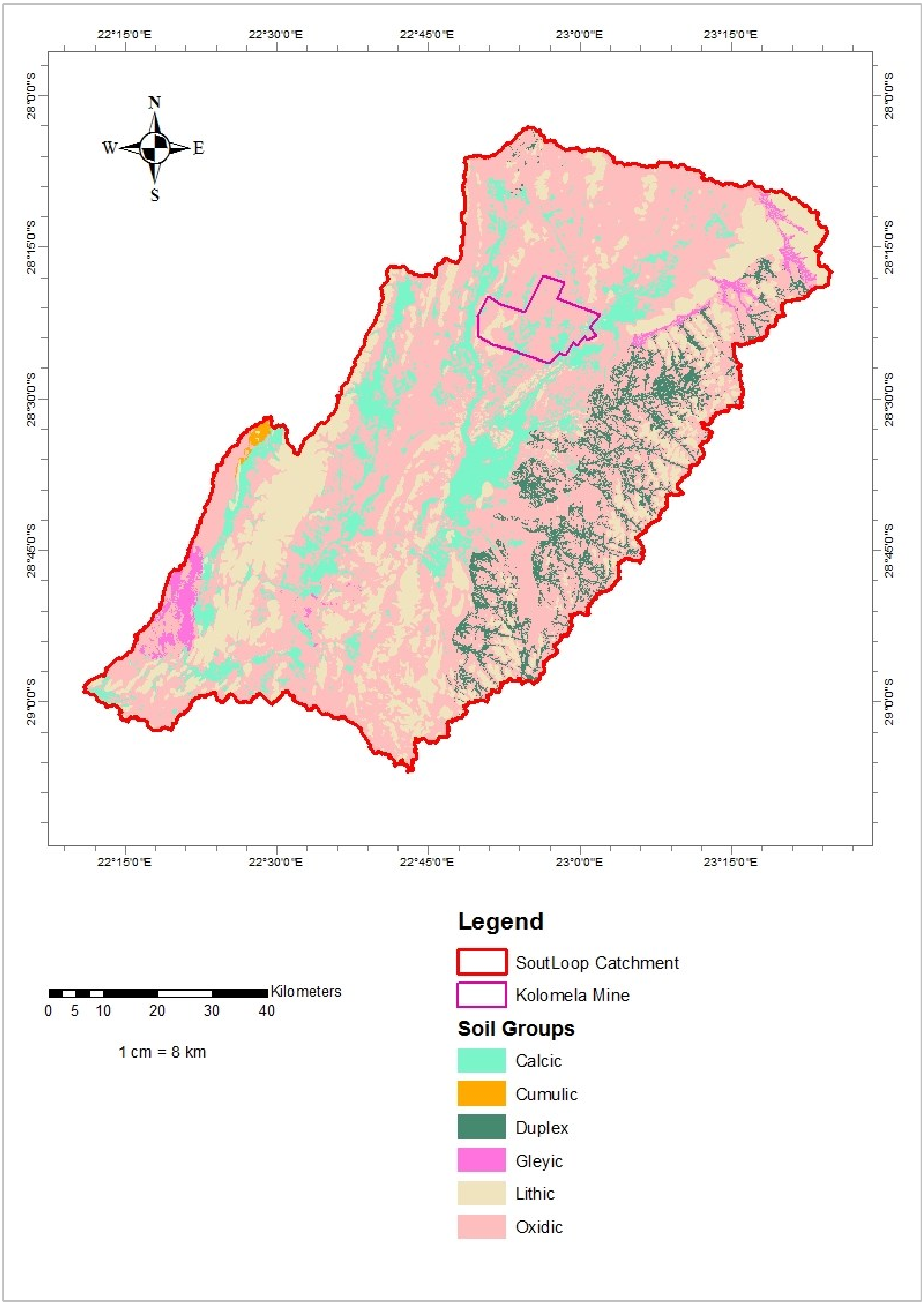

Figure 3.3: Major soil groups in the study catchment.

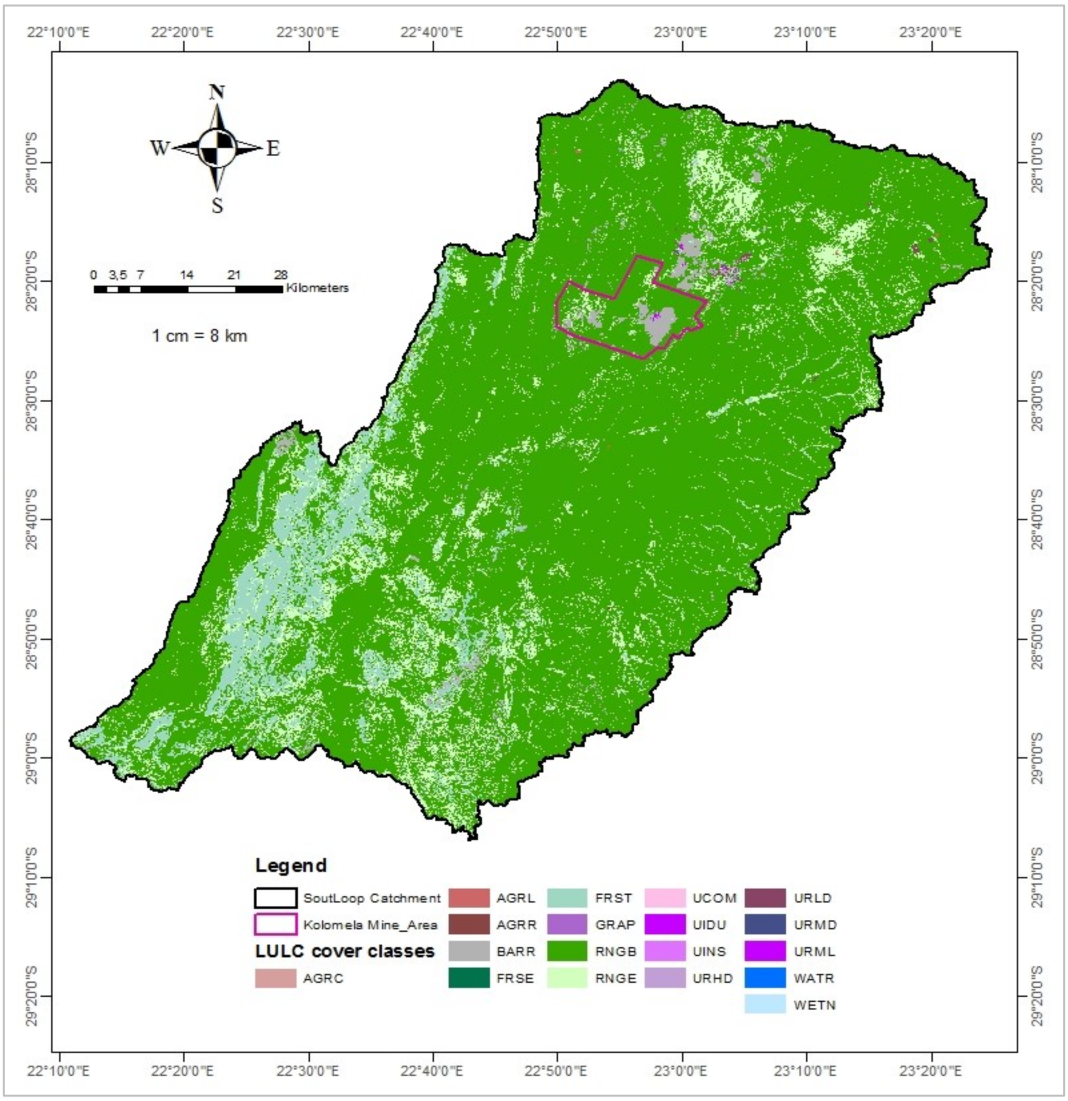

Figure 3.4: The spatial variation of LULC classes in the catchment.

3.2.2 SWAT model inputs

Other than the topographic, soil and LULC data, SWAT requires spatially explicit datasets of climatic data at daily/sub-daily time steps. Major input data for SWAT include DEM, LULC, soil properties, and daily weather data (precipitation, maximum and minimum air temperature, relative humidity, wind speed and solar radiation).

3.2.2.1 Digital Elevation Model (DEM)

Digital elevation model is an important data, since all the topographic attributes of the catchment, sub-catchment up to the HRUs level are derived from this dataset. Some of the attributes include area, slope, slope length, channel length, channel slope, channel width, and channel depth. For this study, a 30-metre spatial resolution SRTM (Shuttle Radar Topography

Mission) DEM was downloaded from the USGS website (link: https://lpdaac.usgs.gov/data_access/data_pool) and was used as an input dataset.

3.2.2.2 Land use/land cover data

Details of LULC comprise one of the most determinant datasets required in hydrologic models, like SWAT, when creating the HRUs. For this study, the national LULC layer of South Africa for the 2013/2014 year, with a 30-metre spatial resolution (GEOTERRAIMAGE, 2015), was used. It was also modified slightly so that it would be consistent with the plant databases of SWAT.

3.2.2.3 Soil type and characteristics

Soil is another data that have major influence in catchment hydrology. In this study, the different soil classes were defined based on the Land Type Survey database compiled by the Agricultural Research Institute of South Africa (ARC), Institute of Soil, Climate and Water (Land Type Survey Staff, 1972). The Land Type Survey data of South Africa do not consist of soil types only. Rather, it is a combined spatial data that consists of mainly terrain, climate and

Table 3.1: Keys to the classification of dominant soil forms into soil groups

No	Dominant soil forms	Soil group	Major characteristics	Diagnostic horizon/material for classification
1	Coega	Calcic	Presence of carbonate or gypsum enrichment in arid climate	Soft or hardpan carbonate or gypsic B
2	Dundee and Fernwood	Cumulic	Incipient soil formation in colluvial, alluvial or aeolian sediment	Neocutanic or neocarbonate B, regic sand, thick E horizon or stratified alluvium
3	Valsrivier	Duplex	Marked textural contrast through clay enrichment	Pedocutanic or prismacutanic B
4	Katspruit and Kroonstad	Gleyic	Protracted reduction in an aquic subsoil or wetland	G horizon
5	Rocky surfaces and Mispah	Lithic	Incipient soil formation on weathering rock or saprolite	Lithocutanic B or hard rock
6	Hutton and Clovelly	Oxidic	Residual iron enrichment through weathering; uniform colour	Red apedal, yellow-brown apedal or red structured B

(Source: Fey, 2010)

soil distribution patterns. This Land Type data was also produced at courser scale (1:250,000 scale). Therefore, there was a need to get the actual data of soil types and increase the scale of the data. As a result of this, the soil units were disaggregated from the Land Type Survey data by the use of satellite data (e.g., DEM, Satellite Imagery), software programs (ArcGIS, SoLIMthe Soil-Land Inference Model (Zhu 1997), 3dMapper), field inspections, and expert knowledge. The details of this procedure is explained in detail in Van Zijl *et al.* (2013).

Finally, ten soil forms were identified in the study catchment. Then, the soil forms were grouped into six soil groups and mapped for the area, based on the criteria of Fey (2010), as shown in Table 3.1. The spatial variations of the major soil groups of the catchment are also depicted in Figure 3.3.

The values of all the soil characteristics required by SWAT were collected by field survey using the soil groups as a base map. As a result, a profile was opened for each soil groups for soil sampling for laboratory and field analysis and also for field verification of the soil groups.

3.2.2.4 Climatic data

The SWAT2012 model requires daily variables of precipitation, temperature, relative humidity, solar energy, and wind speed. The SWAT software also has a weather generator tool that assists us to fill in missing data for certain periods of time in the simulation periods. This tool also enables us to generate the relative humidity, solar energy and wind speed, if we can provide it with a long-term daily precipitation rate and maximum and minimum temperatures. This study relies on meteorological stations inside, and in close proximity to, the study catchment, as seen in Figure 3.5 and Table 3.2. The long-term data details were provided by two organizations – the South African Weather Service (SAWS) and the Agricultural Research Centre, Institute for Soil, Climate and Water.

Table 3.2: Meteorological stations used for the generation of weather parameters in the study catchment

No.	Station Name	Longitude	Latitude	Elevation	Owner organization
1	Olifantshoek	-27.950	22.733	1341	ARC_ISCW and SAWS
2	Onder-Ongeluk	-28.683	23.033	1311	ARC_ISCW
3	Roodemanskloof	-28.583	22.600	1204	ARC_ISCW
4	VaalWater	-28.733	22.800	1109	ARC_ISCW
5	Marydale	-29.324	22.246	928	ARC_ISCW
6	Saalskop	-28.760	21.847	861	ARC_ISCW
7	Postmasburg	-28.345	23.079	1321	SAWS
8	Woolharkop	-28.400	22.859	1221	ARC_ISCW and SAWS
9	Aucampsrus	-28.275	22.962	1293	ARC_ISCW and SAWS

ARC_ISCW refers to the Agricultural Research Commission, Institute for Soil, Climate and Water
SAWS refers to the South African Weather Service

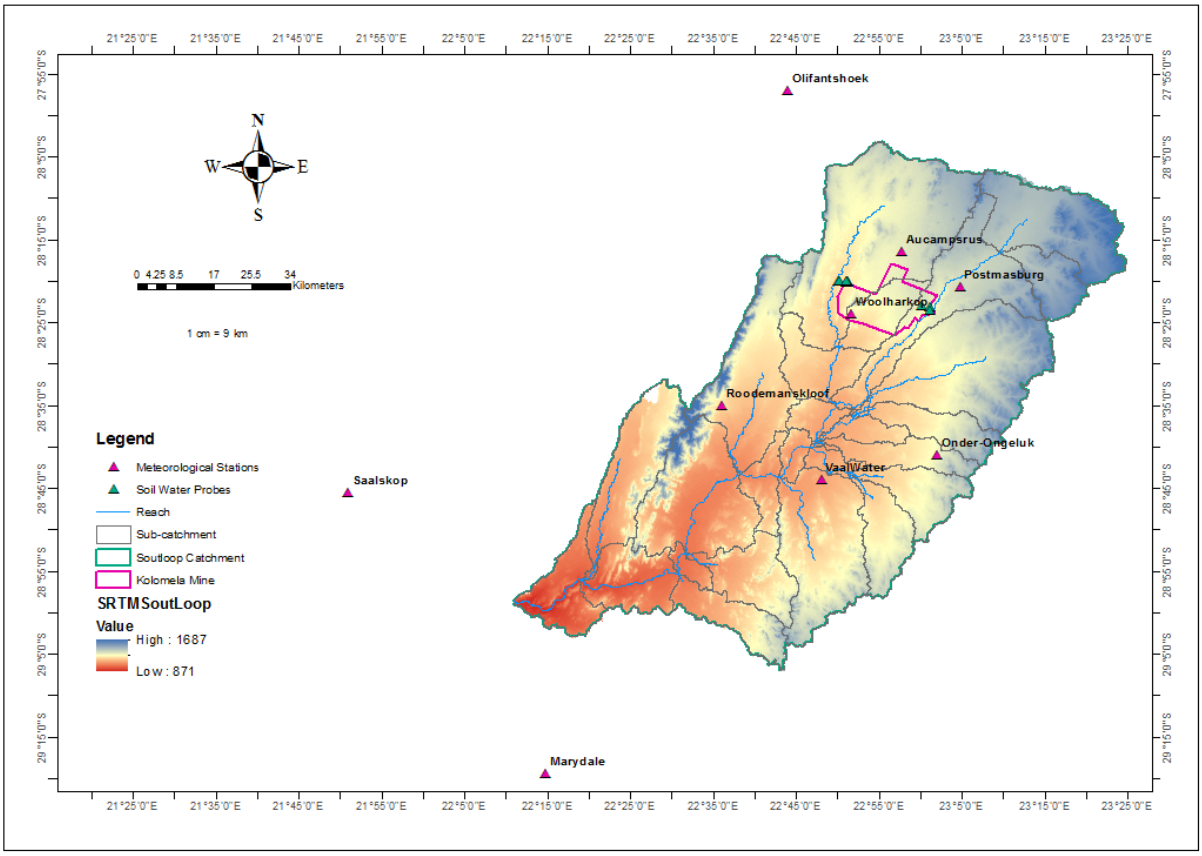

Figure 3.5: Some hydrologic features in the study catchment.

3.2.2.5 Other data for model calibration and validation

For this study, two datasets were collected for calibration and validation purposes. These are the daily runoff (from the donor catchment, A21C quaternary catchment) and daily soil water content from the target catchment (Soutloop River Catchment). As a result, daily discharge data for the donor catchment were obtained from the Department of Water and Sanitation Affairs of South Africa. Whereas the profile water content was measured *in situ* from the target catchment with DFM capacitance probes (installed in four HRUs). The details for DFM capacitance probes can be referred from Zerizghy *et al.* (2013) and from the official website of DFM Technologies at: https://dfmtechnologies.co.za/product/probes.

3.2.3 Model setup and configuration

In this study, SWAT model was used to estimate all the components of the water balance in the study catchment. In the simulation procedure, catchment delineation was the first procedure. The study catchment was delineated using GIS interface of the Soil and Water Assessment Tool (SWAT2012). An SRTM DEM (digital elevation modelling), with 30-metre spatial resolution, was downloaded from LP DAAC (being one of USGS's data distribution centres, at link https://lpdaac.usgs.gov/data_access/data_pool) and was used for this study. The details of the procedures can be referred to Neitsch *et al.* (2011) and Arnold *et al.* (2012).

After the catchment delineation process was completed, the definition of HRUs was continued. The definition of HRUs are also done in the SWAT2012 interface. Three spatial data sets (slope, LULC, and soil maps) are important for the definition of HRUs. Therefore, HRUs are lands with similar topography, LULC and soil types and all the components of the soil water balance could be determined on an HRU basis, with the assumption that similar HRUs would have similar hydrologic characteristics (Neitsch *et al.*, 2011; Arnold *et al.*, 2012; Winchell *et al.*, 2013).

Then, all the required climatic variables were fed to the model, comprising rainfall, minimum and maximum temperature, relative humidity, average wind speed, and solar radiation data. The weather generator tool in the ArcSWAT interface was assigned to fill in the case of unavailability of station data. This tool also enables us to generate the relative humidity, solar energy and wind speed from a long-term daily precipitation and maximum and minimum temperature (Neitsch *et al.*, 2011). The rainfall runoff process was set to be estimated by the curve number (CN-method), the potential evapo-transpiration was estimated by the Penman-Monteith equation, and the channel water routing was simulated by the Variable Storage Routing. After all the above processes were completed, the SWAT simulation was activated. During simulation, a three-year warming-up period was given. Including the three-year warming-up period, the total simulation period (including the warmup periods) was set to run from 1977 to 2018 (i.e. 42 years). Hence, a 39-year period of hydrologic variables were simulated for the study catchment (excluding the warmup periods). The framework, showing major procedures in the simulation process, is summarized in Figure 3.6.

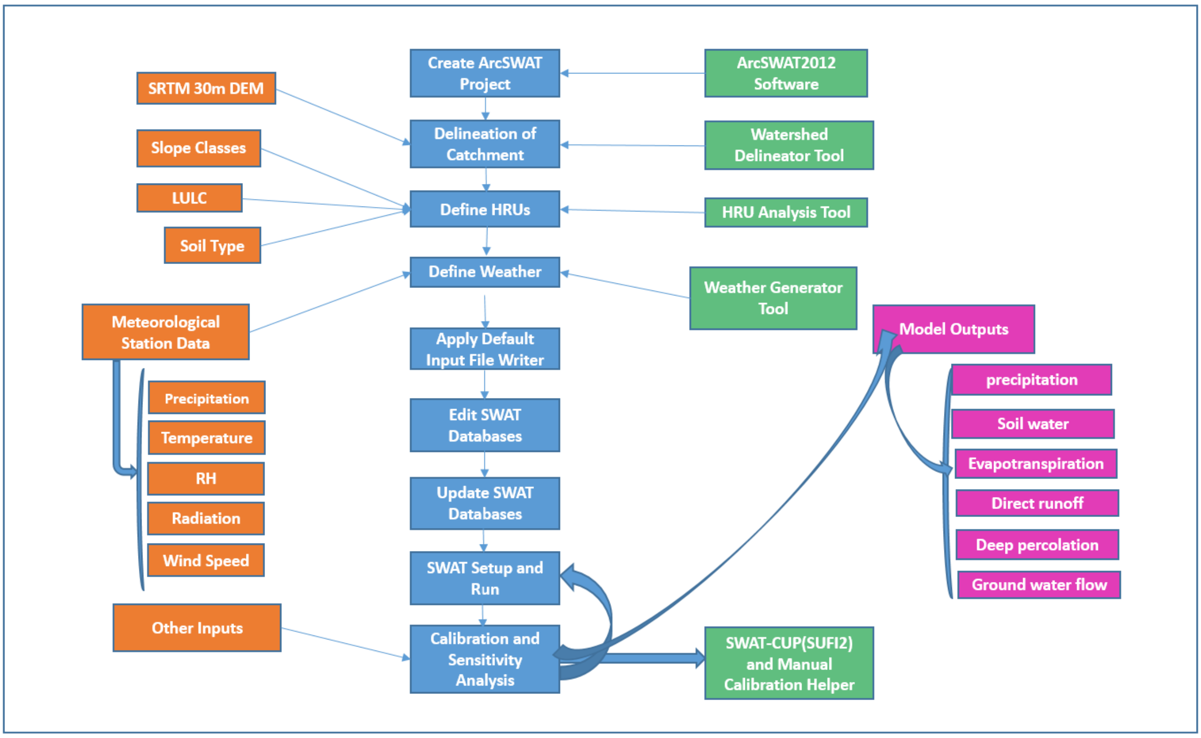

Figure 3.6: General framework followed in the modelling process using SWAT2012.

3.2.4 Model calibration, validation and sensitivity analysis

3.2.4.1 The calibration approach

The successful application of hydrologic models is highly dependent on the calibration and sensitivity analysis of the parameters (Abbaspour, 2015; Kouchi *et al.*, 2017). The calibration and validation processes are only employed efficiently with observed data. Particularly discharge data plays a critical role for this procedure. However, the study area does not have a gauging station for stream flow measurement. Therefore, the regionalization with physical similarity approach (Bárdossy, 2007; Wheater *et al.*, 2008; Blöschl *et al.*, 2013) was adopted here for the calibration and validation of the model. The regionalization approach is usually based on the assumption that catchments with similar physiographic and climatic attributes would have similar hydrologic responses. As a result, the selection of a catchment that has similar attributes to the catchment of interest and that has a fully functional gauging station is a prerequisite. Therefore, there is a need to characterize, evaluate and categorize catchments for this purpose.

Table 3.3: Catchment descriptors used for the evaluation of the similarity between the donor and study catchments.

No.	Catchment descriptors	Donor catchment	Study catchment
1	Annual precipitation (mm)	320-497	214-365
2	Annual PET (mm)	1722-2644	1512.06-2802.07
3	Ratio of Precipitation to PET	0.19	0.13-0.14
4	Ratio of ET to PET	0.15-0.70	0.08-0.70
5	Soil textural class variation	Sandy-loam to Sandy-clay-loam	Clay-Loam to Sandy-loam
6	Dominant LULC	Grasslands, residential with dense trees/bush and mixed forest	Low shrub lands, Grasslands and open bushlands
7	Slope class (percentage)	80% of the catchment is <10%	86% of the catchment is <10%
8	Altitudinal range (masl)	1242-1825	871-1687
9	Runoff coefficients	0-0.12	0-0.1
10	Annual ET (mm)	252-1851	118-1961
11	Annual air temp (ºC)	17-18.7	17.7-19.7
12	Mean solar radiation (MJ m^{-2})	22.6-21.7	21.2-23.1

PET - potential evapotranspiration *ET - evapotranspiration*
LULC - land use and land cover *masl - meter above sea level*

The evaluation and categorization of catchments is based on at least four types of information, i.e. soil type, land use, topographic features, and potential natural vegetation (Omernik, 1987; Blöschl *et al.*, 2013). For this study, however, the eco-regional typing and river classification study conducted by the Department of Water Affairs and Forestry (Kleynhans *et al.*, 2005; Kleynhans *et al.*, 2007) was used. This study covers the whole areas of South Africa and grouped rivers based on their similarity. The main aim of the river eco-regional classification was to group areas according to their similarities using a top-down nested hierarchy. The report also indicates that river eco-regional classification helps to extrapolate information from data-rich to data-scarce catchments within the same hierarchical typing concepts. Hence, the quaternary catchment called A21C (Figure 3.7) was selected as a donor catchment for the calibration, validation and sensitivity analysis for this study. The details of the river eco-regional classification for South Africa can be referred to in Kleynhans *et al.* (2005) and Kleynhans *et al.* (2007). Some of the major attributes used in the classification include terrain morphology, main vegetation types, mean annual precipitation, coefficient of variation of annual precipitation, drainage density, stream frequency, slopes, median annual simulated runoff, and mean annual temperature of catchments. Some of the catchment descriptors used in the evaluation between the donor and study catchments can be seen in Table 3. The comparison table shows that the two catchments are more or less in a physically similar hydro-

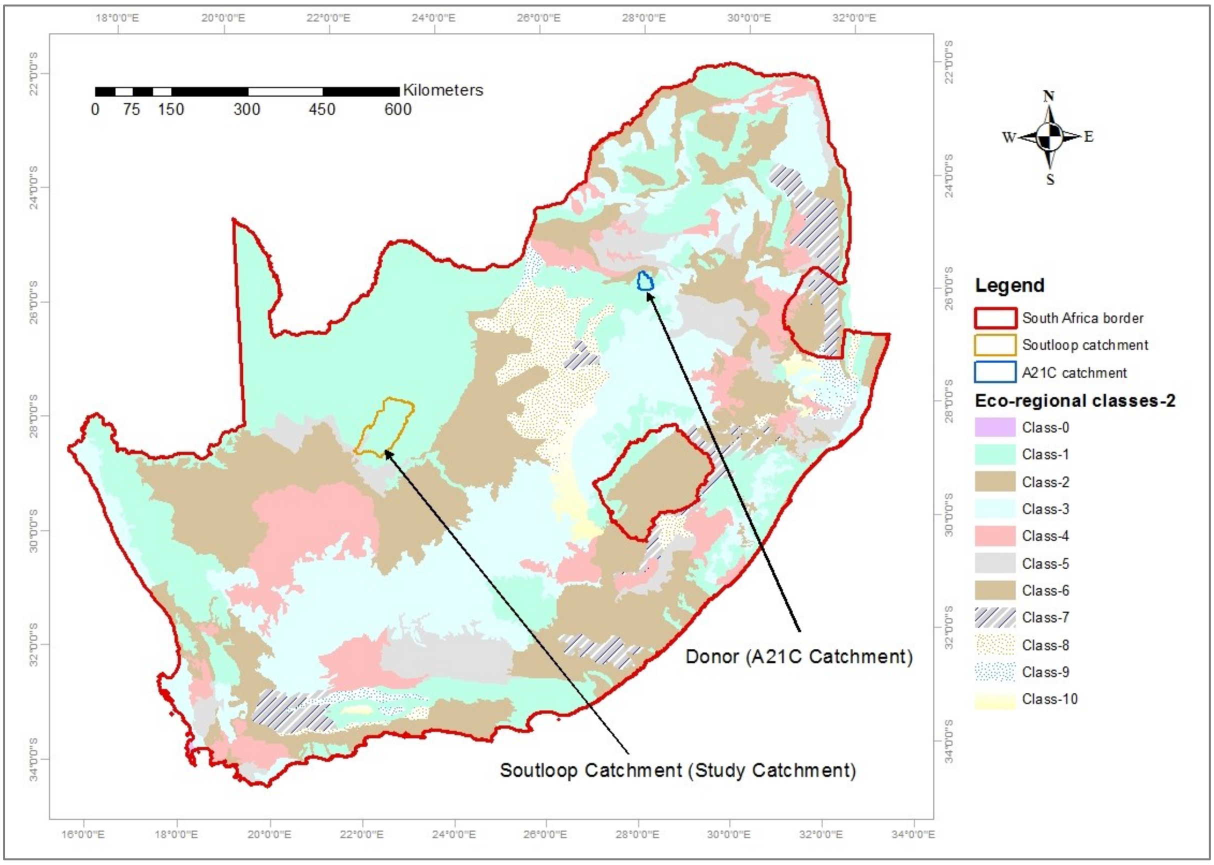

Figure 3.7: Location of the study catchment (Soutloop) and the donor catchment (A21C) showing that both are in the same river eco-regional class (Class-1).

climatic and physiographic conditions. It is also worthy to note that the two catchments have different sizes that may influence some hydrologic variables. However, the influence of catchment sizes on the uncertainty of model outputs is primarily on sediment, nitrogen and phosphorus loadings (FitzHugh and Mackay, 2000; Jha et al., 2004; Kumar and Merwade, 2009; Wallace et al., 2018). Therefore, the difference in the size of the donor and target catchments have insignificant influences on streamflow estimations. As the focus of this paper is on the calibration of SWAT for estimation of flow in arid and semi-arid catchments, the difference in the size of the donor and target catchments is ignored. However, during the study of point and non-point source pollution, sediment, nitrogen and phosphorus loadings, the influence of catchment sizes could matter on the regionalization process.

3.2.4.2 Procedures in the regionalization approach

In this study, all the sensitivity, calibration and validation procedures were facilitated by the use of a specialized computer program, SWAT-CUP ver-2012 (the SWAT Calibration and

Uncertainty Programs), particularly SUFI2 (Sequential Uncertainty Fitting ver. 2). SUFI2 is one of the stochastic calibration programs in SWAT-CUP that was used in this study. The details for the description of SUFI-2 in the whole calibration procedure can be referred to in Abbaspour *et al.* (2004), Abbaspour *et al.* (2007), and Abbaspour (2015). First, the calibration, sensitivity analysis and model validation were conducted on the donor catchment (A21C quaternary catchment) and then the model parameters were transferred to the ungauged catchment (Soutloop Catchment), based on the regionalization with physical similarity approach. After the transfer of calibrated parameter values, the model was run, and the major components of the catchment water balance (particularly long-term annual runoff volume and evapotranspiration) were compared with previous studies of the area for simple inspection of model results. Based on this comparison with other similar studies, a manual calibration helper was employed in the ArcSWAT interface for further parameter adjustments.

During calibration of parameters in the donor catchment, only sensitive parameters were calibrated, based on the results of the sensitivity analysis in SWAT-CUP. The soil and some weather parameters were also excluded from the calibration processes since all the soil parameters were measured directly by the field survey. Similarly, the weather parameters were derived from weather station in the study area. To prioritize other sensitive parameters (other than the excluded parameters), a one parameter at a time (OAT) procedure was followed. This was used to select sensitive parameters to stream flow as a first inspection for sensitivity. Then, the sensitivities of all parameters, selected by one-at-a-time option, were further prioritized by the global sensitivity option. This was done by running SUFI2 for one complete iteration (1000 simulations). The global sensitivity uses the p-value and t-stats for prioritization. The general workflow of the calibration process is depicted in Figure 3.8. The flow data from the donor catchment (A21C) were divided into two, one for calibration and the other half for validating the model. Generally, a two-step calibration and validation procedure was employed here; one in the donor catchment and the other in the study catchment. The calibration in the study catchment was assisted by the ArcSWAT manual calibration helper whereas the validation was outside SWAT-CUP, which was in MS excel with simple comparison of simulated versus *in situ* measured soil water content data.

The second model validation that was conducted in the target catchment was actually a simple verification of model results with respect to simulated water content. The SWAT output for soil water content is in millimetre of depths and also excludes the residual water content. Therefore, the observed soil water content at four HRUs measured by DFM capacitance probes

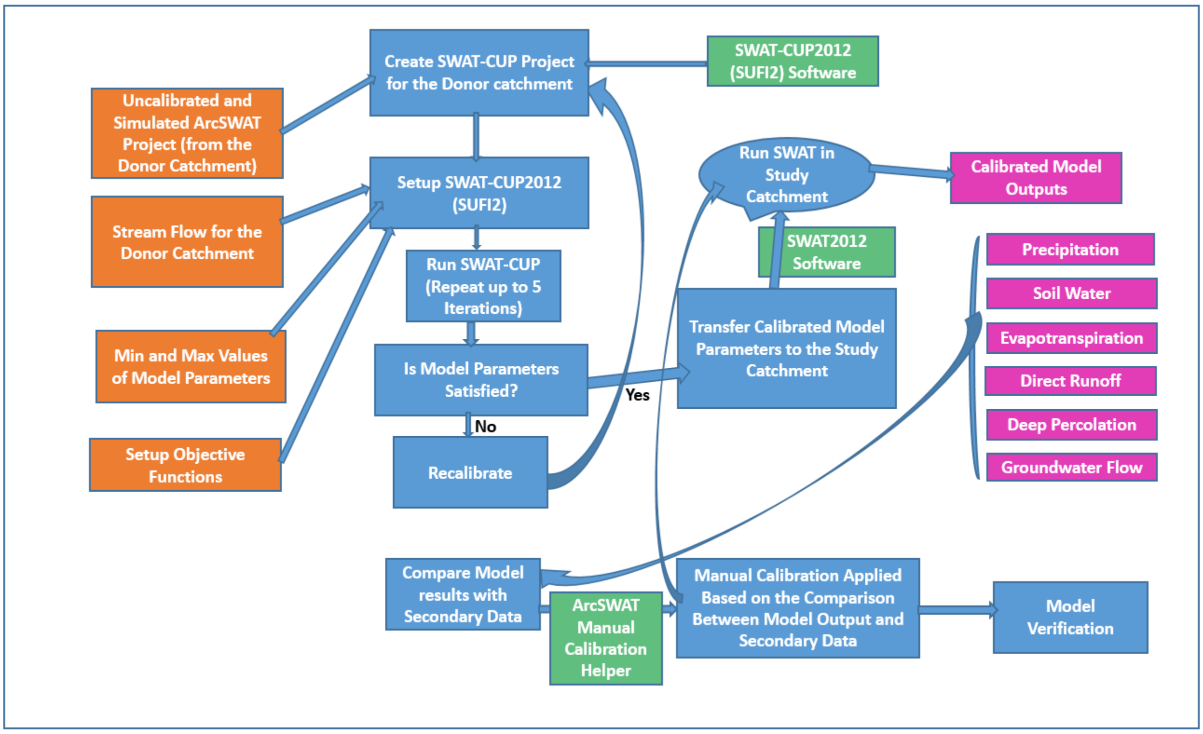

Figure 3.8: Workflow for the calibration and sensitivity analysis using SWAT-CUP.

(Zerizghy et al., 2013) must also have similar units of depth. The readings from the probes is normally in percentage of total soil volume and it measures at six depths at a time down the soil profile. The average of the six depths was multiplied by the bulk density of the soil profile and this product again multiplied by the soil depth to get the total soil water content in millimetre of depth in the profile at that specific measurement time. The residual water content (permanent wilting point) of the soil (estimated by SWAT model) was subtracted from the observed total soil water content of the profile. Then, the resulting soil water content is the observed one and compared to the output from SWAT model for each of the four HRUs.

3.2.4.3 Uncertainty and model performance indices

Reports (Blöschl *et al.*, 2013; Abbaspour, 2015) indicate that the sources of model uncertainties could be from driving variables (e.g. climate data), the conceptual model itself, measured data, or uncertainty during parametrization. The propagation of all sources of model uncertainties to parameters and model outputs in SWAT-CUP is expressed as the 95% probability distributions, by using the Latin Hypercube Sampling. The 95% probability distributions are calculated at the 2.5% and 97.5% levels of the cumulative distribution of an output variable and it is called 95% prediction uncertainty (95PPU). SWAT-CUP calculates two statistical indicators to quantify all the sources of uncertainty. These are the P-factor, which is the percentage of observed data enveloped by the modelling result (the 95PPU), and the R-factor, which is the thickness of the 95PPU envelope.

Regarding the model performance indicators, SUFI2 has many options of model performance indicators. For this study, the Nash-Sutcliffe coefficient (NS) was used as a major objective function in the calibration and validation process. The coefficient of determination (R^2), percent bias (PBIAS), and ratio of the root mean squared error to the standard deviation of measured data (RSR) were also additional criteria used for the evaluation. Equations 1 to 4 were used to calculate the performance indices:

$$NS = 1 - \frac{\sum_i (Q_m - Q_s)_i^2}{\sum_i (Q_{m,i} - Q_m)^2} \tag{1}$$

$$R^2 = \frac{\left[\sum_i (Q_{m,i} - \overline{Q}_m)(Q_{s,i} - \overline{Q}_s)\right]^2}{\sum_i (Q_{m,i} - \overline{Q}_m)^2 \sum_i (Q_{s,i} - \overline{Q}_s)^2} \tag{2}$$

$$PBIAS = 100 \times \left[\frac{\sum_{i=1}^{n} (Q_m - Q_s)_i}{\sum_{i=1}^{n} Q_{m,i}}\right] \tag{3}$$

$$RSR = \frac{\sqrt{\sum_{i=1}^{n} (Q_m - Q_s)_i^2}}{\sqrt{\sum_{i=1}^{n} (Q_{m,i} - Q_m)^2}} \tag{4}$$

where *NS* is the Nash-Sutcliffe coefficient, R^2 is the coefficient of determination, *PBIAS* is the percent bias, *RSR* is ratio of the root mean square error to the standard deviation of measured data, *Q* is a variable (e.g., discharge), *m* and *s* stand for measured and simulated variables, and *i* is the i^{th} measured or simulated data.

3.3 Results

3.3.1 Parameterization and parameter sensitivity analysis

As stated earlier, the study area is an ungauged catchment and accordingly all the possibilities of using *in situ* measured data (whether collected by the authors or second party, such as meteorological stations) were given priority. As a result, parameters that were derived from the *in situ* measured data were not considered in the calibration and sensitivity analysis. On the other hand, parameters other than the ones mentioned above and that are highly sensitive were calibrated by the regionalization with physical similarity approach. The list of sensitive parameters is given in Table 3.4. Parameters are listed based on their sensitivity levels as analysed by SWAT-CUP with the global sensitivity option. It shows that the top sixteen parameters were sensitive and were considered for calibration, from which the first three (the base flow alpha factor, curve number II and initial depth of water in the shallow aquifer) were found to be the top sensitive parameters.

Table 3.4: List of parameters, definitions and sensitivity analysis

No.	Parameter Name	t-Stat	P-Value	Definitions of abbreviations
1	ALPHA_BF.gw	-9.3448	0.0000	Base flow alpha factor (days).
2	CN2.mgt	-8.3021	0.0000	Curve number for soil water condition 2.
3	SHALLST.gw	-7.9193	0.0000	Initial depth of water in the shallow aquifer (mm).
4	OV_N.hru	-1.4871	0.1381	Manning's "n" value for overland flow.
5	CH_N2.rte	1.3869	0.1666	Manning's "n" value for the main channel.
6	CH_K2.rte	1.2528	0.2113	Effective hydraulic conductivity in main channel alluvium.
7	REVAPMN.gw	-1.2125	0.2264	Threshold depth of water in the shallow aquifer for "revap" to occur (mm).
8	ESCO.bsn	1.06	0.2901	Soil evaporation compensation factor.
9	FFCB.bsn	0.9859	0.3250	Initial soil water storage expressed as a fraction of field capacity water content.
10	GWQMN.gw	0.9019	0.3679	Threshold depth of water in the shallow aquifer required for return flow to occur (mm).
11	GW_DELAY.gw	0.8032	0.4225	Groundwater delay (days).
12	EPCO.hru	-0.67	0.5034	Plant uptake compensation factor.
13	MSK_CO1.bsn	0.6601	0.5097	Calibration coefficient used to control impact of the storage time constant for normal flow.
14	SURLAG.bsn	-0.6265	0.5315	Surface runoff lag time.
15	GW_REVAP.gw	0.5637	0.5734	Groundwater "revap" coefficient.
16	RCHRG_DP.gw	-0.2052	0.8376	Deep aquifer percolation fraction.

3.3.2 Model calibration and validation

The lists of calibrated model parameters, methods of change used and the final calibrated values are shown in Table 5. The graphical comparisons of measured stream flow at the outlet of the donor catchment and its simulated discharge values are depicted in Figures 3.9 and 3.10 for the calibration and validation processes, respectively. Similarly, the performance indices for the calibration and validation processes are given in Table 6.

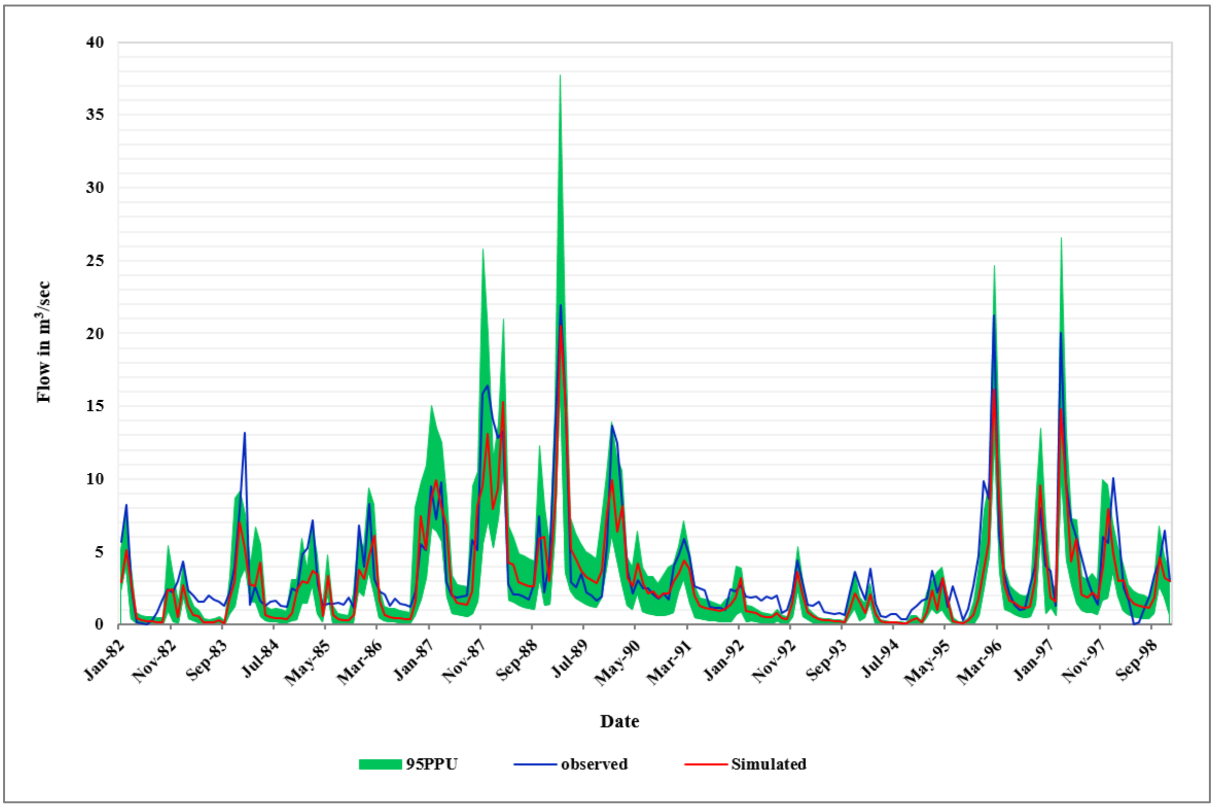

Figure 3.9: Comparison of measured and predicted monthly stream flow during the calibration period (1982–1998).

The performance of the best parameter sets selected in the sensitivity analysis (in Subsection 3.1 above) were evaluated by two major types of statistical evaluations, i.e. model prediction uncertainty and model performance evaluation. The prediction uncertainty in SUFI2 (one of the programs in SWAT-CUP) is expressed by the 95PPU (95 percent prediction uncertainty), which is represented by the green-coloured region in Figures 9 and 10 for the calibration and validation processes, respectively. Two indices are calculated to evaluate the model uncertainty, the P-factor, and the R-factor. Table 3.6 shows that the P-factor estimated was 0.73 and 0.65 for calibration and validation, respectively. This means that 73% and 65% of the observed discharge is enveloped by the 95PPU during the calibration (1982–1998) and validation periods (2000–2013), respectively. On the other hand, the R-factor, which is the thickness of the 95PPU envelop, was 0.93 for calibration and 0.66 for validation periods, respectively.

Table 3.5: Methods of a parameter change, initial adjustment intervals, and calibrated values for each parameter

No.	Parameter Name	Method of change	Min value	Max value	Fitted value one*	Fitted value two**
1	ALPHA_BF.gw	Replace	0.05	0.65	0.269	0.15
2	CN2.mgt	Relative	-0.15	0.48	-0.434	-0.10
3	SHALLST.gw	Replace	500	10000	2100	1650
4	OV_N.hru	Replace	0.01	0.48	0.435	0.21
5	GW_DELAY.gw	Replace	20	566	496	35
6	EPCO.hru	Replace	0.2993	0.82	0.439	0.67
7	GWQMN.gw	Replace	500	3536	2898	1200
8	FFCB.bsn	Replace	0.12	0.69	0.52	0.52
9	CH_K2.rte	Replace	2.14	185.82	52.93	52.93
10	CH_N2.rte	Replace	0.25	0.76	0.56	0.25
11	MSK_CO1.bsn	Replace	1.33	8.15	5.75	5.75
12	ESCO.bsn	Replace	0.11	0.94	0.201	0.85
13	REVAPMN.gw	Replace	122	3670	285.51	850
14	SURLAG.bsn	Replace	0.98	21.77	6.63	6.61
15	GW_REVAP.gw	Replace	0.014	0.30	0.288	0.033
16	RCHRG_DP.gw	Replace	0.01	0.51	0.367	0.072

** Fitted value one-it is the transposed value fitted by the SWAT-CUP program in the donor catchment.*

*** Fitted value two-it is the final fitted value by the manual calibration helper in ArcSWAT2012 software in the study catchment.*

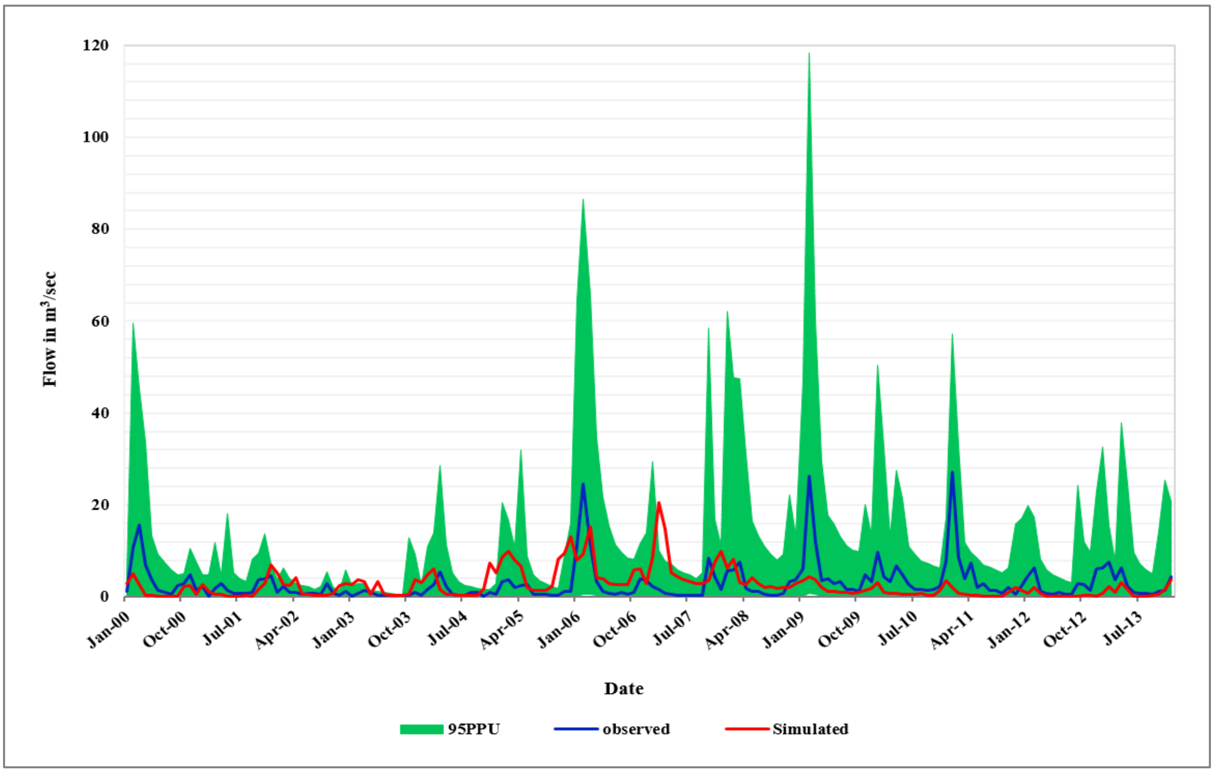

Figure 3.10: Comparison of measured and predicted monthly streamflow during the validation period (2000–2013).

Table 3.6: Summary of statistics for calibration, validation processes with flow data in the outlet of the donor catchment

Process	P-factor	R-factor	R^2	NS	PBIAS	RSR
Calibration	0.73	0.93	0.83	0.82	11.80	0.43
Validation	0.65	0.66	0.72	0.71	-8.10	0.55

Regarding the model performance evaluation, the results of the model performance indicators are shown in Table 3.6. The Nash-Sutcliffe coefficient (NS) was used as the major objective function. Three other performance indices were also selected, namely the coefficient of determination (R^2), the percent bias (PBIAS), and the ratio of the root mean squared error to the standard deviation of measured data (RSR). As the results shows that all the performance indicators for both the calibration and validation periods (R^2 & NS > 0.71, -9 < PBIAS < +12, RSR < 0.6) are in fairly acceptable ranges (Moriasi *et al.*, 2007; Abbaspour, 2015; Almeida *et al.*, 2018). In other words, the statistical indices indicate that there is a good agreement between the measured and simulated streamflow. Moreover, the PBIAS (+11.8 and -8.1 for calibration and validation, respectively) indicates that the model over-estimated by 11.8% during calibration, and under-estimated by 8.1% during validation.

Table 3.7: Performance of the manual calibration after comparison to previous studies of the runoff and evapotranspiration data with model results

Variables compared	Values from previous studies	SWAT-CUP calibration only	SWAT-CUP & manual calibration	Percentage of improvement
Runoff volume*	16.5	25.4	21.6	23
Evapotranspiration**	188.1	268.3	238.5	16

* *Sources for runoff data: DWAF (2009), Schulze et al. (2007), Kleynhans et al. (2005).*

** *Sources of evapotranspiration data: Jovanovic et al. (2015), Bennie and Hensley (2001).*

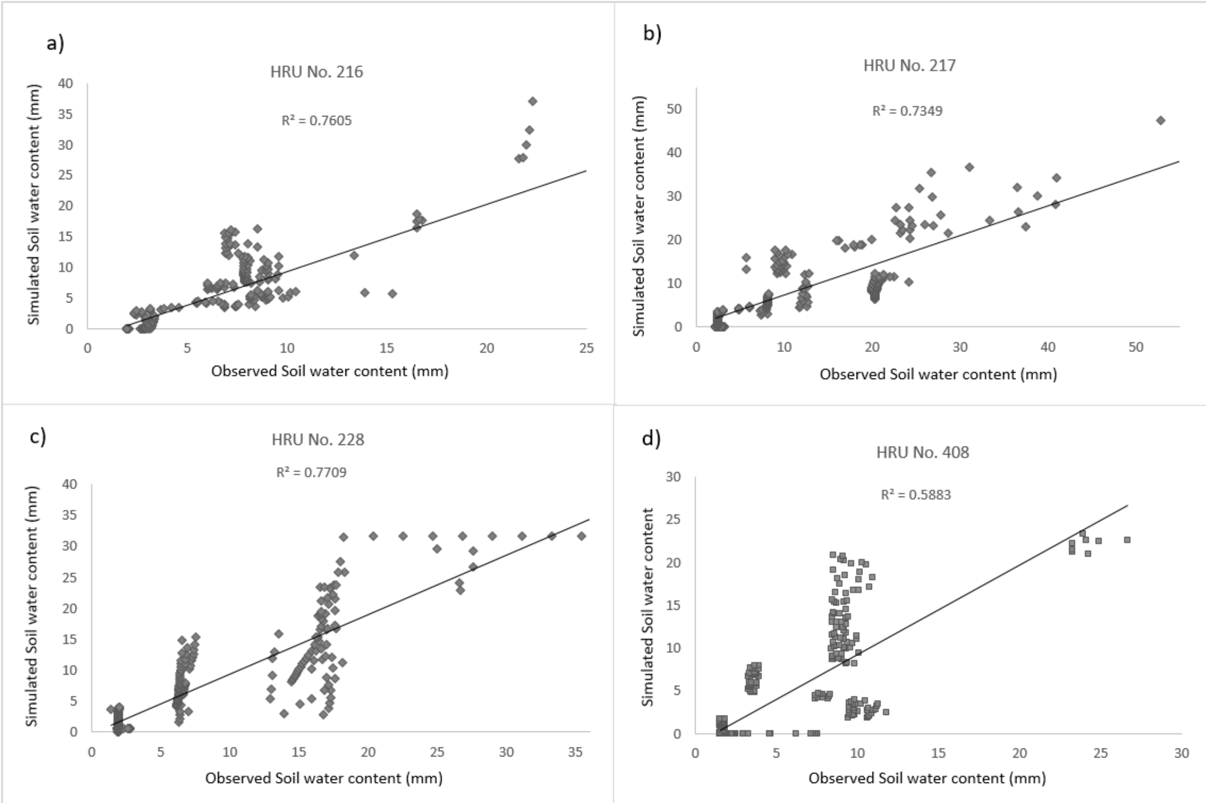

Figure 3.11: Comparisons of measured and simulated daily soil water content variations inside Kolomela Mine.

Note: Water content measured with DFM probes: (a) at HRU No. 216 from 1/1/2013 to 10/30/2013, (b) at HRU No. 217 from 11/16/2016 to 8/22/2017, (c) at HRU No. 228 from 11/15/2016 to 8/24/2017 and at HRU No. 408 from 01/01/2014 to 12/31/2014.

It is worthy to note that all the calibration and validation processes with SUFI2 program was completed in the donor catchment. As a result of this, there was no chance of evaluating the model uncertainty in the catchment of interest. Therefore, after the calibrated model parameters were transposed to the catchment of interest, two model outputs (annual runoff volumes and annual evapotranspiration) were compared with results of similar studies in the past. Then, sensitive model parameters were slightly adjusted with a manual calibration helper in ArcSWAT interface so that the simulated values would be closer to the values gained from previous results. The comparison of the model outputs after SWAT-CUP calibration and after SWAT-CUP plus manual calibration is shown in Table 7. The comparison (Table 7) indicated that the manual calibration helped to improve the annual runoff volume and annual evapotranspiration by 23% and 16%, respectively. Finally, the model performance was also verified by the comparison of the *in situ* measured and simulated soil water content, as shown in Figure 3.11, panels a–d where the soil water content measurement was taken in selected four HRUs in the study catchment.

3.4 Discussion

It is obvious that the different types of regionalization approaches play important roles in the hydrological modelling of ungauged catchments in arid and semi-arid environments. However, it is also true that hydrological modelling in ungauged catchments is exposed to significant amounts of model uncertainty due to the unavailability of data for calibration and validation processes. Hence, the regionalization approach needs to be applied cautiously.

In this study, the regionalization with physical similarity approach was employed and some best practices are also recommended to minimize model uncertainties in hydrological models. In hydrological modelling, sensitivity analysis shows the share of all parameters in the uncertainties of the model output. Hence, more sensitive parameters will have a higher share of model uncertainties than less sensitive ones in the model output, if that parameter is left uncalibrated. Therefore, sensitivity analysis is the first step that should be taken into consideration in model calibration. However, not all the sensitive parameters may be calibrated in ungauged catchments. For instance, in this study, all the soil parameters (collected from field or analysed in laboratory) and some weather parameters (derived from available weather stations in the study area) were excluded from the calibration and validation processes. This is because, as stated by (Faramarzi *et al.*, 2015; Kumarasamy and Belmont, 2018; Abbaspour *et al.*, 2018), measured parameters contribute the least sources of uncertainty in hydrologic modelling. As a result of this, it is recommended to use all available data sources of the catchment understudy and exclude those parameters from calibration to avoid unnecessary and arbitrary adjustments of parameters.

Regarding the evaluation of the modelling process in the donor catchment, two types of statistics were used to, i.e., evaluation with respect to model prediction uncertainty and evaluation of the model with performance indicators. The model uncertainty was shown by the P-factor and R-factor. The P-factor was 0.73 and 0.65 for calibration and validation, respectively; whereas the R-factor was 0.93 for calibration and 0.66 for validation periods. Generally, good model uncertainty is expressed by a higher value of the P-factor (towards 100%) and a lower value of R-factor (towards 0). Abbaspour (2015) has recommended that a P-factor of at least 0.7 and an R-factor of around 1 are acceptable for the calibration and validation of a catchment with respect to its discharge. Therefore, the results of this study indicated that 73% and 65% of the observed data from the donor catchment were enveloped with the 95PPU (the region of lower uncertainty) during calibration and validation processes, respectively. Similarly, the smaller thickness of the 95PPU (R-factor of 0.93 and 0.66 for calibration and validation, respectively) also indicate that there was a lower uncertainty of the modelling process in the donor catchment. Moreover, the model performance indicators (NS, R^2, PBIAS and RSR) also indicated the good performance of the model.

However, all the above model uncertainty and performance indicators were conducted outside the target catchment. There was no any chance to statistically evaluate the model's performance and uncertainty in the catchment of interest. As a result, this study suggests some best practices to inspect model results with other sources of data. For instance, the comparison of long-term annual runoff volume and annual evapotranspiration results from the model were compared with previous similar studies. The comparison indicated that the model overestimated the two parameters and the manual calibration improved the model output by 23% and 16% with respect to the previous results for runoff and evapotranspiration components, respectively. After the manual calibration, the profile soil water content from the model was compared with measured soil water content data in the study catchment as means of verification of the model. Hence, model results of four HRUs from the study catchment were selected and it showed a higher value of coefficient of determination (average R^2 =0.71) indicating a good agreement between the observed and simulated profile soil water content in the study catchment.

Generally, the following best practices are suggested here to minimize the model uncertainty of hydrologic models in arid and semi-arid-catchments. (i) excluding some parameters from calibration: parameters that could be derived from data measured *in situ* from the catchment of interest should be excluded from the calibration and validation processes. (ii) regionalize and transpose model parameters from donor (gauged) to study (ungauged) catchment: this is the method that have been already operational and described in the materials and methods section. (iii) comparison of model outputs to previous studies of any of the components of the catchment water balance and identify the gap between the two results. (iv) Manual calibration: if the difference between the result from the model and the previous study is larger, use manual calibration helper to adjust parameter values until the difference between the two results is minimum. (v) conduct an *in situ* measurement: all possibilities of direct measurement of data from the catchment of interest should be given priority. For instance, measurement of soil water content could be relatively easy. The acquisition of satellite soil water content (e.g., Wanders *et al.* (2014), Alvarez-Garreton *et al.* (2015) and Rajib *et al.* (2016)) or evapotranspiration data (e.g., Franco and Bonumá (2017), Emam *et al.* (2017) and Ha *et al.* (2017)) are also good alternatives nowadays in arid and semi-arid catchments. This data is important and could be used for the model verification and it gives the modeller a confidence on the model outputs.

3.5 Conclusion

The aim of this study was to set up, calibrate and validate SWAT model in a data-scarce catchment by using the regionalization with physical similarity approach. A two-way calibration and validation processes were employed, one in the donor catchment (A21C quaternary catchment) with a semi-automatic calibration program, SWAT-CUP, and the second was conducted in the target catchment (Soutloop) with the ArcSWAT interface of manual calibration helper. Generally, many studies have been conducted to simulate the components of a catchment hydrology through utilizing the regionalization approach. However, this study shows that the transfer of calibrated model parameters from a donor catchment to a target catchment, without further inspection of the outputs of the target catchment, would cause a potential uncertainty in the model outputs. The modeller would then finally draw wrong conclusions. There should be a way to conduct at least a simple inspection. In this study, the simulated values were compared with previous and similar local studies, and additional manual calibration was conducted as one alternative for inspecting uncertainity. Moreover, some *in situ* measurements (such as soil water content or evapotranspiration) are also advisable for model verification. The calibration of some of the parameters that are measured *in situ* (for example, soil parameters in this study) could be unnecessary, since the main calibration process is outside the target catchment. The use of weather station data is also advisable for minimizing the uncertainty in model prediction in ungauged catchments. Finally, as the focus of this study was on the regionalization for streamflow estimation, the influence of catchment sizes were ignored during evaluating the similarity between the donor and target catchments. Therefore, during the study of point and non-point source pollution, sediment, nitrogen and phosphorus loadings, the influence of catchment sizes should also be considered in the regionalization process.

3.6 References

Abbaspour, K.C., 2015. *SWAT-CUP 2012: SWAT calibration and uncertainty programs-a user manual.* Eawag (Swiss Federal Institute of Aquatic Science and Technology): Zurich, Switzerland.

Abbaspour, K.C., Johnson, C.A. and van Genuchten, M.T., 2004. Estimating uncertain flow and transport parameters using a sequential uncertainty fitting procedure. *Vadose Zone Journal*, 3(4), pp.1340-1352.

Abbaspour, K.C., Vaghefi, S.A. and Srinivasan, R., 2018. A guideline for successful calibration and uncertainty analysis for soil and water assessment: a review of papers from the 2016 International SWAT Conference. *Water*, 10(6) p.18.

Abbaspour, K.C., Yang, J., Maximov, I., Siber, R., Bogner, K., Mieleitner, J., Zobrist, J. and Srinivasan, R., 2007. Modelling hydrology and water quality in the pre-alpine/alpine Thur catchment using SWAT. *Journal of Hydrology*, 333(2-4), pp.413-430.

Ajami, N.K., Gupta, H., Wagener, T., Sorooshian, S., 2004. Calibration of a semi-distributed hydrologic model for streamflow estimation along a river system. *Journal of Hydrology*, 298: pp.112–135.

Almeida, R.A., Pereira, S.B. and Pinto, D.B., 2018. Calibration and validation of the SWAT hydrological model for the Mucuri River Basin. *Engenharia Agrícola*, 38(1), pp.55-63.

Alvarez-Garreton, C., Ryu, D., Western, A.W., Su, C.H., Crow, W.T., Robertson, D.E. and Leahy, C., 2015. Improving operational flood ensemble prediction by the assimilation of satellite soil moisture: Comparison between lumped and semi-distributed schemes. *Hydrology and Earth System Sciences*, 19(4), pp.1659-1676.

Arnold, J.G., Kiniry, J.R., Srinivasan, R., Williams, J.R., Haney, E.B. and Neitsch, S.L., 2012. *SWAT input/output documentation version 2012*. Texas Water Resources Institute, 654, pp.1-646.

Babel, L. and Karssenberg, D., 2013. Hydrological models are mediating models. *Hydrology and Earth System Sciences Discussions,* 10(8), pp. 10535-10563.

Bárdossy, A., 2007. Calibration of hydrological model parameters for ungauged catchments. *Hydrology and Earth System Sciences Discussions*, 11(2), pp.703-710.

Bastola, S., Ishidaira, H. and Takeuchi, K., 2008. Regionalisation of hydrological model parameters under parameter uncertainty: A case study involving TOPMODEL and basins across the globe. *Journal of Hydrology*, 357(3-4), pp.188-206.

Bekele, E.G. and Nicklow, J.W., 2007. Multi-objective automatic calibration of SWAT using NSGA-II. *Journal of Hydrology*, 341(3-4), pp.165-176.

Bennie, A. T. P. and Hensley, M., 2001. Maximizing precipitation utilization in dryland agriculture in South Africa-a review. Journal of Hydrology, 241 (1), 124-139.

Blöschl, G., Sivapalan, M., Savenije, H., Wagener, T. and Viglione, A. eds., 2013. *Runoff prediction in ungauged basins: synthesis across processes, places and scales*. Cambridge University Press. Cambridge, UK.

Daniel, E.B., Camp, J.V., LeBoeuf, E.J., Penrod, J.R., Dobbins, J.P. and Abkowitz, M.D., 2011. Catchment modeling and its applications: a state-of-the-art review. *The Open Hydrology Journal,* 5(1), pp. 26-50.

Department of Water Affairs and Forestry (DWAF), 2009. Development of an integrated water quality management strategy for the Upper and Lower Orange Water Management Areas: Desktop Catchment Assessment Study: Lower Orange Water Management Area (WMA 14). Department of Water Affairs and Forestry Report: No: 2.2 (P RSA D000/00/7909/3), Pretoria, South Africa.

Emam, A. R., Kappas, M., Nguyen, L. H. K. and Renchin, T., 2017. Hydrological modeling and runoff mitigation in an ungauged basin of Central Vietnam using SWAT model. *Hydrology,* 4(1), p. 16.

Emam, A.R., Kappas, M., Akhavan, S., Hosseini, S.Z. and Abbaspour, K.C., 2015. Estimation of groundwater recharge and its relation to land degradation: Case study of a semi-arid river basin in Iran. *Environmental Earth Sciences,* Volume 74, p. 6791–6803.

Faramarzi, M., Srinivasan, R., Iravani, M., Bladon, K.D., Abbaspour, K.C., Zehnder, A.J. and Goss, G.G., 2015. Setting up a hydrological model of Alberta: data discrimination analyses prior to calibration. *Environmental Modelling & Software*, 74, pp.48-65.

Farsadnia, F., Kamrood, M.R., Nia, A.M., Modarres, R., Bray, M.T., Han, D. and Sadatinejad, J., 2014. Identification of homogeneous regions for regionalization of watersheds by two-level self-organizing feature maps. *Journal of Hydrology*, 509, pp.387-397.

Fey, M., 2010. *Soils of South Africa*. Cambridge University Press.

FitzHugh, T.W. and Mackay, D.S., 2000. Impacts of input parameter spatial aggregation on an agricultural non-point source pollution model. *Journal of Hydrology*, 236(1-2), pp.35-53.

Franco, A.C.L. and Bonumá, N.B., 2017. Multi-variable SWAT model calibration with remotely sensed evapotranspiration and observed flow. *Brazilian Journal of Water Resources*, 22(e35).

GEOTERRAIMAGE (South Africa), 2015. *South African National Land cover dataset-2013- 2014*. Department of Environmental Affairs. Accessed on 22 Feb, 2017 from this url: https://egis.environment.gov.za/data_egis/data_download/current.

Gitau, M.W. and Chaubey, I., 2010. Regionalization of SWAT model parameters for use in ungauged watersheds. *Water*, 2(4), pp.849-871.

Ha, L.T., Bastiaanssen, W.G., van Griensven, A., van Dijk, A.I. and Senay, G.B., 2017. SWAT-CUP for calibration of spatially distributed hydrological processes and ecosystem services in a Vietnamese river basin using remote sensing. *Hydrology and Earth System Science*, https://doi.org/10.5194/hess-2017-251.

Jajarmizadeh, M., Harun, S., and Salarpour, M., 2012. A review on theoretical consideration and types of models in hydrology. *Journal of Environmental Science and Technology*, 5 (5), 249–261.

Jha, M., Gassman, P.W., Secchi, S., Gu, R. and Arnold, J., 2004. Effect of watershed subdivision on SWAT flow, sediment, and nutrient predictions. *JAWRA Journal of the American Water Resources Association*, 40(3), pp.811-825.

Jovanovic, N., Mu, Q., Bugan, R.D. and Zhao, M., 2015. Dynamics of MODIS evapotranspiration in South Africa. Water SA, 41(1), pp.79-90.

Kan, G., He, X., Ding, L., Li, J., Liang, K. and Hong, Y., 2017. Study on applicability of conceptual hydrological models for flood forecasting in humid, semi-humid semi-arid and arid basins in China. *Water*, 9(10), p.719.

Kleynhans, C.J., Thirion, C. and Moolman, J., 2005. *A level I river ecoregion classification system for South Africa, Lesotho and Swaziland*. Report No. N/0000/00/REQ0104. Department of Water Affairs and Forestry, Resource Quality Services, Pretoria, South Africa.

Kleynhans, C.J., Thirion, C., Moolman, J. and Gaulana, L., 2007. *A level II river ecoregion classification system for South Africa, Lesotho and Swaziland*. Report No. N/000/00/REQ0XXX. Department of Water Affairs and Forestry, Resource Quality Services, Pretoria, South Africa.

Kouchi, D.H., Esmaili, K., Faridhosseini, A., Sanaeinejad, S.H., Khalili, D. and Abbaspour, K.C., 2017. Sensitivity of calibrated parameters and water resource estimates on different objective functions and optimization algorithms. *Water*, 9(6), p.384.

Kumar, S. and Merwade, V., 2009. Impact of watershed subdivision and soil data resolution on SWAT model calibration and parameter uncertainty. *JAWRA Journal of the American Water Resources Association*, 45(5), pp.1179-1196.

Kumarasamy, K. and Belmont, P., 2018. Calibration parameter selection and catchment hydrology model evaluation in time and frequency domains. *Water*, 10(6), p.1.

Land Type Survey Staff, 1972. Land types of South Africa: digital map (1: 250 000 scale) and soil inventory databases. Agricultural Research Council, Institute for Soil, Water and Climate, Pretoria, South Africa.

Li, J., Mao, X., Kang, S. and Barry, D.A., 2015. Modeling of hydrological processes in arid agricultural regions. *Frontiers of Agricultural Science and Engineering*, 2, pp.283-294.

Lundin, L.-C., Bergström, S., Eriksson, E. and Seibert, J., 1999. Hydrological models and modelling. In: Lundin, L., ed. Sustainable water management in the Baltic Sea Basin. Uppsala, Sweden: The Baltic University Program, pp. 129-140.

Merz, R. and Blöschl, G., 2004. Regionalisation of catchment model parameters. *Journal of hydrology*, 287(1-4), pp.95-123.

Moriasi, D.N., Arnold, J.G., van Liew, M.W., Bingner, R.L., Harmel, R.D. and Veith, T.L., 2007. Model evaluation guidelines for systematic quantification of accuracy in catchment simulations. *Transactions of the ASABE*, 50(3), pp.885-900.

Nair, S.S., King, K.W., Witter, J.D., Sohngen, B.L. and Fausey, N.R., 2011. Importance of crop yield in calibrating watershed water quality simulation tools. *JAWRA Journal of the American Water Resources Association*, 47(6), pp.1285-1297.

Neitsch, S.L., Arnold, J.G., Kiniry, J.R. and Williams, J.R., 2011. *Soil and water assessment tool: theoretical documentation, Version 2009.* Texas Water Resources Institute Technical Report No. 406. Texas A&M University, Texas, USA.

Odusanya, A.E., Mehdi, B., Schürz, C., Oke, A.O., Awokola, O.S., Awomeso, J.A., Adejuwon, J.O. and Schulz, K., 2019. Multi-site calibration and validation of SWAT with satellite-based evapotranspiration in a data-sparse catchment in south-western Nigeria. *Hydrology and Earth System Sciences*, 23(2), pp.1113-1144.

Omernik, J.M., 1987. Ecoregions of the conterminous United States. *Annals of the Association of American geographers*, 77(1), pp.118-125.

Parajuli, P.B. and Ouyang, Y., 2013. Catchment-scale hydrological modelling methods and applications. *In: Bradley, P.M., ed. Current Perspectives in Contaminant Hydrology and Water Resources Sustainability*. ISBN 980-953-307-926-9. InTech, pp.57-80.

Pechlivanidis, I., Jackson, B., McIntyre, N. and Wheater, H., 2011. Catchment scale hydrological modelling: a review of model types, calibration approaches and uncertainty analysis methods in the context of recent developments in technology and applications. *Global NEST Journal,* 13(3), pp. 193-214.

Pilgrim, D.H., Chapman, T.G. and Doran, D.G., 1988. Problems of rainfall-runoff modelling in arid and semiarid regions. *Hydrological Sciences Journal*, 33(4), pp.379-400.

Rajib, A., Evenson, G.R., Golden, H.E. and Lane, C.R., 2018. Hydrologic model predictability improves with spatially explicit calibration using remotely sensed evapotranspiration and biophysical parameters. *Journal of Hydrology*, 567, pp.668-683.

Rajib, M.A., Merwade, V. and Yu, Z., 2016. Multi-objective calibration of a hydrologic model using spatially distributed remotely sensed/in-situ soil moisture. *Journal of Hydrology*, 536, pp.192-207.

Reichl, J.P.C., Western, A.W., McIntyre, N.R. and Chiew, F.H.S., 2009. Optimization of a similarity measure for estimating ungauged streamflow. *Water Resources Research*, 45(10).

Sinnathamby, S., Douglas-Mankin, K.R. and Craige, C., 2017. Field-scale calibration of crop-yield parameters in the Soil and Water Assessment Tool (SWAT). *Agricultural Water Management*, 180, pp.61-69.

Sokolowski, J. and Banks, C., 2010. *Modeling and simulation fundamentals: theoretical underpinnings and practical domains.* John Wiley and Sons, Hoboken, New Jersey, USA.

Sokolowski, J. and Banks, C., 2011. *Principles of modeling and simulation: a multidisciplinary approach.* John Wiley and Sons, Hoboken, New Jersey, USA.

Swain, J.B. and Patra, K.C., 2017. Streamflow estimation in ungauged catchments using regionalization techniques. *Journal of hydrology*, 554, pp.420-433.

Tessema, S., 2011. Hydrological modeling as a tool for sustainable water resources management: a case study of the Awash River Basin (Doctoral dissertation), KTH Royal Institute of Technology, Stockholm, Sweden.

Tobin, K.J. and Bennett, M.E., 2017. Constraining SWAT calibration with remotely sensed evapotranspiration data. *JAWRA Journal of the American Water Resources Association*, 53(3), pp.593-604.

Van Zijl, G., Le Roux, Pieter A.L., and Turner, D.P., 2013. Disaggregation of land types using terrain analysis, expert knowledge and GIS methods, South African Journal of Plant and Soil, 30:3, 123-129, DOI: 10.1080/02571862.2013.806679.

Wallace, C., Flanagan, D. and Engel, B., 2018. Evaluating the effects of watershed size on SWAT calibration. *Water*, 10(7), p.898.

Wanders, N., Bierkens, M.F., de Jong, S.M., de Roo, A. and Karssenberg, D., 2014. The benefits of using remotely sensed soil moisture in parameter identification of large-scale hydrological models. *Water Resources Research*, 50(8), pp.6874-6891.

Wheater, H., Sorooshian, S. and Sharma, K.D. eds., 2008. *Hydrological modelling in arid and semi-arid areas*. Cambridge University Press. Cambridge, UK.

Wheater, H.S., 2005. Modelling hydrological processes in arid and semi-arid areas. AWADI workshop, Roorkee, Imperial College, London.

Winchell M.F., Srinivasan R., Di Luzio M., Arnold J., 2013. *ArcSWAT interface for SWAT 2012 user's guide*. Black land Research and Extension Centre. P.464, Temple, Texas, USA.

Zhang, Y., Zhang, L., Hou, J., Gu, J. and Huang, C., 2017. Development of an evapotranspiration data assimilation technique for streamflow estimates: a case study in a semi-arid region. *Sustainability*, 9(10), p.1658.

Zhu AX. 1997. A similarity model for representing soil spatial information. *Geoderma* 77: 217–242.

CHAPTER 4
ANALYSIS OF THE SPATIO-TEMPORAL VARIATION OF PRECIPITATION AND WATER DEFICIT

4.1 Introduction

Precipitation and its characteristics (amount, intensity, duration, and frequency or return period) are the most important climatological variables for specifying the state of the climate system of an area (Longobardi and Villani, 2010; He and Gautam, 2016; Donat *et al*., 2016). An analysis and understanding of precipitation and its changes are crucial for the assessment of climate change (Lima *et al*., 2013; Javari, 2016). Gaining an understanding of precipitation behaviours and the extremes is also of great concern, as these factors have inevitable impacts on environmental and socio-economic development (Munodawafa, 2012; Lima *et al*., 2013; Botai *et al*., 2015). Understanding the spatio-temporal variability of precipitation and its extreme events has theoretical and practical importance (He and Gautam, 2016). From a theoretical point of view, this understanding sheds a light on the evolving characteristics of the hydro-climatic variables and lays the foundation for developing predictive models for forecasting their future behaviour. On the other hand, from a practical point of view, this understanding assists us in water resources management practices in terms of better adapted planning and informed decision making, which is particularly important in arid and semi-arid areas.

The spatial and temporal variation of precipitation is affected by many factors. Generally, altitude, distance from the sea, geographical locations, air pressure, temperature and wind direction play an interactive and vital role in effecting differences in spatial and temporal variations of precipitation on the earth's surface (Grist and Nicholson, 2001; Liu and Shen, 2008; González *et al*., 2012; Sabziparvar *et al*., 2015). Focusing on their influence on a catchment scale, the major topographic properties include altitude, aspect, direction of mountain ranges (Sevruk *et al*., 1998; Nel and Sumner, 2006; Daly, 2006), and orographic enhancement, which is affected by wind speed and direction (Johansson and Chen, 2003; Daly, 2006). Augustine (2010) has stated that orographic variation has minimal influence on precipitation in arid and semi-arid areas, since such ecosystems are characterized by flat to gently undulating topography. Based on his statement, the source of variation in these landscapes could be local variation in intensity and path of convective thunderstorms.

Moreover, the differences in surface albedo, cloud cover, and general atmospheric circulations are also important factors on larger scales, like regional climate (Türkeş, 1996).

Rainfall is one of the most challenging meteorological parameters to measure because of its spatial and temporal variability (Kidd, 2001; Kidd and Huffman, 2011). Conventional observations made through surface gauge networks provide the most valuable direct measurement of precipitation data on the earth's surface and are primarily important for catchment-wide area coverages (Kidd, 2001; New *et al.*, 2001; Kidd and Huffman 2011; Sene, 2013). However, surface gauge networks provide point data and are limited to covering the land surface, although a few are available over oceans. Weather radar networks are also important technologies that provide data with better spatial coverage (e.g. in national weather forecasts) than surface gauges do, but it is limited in extent and number due to its high cost (Kidd and Huffman, 2011; Sene, 2013). Nowadays, satellite observation systems receive great attention since these have better spatial coverage both over land surfaces and over oceans; however, these have coarser spatial and temporal resolutions than the other systems do (Kidd, 2001; New *et al.*, 2001; Sene, 2013). All the three of these systems used to determine precipitation have their own advantages and disadvantages. The final method that combines all the three systems together is called multi-sensor precipitation estimates (MPE), combining the best features from each measurement systems in to a single estimate (New *et al.*, 2001; Sene, 2013).

Many studies have been conducted on precipitation and its distribution patterns, at different scales. A substantial impact of global warming on the hydrology is also expected (Olsson *et al*., 2016). As a result of this, much effort has been spent on the assessment of hydro-climatology at global, national, regional, and catchment scales. To mention some of these efforts: at global level, the studies of Thomas and Henderson-Sellers (1992), Shiklomanov and Rodda (2003), Trenberth *et al*., (2007), Güntner *et al*. (2007) and McCabe and Wolock (2013) are groundbreaking. The findings of Makurira *et al*. (2010), Brooks *et al*. (2011), Herrmann *et al*. (2015), and Barthel and Banzhaf (2016) are also key contributors in gaining an understanding of the regional scale. On the catchment scale, an even greater number of studies has been conducted. However, the study of precipitation variation at both catchment and national scales in South Africa is better compared with the other components of the catchment water balance. Botai *et al*. (2015) reported that the study of hydro-meteorological variables dates back four decades in South Africa, although most of them are at catchment scales. Roy and Rouault (2013) and DEA (2013) could be mentioned as national studies. Roy and Rouault

(2013) showed a positive trend of precipitation in summer, whereas during winter, the reverse was true in South Africa. The study conducted by the Department of Environmental Affairs (DEA, 2013) indicated that there was a high inter-annual variability of rainfall in the country. The trend from 1950 to 2010 showed that it was above average in the 1970s, the late 1980s, and the mid to late 1990s, and below average in the 1960s and in the early 2000s, while reverting to mean rainfall towards 2010. There was also a significant decrease in the number of rainy days and an increase in intensity of rain events, leading to an increase in dry spell durations.

Although some catchment scale studies have been done in a South African context (Gertenbach, 1980; Dollar and Rowntree, 1995; Reason *et al*., 2005; Nel and Sumner, 2006; Hewitson and Crane, 2006), most of their analyses relied on point data, i.e. they do not show spatial variability very well. On the other hand, the spatial and temporal variations in precipitation constitute a key input for the estimation of other hydro-climatic variables. Therefore, this study was conducted to characterize the spatial and temporal variations of precipitation in the Soutloop Catchment in the Northern Cape Province, South Africa. The trend of long-term (1980–2018) precipitation events were also analysed in the catchment. Finally, the catchment was evaluated for precipitation deficits within the study period, by using the aridity index (AI) and standardized precipitation index (SPI).

4.2 Materials and methods

4.2.1 Description of the study area

The study catchment is located in the Northern Cape Province, South Africa, with a geographic location of between 22°11’00” and 23°28”00” E longitudes, and between 28°03’00” to 29°06’00” S latitudes. The details for the location and description of the study catchment can be seen in Chapter 3, Subsection 3.2.1.

4.2.2 Testing normality of time series data

It is a pre-requisite to conduct a test of normality before any statistical analysis is employed, for the sake of choosing the right statistical analysis. This test is particularly important for applying parametric statistics which assume that the data is collected from a normally distributed population. In this study, the two most-used types of normality test were used, i.e.

the graphical method (probability-probability (P-P plot) and quantile-quantile (Q-Q plot)) and the statistical method (Shapiro-Wilk test), assisted by XLSTAT ver-2018.6, build ver-53390.

4.2.3 Precipitation trend analysis

The trend analysis in the long-term (1980–2018) precipitation data was investigated by the non-parametric Mann-Kendall test (Mann, 1945; Kendall, 1975) to verify and detect trends in time series data. In this test, all the data values were evaluated as an ordered time series. Each data value was compared to the subsequent data values. The initial value of the Mann-Kendall test, *S,* in the time series was considered to be zero or no trend (Shahid, 2010; Dindang *et al.*, 2013). If a data value is greater than the previous value, then it was considered to be incremental by +1, whereas if the value was lower than the previous value, it was considered to be decremental by -1. The resultant of all such incremental and decremental values gives the final S value, and is given by the following equation:

$$S = \sum_{k=1}^{n-1} \sum_{j=k+1}^{n} Sign\left(X_j - X_k\right) \tag{4.1}$$

where $\left(X_j - X_k\right) = +1$, if $\left(X_j - X_k\right) > 0$

$\left(X_j - X_k\right) = 0$, if $\left(X_j - X_k\right) = 0$

$\left(X_j - X_k\right) = -1$, if $\left(X_j - X_k\right) < 0$

$X_1, X_2, \ldots X_i$ represents n data points, X_j represents the data point at time j, and n is the sample size.

The presence of significance between trends was tested by the normalized statistical test (*Z*-score) and computed by the following formula:

$$Z = \frac{S-1}{\sqrt{VAR(S)}}, \text{ if } S > 0$$

$$Z = 0, \text{ if } S = 0$$

$$Z = \frac{S+1}{\sqrt{VAR(S)}}, \text{ if } S < 0 \tag{4.2}$$

where *VAR* refers to the variance of the population.

On the other hand, the magnitude of the trend was calculated using the Sen's method (Sen, 1968; Adarsh and Reddy, 2015). Sen's method is useful for estimating the slope of a linear trend and it has been widely used for determining the magnitude of a trend in hydro-meteorological time series data. First, the slope of all the data pairs was calculated, as follows (Sen, 1968; Adarsh and Reddy, 2015):

$$m_i = \frac{\left(X_j - X_k\right)}{\left(j-k\right)}, \text{ for } i = 1, 2, 3, \ldots, N \qquad (4.3)$$

where N is the number of data points in the time series; and X_j and X_k are data values at times *j* and *k* (*j>k*), respectively.

Then, the median of these *N* values, m_i is Sen's estimator of slope, which is calculated as follows:

$$\beta = \begin{cases} m\dfrac{N+1}{2}, & if\ N\ is\ odd \\ \dfrac{1}{2}\left(m\dfrac{N}{2} + m\dfrac{N+1}{2}\right), & if\ N\ is\ even \end{cases} \qquad (4.4)$$

All these procedures were assisted by using an Excel add in, XLSTAT ver-2018.6, build ver-53390, which was downloaded from the following url: https://www.xlstat.com/en/download.

4.2.4 The spatial variation of precipitation

The spatial variation of precipitation in the catchment was estimated at HRU, Sub-basin, and catchment scale as a whole by the Soil and Water Assessment Tool (SWAT), as discussed in Chapter 3. All the theories and equations used to convert station data to raster values are discussed in Chapter 2, Subsection 2.5.2.1. In this section, therefore, the mean values of the long-term monthly and yearly variations of precipitation were displayed spatially. Since SWAT only generates precipitation data at sub-basin levels, the mean annual and monthly precipitation figures were interpolated by the IDW (inverse distance weighted method) in ArcGIS 10.4 software in order to gain better spatial estimates of precipitation in the catchment.

4.2.5 Precipitation deficit

The presence of precipitation deficit in the catchment was evaluated by utilizing two commonly used indicators. These are the Standardized Precipitation Index and the Aridity Index, explained as follows.

4.2.5.1 Aridity Index (AI)

The aridity index (AI) is another index that has been proposed to quantify the degree of dryness of a given location. It is commonly defined as the ratio of the annual precipitation to the evapotranspiration (UNESCO, 1979):

$$AI = \frac{P}{PET} \tag{4.5}$$

where P is the annual precipitation (mm) and PET is the potential evapotranspiration (mm).

Table 4.1 Aridity classes used for interpretation of the aridity in the catchment

No.	Aridity Class	Ranges of values
1	Hyper-arid	AI < 0.03
2	Arid	0.03 < AI<0.20
3	Semi-arid	0.20 < AI < 0.50
4	Sub-humid	0.50 < AI < 0.75
5	Humid	AI > 0.75

(Source: UNESCO, 1979)

4.2.5.2 Standardized Precipitation Index (SPI)

The Standardized Precipitation Index (SPI) was developed to monitor drought occurrence from precipitation data. This index quantifies the precipitation deficits and drought severity on different time scales in the catchment, and is calculated by the following equation (McKee *et al*., 1993; Agnew, 2000):

$$SPI = \left(\frac{P_{ik} - \overline{P}_i}{Std_i} \right) \tag{4.6}$$

where P_{ik} is precipitation for the i^{th} station and k^{th} observation, $\overline{P}_i$ is the mean precipitation for the i^{th} station, and Std_i is the standardized deviation for the i^{th} station.

Table 4.2: Drought categories based on SPI values

No.	SPI value	Drought category
1	0 to -0.99	Mild drought
2	-1.0 to -1.49	Moderate drought
3	-1.5 to -1.99	Severe drought
4	<=-2.0	Extreme drought

(Sources : McKee *et al*., 1993; Komuscu, 1999)

The calculation of SPI was assisted by using a computer program downloaded from the US National Drought Mitigation Centre website, managed by the University of Nebraska, at: https://drought.unl.edu/droughtmonitoring/SPI/SPIProgram.aspx.

4.3 Results

4.3.1 Tests of normality

The tests of the normality of the time series annual and monthly precipitation (from 1980 to 2018) were conducted in two ways; one is graphic, with a visual assessment, and the second is numerical, with statistical tests. The graphical assessment of the normality of the annual and monthly precipitation is depicted in Figures 4.1 below, panels a–d, and the numerical tests are reflected in Table 4.3 below.

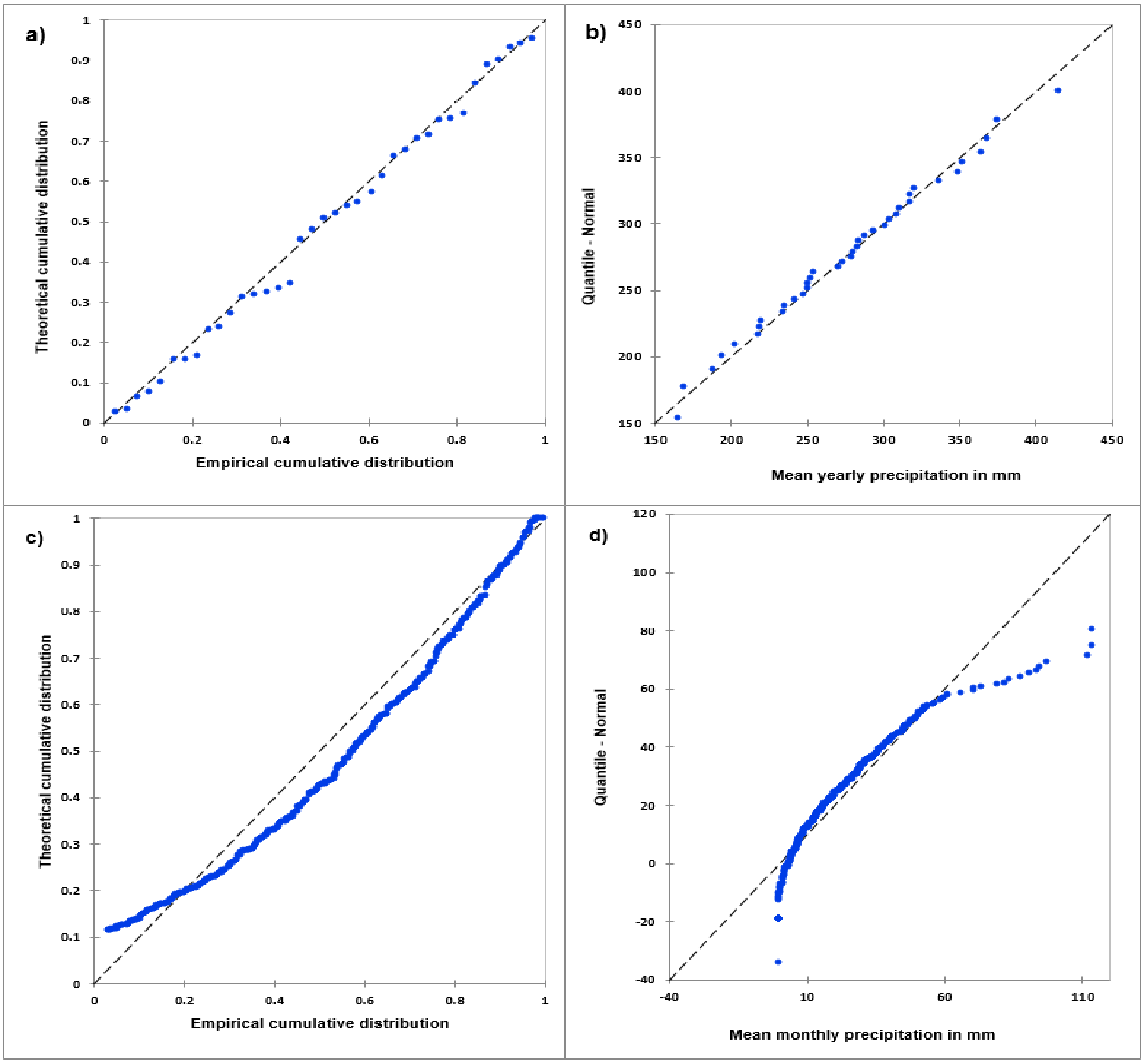

Figure 4.1: Graphical sketches showing the normality of precipitation data

Notes: (a) probability-probability (P-P plot) for mean annual precipitation, (b) quantile-quantile (Q-Q plot) for mean annual precipitation, (c) probability-probability (P-P plot) for mean monthly precipitation, and (d) quantile-quantile (Q-Q plot) for mean monthly precipitation.

Table 4.3: Tests of normality for the time series of precipitation data

Variable	Observations	Minimum	Maximum	Mean	Std. deviation	Shapiro-Wilk test	
						W	p-value
Annual Precipitation	38	165.17	415.08	277.16	59.52	0.9887	0.8829
monthly Precipitation	467	0	113.82	22.98	19.30	0.9624	< 0.0001

The simple visual assessment was conducted by utilizing two graphical sketches, as shown in Figure 4.1 above. The first one is with a P-P plot (Probability-Probability plot, Figure 4.1, panels a and c), which compares the cumulative probability of the empirical data with an ideal normal distribution. In normally distributed data, most of the data will fall on, or in close proximity around, a straight line. Based on this, the annual precipitation meets the criteria of normal distribution. The other graphical sketch, the Q-Q plot (quantile-quantile plot) in Figure 4.1, panels b and d, also shows a normal distribution for the annual precipitation, since the observed values are distributed in close proximity with the trend line of a theoretically normal distribution. Although visual inspections are easy to understand and interpret, in some cases this might be unreliable and does not guarantee that the distribution is normal (Öztuna *et al.*, 2006; Ghasemi and Zahediasl, 2012). Therefore, the statistical test could be applied. Table 4.3 above shows that the p-values of the Shapiro-Wilk test (0.8829 and < 0.0001 for annual and monthly precipitation data sets, respectively) of the annual precipitation data are normally distributed, whereas the monthly data are not normally distributed.

Generally, the analysis of normality of data, particularly for time series data sets, is a prerequisite and is the first analysis to be done before any statistical tests are made. This is because the choice of a statistical analysis is based on certain assumptions. For example, the parametric tests are based on the assumption that observations are normally distributed. Therefore, the time series data of annual precipitation for this study is normally distributed and accordingly parametric tests can be applied for conducting further data analysis. However, non-parametric tests are recommended to analyse the monthly precipitation data.

4.3.2 Trends of precipitation

The distribution of mean daily precipitation throughout the year is shown in Figure 4.2 below. It was calculated from the long-term trends (1980–2018) of precipitation records in the study catchment. The mean monthly records are also shown in Figure 4.3 below.

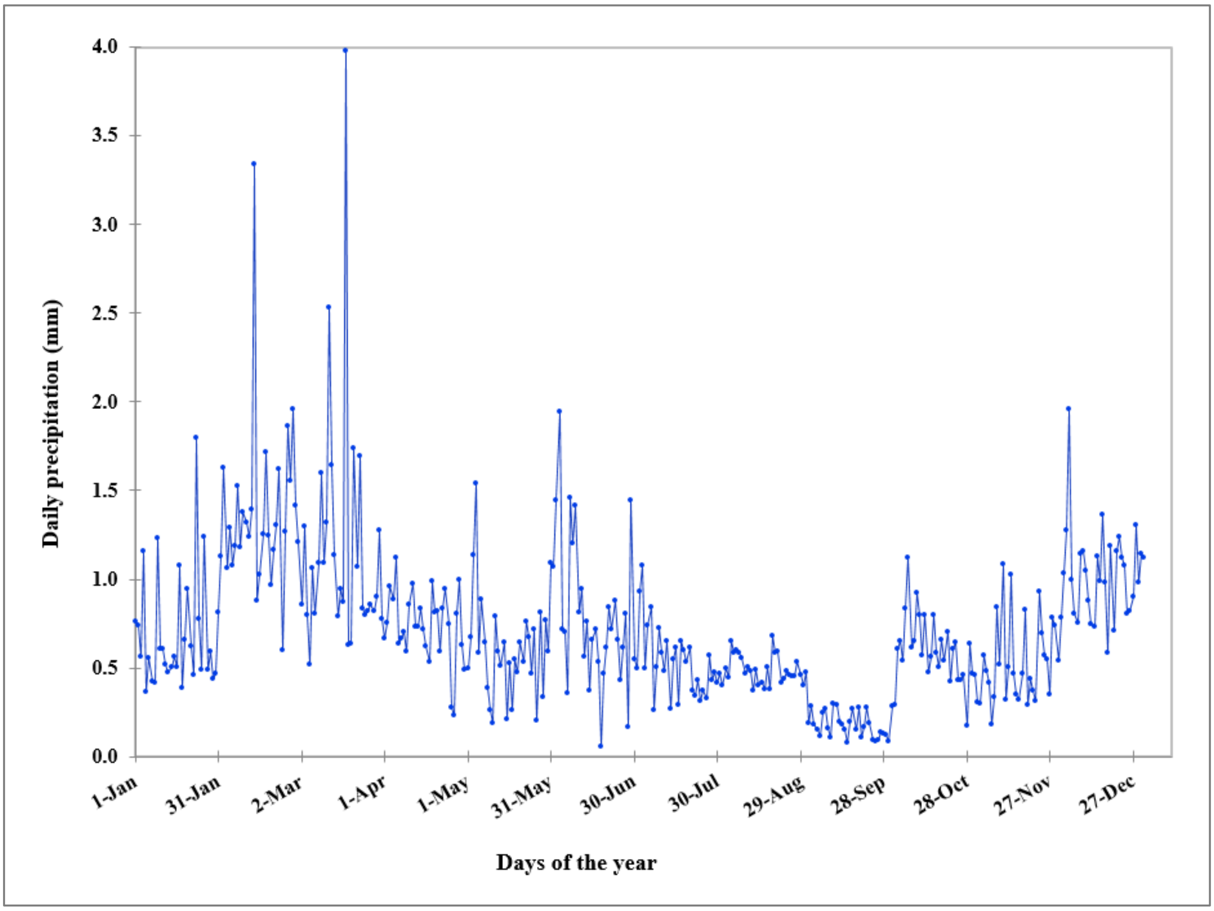

Figure 4.2: Mean daily precipitation calculated from the 39-year trend in Soutloop Catchment

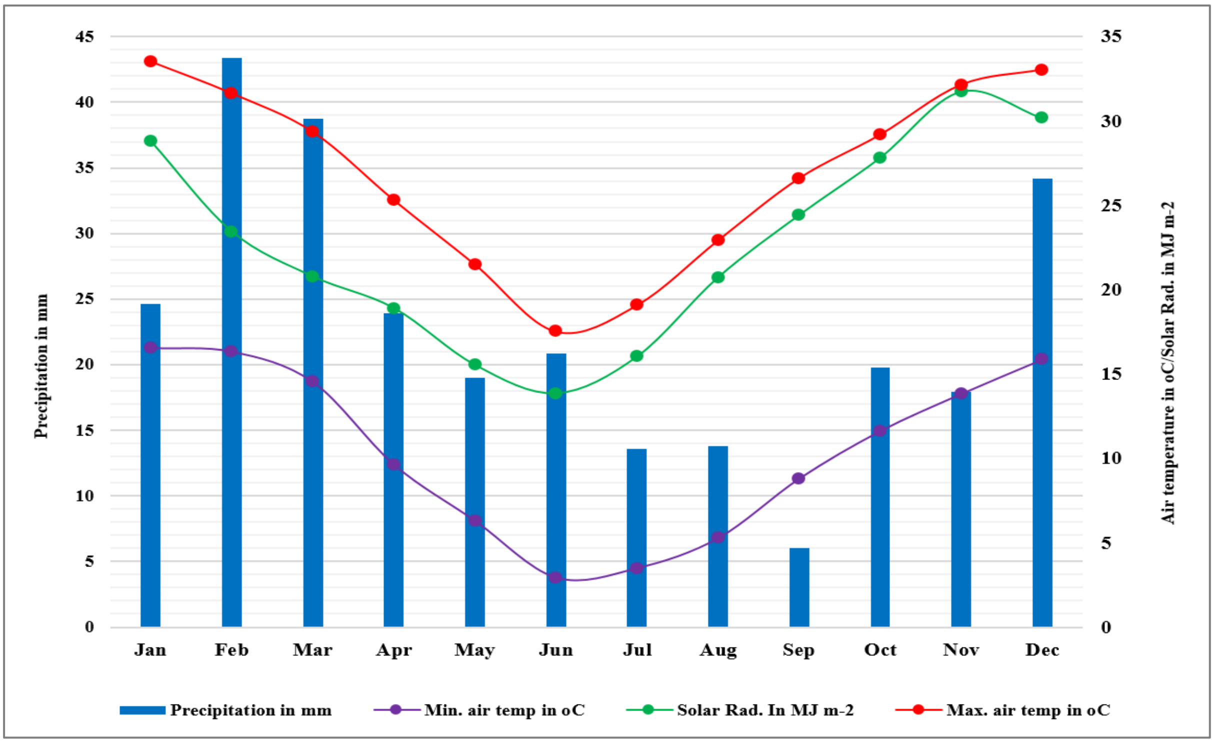

Figure 4.3: Long-term average monthly precipitation and other weather parameters in Soutloop Catchment.

As indicated in Figure 4.2 above, the long-term average minimum and maximum records for mean daily precipitation were 0.1 and 4.0 mm, respectively. The average monthly records show that September is the lowest month for precipitation, with a mean value of 6.0 mm, and that February reflects, relatively, the highest records of all the months, with a mean rainfall of 43.4 mm. In terms of seasonal distribution, summer (December, January and February) has the highest rainfall record (102 mm) in the catchment, whereas spring (September, October and November) is the lowest rainfall season, with a mean record of 44 mm. Comparing the trends of the annual precipitation in the catchment (Figure 4.4), 1983 was the lowest year for precipitation, with a record of 169 mm, whereas 2003 was the year with the highest precipitation record, at 415 mm, in the last 4 decades.

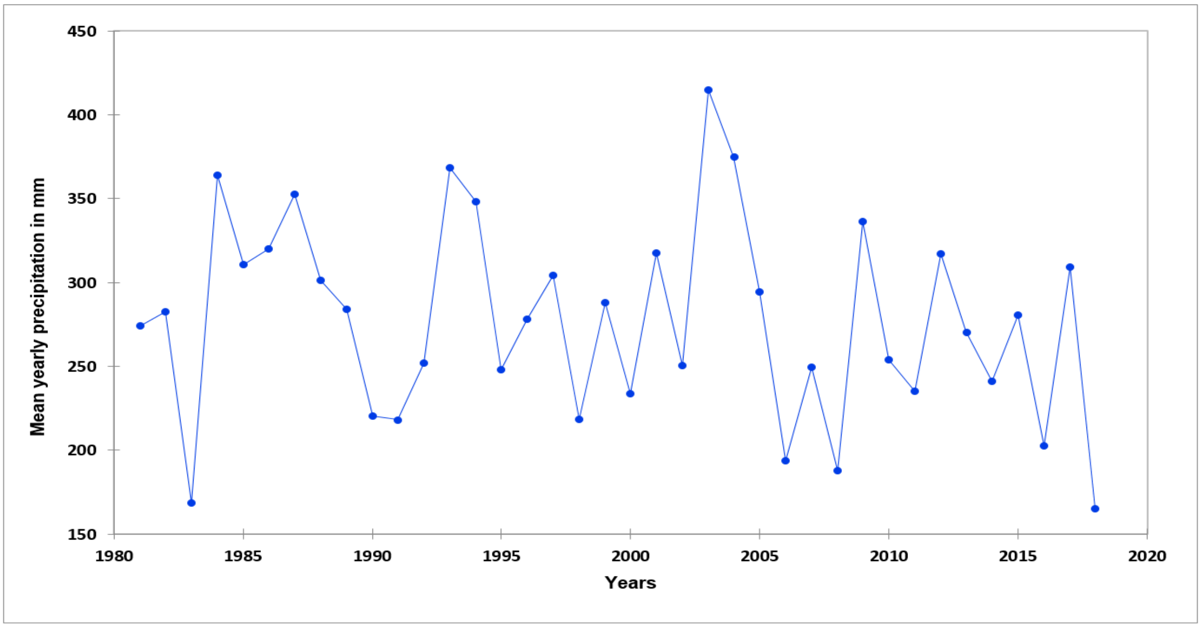

Figure 4.4: Trends of yearly precipitation in Soutloop Catchment

Regarding the trends of precipitation in the Soutloop Catchment, the Mann-Kendall trend test (Table 4.4 below) shows that there was no significant evidence for the presence of trend in annual precipitation. In the mean monthly precipitation, however, there was a negative or decreasing trend in the catchment. Figure 4.5 also shows the monthly time series variation of precipitation in the catchment. The magnitude of the decrease in the monthly precipitation was estimated by Sen's slope method. As a result, it was found that there has been an average decrease of 0.01 mm per month over the last 4 decades in the catchment.

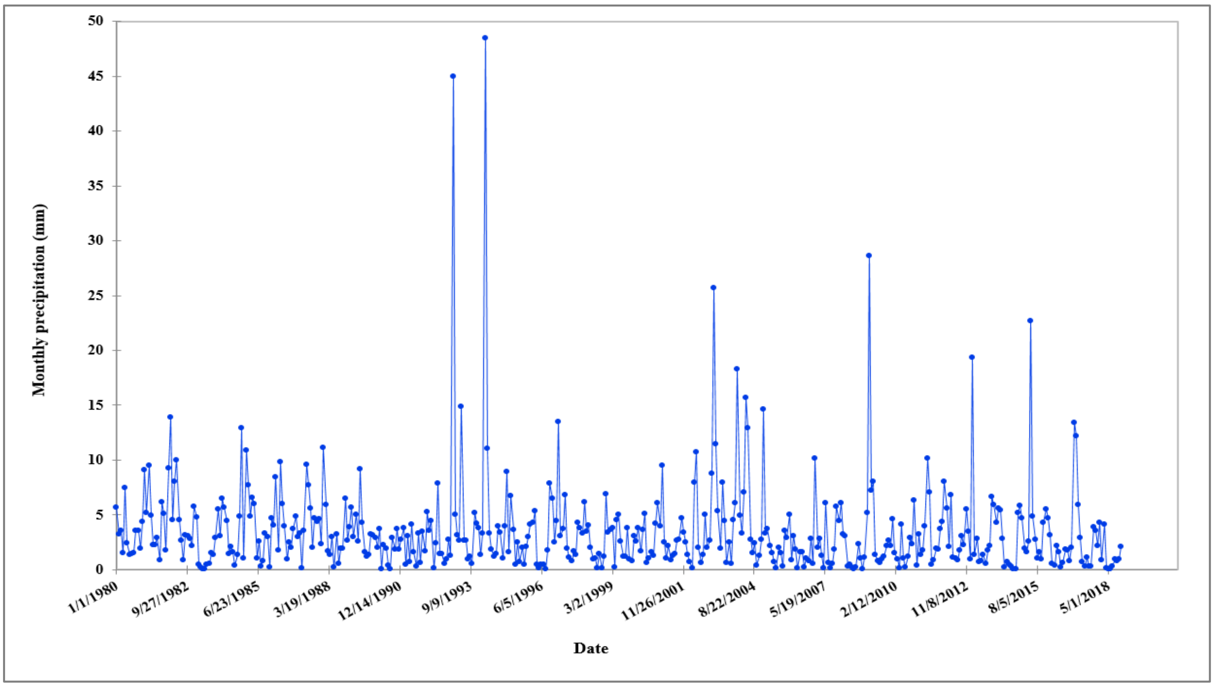

Figure 4.5: Trends of monthly precipitation in Soutloop Catchment.

Table 4.4: Statistics of the Mann-Kendall trend test for the mean yearly and monthly precipitation

Parameters	Annual Precipitation	Monthly Precipitation
Kendall's tau	-0.149	-0.061
S stat	-105	-6619
Var(S)	6327	11352277
p-value	0.191	0.05
Sen's slope	-1.355	-0.011

4.3.3 Spatial variation of precipitation

The spatial variation of the mean annual precipitation is depicted in Figure 4.6 below. The long-term (1980–2018) annual precipitation was averaged and interpolated by the IDW (inverse distance weighted method) in ArcGIS 10.4 software. A similar method was applied for the long-term mean monthly precipitation, and the results are displayed in Figures 4.7 to 4.10 below. The mean annual precipitation showed a spatial and temporal variation in the catchment. Hence, the mean annual precipitation varies from a minimum of 214 mm in the southern and south-western parts of the catchment to a maximum record of 365 mm per annum in the north and north-western parts (Figure 4.6 below). Therefore, the annual precipitation decreases as one goes from north to south in the catchment.

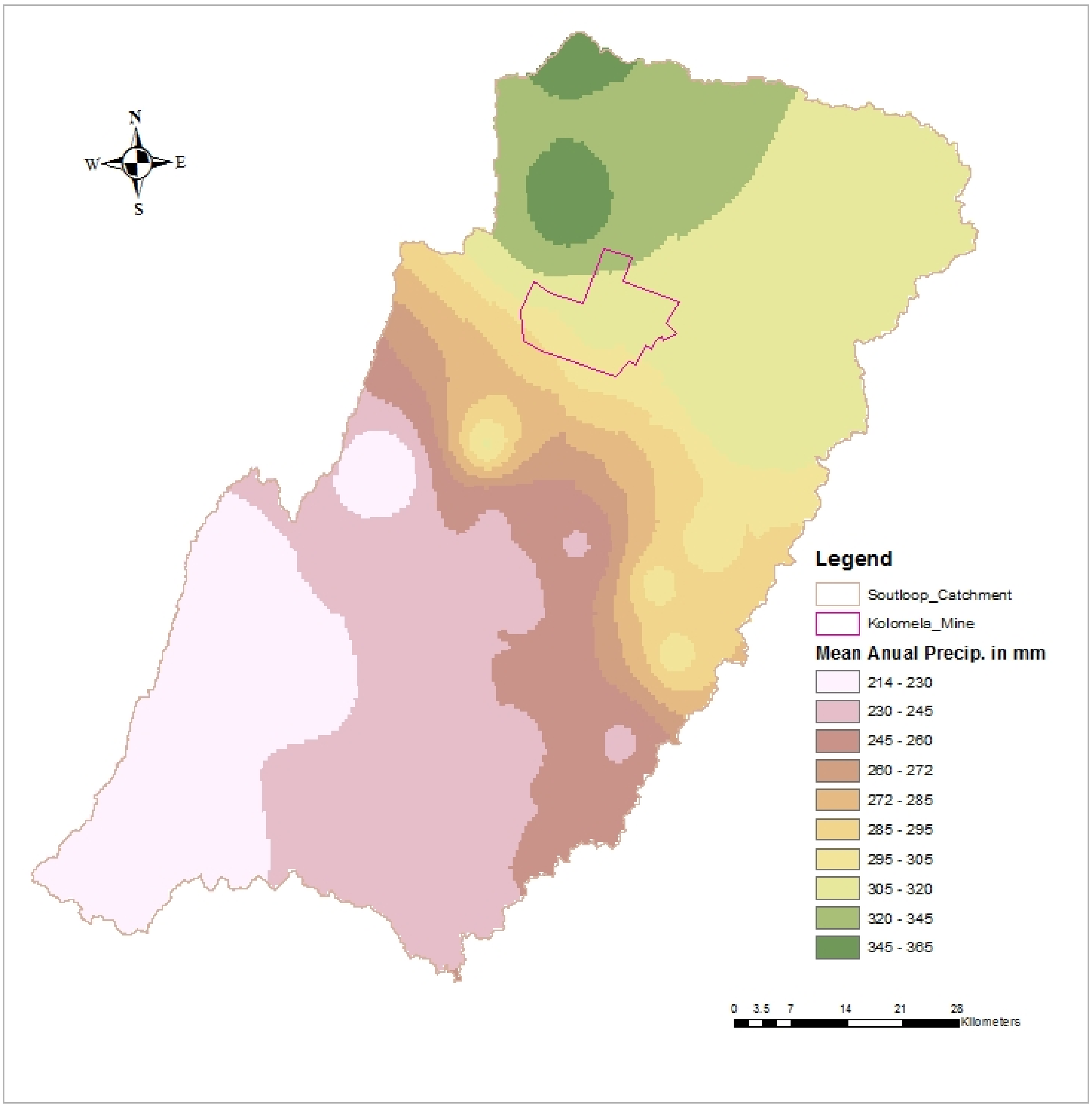

Figure 4.6: Spatial variation mean annual precipitation in Soutloop Catchment

The long-term mean monthly precipitation in Soutloop Catchment also showed both spatial and temporal variations, as seen in Figures 4.7 to 4.10 below. Hence, February is the month with the highest precipitation record, while September is the month with the lowest precipitation record in the catchment. The patterns of the spatial variation can also be seen in meteorological seasons. The comparison of seasons regarding their spatial precipitation variations shows that during summer, precipitation increased from a north to south direction in the catchment (Figure 4.7 below). This variation is also true for autumn, except for May (Figure 4.8 below). However, precipitation increased as one moves from south to north during winter time, which is the opposite of the summer season (Figure 4.9 below). There were no clear trends of spatial variation detected during the spring season, (Figure 4.10 below).

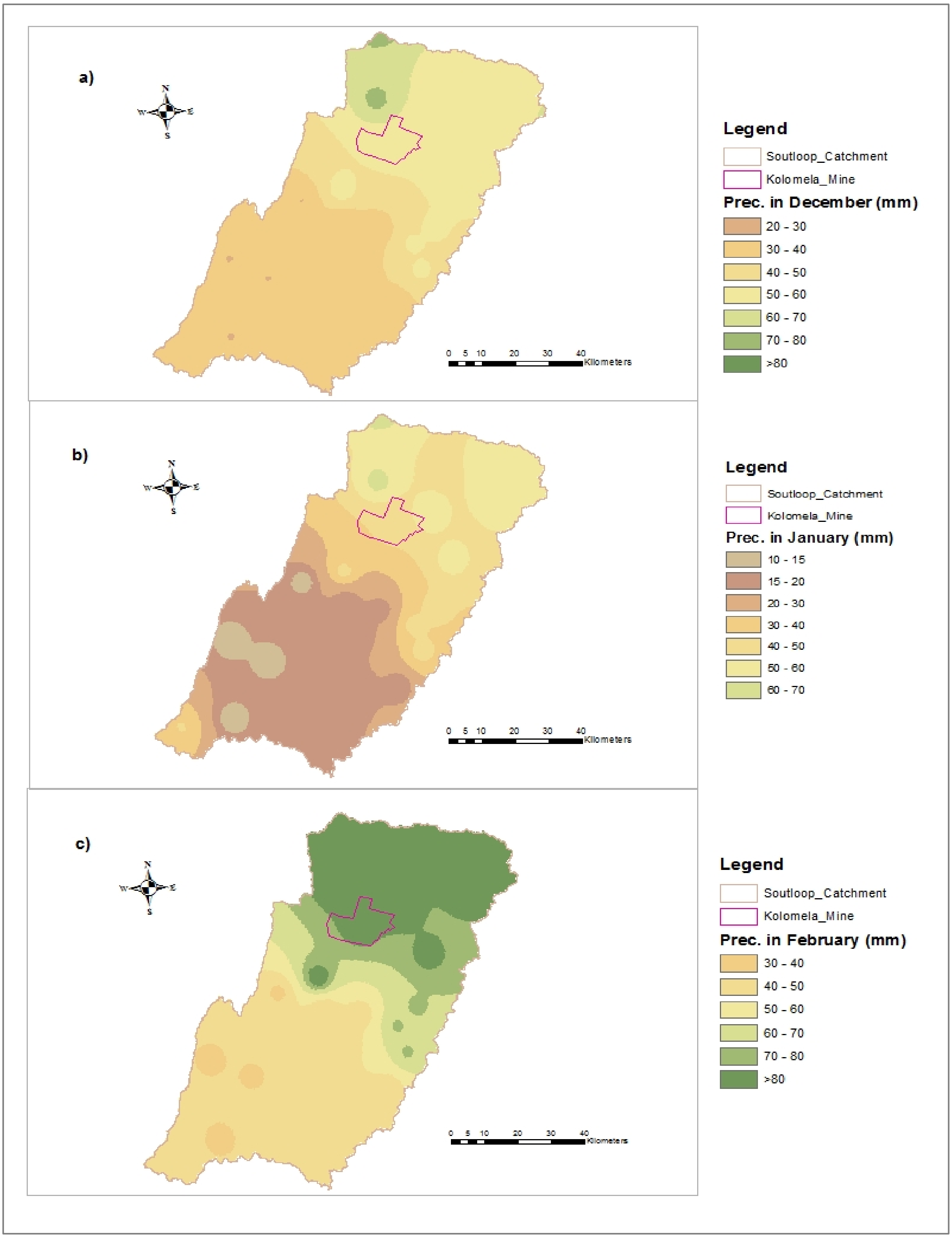

Figure 4.7: Spatial variation of the mean monthly precipitation (a) December, (b) January and (c) February

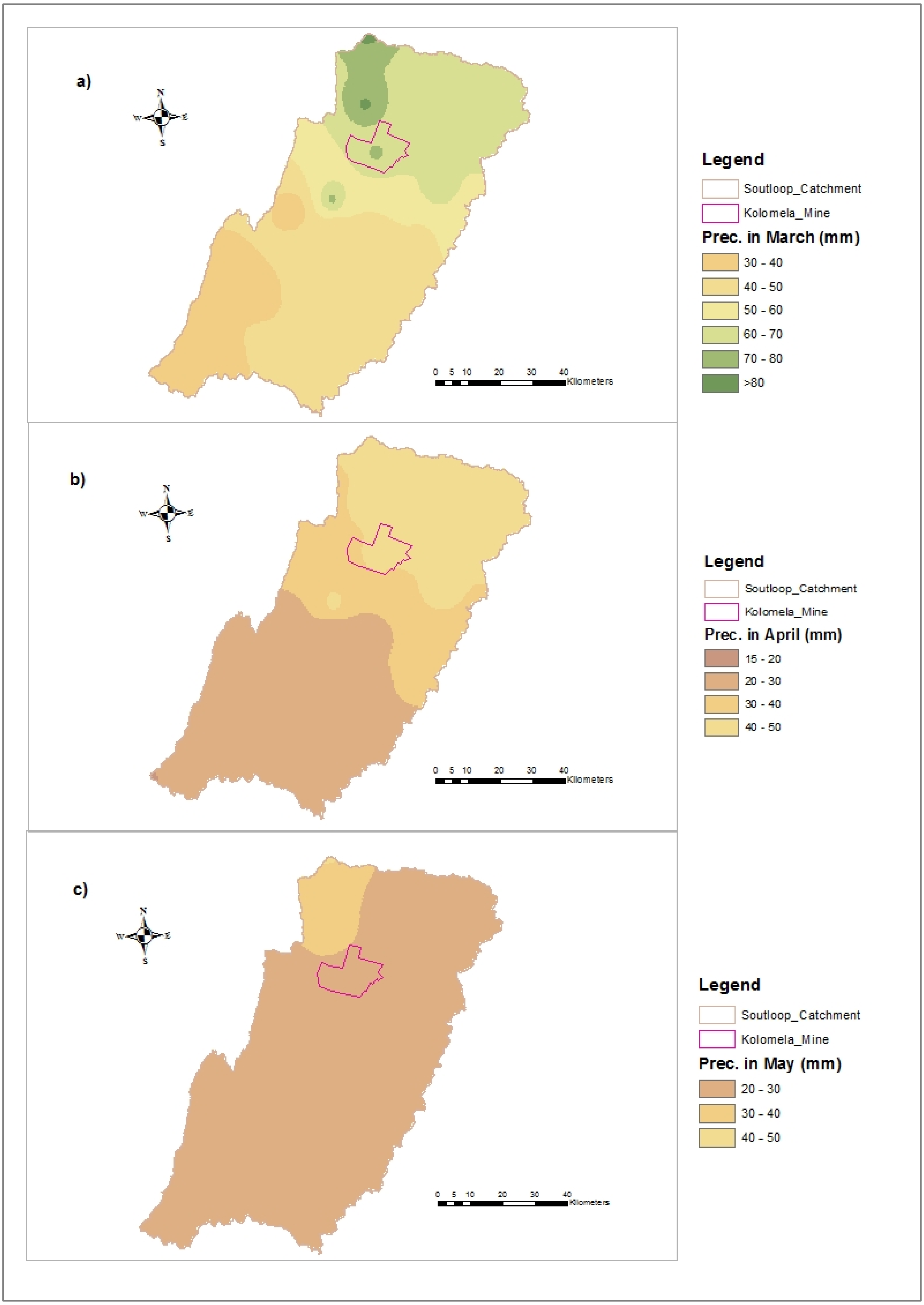

Figure 4.8: Spatial variation of the mean monthly precipitation (a) March, (b) April and (c) May

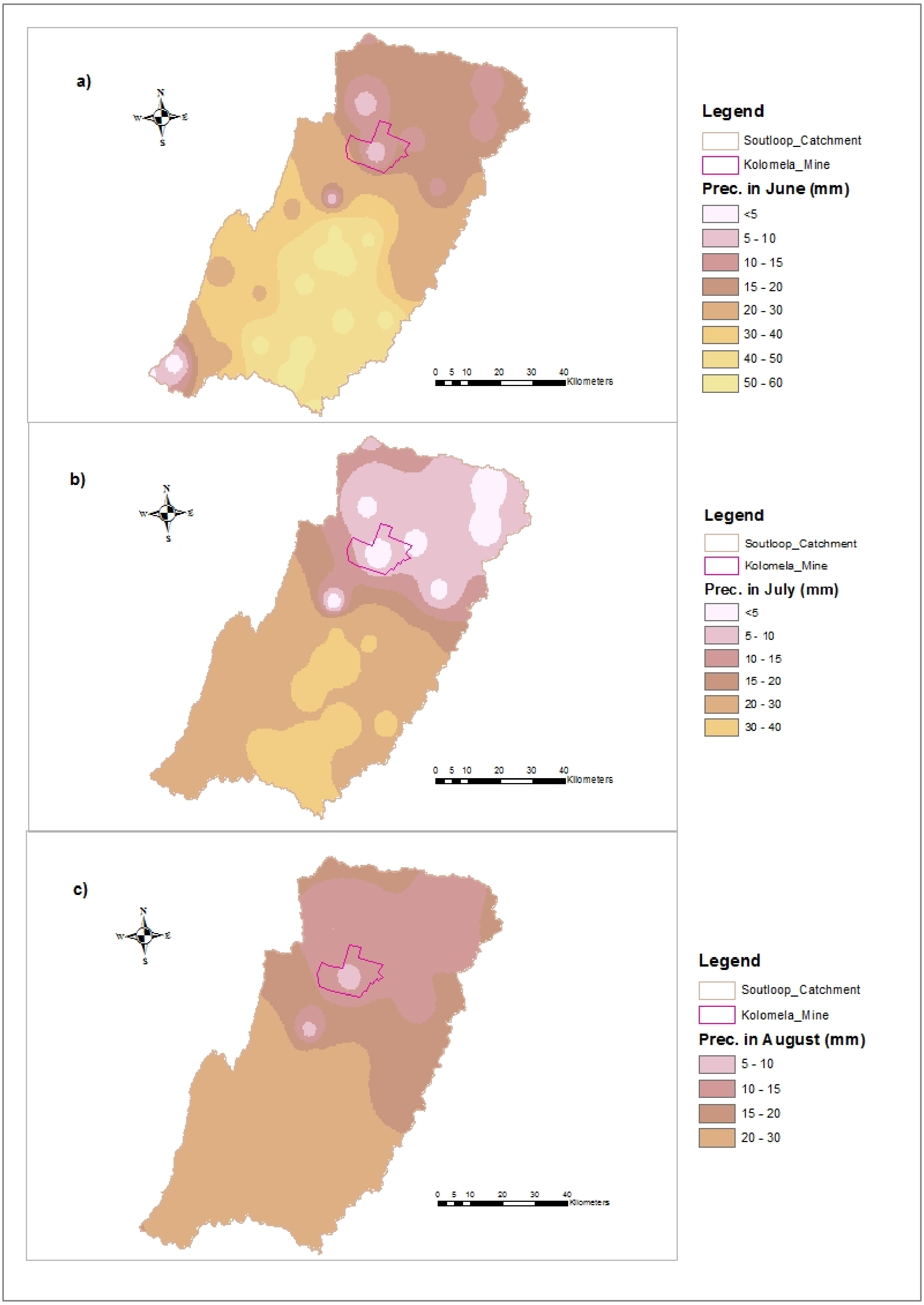

Figure 4.9: Spatial variation of the mean monthly precipitation (a) June, (b) July and (c) August

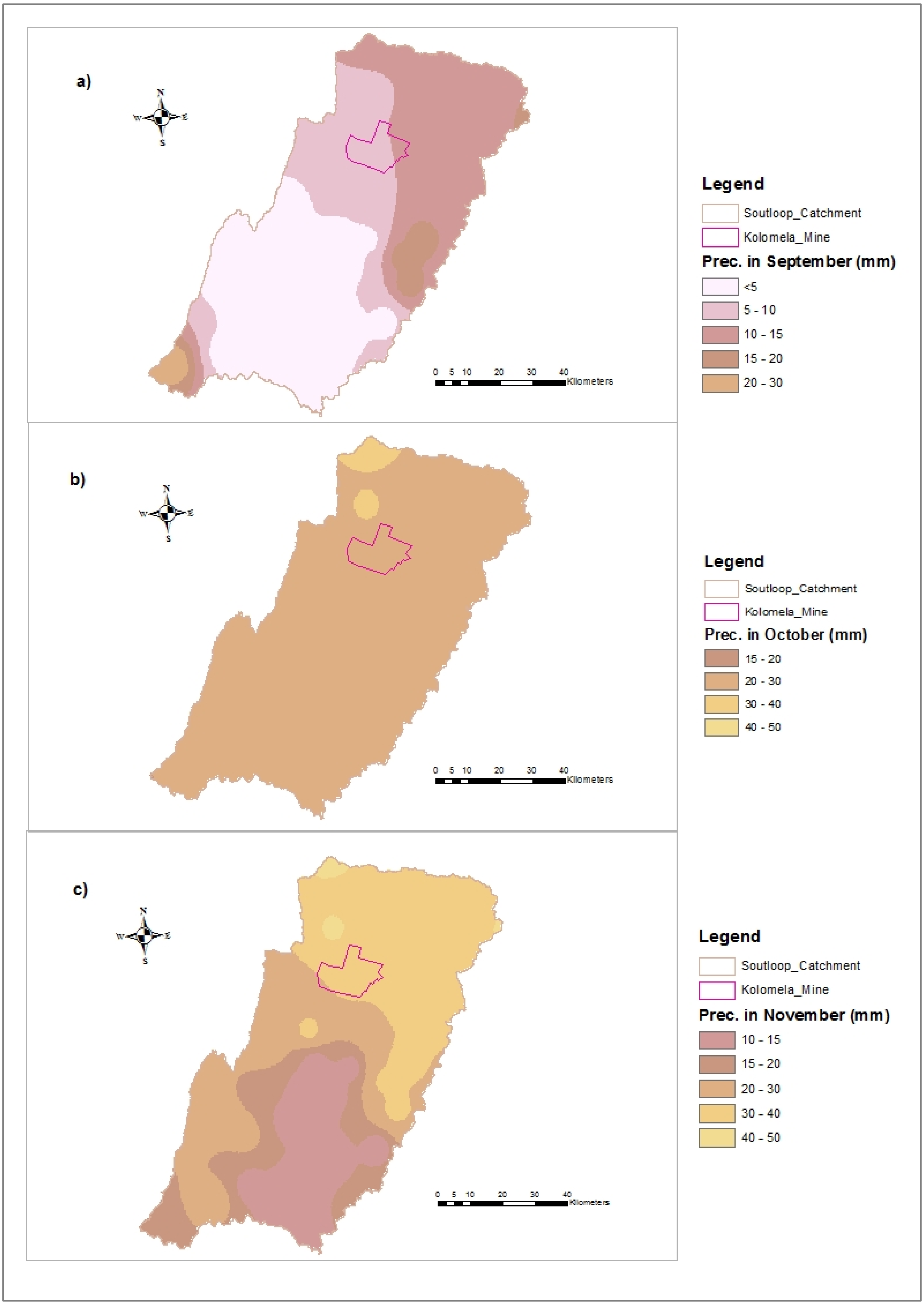

Figure 4.10: spatial variation of the mean monthly precipitation (a) September, (b) October and (c) November

4.3.4 Indicators of precipitation deficit

As discussed in this subsection, two important indices were used to assess the deficit of precipitation in the Soutloop Catchment. These are the aridity index and the standardized precipitation index. The aridity index (AI) is a measure of the climatic condition for a given place, whereas the standardized precipitation index (SPI) is a measure of the climatic condition for a specific time period. In other words, aridity is more or less a permanent index, whereas SPI shows the deviation of precipitation from the normal period, hence, it changes over time. Figure 4.11 below shows the spatial variation of the aridity index in the Soutloop Catchment. It shows that the catchment is categorized as an arid catchment (AI value varies from 0.0774 to 0.153), with no spatial variation in terms of the aridity class (UNESCO, 1979), as depicted in Table 4.2 above.

Similarly, the SPI is important to show the time series variation of rainfall variability of an area, which is shown in Figure 4.12 below for different seasons. Table 4.5 below also shows the trends of the standardized precipitation index in Soutloop Catchment, tested for five inter-annual periods, selected from the 1980 to 2018 simulation years. Based on the Mann-Kendall test (Table 4.5 below), there was no significant difference found within the trends of the one month-SPI. However, there was a significant trend in the 3-, 6-, 9- and 12-month SPIs from 1980 to 2018 in the catchment. The Sen's slope value also shows that there were average decreasing trends of 0.0007, 0.0006, 0.0006 and 0.0007 for the 3-, 6-, 9- and 12-month SPIs, respectively.

The time series analysis of the inter-annual SPI values (Figure 4.12 below, panels a–d) shows that the 1983 drought was the worst ever over the last four decades (1980–2018). Based on McKee *et al*. (1993) and Komuscu (1999), this drought can be categorized as a moderate drought. Similarly, mild droughts occurred between 1990 and 1992, 1995 and 1996, 1998 and 2000, 2006 and 2008, and 2014 and the current time. Accordingly, the mild drought that started in 2014, and currently continues, is the longest consecutive drought experienced since 1980 in the catchment. On the other hand, Figure 4.12 below, panels a–d, also shows periods with above-normal rainfall in the region. The 2003–2004 years were the best wet years that had above-normal rainfall. The 1985–1989 years constitute the longest period with above-normal rainfall since 1980 in the catchment.

The spatial variation of the standardized precipitation index (SPI) in the Soutloop Catchment is depicted in Figure 4.13 below for different years of the 12 month-SPI. The selected periods for the comparison of the spatial variations of the 12 month-SPI were the months of January in 2000, 2005, 2010 and 2015. The January, 2000, SPI (Figure 4.13 below, panel a) shows that mild to moderate drought conditions were experienced in all the northern parts, in the tips of the south-western part, and in the south-eastern part of the catchment. However, the other part of the catchment was receiving rainfall that was slightly above normal. In 2005, most of the catchment was getting above-normal rainfall, except the south-western tip. During this time, the catchment had even experienced a very high rainfall, as compared with the catchment's mean rainfall value. Similarly, the January, 2010, SPI shows that much of the northern, eastern and south-eastern parts had experienced precipitation that was slightly above normal for a wet season. The south-western part experienced mildly dry to dry conditions. Finally, the January, 2015, SPI shows that the catchment experienced one of the largest droughts that covered most of its parts, except for its south-western part and some pocket areas in the north.

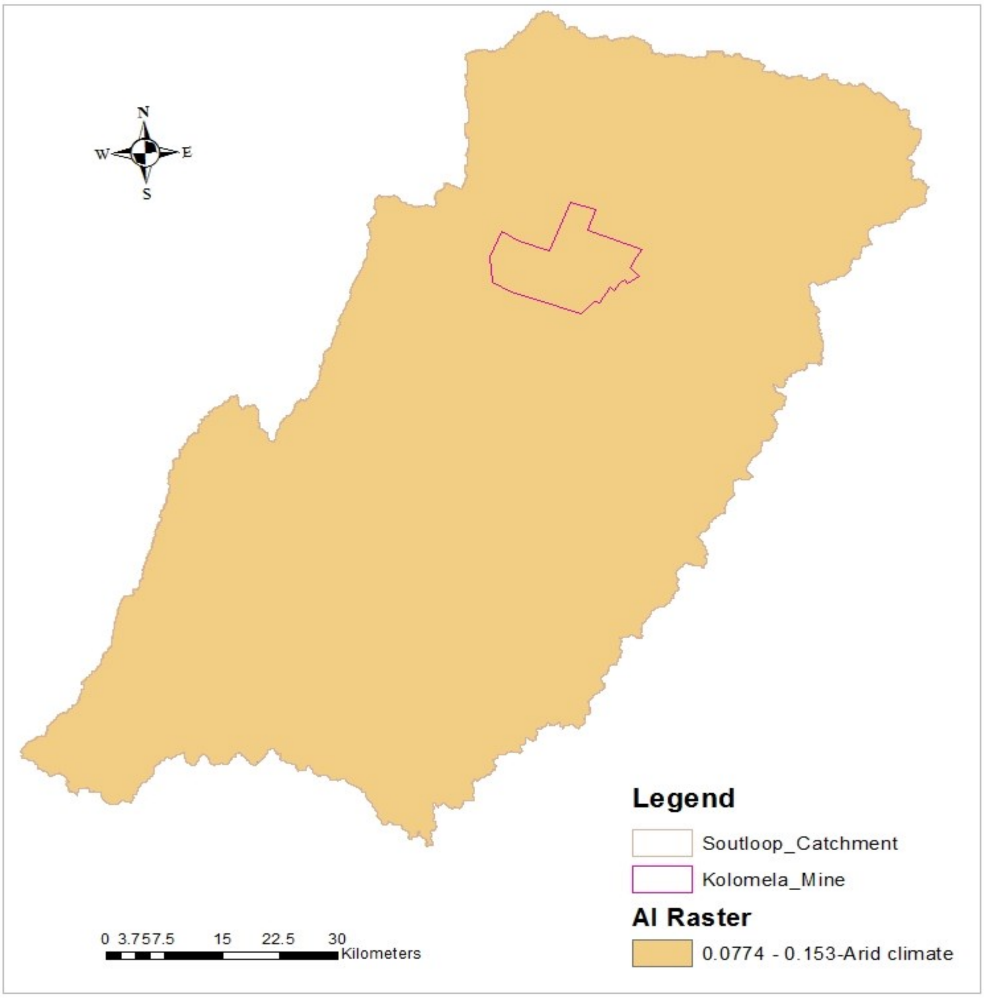

Figure 4.11: Spatial variation of the aridity index (AI) in Soutloop Catchment

Table 4.5: Statistics of the Mann-Kendall trend test for the different period SPIs

parameters	1-month SPI	3-month SPI	6-month SPI	9-month SPI	12-month SPI
Kendall's tau	-0.0251	-0.0736	-0.0792	-0.0837	-0.0933
S	-2739	-7975	-8465	-8832	-9723
Var(S)	11425577	11279892	11063684	10850226	10639550
p-value	0.4179	0.0176	0.0109	0.0073	0.0029
Sen's slope	-0.0002	-0.0007	-0.0006	-0.0006	-0.0007

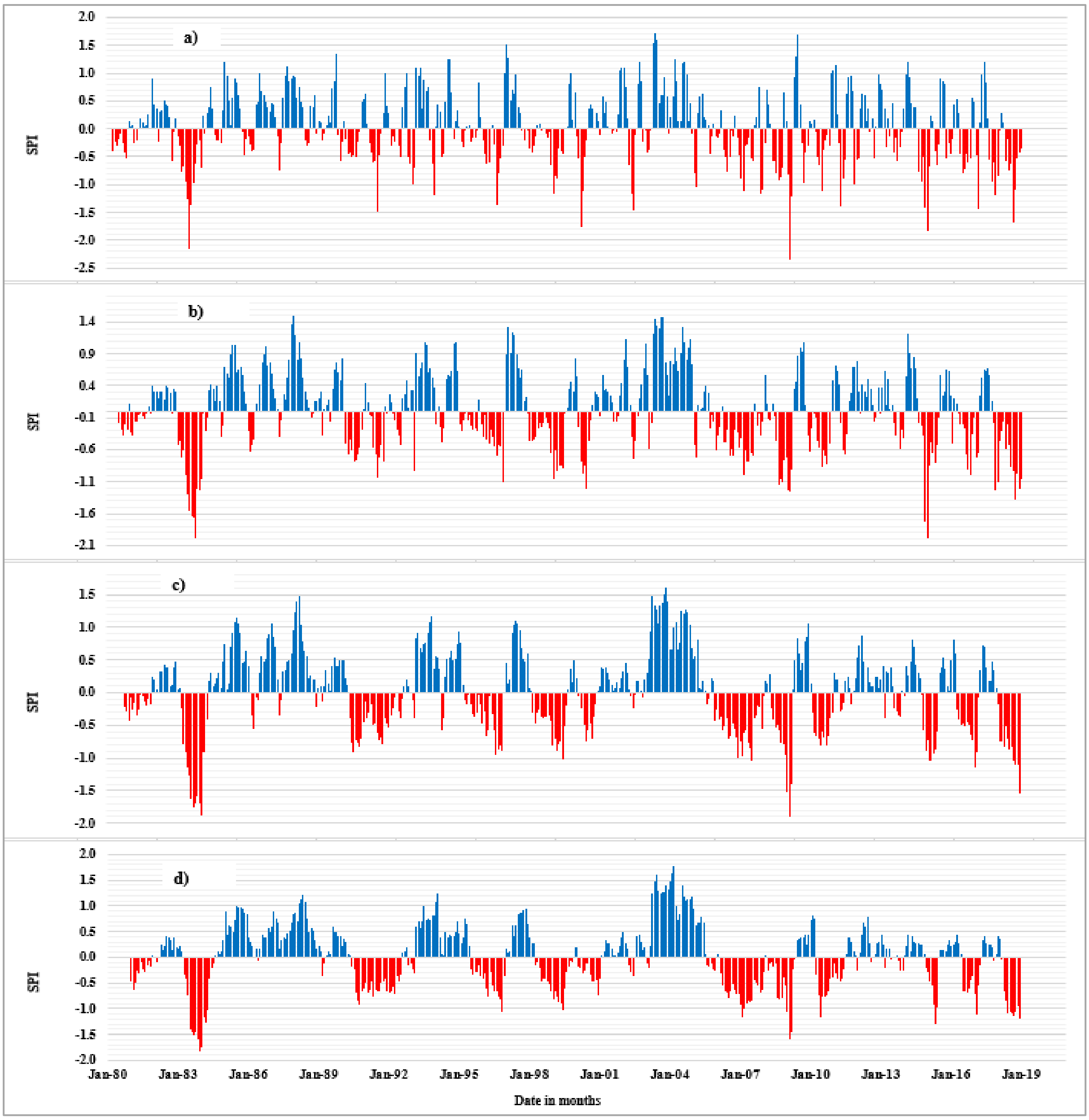

Figure 4.12: Trends of the standardized precipitation index in the Soutloop Catchment

Notes: (a) a 3-month SPI, (b) a 6-month SPI, (c) a 9-month SPI, and (d) a 12-month SPI.

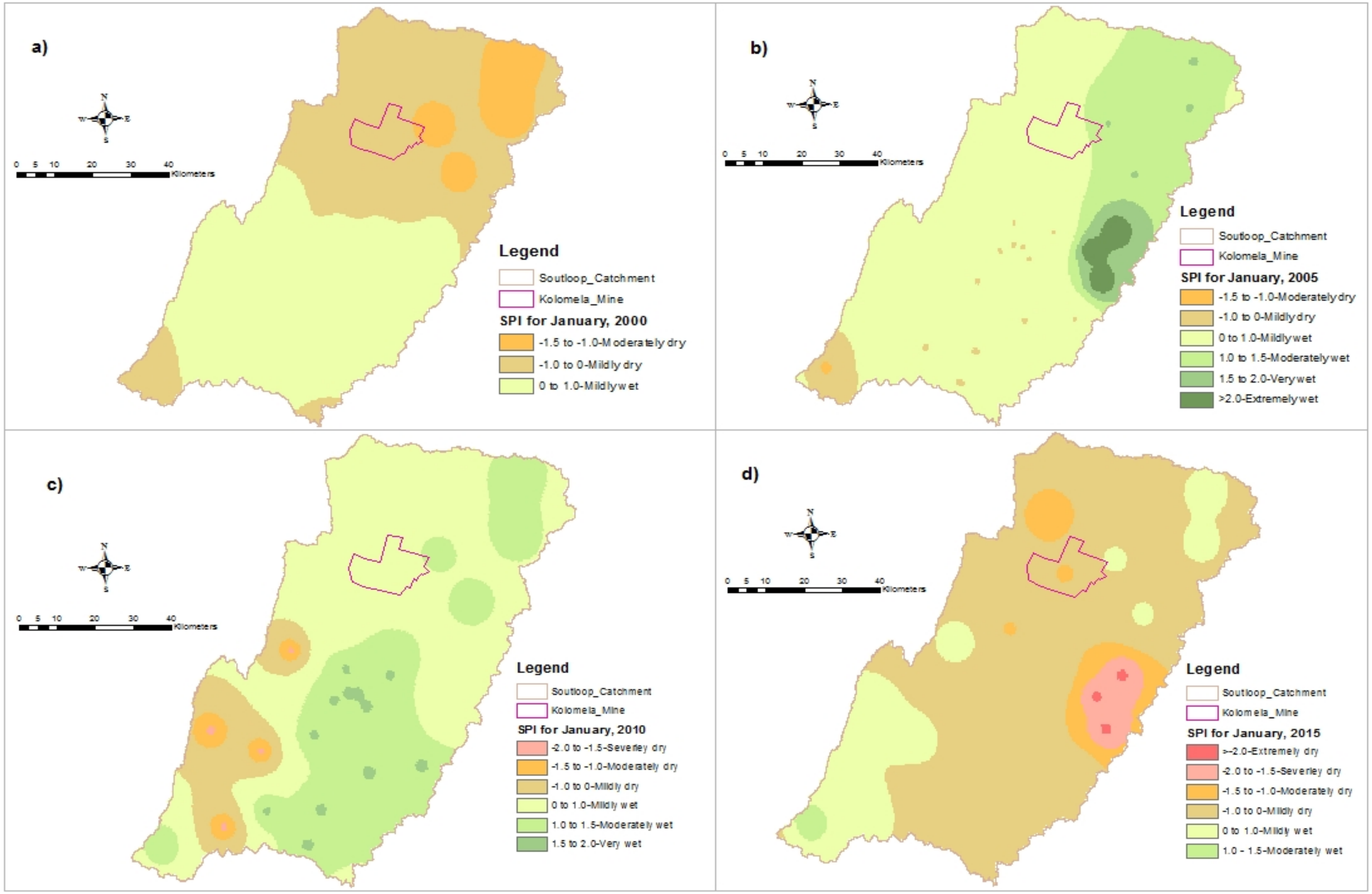

Figure 4.13: Spatial variations of twelve-month SPI in Soutloop Catchment at different time periods

Notes: (a) January, 2000, (b) January, 2005, (c) January, 2010, and (d) January, 2015.

4.4 Discussions

4.4.1 Precipitation variability

South Africa is a semi-arid country, characterized by a variable precipitation at diurnal, intra-seasonal, and annual timescales (CSIR, 2010; Colvin *et al*., 2016; Botai *et al*., 2018). Besides its temporal variation, the spatial variation of precipitation is also significant in the country (Richard *et al*., 2001; Roy and Rouault, 2013; Botai *et al*., 2018). In the study catchment, particularly, the precipitation is highly variable both in a spatially and a temporal manner, where the intensity, frequency, duration and distribution should always be of concern to farmers and water resource managers.

The Soutloop Catchment receives mainly summer precipitation, which usually starts in December and ends in February. However, significant amounts of precipitation are also recorded in other seasons. Although the general yearly trend was more or less constant in the consecutive years under study, the 1983 mean annual precipitation registered the lowest record of precipitation, whereas 2003 experienced the maximum mean annual precipitation in the catchment. The minimum annual precipitation of 1983 exactly matches the occurrence of drought in South Africa, as reported by other researchers (Rouault and Richard, 2003; Kane, 2009). The absence of a significant trend in the annual precipitation is also consistent with the reports of Kane (2009), MacKellar *et al*. (2014), Davis *et al*. (2016), Kruger and Nxumalo, (2017), Tfwala *et al*. (2018) and Botai *et al*. (2018). However, the Mann-Kendall trend test on the mean monthly values showed decreasing trends in the catchment. This shows that the intra-annual variations (seasonal and monthly variability) are more prevalent than the yearly variations in the catchment area. This result is consistent with the findings of Davis *et al*. (2016) that was conducted in the Namaqualand area, situated in the south-western part of the Northern Cape Province. However, it is in contrast to other studies (DEA, 2013; MacKellar *et al*., 2014) that have been conducted in the Northern Cape Province, although the scale of those studies was on a provincial level.

Similarly, this study shows the presence of a spatial variation, as it is true for an intra-annual variation in the study catchment. For example, the mean annual precipitation varies from 214 mm in the southern and south-western parts of the catchment to a maximum record of 365 mm per annum in the north and north-western parts (Figure 4.6 above). Hence, precipitation decreases from north to south, annually. The possible reason for these local variations of precipitation could be: (i) it is evidenced in Chapter 3 that the northern part has a higher altitude than the southern part has, and as a result, the difference in altitude could have contributed towards the local variations; and (ii) the main rainfall season in the south-western part of the Northern Cape province, for example, the Namaqualand region, is in the winter season (Hoffman *et al*., 2009; Davis *et al*., 2016). Hence, it is believed that the southern part of Soutloop Catchment could have been influenced by the rain-bearing conditions of the Namaqualand area and its surroundings. There is other evidence that shows the impact of the Namaqualand area on the effect of seasonal changes in the Soutloop Catchment. The rainfall totals in the winter seasons (June to August) in the central and southern sub-basins in the catchment are higher than the northern sub-basin totals. However, the annual rainfall totals increase as one moves from south to north, which is a good indicator that the winter rainfall areas in the south-western Northern Cape Province are influencing the spatial variability of rainfall in the Soutloop Catchment.

4.4.2 Evaluation of precipitation deficit

The deficit in atmospheric precipitation is the cause of drought and shortages of water for all forms and activities of life on earth. The precipitation deficit can be defined as the difference between the potential evapotranspiration and the actual mean precipitation record. Hence, as the amount of recorded precipitation decreases below the potential evapotranspiration, the precipitation deficit soon starts. However, this deficit could not be called a drought for only a certain, limited period of time. Hence, drought is properly understood to be an accumulated water deficit that imposes significant influences on the economic, social, and environmental entities of an area (UNESCO, 1979; Agnew, 2000; Komuscu, 1999; WMO, 2012). However, some parts of the world receive a lower mean precipitation for an indeterminate time period. Such areas are called arid areas. Therefore, drought is a departure from the usual or mean precipitation, while ‘aridity’ refers to the average conditions of limited rainfall and water supplies for an area.

Two main indices were used to evaluate the presence of a precipitation deficit and its severity levels in the catchment. The first and the simpler indicator is the aridity index (AI). As depicted in Figure 4.11 above, the AI values vary from 0.0774 to 0.153 in the catchment. Moreover, based on the classification of aridity classes by UNESCO (1979) given in Table 4.2 above, the catchment is classified as an arid catchment. The second and relatively more complex index is the standardized precipitation index (SPI), which shows the time series variability of precipitation, and is perhaps a good indicator for water deficit and drought. The time series trends of SPI at different time scales are given in Figure 4.12 above. The relatively wettest year was 2003/2004, with average SPI values of 0.65, 0.92, 1.20 and 1.17, at 3-, 6-, 9- and 12-month time scales, respectively. Similarly, the driest year was 1983, with average SPI values of -0.86, -1.16, -1.21 and -1.01, at 3-, 6-, 9- and 12-month time scales, respectively, and the drought is categorized as mild to moderate drought, based on the time scales. Mild droughts occurred between 1990 and 1992, 1995 and 1996, 1998 and 2000, 2006 and 2008, and 2014 and the current time. The droughts of 1983 and 1992 are also reported on by Rouault and Richard (2003) and Kane (2009). Rouault and Richard (2003) and Kane (2009) also suggested El Nino as being the cause of droughts experienced since 1960. The precipitation deficit and drought are also spatially variable, as shown in Figure 4.13 above, panels a–d.

Most of the droughts that have occurred in the study area have been mild droughts. However, this does not mean that there is not a problem regarding water scarcity. The area is already arid and accordingly water availability is a problem of indefinite duration. However, the SPI values are still important for showing the rainfall variability and the intensification of water deficit from the normal rainfall years, and for predicting the additional burdens placed on the catchment during times of drought. The additional burdens might be different in nature, based on the intensity of the SPI values. Based on WMO (2012) and Zargar *et al*. (2011), a 3-month SPI is used to evaluate short-term soil water conditions with respect to seasonal crop growth. The 6-month SPI indicates seasonal to medium-term trends in precipitation. Similarly, the 9-month SPI provides an indication of inter-seasonal precipitation patterns over a medium timescale, and is a good indicator for agricultural drought. The 12-month SPI, on the other hand, reflects long-term precipitation patterns in the catchment and shows the impact of drought on stream flow, and on reservoir and groundwater levels. However, it is difficult to interpret and predict the impacts of drought, and draw conclusions based on the SPI values directly in low-rainfall areas, as arid catchments experience a more or less permanent water stress. For example, the 12-month SPI of 2003 was 1.13, i.e. it was moderately wet, which seems to suggest that no water stress was experienced in that time. However, the precipitation was 415.08 mm per annum, yet there was water scarcity. It is also shown that the 1983 drought was the worst experienced over the last 4 decades in the catchment. Based on the values of the 6- and 9-month SPIs, this drought could have had a significant impact on agriculture. Similarly, the 12-month SPI could also interpreted that there was a significant impact on stream flow, and on water levels in reservoirs and groundwater tables (WMO, 2012; Zargar *et al*., 2011).

However, in reality there is no cultivation of crops and no surface water, even during normal rain years, which is caused by the normal climate of the catchment, and not just drought. Therefore, the interpretation of SPI values must be conducted cautiously for arid catchments.

4.5 Conclusion

The aim of this study was to analyse the spatial and temporal variability of precipitation and its impact on the Soutloop River Catchment by using the Soil and Water Assessment Tool (SWAT). The output from the SWAT model could not describe the spatial variations of precipitation properly, since the model generates the time series precipitation values on sub-basin levels. This is a limitation of the model that does not apply to other components of the catchment water balance. As a result of this, the spatial variation was successfully analysed by using the inverse distance weighted method (IDW). However, the SWAT weather generator tool was successful in estimating time series precipitation for ungauged sub-basins and in filling missing values for some precipitation gauges.

The precipitation in the catchment varies from 214-365 mm per annum, which is nearly half of the South African average annual precipitation. Therefore, precipitation deficit is a permanent occurrence in the catchment. The study shows that the precipitation displays spatial and temporal variations in the catchment. It is also shown that the intra-annual (within months, seasons, etc.) variability is more prevalent than the inter-annual variability is.

The standardized precipitation index is good for showing water availability and the occurrence of drought. It can be applied in arid catchments to show the extra burdens that are placed on top of the aridity to the water deficit to the area. However, further analysis and conclusions regarding the possible consequences for the water resources of arid-catchments could be misleading, since arid catchments have unique hydro-meteorological characteristics. Therefore, the evaluation of the precipitation deficit and further inference of consequences based on the standardized precipitation index (SPI) in arid catchments should be interpreted cautiously.

4.6 References

Adarsh, S. and Janga Reddy, M., 2015. Trend analysis of rainfall in four meteorological subdivisions of southern India using nonparametric methods and discrete wavelet transforms. *International Journal of Climatology*, 35(6), pp.1107-1124.

Agnew, C.T., 2000. *Using the SPI to identify drought*. University of Nebraska-Lincoln, Lincoln, Nebraska, USA.

Augustine, D.J., 2010. Spatial versus temporal variation in precipitation in a semiarid ecosystem. *Landscape Ecology*, 25(6), pp.913-925.

Barthel, R. and Banzhaf, S., 2016. Groundwater and surface water interaction at the regional-scale–a review with focus on regional integrated models. *Water Resources Management*, 30(1), pp.1- 32.

Botai, C.M., Botai, J.O. and Adeola, A.M., 2018. Spatial distribution of temporal precipitation contrasts in South Africa. *South African Journal of Science*, 114(7-8), pp.70-78.

Botai, C.M., Botai, J.O., Muchuru, S. and Ngwana, I., 2015. Hydro-meteorological research in South Africa: a review. *Water*, 7(4), pp.1580-1594.

Brooks, P.D., Troch, P.A., Durcik, M., Gallo, E. and Schlegel, M., 2011. Quantifying regional scale ecosystem response to changes in precipitation: not all rain is created equal. *Water Resources Research*, 47(10).

Colvin, C., Muruven, D., Lindley, D., Gordon, H. and Schachtschneider, K., 2016. *Water Facts and Futures: rethinking South Africa's water future*. WWF-SA 2016: water facts and futures, pp.2-96.

Council for Scientific and Industrial Research (CSIR), 2010. *A CSIR perspective on water in South Africa–2010*. CSIR Report No. CSIR/NRE/PW/IR/2011/0012/A, ISBN: 978-0-7988-5595-2.

Daly, C., 2006. Guidelines for assessing the suitability of spatial climate data sets. *International Journal of Climatology,* 26(6), pp.707-721.

Davis, C.L., Timm Hoffman, M. and Roberts, W., 2016. Recent trends in the climate of Namaqualand, a megadiverse arid region of South Africa. *South African Journal of Science*, 112(3-4), pp.1-9.

Department of Environmental Affairs (DEA), 2013. *Long-term adaptation scenarios flagship research programme (LTAS) for South Africa: climate trends and scenarios.* Department of Environmental Affairs, Pretoria, South Africa.

Dindang, A., Taat, A., Beng, P.E., Alwi, A.M., Mandai, A., Adam, S.M., Othman, F., Bima, D.A. and Lah, D., 2013. Statistical and trend analysis of rainfall data in Kuching, Sarawak from 1968–2010. *Journal of Medical Microbiology*, 6, p.17.

Dollar, E.S.J. and Rowntree, K.M., 1995. Hydro-climatic trends, sediment sources and geomorphic response in the Bell River catchment, Eastern Cape Drakensberg, South Africa. *South African Geographical Journal*, 77(1), pp.21-32.

Donat, M.G., Lowry, A.L., Alexander, L.V., O'Gorman, P.A. and Maher, N., 2016. More extreme precipitation in the world's dry and wet regions. *Nature Climate Change*, 6(5), p.508.

Gertenbach, W.D., 1980. Rainfall patterns in the Kruger National Park. *Koedoe*, 23(1), pp.35-43.

Ghasemi, A. and Zahediasl, S., 2012. Normality tests for statistical analysis: a guide for non-statisticians. *International journal of endocrinology and metabolism*, 10(2), p.486.

González, M.H., Cariaga, M.L. and Skansi, M.D.L.M., 2012. Some factors that influence seasonal precipitation in Argentinean Chaco. *Advances in Meteorology*, 2012.

Grist, J.P. and Nicholson, S.E., 2001. A study of the dynamic factors influencing the rainfall variability in the West African Sahel. *Journal of climate*, 14(7), pp.1337-1359.

Güntner, A., Stuck, J., Werth, S., Döll, P., Verzano, K. and Merz, B., 2007. A global analysis of temporal and spatial variations in continental water storage. *Water Resources Research*, 43(5).

He, M. and Gautam, M., 2016. Variability and trends in precipitation, temperature and drought indices in the State of California. *Hydrology*, 3(2), p.14.

Herrmann, F., Keller, L., Kunkel, R., Vereecken, H. and Wendland, F., 2015. Determination of spatially differentiated water balance components including groundwater recharge on the federal state level–a case study using the mGROWA model in North Rhine-Westphalia (Germany). *Journal of Hydrology: Regional Studies*, 4, pp.294-312.

Hewitson, B.C. and Crane, R.G., 2006. Consensus between GCM climate change projections with empirical downscaling: precipitation downscaling over South Africa. *International Journal of Climatology*, 26(10), pp.1315-1337.

Hoffman, M.T., Carrick, P.J., Gillson, L. and West, A.G., 2009. Drought, climate change and vegetation response in the succulent Karoo, South Africa. *South African Journal of Science*, 105(1-2), pp.54-60.

Javari, M., 2016. Trend and homogeneity analysis of precipitation in Iran. *Climate*, 4(3), p.44.

Johansson, B. and Chen, D., 2003. The influence of wind and topography on precipitation distribution in Sweden: Statistical analysis and modelling. *International Journal of Climatology*, 23(12), pp.1523-1535.

Kane, R.P., 2009. Periodicities, ENSO effects and trends of some South African rainfall series: an update. *South African Journal of Science*, 105(5-6), pp.199-207.

Kendall, M. G., 1975. *Rank correlation methods*, 4th ed., Charles Griffin: London, UK.

Kidd, C. and Huffman, G., 2011. Global precipitation measurement. *Meteorological Applications*, 18(3), pp.334-353.

Kidd, C., 2001. Satellite rainfall climatology: a review. *International Journal of Climatology*, 21(9), pp.1041-1066.

Kruger, A.C. and Nxumalo, M.P., 2017. Historical rainfall trends in South Africa: 1921– 2015. *Water SA*, 43(2), pp.285-297.

Lima, C.A.D., Palácio, H.A.D.Q., Andrade, E.M.D., dos Santos, J.C. and Brasil, P.P., 2013. Characteristics of rainfall and erosion under natural conditions of land use in semiarid regions. *Revista Brasileira de Engenharia Agrícola e Ambiental*, 17(11), pp.1222-1229.

Liu, R. and Shen, Z., 2008. Temporal-spatial variation and the influence factors of precipitation in Sichuan Province, China. *Frontiers of Biology in China*, 3(2), pp.236- 240.

Longobardi, A. and Villani, P., 2010. Trend analysis of annual and seasonal rainfall time series in the mediterranean area. *International journal of Climatology*, 30(10), pp.1538-1546.

MacKellar, N., New, M. and Jack, C., 2014. Observed and modelled trends in rainfall and temperature for South Africa: 1960-2010. *South African Journal of Science*, 110(7-8), pp.1-13.

Makurira, H., Savenije, H.H.G. and Uhlenbrook, S., 2010. Modelling field scale water partitioning using on-site observations in sub-Saharan rain-fed agriculture. *Hydrology and Earth System Sciences*, 14(4), pp.627-638.

Mann, H.B., 1945. Nonparametric tests against trend. *Econometrica*, pp.245-259.

McCabe, G.J. and Wolock, D.M., 2013. Temporal and spatial variability of the global water balance. *Climatic Change*, 120(1-2), pp.375-387.

McKee, T.B., Doesken, N.J. and Kleist, J., 1993. The relationship of drought frequency and duration to time scales. *In Proceedings of the 8th Conference on Applied Climatology,* American Meteorological Society, Vol. 17, No. 22, pp. 179-183: Boston, Massachusetts, USA.

Munodawafa, A., 2012. The effect of rainfall characteristics and tillage on sheet erosion and maize grain yield in semiarid conditions and granitic sandy soils of Zimbabwe. *Applied and Environmental Soil Science*, 2012.

Nel, W. and Sumner, P.D., 2006. Trends in rainfall total and variability (1970–2000) along the KwaZulu-Natal Drakensberg foothills. *South African Geographical Journal*, 88(2), pp.130-137.

New, M., Todd, M., Hulme, M. and Jones, P., 2001. Precipitation measurements and trends in the twentieth century. *International Journal of Climatology*, 21(15), pp.1889-1922.

Olsson, J., Arheimer, B., Borris, M., Donnelly, C., Foster, K., Nikulin, G., Persson, M., Perttu, A.M., Uvo, C.B., Viklander, M. and Yang, W., 2016. Hydrological climate change impact assessment at small and large scales: key messages from recent progress in Sweden. *Climate*, 4(3), p.39.

Öztuna, D., Elhan, A.H. and Tüccar, E., 2006. Investigation of four different normality tests in terms of type 1 error rate and power under different distributions. *Turkish Journal of Medical Sciences*, 36(3), pp.171-176.

Reason, C.J.C., Hachigonta, S. and Phaladi, R.F., 2005. Inter-annual variability in rainy season characteristics over the Limpopo region of Southern Africa. *International Journal of Climatology*, 25(14), pp.1835-1853.

Richard, Y., Fauchereau, N., Poccard, I., Rouault, M. and Trzaska, S., 2001. 20th century droughts in Southern Africa: spatial and temporal variability, teleconnections with oceanic and atmospheric conditions. *International Journal of Climatology*, 21(7), pp.873-885.

Rouault, M. and Richard, Y., 2003. Intensity and spatial extension of drought in South Africa at different time scales. *Water SA*, 29(4), pp.489-500.

Roy, S.S. and Rouault, M., 2013. Spatial patterns of seasonal scale trends in extreme hourly precipitation in South Africa. *Applied Geography*, 39, pp.151-157.

Sabziparvar, A.A., Movahedi, S., Asakereh, H., Maryanaji, Z. and Masoodian, S.A., 2015. Geographical factors affecting variability of precipitation regime in Iran. *Theoretical and Applied Climatology*, 120(1-2), pp.367-376.

Sen, P.K., 1968. Estimates of the regression coefficient based on Kendall's tau. *Journal of the American statistical association*, 63(324), pp.1379-1389.

Sene, K., 2013. *Flash floods: forecasting and warning*. Springer Science & Business Media. P.386.

Sevruk, B., Matokova-Sadlonova, K. and Toskano, L., 1998. Topography effects on small-scale precipitation variability in the Swiss pre-Alps. *International Association of Hydrological Sciences (IAHS)*, 248, pp.51-58.

Shahid, S., 2010. Rainfall variability and the trends of wet and dry periods in Bangladesh. *International Journal of Climatology*, 30(15), pp.2299-2313.

Shiklomanov, I.A. and Rodda, J.C. eds., 2003. *World water resources at the beginning of the twenty- first century*. Cambridge University Press.

Tfwala, C.M., van Rensburg, L.D., Schall, R. and Dlamini, P., 2018. Drought dynamics and inter-annual rainfall variability on the Ghaap plateau, South Africa, 1918–2014. *Physics and Chemistry of the Earth, Parts A/B/C*, 107, pp.1-7.

Thomas, G. and Henderson-Sellers, A., 1992. Global and continental water balance in a GCM. *Climatic change*, 20(4), pp.251-276.

Trenberth, K.E., Smith, L., Qian, T., Dai, A. and Fasullo, J., 2007. Estimates of the global water budget and its annual cycle using observational and model data. *Journal of Hydrometeorology*, 8(4), pp.758-769.

Türkeş, M., 1996. Spatial and temporal analysis of annual rainfall variations in Turkey. *International Journal of Climatology*, 16(9), pp.1057-1076.

Umran Komuscu, A., 1999. Using the SPI to analyse spatial and temporal patterns of drought in Turkey. *Drought Network News (1994-2001),* p.49.

UNESCO, 1979. Map of the world distribution of arid regions: explanatory note. UNESCO.

Svoboda, M. and Fuchs, B. and Integrated Drought Management Programme (IDMP), 2016. *Handbook of drought indicators and indices*. University of Nebraska-Lincoln, Drought Mitigation Centre Faculty Publications-117, link: http://digitalcommons.unl.edu/droughtfacpub/117/.

World Meteorological Organization, 2012. *Standardized precipitation index user guide*. *ISBN:* 978-92-63-11091-6.

Zargar, A., Sadiq, R., Naser, B. and Khan, F.I., 2011. A review of drought indices. *Environmental Reviews*, 19, pp.333-349.

CHAPTER 5
SPATIO-TEMPORAL VARIATION OF SOIL WATER

5.1 Introduction

The amount of water associated with a given volume or mass of soil, which is its water content, is an essential component of the soil water balance and plays a central role in hydrology (Hébrard *et al.,* 2006; Endale *et al.,* 2006; Mahanama *et al.,* 2008). It also affects many biophysical processes, including plant growth, decomposition of organic matter in soil, heat and water transfer in the land-atmosphere interface (Wang and Qu, 2009; Bittelli, 2011). It is obvious that plant growth on the land surface is directly influenced by the available water content. Therefore, a change in soil water results a change in the LULC or vegetation. In this regard, soil water contributes in the climate system through influencing vegetation growth on the land surface. The presence of soil water also affects the local air temperature (Whan *et al*., 2015). Similarly, soil water plays a key role in the retention or emission process of greenhouse gases by influencing vegetation growth (Lal, 2004; European Environmental Agency, 2015). Generally, soil water is involved in a number of hydrologic and climatic processes at the local, regional and global scales, and plays a major role in climate-change projections, adaptation and mitigation strategies (Seneviratne *et al*., 2010; European Environmental Agency, 2015). As a result of this, its spatial and temporal variations along land surfaces have received great attention (Porporato *et al.,* 2002; Western, *et al.,* 2004; Hébrard *et al.,* 2006; Endale *et al.,* 2006; Mahanama *et al.,* 2008).

The distribution of the soil water status in an area is the result of the interaction of the local topographic features, climate variation, soil properties, land use, and vegetation types (Western, *et al.,* 2004; Endale *et al.,* 2006; Williams *et al.,* 2009; Mello *et al.,* 2011). However, the levels of influence of these factors on the spatio-temporal distribution differ, depending on other conditions such as the location of the area and the time of measurement. The other factor influencing the water distribution in landscapes is the size of the runoff contributing area above the point of interest. In principle, it is assumed that as the contributing area increases, the water content will increase, as we approach the runoff outlet (Zhao *et al.,* 2011). The characteristics of topography constitute one of the major factors that play a key role in influencing surface, sub-surface, and hydraulic head flows (Western *et al.,* 2004). Although lower slopes are assumed to have a higher water content than steep slopes do, this may not always true, depending on the textural differences of the soils at different slope classes (Endale *et al.*, 2006).

Aspect, as one of the characteristics of topography, also influences the water distribution due to a difference in insolation on the land surface (Zhao *et al.,* 2011).

In recent decades, a number of methods have been developed to determine the soil water content. The methods can be classified as direct or indirect (Cepuder *et al.*, 2008; Bittelli, 2011; Romano, 2014). In a direct measurement method, the amount of water can be measured directly, for instance, by measuring the mass of the water as a fraction of the total weight of the soil, which is called the gravimetric method (Cepuder *et al.*, 2008; Bittelli, 2011; Romano, 2014). On the other hand, in indirect methods, a variable that is significantly affected by the amount of water in a soil will be measured, and the change of the variable will be related to the change in the soil water content. These physically based or empirical relationships are called calibration curves. Some of the major indirect methods include: the neutron soil water meter (NSWM), time domain reflectometry (TDR), capacitance probes such as DFM probes, ground penetrating radar (GPR), electromagnetic induction (EMI), electrical resistivity tomography (ERT), and remote sensing techniques (Lal, 2004). The remote sensing technique is advantageous over the other methods listed since it has a better spatial coverage. Detailed descriptions of the different types of indirect methods are given in Cepuder *et al.* (2008), Bittelli (2011) and Romano (2014).

Nowadays, the study of the spatial and temporal variations of soil water have drawn special attention in the fields of meteorology, climate change, hydrology and environmental monitoring, at global, continental, national, regional, and catchment or local scales. As a result of this, soil water content was recognized as one of the Essential Climate Variables (ECV) in 2010 by the Global Climate Observing System (GCOS) programme, which is part of the European Space Agency (ESA). Since then, satellite-based global soil water content data is provided by the Soil Moisture Climate Change Initiative (CCI) and is available at http://www.esa-soilmoisture-cci.org/. Another global-scale source of data is provided at http://ismn.geo.tuwien.ac.at/ coordinated by the International Soil Moisture Network. Other regional- and national-scale soil water content databases are also available, such as the North American Soil Moisture Database (NASMID), available at http://soilmoisture.tamu.edu/ and Soil Moisture Outlook for India (http://www.monsoondata.org/wx/soil.html). As far as the author is aware, there is no national soil water monitoring programme in South Africa, except for some site-specific and local-scale measurements. Therefore, it seems that the study of the spatial and temporal variations of soil water is a neglected area of research in South Africa. Therefore, this study was conducted to analyse the spatial and temporal variations of the root zone water content for different soil groups, topographic features, and LULC types at catchment scale. The root zone was also evaluated with one of the drought monitoring indicators, soil water anomaly (SWA), to describe the spatial and temporal soil water variations efficiently.

5.2 Materials and methods

5.2.1 Description of the study area

The study catchment is located in the Northern Cape Province, South Africa, with a geographic location of between 22°11'00" and 23º28"00" E longitudes and between 28°03'00" and 29°06'00" S latitudes. The details for the location and description of the study catchment can be seen in Chapter 3, Subsection 3.2.1.

5.2.2 Testing normality of time series data

As explained in Chapter 4 (Subsection 4.2.2), the test of normality is a pre-requisite in any statistical analysis. In this study, the two most-used types of normality test were used, i.e. the graphical method (probability-probability (P-P plot) and quantile-quantile (Q-Q plot)) and the statistical method (Shapiro-Wilk test).

5.2.3 Soil water time series analysis

The trend analysis in the long-term (1980–2018) time series soil water content data was analysed by using the non-parametric Mann-Kendall test. For details, see Chapter 4 (Subsection 4.2.3).

5.2.4 The spatial variation of soil water content

The spatial variation of the soil water content in the catchment was estimated at HRU, Sub-basin, and catchment level as a whole by the Soil and Water Assessment Tool (SWAT), as discussed in Chapter 3. In this section, therefore, the mean values of the long-term seasonal and annual variations of water contents were analysed spatially regarding the catchment, assisted by ArcGIS software ver 9.4.

5.2.5 Soil water anomaly (SWA)

The presence of a soil water deficit in the catchment was evaluated by the soil water anomaly, which is commonly used as a water deficit indicator. The soil water anomaly is a very important indicator for monitoring daily, weekly, and monthly water contents and anomalies in the soil, relative to a defined climatological period (EDO and JRC, 2018). It can be calculated as described below.

For each location (HRU), the daily soil moisture anomaly is calculated as follows:

$$SWA = \frac{SWC_i - SWC_{MN}}{STD} \tag{5.1}$$

where SWC_i is the soil water of the time scale (month or year) i, SWC_{MN} is the long-term average value for the total time scale i, and STD is the standard deviation, which are calculated for the same period i over the available time series (1980–2018). According to this definition, the anomaly values are expressed as units of standard deviation.

5.3 Results

5.3.1 Normality test

The tests of the normality of the time series data (both mean annual and monthly soil water content) were conducted by visual assessment and with statistical tests. The graphical assessment is depicted in Figure 5.1 below, panels a–d, and the numerical tests are given in Table 5.1 below. As explained in in detail in Chapter 4, Subsections 4.3.1 and 4.2.2, the P-P plot (Figure 5.1, panels a and c) compares the cumulative probability of the empirical data with an ideal normal distribution. The other graphical method, which is the Q-Q plot (Figure 5.1, panels b and d), compares the quantile of an observation with a quantile of a standardized theoretical dataset. Figure 5.1, panels a to d, shows that both the graphical sketches of the mean monthly and annual soil water content data do not meet the criteria of normal distribution.

The statistical test (the Shapiro-Wilk test, shown in Table 5.1 below) also shows that both the annual and monthly time series data are not normally distributed. Therefore, it can be concluded that parametric statistics cannot be applied to the time series data of annual and monthly soil water content for further analysis; thus, non-parametric tests are appropriate. It is important to note that the soil water content simulated by SWAT and its analysis in this thesis is a fraction of the available water capacity. This means that the analyses do not consider the amount of water below the permanent wilting point.

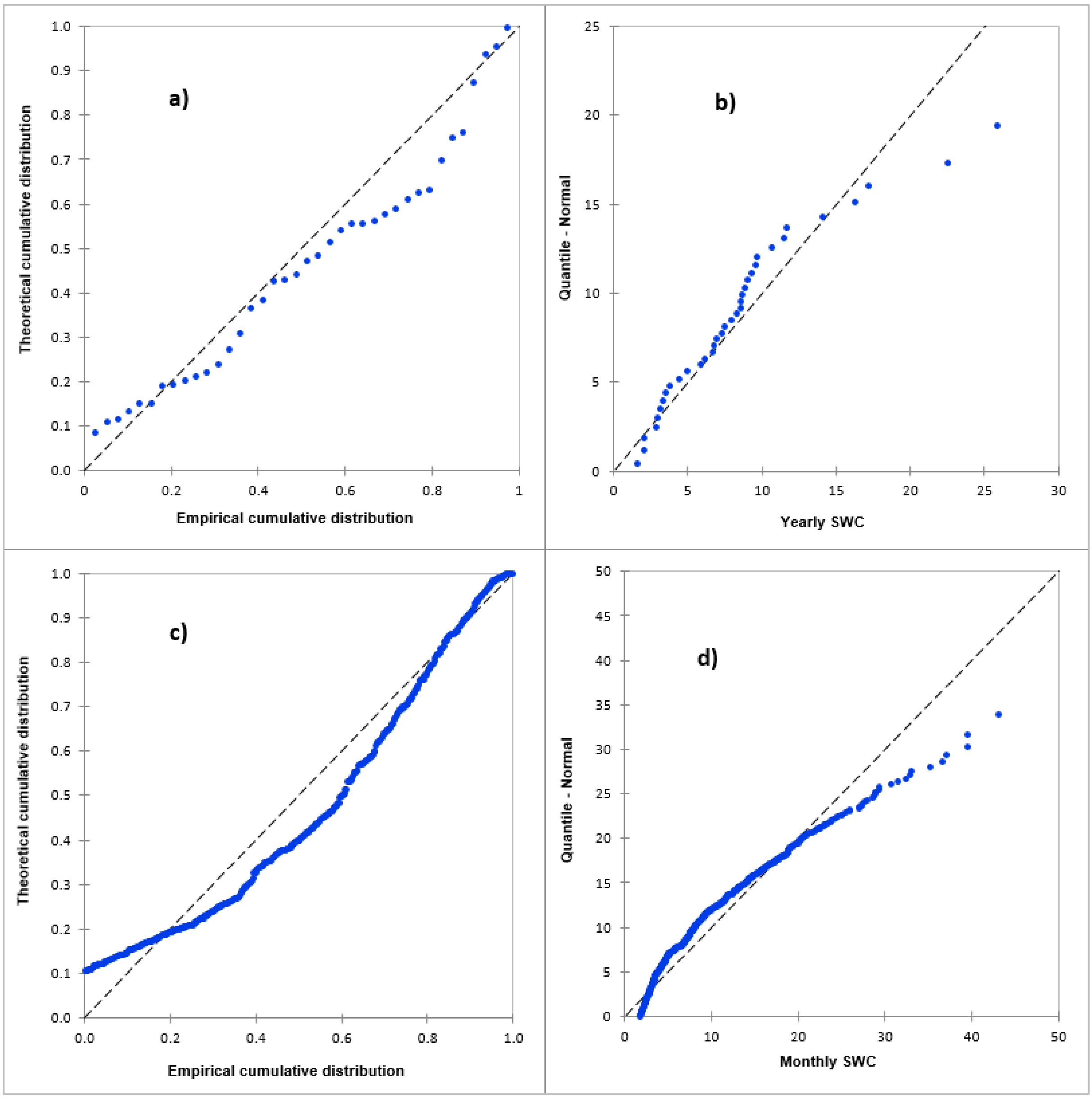

Figure 5.1: Graphical sketches showing the normality of soil water content data

Notes: (a) probability-probability (P-P plot) for mean annual soil water content, (b) quantile-quantile (Q-Q plot) for mean annual soil water content, (c) probability-probability (P-P plot) for mean monthly soil water content, and (d) quantile-quantile (Q-Q plot) for mean monthly soil water content.

Table 5.1: Tests of normality for the time series of soil water content (SWC) data

Variable	Observations	Minimum	Maximum	Mean	Std. deviation	Shapiro-Wilk test	
						W	p-value
Annual SWC	39	0.120	25.860	7.762	5.629	0.892	0.001
Monthly	468	0.030	43.170	10.031	8.029	0.903	< 0.001

5.3.2 Trends of soil water content

In this subsection, two major characteristics of the soil water content are explained. Firstly, the variation of the long-term mean (which is a double mean that is averaged spatially for the catchment and again for the time series mean) of the soil water content at different time scales (daily, monthly and yearly variations) are described. Secondly, the long-term trends of the time series soil water content at monthly and yearly time scales are described. Figure 5.2 below shows the variation of the long-term (1980–2018) mean daily soil water content throughout a year, together with its comparison with the monthly and yearly values. The daily mean precipitation and percolation are also plotted to show the impact of precipitation on the soil water content and percolation. The daily soil water content varies from 3.6 mm during the start of summer and 15.0 mm in the winter season. Generally, spring is the season with the lowest record of soil water content, and late summer (February) and the early winter season (June and July) are the seasons with relatively higher soil water contents. The pattern of the soil water content and percolation is also consistent with the precipitation trend, as expected, i.e. the soil water content and percolation out of the root zone increases as precipitation increases. The monthly values of the soil water contents also follow the trends of daily soil water content. The result also indicates that the monthly and daily mean values vary around the long-term mean annual soil water content throughout the year.

Regarding the long-term monthly soil water distribution in the catchment (Figure 5.3 below), the fate of water that has infiltrated the soil profile primarily depends on the season and precipitation intensity. As a result, late summer and winters had higher water content, percolation and lateral flow, but the revap water (which contains the sum of the water transpired by deep-rooted vegetation and the amount of water moved upwards due to water deficit in the root zone from the shallow aquifer) was less than the percolation and lateral flows. However, during lower precipitation times (spring and early summer seasons), the revap water was higher than the percolation and lateral flows. Moreover, the response of percolation and lateral flows to precipitation followed a similar pattern, i.e. both of them increased as precipitation increased. Figure 5.3 below also shows the relative contribution of the revap water to evapotranspiration. It shows that the revap water contributes to evapotranspiration from a minimum of 9% during late summer (where the soil water content is relatively higher) up to 32% during early spring season (where soil water is at its minimum value).

The trends of the time series catchment mean soil water storage, percolation and revap water are shown in Figures 5.4 and 5.5 below for annual and monthly values, respectively. The statistical analysis was conducted by using the Mann-Kendall trend test and the results are shown in Table 5.2 below. The annual trends (Figure 5.4 below) and monthly trends (Figure 5.5 below) indicate that there is no significant trend for mean annual and monthly soil water content and percolation at $p < 0.05$. However, there is a highly significant trend (negative trend) in both the mean annual and monthly revap water from the shallow aquifer at $p < 0.01$. Hence, the Sen's slope value shows that the revap water decreases at a mean rate of 1.091 mm per annum. Whereas as in the monthly time scales, the rate was estimated to be 0.007 mm.

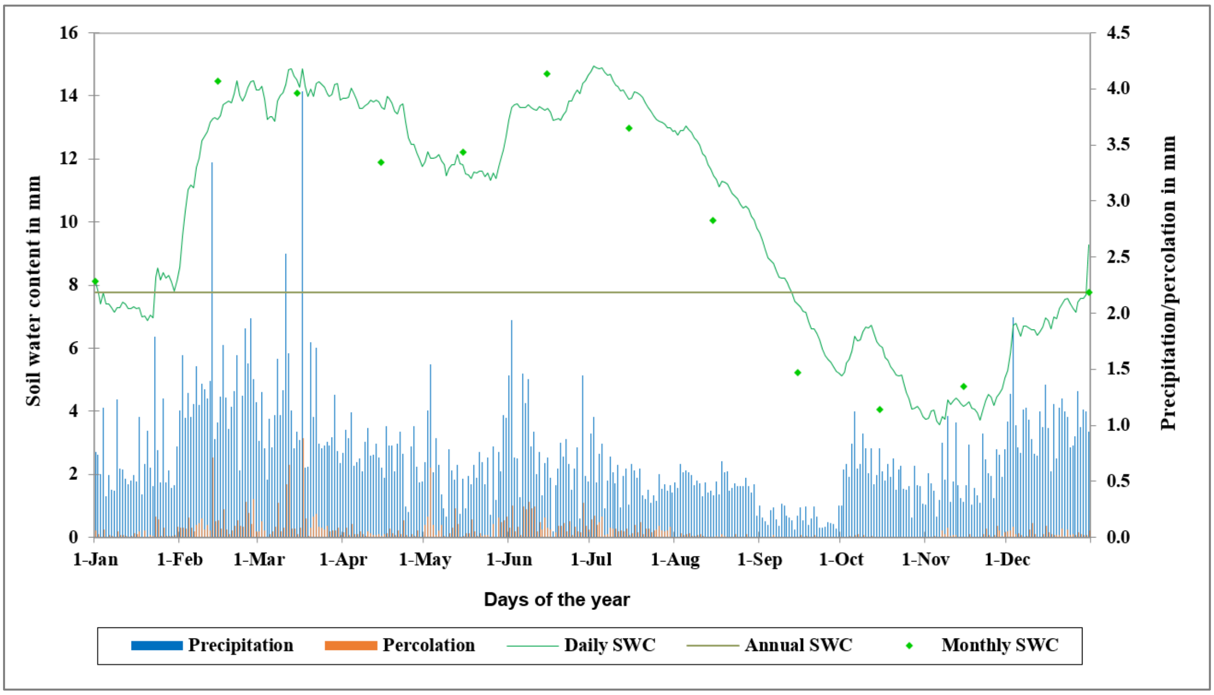

Figure 5.2: Comparison of the long-term mean daily, monthly and annual soil water contents with the corresponding long-term mean values of percolation and precipitation in the catchment

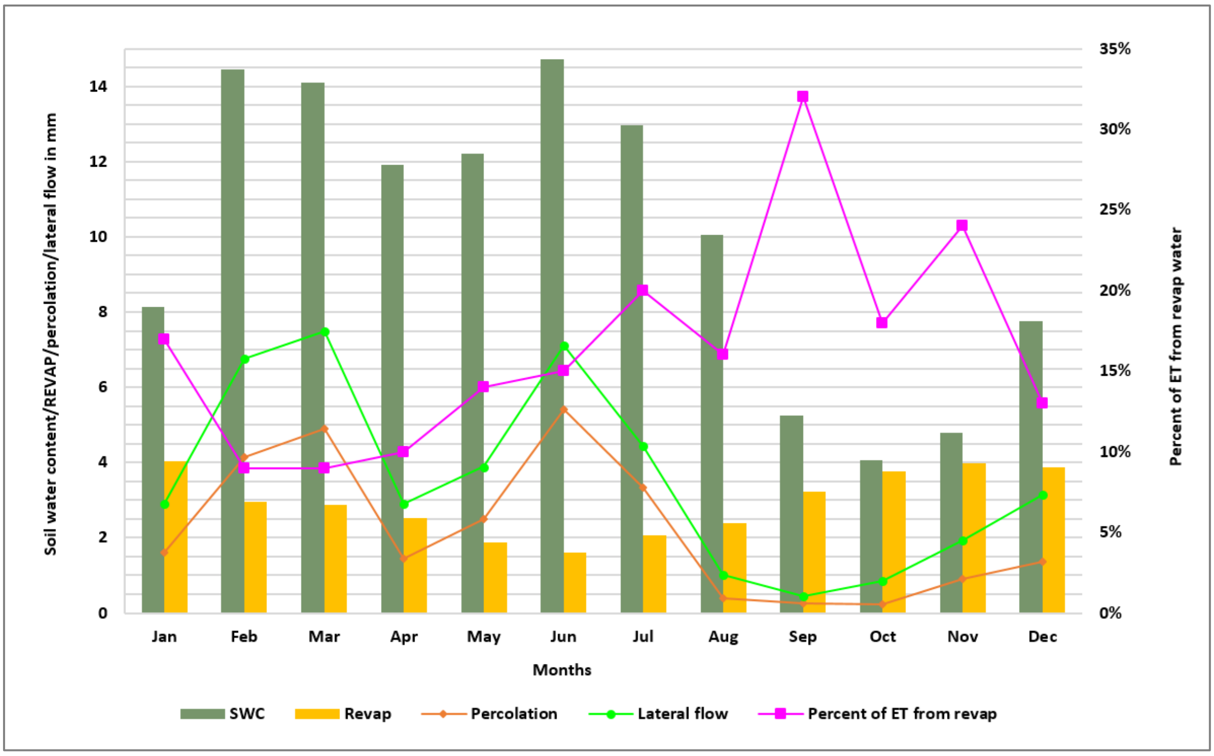

Figure 5.3: Long-term monthly mean soil water content variation, percolation bellow the root zone and the contribution of revap water to evapotranspiration

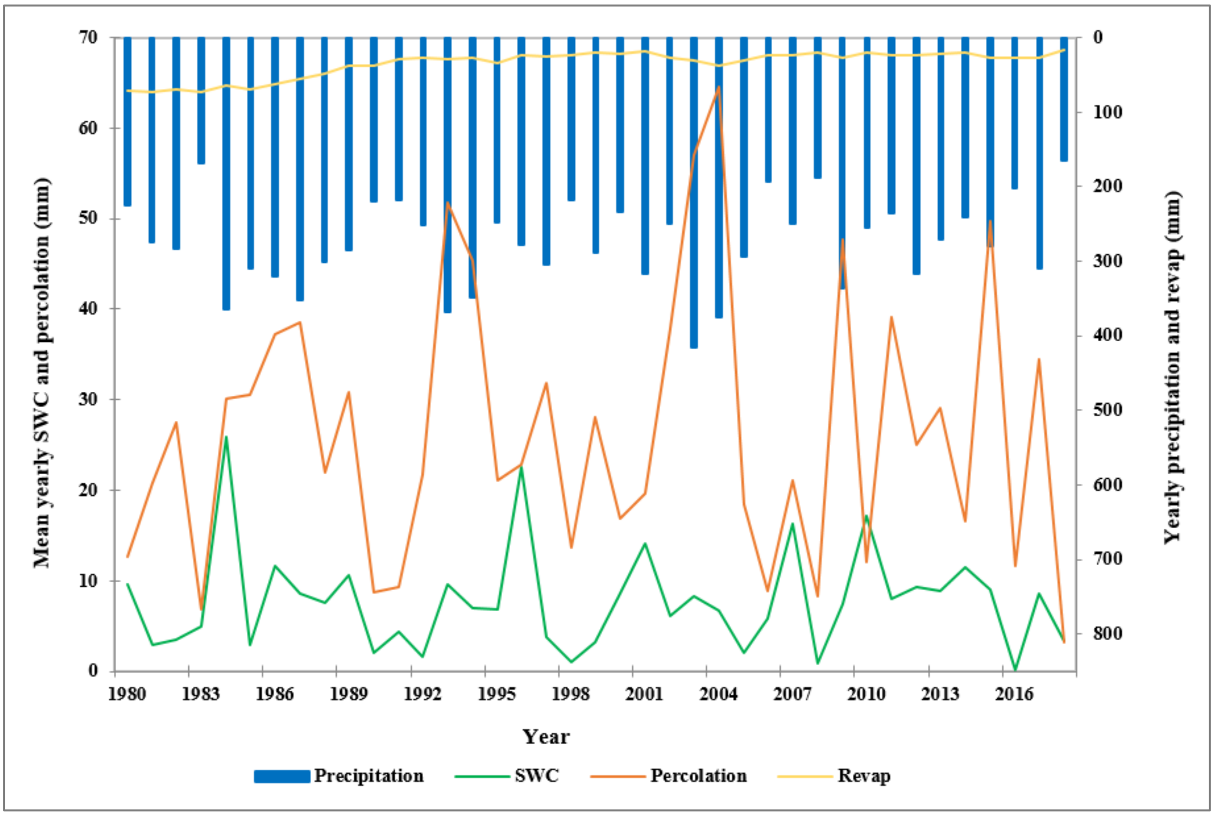

Figure 5.4: Trends of annual soil water content in Soutloop Catchment

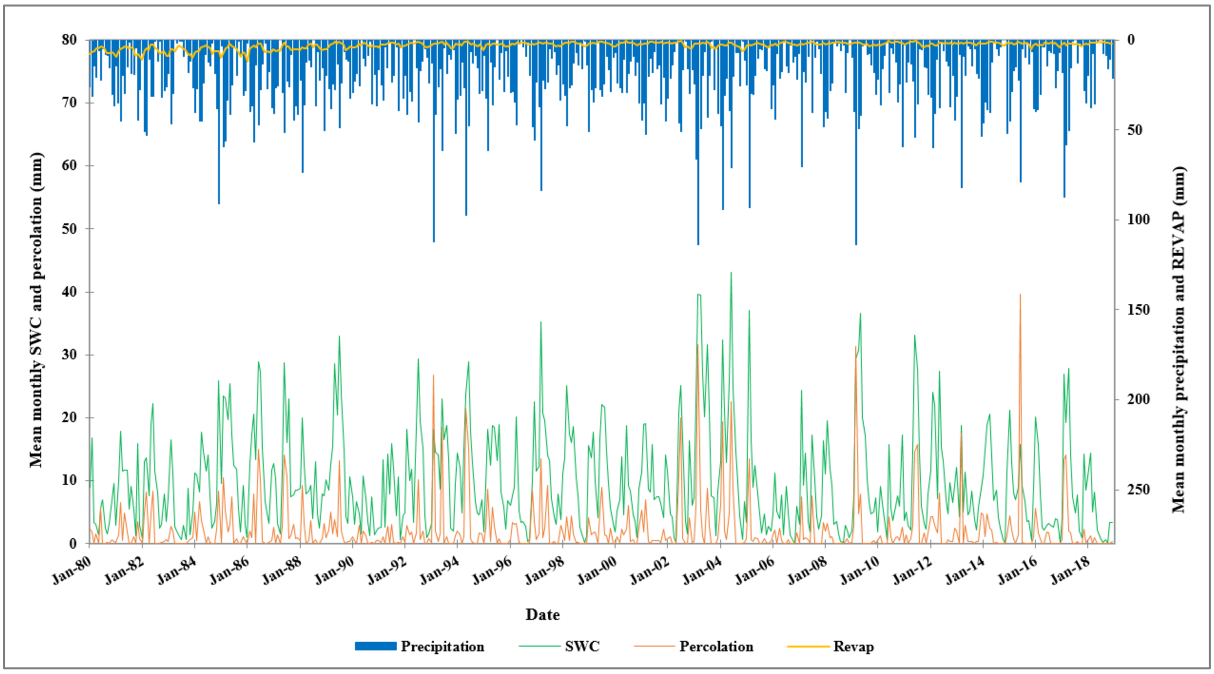

Figure 5.5: Trends of monthly soil water content in Soutloop Catchment

The long-term volumetric soil water distribution along the two layers and the surface water content (up to 10 millimetres deep from the land surface) are depicted in Figure 5.6 below. Regarding the surface soil water content, it was very dry throughout the different time scales and this content varies relatively very little, as compared with layer 1 and layer 2, irrespective of the time scales. It varied from 0.0006 to 0.005, 0.001 to 0.004 and 0.0012 to 0.0035% for the mean daily, mean monthly and mean annual time series, respectively. However, the variations in layer 1 and layer 2 were very high, relatively. For example, at layer 1, daily soil water varied from 0.025 to 0.116%, whereas at layer 2, it varied from 0.026 to 0.11%. (See further details in Table 5.3 below.) The daily variation throughout a year follows a similar pattern to that of the monthly variation. Therefore, during late spring, summer and autumn, the water content in layer 1 was higher than in layer 2. The reverse was true during winter and early spring seasons. However, in the case of annual time series soil water, there is no clear pattern, especially between layer 1 and layer 2. Generally, the surface water content was the most stable, followed by layer 1, whereas layer 2 was the most variable of all soil water contents. Note that soil depth varies based on the soil type. The surface layer refers to the top 10 mm, whereas layer 1 and layer 2 vary, based on the soil type. Hence, layer 1 has an average depth of 247 mm, whereas layer 2 averages 586 mm.

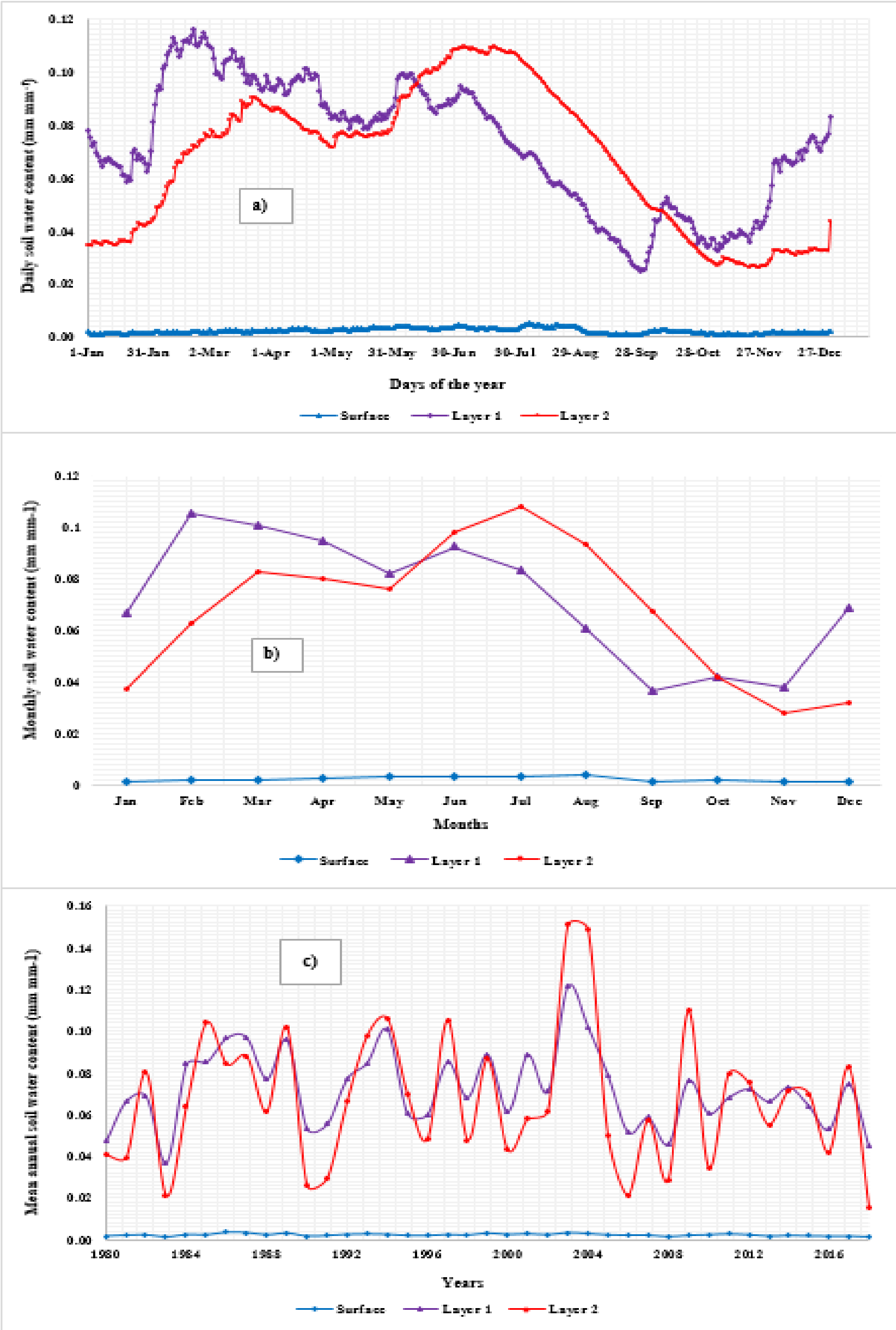

N.B. Surface layer – the top 10 mm deep   Layer 1 – on average, 247 mm   Layer 2 – on average, 586 mm deep.

Figure 5.6: The long-term mean soil profile water distribution in three soil layers

Notes: three soil layers (surface, first layer and second layer) as a fraction of the available water capacity at different time scales: a) daily means in the year, b) monthly means in the year, and c) annual time series from 1980 to 2018.

Table 5.2: Statistics of the Mann-Kendall trend test for the mean yearly and monthly soil water content, percolation and revap water from the shallow aquifer

Parameters	Annual means			Monthly means		
	SWC	Percolation	revap	SWC	Percolation	revap
Kendall's tau	0.028	0.007	-0.595	-0.054	-0.060	-0.396
S stat	21	5	-441	-5907	-6367	-43306
Var(S)	6834	6834	6834	11425582	11258872	11425622
p-value	0.809	0.961	< 0.01	0.081	0.058	< 0.01
Sen's slope	0.016	0.013	-1.091	-0.004	0	-0.007

Table 5.3: Variation of soil water content (as a fraction of the available water content) at different soil layers and time scales

Time scales	Surface		Layer 1		Layer 2	
	Min	Max	Min	Max	Min	Max
Daily	0.0006	0.005	0.025	0.116	0.026	0.11
Monthly	0.001	0.004	0.037	0.105	0.028	0.108
Yearly	0.0012	0.004	0.037	0.12	0.015	0.151

5.3.3 Spatial variation of the soil water content

This subsection focuses on the description of the spatial variation of soil water content, based on the long-term mean values, on annual and seasonal time scales. The soil water content was expressed as a fraction of the available water capacity. This was done by dividing the total profile water content (corresponding depth of water in mm) by the available water capacity (AWC in mm). Accordingly, the spatial variation of the mean annual soil water content is depicted in Figure 5.7 below, while the seasonal variations are shown in Figure 5.8 below. The soil water content showed a higher spatial variation at both time scales (both seasonally and annually). Regarding the annual soil water content (Figure 5.7 below), most of the catchment area reflects between 0.1 and 0.2 mm mm^{-1} water content. The annual soil water content of the north-western and south-eastern parts of the catchment varies between 0.15 and 0.2 mm mm^{-1}, whereas most of the north-eastern and the south-western parts lie between 0.1 and 0.15 mm mm^{-1}. The driest area (a water content of <0.1 mm mm^{-1}) in the catchment is found mainly in the south-western and north-eastern part in smaller patches of area. The wettest area in the catchment (> 0.25 mm mm^{-1}) is found in the north-western part in very small and sparsely distributed patches of land.

The seasonal soil water content variation of the Soutloop Catchment was also analysed based on the long-term (1980–2018) mean monthly soil water content. As it is shown in Figure 5.8 below, autumn is the season during which most of the catchment experienced a relatively wetter (> 0.2 mm mm^{-1}) and uniform distribution of soil water. On the other hand, spring was a season of low water content (< 0.1 mm mm^{-1}) in most parts of the catchment. In the summer season, the catchment can be classified into two regions, the northern part where the catchment is relatively wet (>0.15 mm mm^{-1}) and the southern part where the water content is very low (< 0.15 mm mm^{-1}). Similarly, in the winter season, the patterns of the distribution of the soil water content divide the catchment into two, i.e. the drier region (< 0.1 mm mm^{-1}) that covers the larger area of the northern part, and the wetter part (SWC > 0.15 mm mm^{-1}) which covers the southern part of the catchment. The long-term mean distribution of water content follows a similar pattern in the seasonal and monthly distribution of precipitation, as discussed in Chapter 4, Subsection 4.3.3. Therefore, it can be generalized that the spatial trends of soil water content were highly influenced by the spatial distribution of rainfall in the study area.

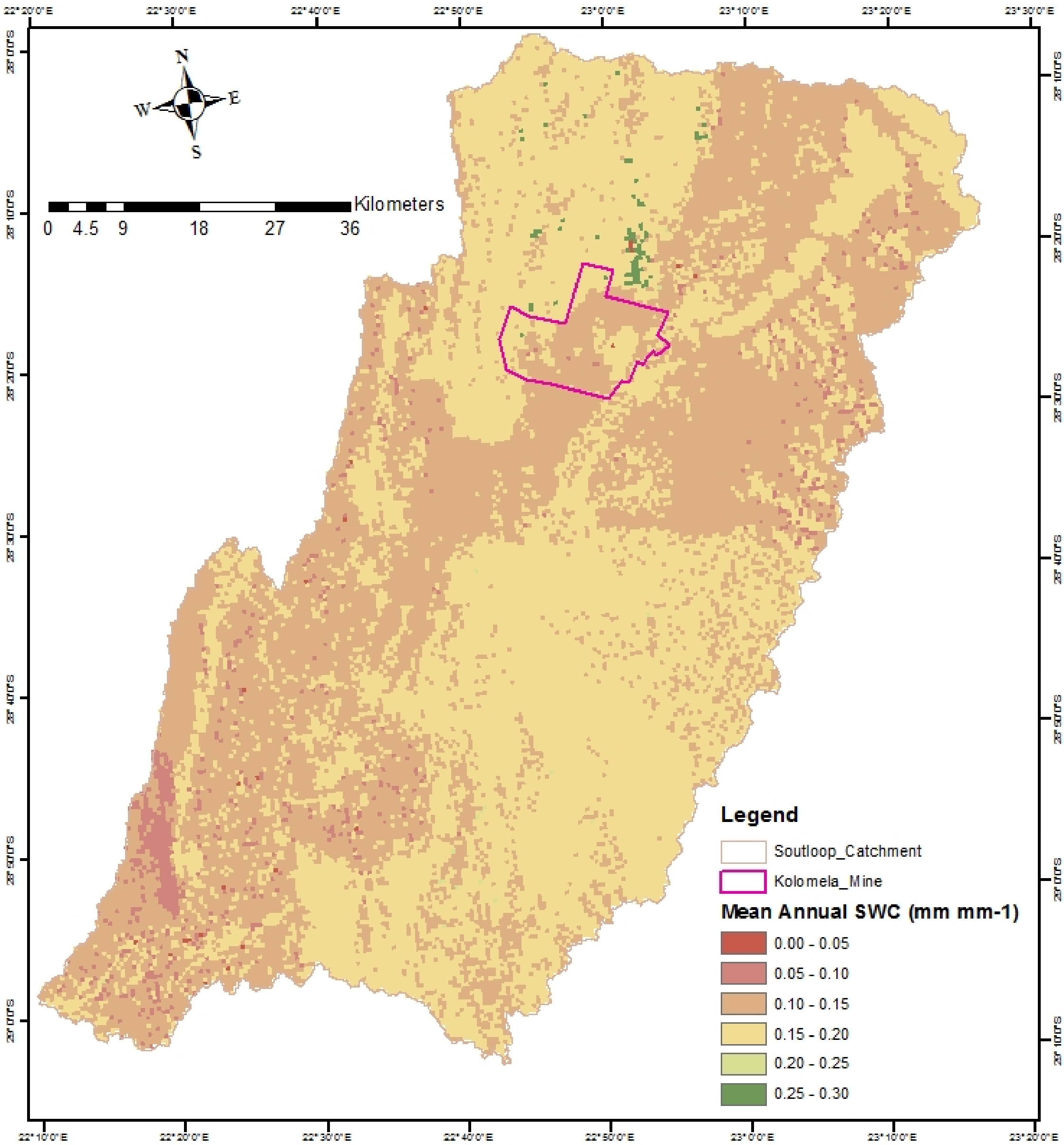

Figure 5.7: The spatial variations of the long-term mean annual soil water content (as a fraction of the available water content) in Soutloop Catchment

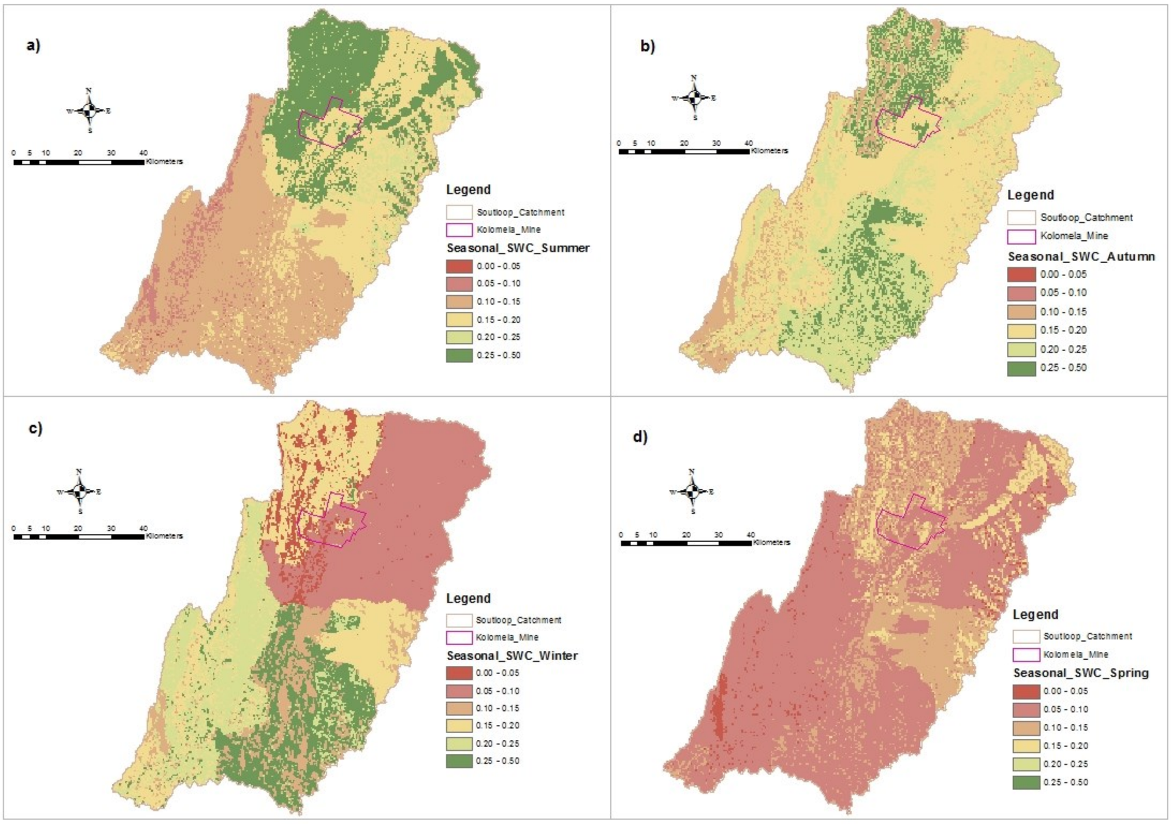

Figure 5.8: The spatial variations of the long-term mean seasonal soil water content (as a fraction of the available water content for the profile) in Soutloop Catchment.

5.3.4 Soil water anomaly

The soil water anomaly (SWA) is one of the most important indicators in the evaluation of water deficit in catchments, particularly for monitoring agricultural drought. It compares each time series soil water content record with a normal value (a long-term mean value) to monitor a relative soil water deficit in the catchment. Accordingly, in this subsection, the time series mean monthly soil water anomaly (Figure 5.9 below) and the mean annual anomaly (Figure 5.10 below) are described. The spatial variation of the mean annual soil water anomaly is depicted in Figure 5.11 below.

Based on the time series monthly soil water anomaly (Figure 5.9 below), June, 2004, was relatively the wettest month (which recorded the highest above-normal soil water content) within the study period. Similarly, the driest period (which recorded the highest below-normal soil water content) was September, 2008. The longest period with consecutive months that experienced above-normal soil water content ran from November, 1996 to July, 1997. The longest periods with drier months were: March, 1980 – January, 1981; March, 2006 – January, 2007; April, 2008 – February, 2009; and March, 2016 – January, 2017. Regarding the annual soil water anomaly (Figure 5.10 below), 1984 was the wettest year in terms of soil water content, whereas 2016 was the driest year of all in the study time period. Moreover, the longest period of consecutive years with above-normal soil water content was 2010–2015 (more than 5-years long), while the longest period of consecutive years with below-normal soil water content were: 1981 – 1983; 1990 – 1992; 1997 – 1999; and 2004 – 2006, which were all nearly 3 years in duration.

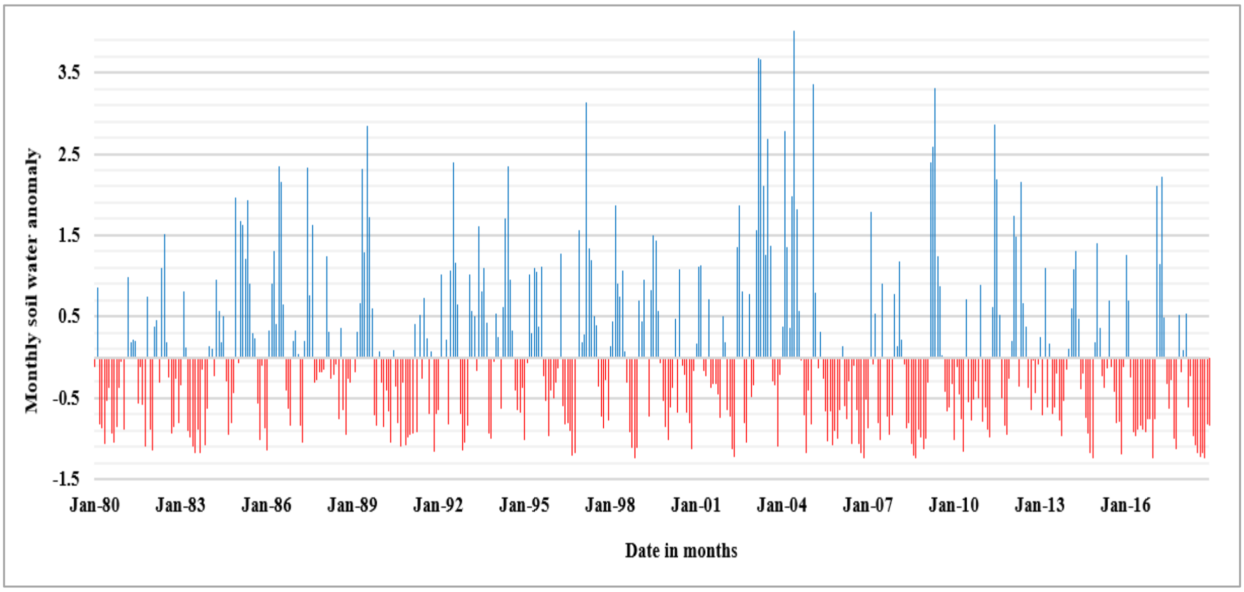

Figure 5.9: Long-term soil water anomaly showing the soil water deviation at monthly time scale.

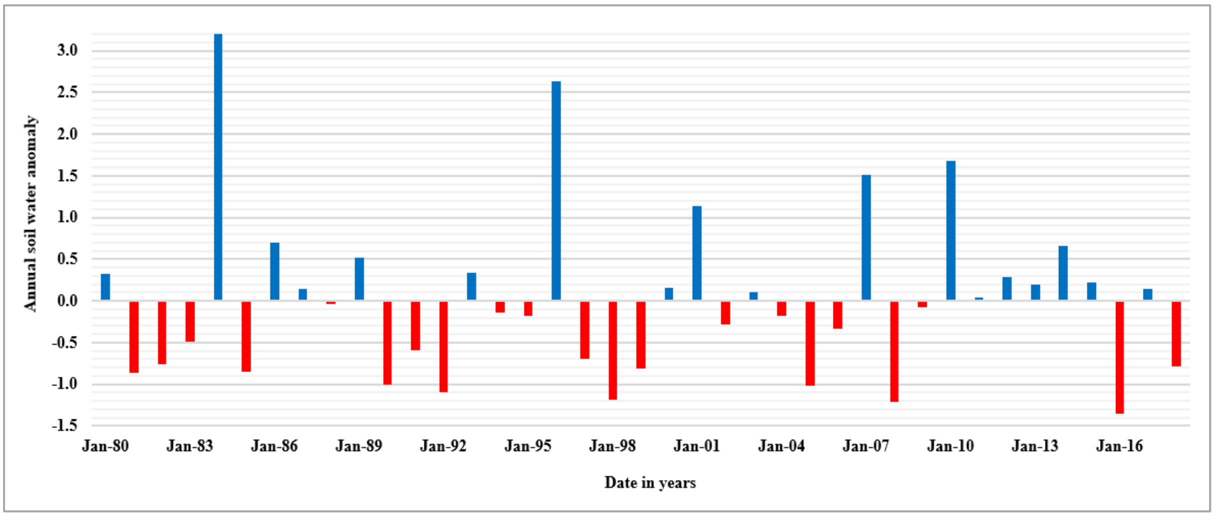

Figure 5.10: Long-term soil water anomaly showing the soil water deviation at a yearly time scale

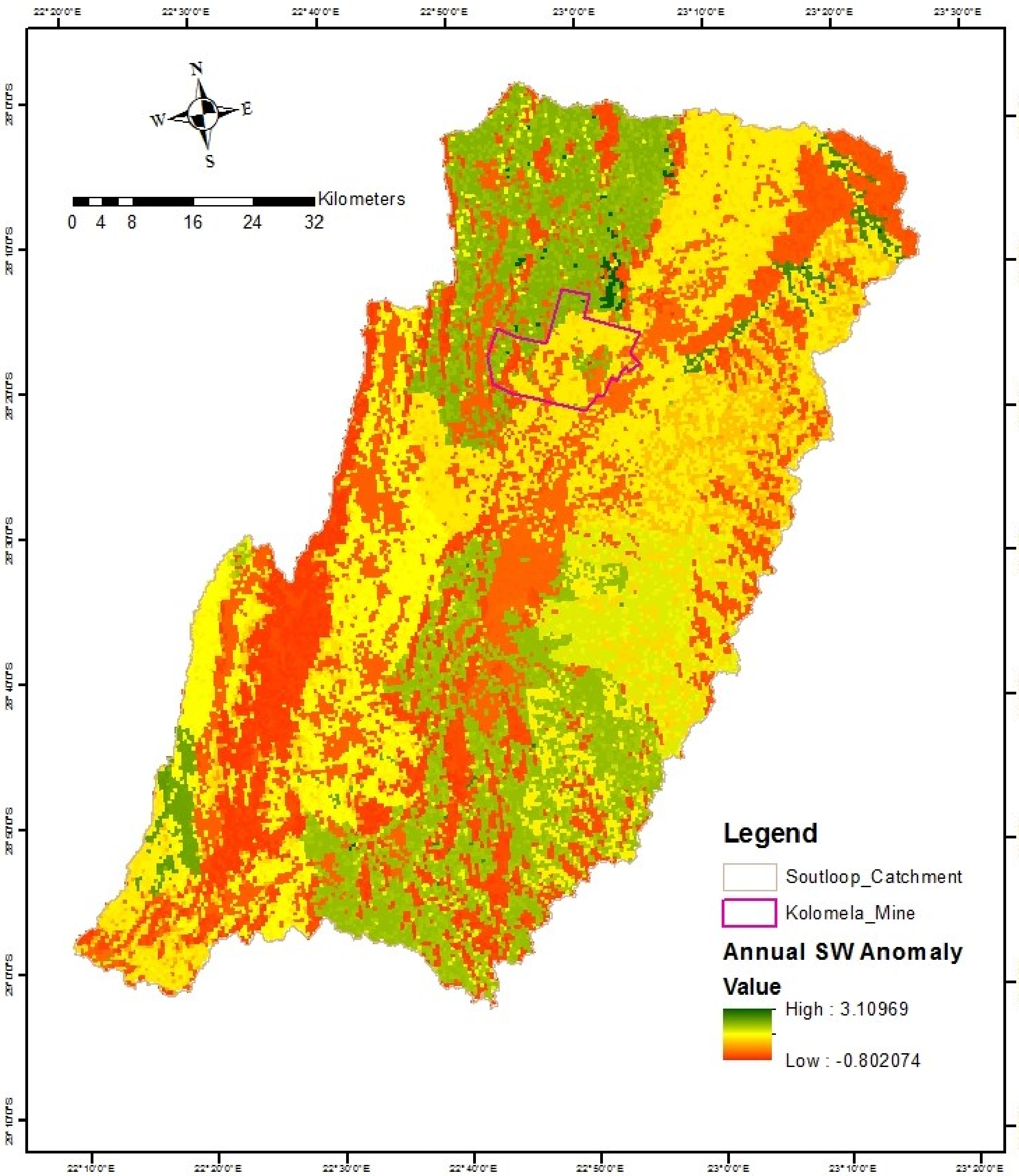

Figure 5.11: The spatial variation of long-term soil water anomaly showing the soil water deviation from the normal value at yearly time scale.

The spatial variation of the annual soil water anomaly is depicted in Figure 5.11 above. It is calculated based on the mean long-term annual soil water content of the hydrological response units (HRUs, as discussed in Chapter 3, Subsection 3.2.1.3). It shows the relative comparison of the mean annual soil water content at HRU level. Generally, larger part of the north-western and south-eastern parts of the catchment have experienced above-normal soil water (SWA > 0 and shaded with deep green), while the north-eastern, central and a considerable area of south and south-western parts experienced a nearly normal soil water content (SWA closer to 0 and shaded yellow). On the other hand, areas that have experienced below-normal soil water content (SWA < 0 and shaded red) are distributed throughout the catchment, specifically dominating the western, south-western, some central and north-eastern tips.

5.4 Discussions

5.4.1 Variations of soil water content

The soil water content in Soutloop Catchment exhibited spatial and temporal variability that demands clarification and contextualization. The temporal variations are given in Figure 5.2 above (long-term mean daily, monthly and annual variations), Figure 5.3 above (long-term mean monthly variations), Figure 5.4 above (time series mean annual variations in the 39-year study period) and Figure 5.5 above (which shows time series mean monthly variations for the 39 years of simulations). On the other hand, the spatial variations show changes in soil water content, as the latitude and longitude of the area are increases/decreases. Therefore, Figures 5.7 and 5.8 above have been included to show the two-dimensional variations of the annual and seasonal soil water contents, respectively. Moreover, Figure 5.6 above is given to show the variation of the soil water content along the profile depth (which can be taken as the third dimension of variation).

The temporal variations of the soil water content can be seen in two ways: the long-term averages and the trends of the time series for different time scales in the simulation period (1980–2018). Generally, the results reflected in Figures 5.2 and 5.3 above indicate that the daily and monthly averages follow similar patterns, i.e. if one increases, the other also increases, and vice versa, although the rate of change varies. It is also important to note that the daily and monthly average values vary around the mean annual soil water content for the different seasons of the year. Hence, the daily and monthly averages were the lowest in spring, and relatively higher during the late summer and early winter seasons. The reason for this might be the lower amounts of precipitation, but with higher figures for other weather parameters, such as temperature and solar radiation, experienced in spring seasons. However, the reverse was true in late summer and early winter season, as discussed in Chapter 4, Subsection 4.3.2 for the seasonal variation of different weather parameters.

Water infiltrating into the root zone could be stored as soil water until the field capacity, or it could be converted to lateral flow in the presence of impervious layers in the sub-soil, or it could experience deep percolation to shallow aquifers. This is the usual process, especially in most humid areas. However, during dry periods and with the unavailability of sufficient soil water in the root zone to meet the requirements of evapotranspiration, water from the shallow aquifer will move upwards to the root zone. This water is called the revap water (Neitsch *et al*., 2011; Arnold *et al*., 2012; Winchell *et al*., 2013). The revap process is most common in the presence of shallow aquifers in close proximity to the root zone, and also in the presence of deep-rooted vegetation in arid and semi-arid areas. Details of the monthly values of the soil water content, contribution of the revap water to soil water, lateral flow, percolation and percent contribution of the revap water to evapotranspiration are given in Figure 5.3 above. The percolated water and lateral flow positively follows the magnitude of the soil water content. However, the revap water increased as the precipitation and soil water content decreased. As a result, the revap water was at a maximum during the spring season where the soil water was at its minimum, whereas it was at a minimum during the late summer and early autumn seasons where the soil water content was at its maximum. Similarly, the contribution of revap water to evapotranspiration varied between 9% during late summer and 32% during the early spring season. The seasonality of the revap water and its dependence on precipitation intensity is consistent with the results of Adrià Barbeta and Peñuelas (2017). They also indicated that the presence of perennial vegetation (trees, shrubs, etc.), as is true for the case of Soutloop Catchment, contributes significantly to the increase of the revap water. Different researchers have calculated different percentages of contribution of the revap water to soil water and evapotranspiration: e.g. Yeh and Famiglietti (2009) estimated an average of up to 20% in dry seasons, Adrià Barbeta and Peñuelas (2017) found an average of 38.5%, and Balugani *et al*. (2017) found an average value of nearly 33%.

The other type of temporal variation, which is the detection of trends in a time series soil water content, percolation and revap water, is given in Figures 5.4 and 5.5 above for annual and monthly time series data, respectively. The Mann-Kendall trend test shows that there is no significant trend in soil water and percolation; however, there was a highly significant negative trend in both annual and monthly time series values on the revap water. On average, the annual revap water decreased by 1.1 mm, whereas the monthly revap water decreased at a rate of 0.01mm. The impacts of climate change could be the main cause for the decrease of the revap water. Some reports (Gillson *et al*., 2012; Schoeman *et al*., 2013; Schoeman *et al*., 2010) also show that a significant transformation of land cover characteristics in South Africa is being experienced. Changes in land cover include the conversion of natural vegetation to agricultural lands, changes to natural vegetation through bush encroachment and overgrazing, soil erosion, invasion by alien plant species, and accelerating urbanization. Therefore, the impacts of LULC change (whether natural or anthropogenic) could constitute another possible cause for the results discussed in this paragraph. However, further research should be conducted to identify the real cause for the decrease of revap water in the catchment.

The spatial variations of soil water content were also seen in two ways, i.e. the two-dimensional variations shown in Figures 5.7 and 5.8 above for the mean annual and seasonal soil water content, respectively, and the variation of the soil water content in depth (Figure 5.6 above) as a third dimension of the variations. Both the annual and seasonal soil water content figures showed a higher spatial variation in the catchment. The annual mean variation (Figure 5.7 above) shows a lower soil water content in the north-eastern and south-western parts of the catchment. Regarding the seasonal distribution, autumn is the season during which most of the catchment had a relatively wetter (> 0.2 mm mm^{-1}) and uniform distribution of soil water. On the other hand, spring was a season of low water content (< 0.1 mm mm^{-1}) in most parts of the catchment. In the summer season, the northern part is relatively wet (>0.15 mm mm^{-1}) and the southern part is very dry (< 0.15 mm mm^{-1}). Similarly, in the winter season, a larger area of the northern part was drier, whereas the southern part of the catchment was relatively wetter. The long-term mean distribution of water content follows a similar pattern in the seasonal and monthly distribution of precipitation, as discussed in Chapter 4, Subsection 4.3.3. Therefore, it can be generalized that the spatial trends of soil water content were influenced mainly by the spatial distribution of rainfall in the study area. However, the influence of other factors, such as variation in LULC, soil type, topographic features and weather parameters other than precipitation, could have also played a vital role (Bárdossy and Lehmann, 1998; Gómez-Plaza *et al*., 2001).

The other soil water variation, which can be seen as a third dimension, is the variability of soil water content by its depth. This is shown in Figure 5.6 above, panels a, b and c, for the daily means, monthly means and annual time series, respectively. Regarding the surface soil water content (the top 10 mm), it was very dry throughout the different time scales and very stable as compared with layer 1 and layer 2, irrespective of the time scales. This result gives rise to a special interest, as it contrasts with the usual trend whereby the variation in soil surface water is higher than sub-soil horizons in humid areas, as has been indicated by many reports (e.g., Zhang and Huang, 2004; Gao *et al*., 2016; Chandler *et al*., 2017). On the other hand, the variation in the soil water content depends on the season. Hence, during late spring, summer, and autumn, the water content in layer 1 was higher than in layer 2, and the reverse was true during the winter and early spring seasons. This result was the same for the monthly soil water content variations. This might be attributable the fact that during relatively wet seasons (late spring, summer and autumn), the soil water content in the deeper horizons would have been extracted by the perennial vegetation (which is the dominant vegetation in the catchment), whereas during dry seasons, the deeper horizons would have been subsidized with the shallow aquifer (the revap water), as discussed above in this section. For the case of time series mean annual soil water content, there is no clear trend between the layers. Generally, the spatial variation was mainly influenced by the complex interactions of soil, land use, topographic feature and the weather parameters, whereas for temporal variations, the weather parameters play the major role.

5.4.2 Soil water deficit and anomaly

The soil water deficit can be defined as the difference between the actual soil water content and the potential of the soil to retain a water content, called the field water capacity (American Meteorological Society, 2018; NIWA, 2018). On the other hand, the soil water anomaly shows the time series deviation of soil water from the normal value (usually a long-term mean) of soil profiles (EDO and JRC, 2018; NIWA, 2018). Therefore, for arid areas like the Soutloop Catchment, the description of the soil water anomaly would be more important than the soil water deficit. This is because it is obvious that arid climates are always in a water deficit condition; hence, the relative description of soil water availability (called soil water anomaly) would be a better indicator for drought monitoring and management. Therefore, the temporal variations of the monthly and annual soil water anomaly are given in Figures 5.9 and 5.10 above, respectively. The spatial variation of the mean soil water anomaly in the catchment is also given in Figure 5.11 above.

Regarding the time series monthly soil water anomaly (Figure 5.9 above), June 2004 was relatively the wettest month (which recorded the highest above-normal soil water content), whereas September 2008 was the driest period within the study period. Similarly, in the annual soil water anomaly (Figure 5.10 above), 1984 was the wettest year, whereas 2016 was the driest year. Moreover, the longest consecutive period of years with above-normal soil water content was 2010 – 2015 (more than 5-years long), while the longest consecutive periods of years with below-normal soil water content were: 1981 – 1983; 1990 – 1992; 1997 – 1999; and 2004 – 2006, which all are nearly 3-years long. Generally, most of the soil water anomaly calculated was consistent with both the extreme rainfall events (for both the occurrence of drought or above-normal rainfall). Therefore, this result indicates that the temporal rainfall variation was the major cause of the variation of the soil water anomaly in the catchment. Besides the rainfall variation, the presence of higher evaporative demand (high temperature, solar radiation, low relative humidity, and high wind speed) would exacerbate the loss of soil water through evapotranspiration.

The spatial variation of the soil water anomaly (Figure 5.11 above) shows that a larger part of the north-western and south-eastern parts of the catchment has experienced above-normal soil water content (SWA > 0 and shaded with deep green), while the north-eastern, central, and a considerable area of the south and south-western parts experienced a nearly normal soil water content (SWA closer to 0 and shaded yellow). On the other hand, the areas that experienced below-normal soil water content (SWA < 0 and shaded red) are distributed throughout the catchment, specifically dominating the western, south-western, some central, and north-eastern tips. The causes for the spatial variation of the soil water anomaly might be similar to the causes of the variation in soil water content. Therefore, the spatial distributions of the rainfall, topographic features, LULC and soil type played a key role in the spatial variation of the soil water anomaly in Soutloop Catchment.

5.5 Conclusion

This study was conducted to analyse the spatial and temporal variations of the root zone water content according to different soil, topographic features and LULC types, at a catchment scale. Since long-term, continuous observations of soil water were not readily available, this study also aimed at documenting such long-term time series variability of soil water with the application of distributed hydrological models. It can be said that the soil and water assessment tool (SWAT model) has successfully simulated the different processes of soil water variability in the Soutloop Catchment. However, it is expected that there might be considerable uncertainty in the results generated by the model, which could be related to the unavailability of flow data for *in situ* model calibration and validation, where the regionalization approach in a similar catchment was adopted here (see Chapter 3, Subsection 3.2.5).

The soil water in the Soutloop Catchment exhibited a higher spatial and temporal variation. Unlike the total soil water storage, this study identified a significant negative trend in the revap water. Although it is believed that the temporal variations of the soil water, including the contributions from the revap water, were mainly caused by the variations of daily weather parameters, the absence of a significant trend in the total soil water content shows that it needs a further study. It was also found that the environmental attributes, such as land use, topography and soil type, play controlling roles in the spatial distribution of soil water, other than the precipitation distribution. The results regarding the variation of soil water storage by depth were also interesting, which is inconsistent with the processes in humid areas where the surface variation of soil water is higher than in the sub-soil layers. Generally, confirmation of the suggested variability on temporal and spatial scales of soil water across the entire catchment requires further verification, over much larger scales, to increase the reliability of results.

The results in this study also showed that it is an added value to use the soil water anomaly (SWA) for agricultural drought monitoring and forecasting, in combination with the commonly recommended SPI (see Chapter 4, Subsection 4.3.4). It also provides an alternative approach that encourages making use of model-derived simulations as a new data source for drought investigations. This may be particularly relevant for planning in agriculture and for supporting decision makers and farmers in monitoring potential impacts on water resources and agriculture in the study catchment.

5.6 References

American Meteorological Society, 2018. *Meteorological glossary*, accessed on November 27, 2018. url: http://glossary.ametsoc.org/wiki/Soil_moisture_deficit.

Arnold, J.G., Moriasi, D.N., Gassman, P.W., Abbaspour, K.C., White, M.J., Srinivasan, R., Santhi, C., Harmel, R.D., van Griensven, A., van Liew, M.W. and Kannan, N., 2012. SWAT: model use, calibration, and validation. *Transactions of the ASABE*, 55(4), pp. 1491-1508.

Balugani, E., Lubczynski, M.W., Reyes-Acosta, L., van Der Tol, C., Francés, A.P. and Metselaar, K., 2017. Groundwater and unsaturated zone evaporation and transpiration in a semi-arid open woodland. *Journal of Hydrology*, 547, pp.54-66.

Barbeta, A. and Peñuelas, J., 2017. Relative contribution of groundwater to plant transpiration estimated with stable isotopes. *Scientific Reports*, 7(1), p.10580.

Bárdossy, A. and Lehmann, W., 1998. Spatial distribution of soil moisture in a small catchment. Part 1: geostatistical analysis. *Journal of Hydrology*, 206(1-2), pp.1-15.

Bittelli, M., 2011. Measuring soil water content: a review. *HortTechnology,* 21(3), pp.293-300.

Cepuder, P., Evett, S., Heng, L. K., Hignett, C., Laurent, J.P., Ruelle, P., 2008. *Field estimation of soil water content: a practical guide to methods, instrumentation and sensor technology*. International Atomic Energy Agency. Vienna, Austria.

Chandler, D.G., Seyfried, M.S., McNamara, J.P. and Hwang, K., 2017. Inference of soil hydrologic parameters from electronic soil moisture records. *Frontiers in Earth Science*, 5, p.25.

European Drought Observatory (EDO) and Joint Research Centre (JRC), 2018. *Soil moisture anomaly (SMA): EDO indicator factsheet*. European Commission. Accessed from url: http://edo.jrc.ec.europa.eu/documents/factsheets/factsheet_soilmoisture.pdf.

Endale, D., Fisher, D. and Schomberg, H., 2006. Soil water regime in space and time in a small Georgia Piedmont catchment under pasture. *Soil Science Society of America Journal,* 70(1), pp. 1-13.

European Environment Agency, 2015. *Signals 2015 - living in a changing climate*. Accessed from the following URL: https://www.eea.europa.eu/signals/signals-2015/articles.

Gao, X., Zhao, X., Brocca, L., Lv, T., Huo, G. and Wu, P., 2016. Upscaling of soil moisture content from surface to profile: multi-station testing of observation operators. *Hydrology and Earth System Sciences Discussions*, published online and accessed: https://doi.org/10.5194/hess-2016-617.

Gillson, L., Midgley, G.F. and Wakeling, J.L., 2012. Exploring the significance of land-cover change in South Africa. *South African Journal of Science,* 108(5-6), pp.03-05.

Gómez-Plaza, A., Martınez-Mena, M., Albaladejo, J. and Castillo, V.M., 2001. Factors regulating spatial distribution of soil water content in small semiarid catchments. *Journal of hydrology,* 253(1-4), pp.211-226.

Hébrard, O., Voltz, M., Andrieux, P. and Moussa, R., 2006. Spatio-temporal distribution of soil surface moisture in a heterogeneously farmed mediterranean catchment. *Journal of Hydrology,* 329(1), pp. 110-121.

Lal, R., 2004. Soil carbon sequestration impacts on global climate change and food security. *Science*, 304(5677), pp.1623-1627.

Mahanama, S., Koster, R., Reichle, R. and Zubair, L., 2008. The role of soil moisture initialization in sub-seasonal and seasonal streamflow prediction–a case study in Sri Lanka. *Advances in Water Resources,* 31(10), pp. 1333-1343.

Mello, C.R.D., Ávila, L.F., Norton, L.D., Silva, A.M.D., Mello, J.M.D. and Beskow, S., 2011. Spatial distribution of top soil water content in an experimental catchment of Southeast Brazil. Scientia Agricola, 68(3), pp.285-294.

Neitsch, S.L., Arnold, J.G., Kiniry, J.R. and Williams, J.R., 2011. *Soil and water assessment tool: theoretical documentation, Version 2009.* Texas Water Resources Institute Technical Report No. 406. Texas A&M University, Texas, USA.

Porporato, A., D'odorico, P., Laio, F., Ridolfi, L. and Rodriguez-Iturbe, I., 2002. Eco-hydrology of water-controlled ecosystems. *Advances in Water Resources*, 25(8), pp. 1335-1348.

Romano, N., 2014. Soil moisture at local scale: measurements and simulations. *Journal of Hydrology*, Volume 516, pp. 6-20.

Schoeman, F., Newby, T.S., Thompson, M.W. and van den Berg, E.C., 2013. South African national land-cover change map. *South African Journal of Geomatics*, 2(2), pp.94-105.

Schoeman, F., Newby, T.S., Thompson, M.W. and Van den Berg, E.C., 2010. *South African national land-cover change map*. A FAO report (Report No GW/A/2010/47) produced by the Agricultural Research Council-Institute for Soil, Climate and Water (ARC-ISCW), Pretoria, South Africa.

Seneviratne, S.I., Corti, T., Davin, E.L., Hirschi, M., Jaeger, E.B., Lehner, I., Orlowsky, B. and Teuling, A.J., 2010. Investigating soil moisture–climate interactions in a changing climate: a review. *Earth-Science Reviews*, 99(3-4), pp.125-161.

The National Institute of Water and Atmospheric Research (NIWA), 2018. Official website of NIWA, Accessed on November 27, 2018. url: https://www.niwa.co.nz/climate/nz-drought-monitor/droughtindicatormaps/soil-moisture-deficit-smd.

Wang, L. and Qu, J.J., 2009. Satellite remote sensing applications for surface soil moisture monitoring: a review. *Frontiers of Earth Science in China*, 3(2), pp.237-247.

Western, A.W., Zhou, S.L., Grayson, R.B., McMahon, T.A., Blöschl, G. and Wilson, D.J., 2004. Spatial correlation of soil moisture in small catchments and its relationship to dominant spatial hydrological processes. *Journal of Hydrology*, 286(1), pp. 113-134.

Whan, K., Zscheischler, J., Orth, R., Shongwe, M., Rahimi, M., Asare, E.O. and Seneviratne, S.I., 2015. Impact of soil moisture on extreme maximum temperatures in Europe. *Weather and Climate Extremes*, 9, pp.57-67.

Williams, C.J., McNamara, J.P. and Chandler, D.G., 2009. Controls on the temporal and spatial variability of soil moisture in a mountainous landscape: the signature of snow and complex terrain. *Hydrology and Earth System Sciences*, 13(7), pp.1325-1336.

Winchell, M., Srinivasan, R., Di Luzio, M. and Arnold, J., 2013. *ArcSWAT interface for SWAT2012: user's guide.* Blackland Research and Extension Centre, Blackland, Texas, USA.

Yeh, P.J. and Famiglietti, J.S., 2009. Regional groundwater evapotranspiration in Illinois. *Journal of Hydrometeorology*, 10(2), pp.464-478.

Zhang, Q. and Huang, R., 2004. Water vapour exchange between soil and atmosphere over a Gobi surface near an oasis in the summer. *Journal of Applied Meteorology*, 43(12), pp.1917-1928.

CHAPTER 6
VARIABILITY OF EVAPO-TRANSPIRATION AND VEGETATION WATER DEFICIT IN THE CATCHMENT

6.1 Introduction

Evapotranspiration (ET) is a combined term consisting of evaporation of water from either bare soil or water body in the presence of energy, whereas transpiration is the loss of water vapour from plant tissues to the atmosphere (Allen *et al*., 1998; Jovanovic and Israel, 2012). ET is an important component of the soil water and energy balance and is usually linked with ecosystem productivity, species distribution and ecosystem health (Christensen *et al*., 2008; Emanuel *et al*., 2010; Schaffrath and Bernhofer, 2013). This is because a significant amount of water is lost through this process. Babkin (2009) estimated that an annual amount of 577 $\times 10^3$ km^3 of water is lost through ET, globally (72 $\times$ 10^3 km^3 $year^{-1}$ being from the terrestrial land mass). Regarding South African conditions, Bennie and Hensley (2001) and Jovanovic *et al*. (2015) reported that, on average, 65% of the annual precipitation is lost through ET from crop fields in semi-arid areas. ET is not a means of water loss only; it is also one of the major ways of losing energy during the conversion of liquid water to vapour. Babkin (2009) estimated that ET consumes 25% of the total energy reaching the earth's surface (which is about 1.26×10^{24} joules). Therefore, ET is a very important process that influences water and energy balances between the earth's surface and the atmosphere. Hence, the accurate determination of ET is a very important task in arid and semi-arid environments.

Evapotranspiration is highly variable, both spatially and temporally. This is because it is affected by the complex interaction of the soil–plant–atmosphere continuum. The interactive influence of topographic features, soil characteristics, vegetation, and climatic factors influence ET significantly (Western, *et al.*, 2004; Babkin, 2009; Zhao and Ji, 2016). These factors determine the rate of ET by influencing the availability of water, energy and vegetation type of an area. However, the influence of this complex interaction in the spatial and temporal distribution of ET differs greatly, depending on other conditions. For example, in dry climates, the water availability is a limiting factor (Zhao *et al.*, 2014), the distribution of the vegetation type is also a limiting factor in catchment-scale studies (Western, *et al.*, 2004; Li *et al.*, 2015), and soil type (due to differences in soil water holding capacity) is another important factor in some instances (Hatfield and Prueger, 2011). Jarmain and Meijninger (2010), Dzikiti *et al*. (2014), and Zhao and Ji (2016) showed that the vapour pressure gradient and plant characteristics are important for the variations of ET in vegetated areas. Zhang *et al*. (2016b) also showed that the vegetation leaf area index is an important driver of evapotranspiration.

Evapotranspiration is one of the most difficult parameters in the soil–plant–atmosphere continuum for determination (Jovanovic and Israel, 2012; Zhao *et al.*, 2013; Banimahd *et al.*, 2015). This is due to the complex nature of the evapotranspiration process. However, a number of methods are proposed in the literature to measure or to estimate evapotranspiration. These include: (i) lysimeters, which provide the most direct method to measure ET (Jovanovic and Israel, 2012; Wang and Dickinson, 2012). (ii) The scintillometers, which estimate the latent and sensible heat by using a device to measure small fluctuations of the refractive index of air (Jarmain *et al*., 2009). (iii) The Eddy Covariance Method, which determines evapotranspiration from the correlation between fluctuations in vertical wind speed and atmospheric humidity (Wang and Dickinson, 2012). (iv) The sap flow technique, whereby transpiration is measured from the rate of sap flow in trees and parts of trees, using heat as a tracer with an estimate of the area of wood through which flow occurs (Nouri *et al*., 2013; Zhang *et al*., 2014; Ferraz *et al*., 2015). Other methods, such as the use of models and remote sensing, are also important improvements in the estimation of ET, with a better spatial and temporal scale.

Numerous studies have been conducted on the spatial and temporal distribution of evapotranspiration. These studies have been conducted at the global scale (Jung *et al*., 2010; Vinukollu *et al*., 2011; Badgley *et al*., 2015; Zhang *et al*., 2016a), the regional scale (Zhao *et al*., 2014; Li *et al*., 2015; Nistor *et al*., 2017; Wang *et al*., 2013; Kramer *et al*., 2015), and a number at the catchment scale. Some studies are available in South African context. For example, Gibson *et al*. (2013) and Jarmain *et al*. (2009) evaluated the applicability of remote sensing for the estimation of spatio-temporal evapotranspiration. Dzikiti *et al*. (2014) estimated an ET of 1460 mm year^{-1}, from a Sandstone Fynbos. Another study by Meijninger and Jarmain (2014) showed that the annual ET had reduced by 9.5%, on average, following the clearance of the alien plant species. Jovanovic *et al*. (2015) analysed MOD16 satellite data and found an average ET for South Africa (from 2000 to 2012) to be 303 mm year^{-1} which comprised 14% of the potential evaporation and 67% of the precipitation. Majozi *et al*. (2017) investigated the performance of satellite-based ET algorithms and two global data products for South Africa. However, they showed that none of the models performed well for South African conditions.

However, studies of the spatial and temporal variation in ET are scarce, at all levels of study, especially arid areas, although evapotranspiration is a crucial component in the hydrologic cycle. The evapotranspiration process is also a complex and dynamic process in both space and time. Therefore, the aim of this chapter is to analyse the spatial and temporal variation of evapotranspiration in an arid catchment in Northern Cape Province, South Africa. The catchment was evaluated with two indicators of vegetation water deficit, namely by the evaporative stress index (ESI) and by the remote sensing-based normalized difference vegetation index (NDVI).

6.2 Materials and methods

6.2.1 Description of the study area

The study catchment is located in the Northern Cape Province, South Africa, with a geographic location of between 22°11’00” and 23º28”00” E longitudes and 28°03’00” and 29°06’00” S latitudes. The details for the location and description of the study catchment can be seen in Chapter 3, Subsection 3.2.1.

6.2.2 Testing normality of time series data

As explained in the previous chapters, the graphical method (probability-probability (P-P plot) and quantile-quantile (Q-Q plot)) and the statistical method (Shapiro-Wilk test) were used to test the normality of the data. For details, see Chapter 4, Subsection 4.2.3.

6.2.3 Trend analysis of evapotranspiration

The trend analysis in the long-term (1980–2016) evapotranspiration data was investigated by the non-parametric Mann-Kendall test. For details, see Chapter 4, Subsection 4.2.3.

6.2.4 The spatial variation of evapotranspiration

SWAT was used to estimate the spatial and temporal values of evapotranspiration at HRU and sub-basin scale, as discussed in Chapter 3. In this section, therefore, the mean value of the long-term monthly and yearly variations of evapotranspiration are analysed spatially with ArcGIS 10.4.

6.2.5 Indicators of vegetation water deficit

6.2.5.1 Evaporative stress index (ESI)

The evaporative stress index shows standardized anomalies in reference ET fractions or vegetation stress attributable to the lack of water. It is regarded as an early indicator of water stress for an area. It was calculated by the following equation (Anderson *et al*., 2007):

$$ESI = 1 - fPET = 1 - \frac{ET}{PET} \tag{6.1}$$

where *ESI* is the Evaporative Stress Index, *ET* is the actual evapotranspiration (mm), and *PET* is the potential evapotranspiration (mm). If the ESI value is closer to zero, it indicates that water is available for the area. On the other hand, as the ESI value approaches towards 1, it shows the area is under a water stress condition.

6.2.5.2 Normalized difference vegetation index (NDVI)

The normalized difference vegetation index (NDVI) is a multi-scale drought indicator that shows the response of vegetation to water stress in the catchment, and is an important indicator in drought-monitoring tasks. The calculation of NDVI is based on the relative differences of the land cover classes to light reflectance at different electromagnetic spectra (Huete *et al*., 1999; Didan *et al*., 2015). As a result, the NDVI is a normalized transform of NIR (near infrared) to red reflectance ratios, and it is expressed as (Huete *et al*., 1999; Senay *et al*., 2015; Didan *et al*., 2015):

$$NDVI = \frac{(\rho_{NIR} - \rho_{RED})}{(\rho_{NIR} + \rho_{RED})} \tag{6.2}$$

where ρ is the spectral reflectance at red and NIR (near infra-red) bands.

However, the Moderate Resolution Imaging Spectroradiometer (MODIS) Normalized Difference Vegetation Index (NDVI), which was used in this study, was processed and produced by the NASA/Goddard Space Flight Centre's Global Inventory Modelling and Mapping Studies (GIMMS) Group, as accessed on October 17, 2018. The URL for the data was found at: https://gimms.gsfc.nasa.gov/MODIS/std/GMOD09Q1/tif/NDVI/. The dataset is divided in tiles of 9x9 degrees for ease of data management. Then, each tile covering the study catchment was downloaded and clipped by the boundary of the study catchment.

6.3 Results

6.3.1 Normality test

The tests of the normality of the time series data (both mean annual and monthly evapotranspiration) were conducted by a visual assessment, together with statistical tests. The results of the graphical assessment are shown in Figure 6.1 below, panels a to d, and the results of the numerical tests are given in Table 6.1. Both the graphical sketches and the statistical tests show that the mean monthly evapotranspiration does not meet the requirements of a normal distribution, while the annual evapotranspiration data follow a normal distribution. Therefore, it can be concluded that parametric statistics can be applied to the time series annual evapotranspiration, but not to the monthly evapotranspiration.

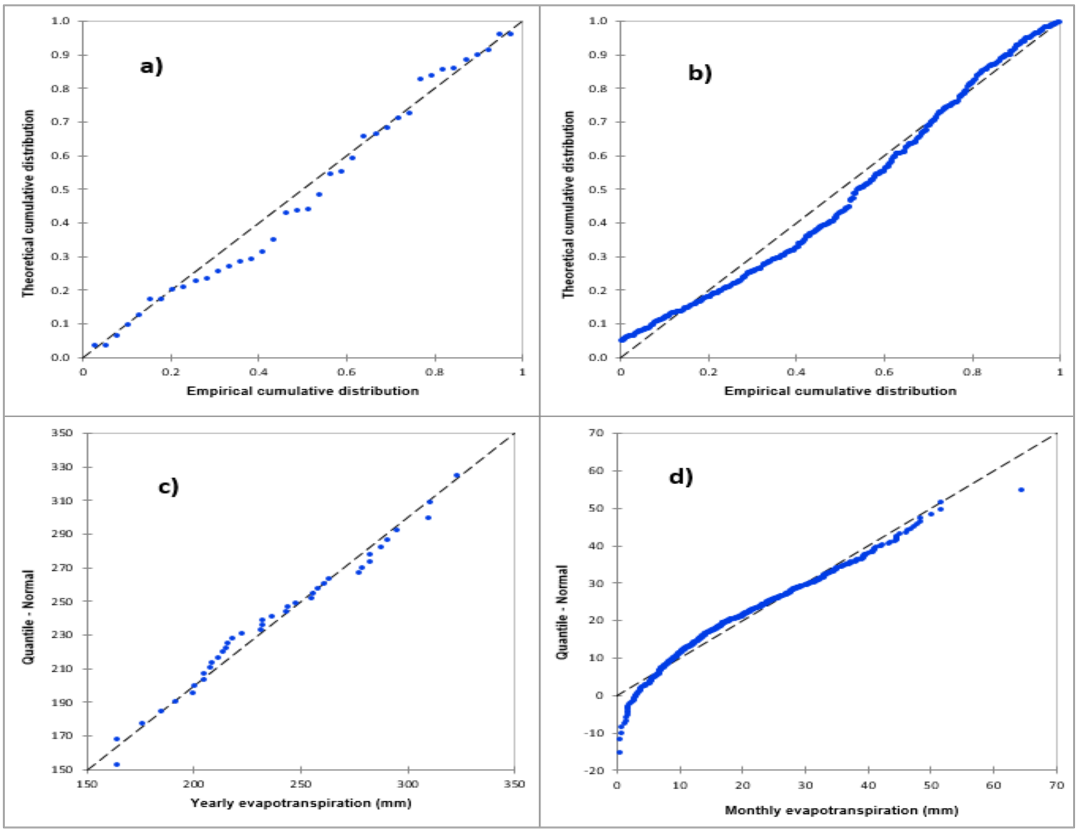

Figure 6.1: Graphical sketches showing the normality of the evapotranspiration data

Notes: (a) probability-probability (P-P plot) for the mean annual evapotranspiration, (b) quantile-quantile (Q-Q plot) for mean annual evapotranspiration, (c) probability-probability (P-P plot) for the mean monthly evapotranspiration, and (d) quantile-quantile (Q-Q plot) for the mean monthly evapotranspiration.

Table 6.1: Tests of normality for the time series of evapotranspiration data

Variable	Observations	Minimum	Maximum	Mean	Std. deviation	Shapiro-Wilk test	
						W	p-value
Annual ET	39	163.89	323.03	238.522	41.407	0.976	0.549
Monthly ET	468	0.51	64.54	19.877	11.816	0.964	< 0.01

6.3.2 Trends of evapotranspiration

In this section, the long-term trends of evapotranspiration, mean daily, monthly and annual values are described in detail. The impacts of other components, such as precipitation, soil water content and revap water from shallow aquifer, are also analysed. Accordingly, the long-term mean daily evapotranspiration, soil water and precipitation are shown in Figure 6.2 below. The 39-year mean monthly values of evapotranspiration and other water balance components mentioned above are shown in Figure 6.3 below. Finally, the long-term time series trends of evapotranspiration are depicted in Figures 6.4 and 6.5 below for the mean annual and monthly evapotranspirations, respectively. The time series trend analyses are conducted by the non-parametric Mann-Kendall test, and the statistics are shown in Table 6.2 below.

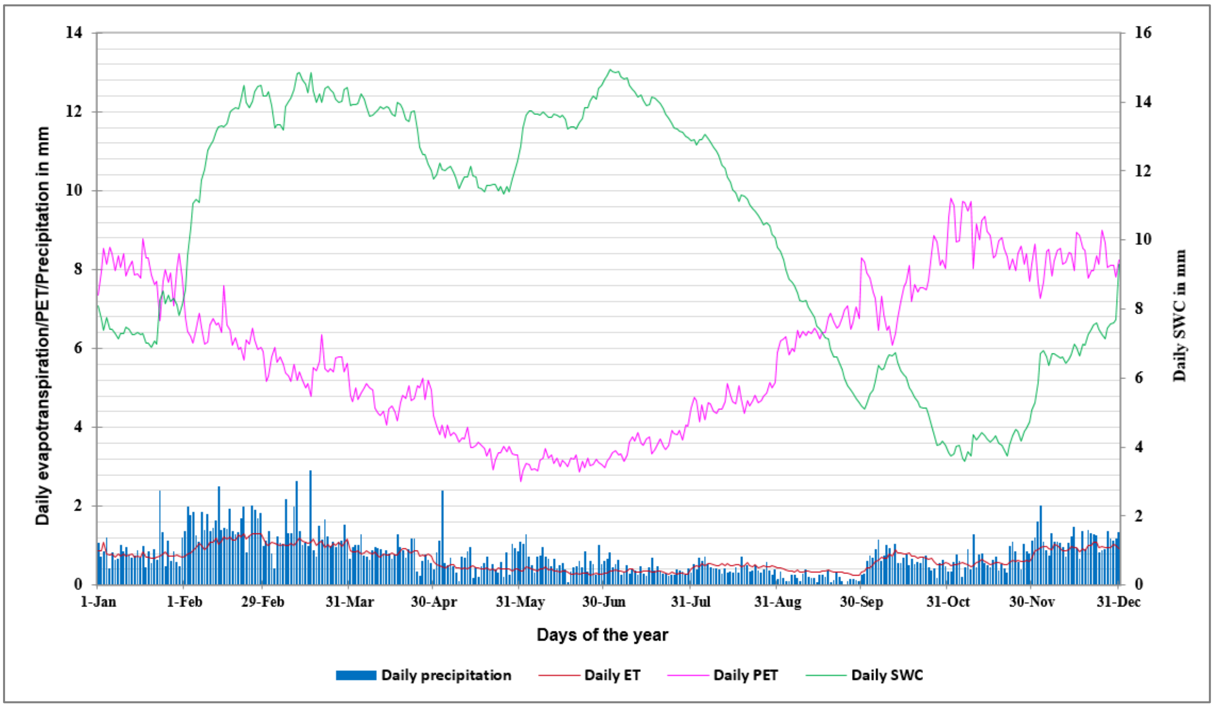

Figure 6.2: Comparison of the long-term mean daily evapotranspiration, soil water content and precipitation in the catchment.

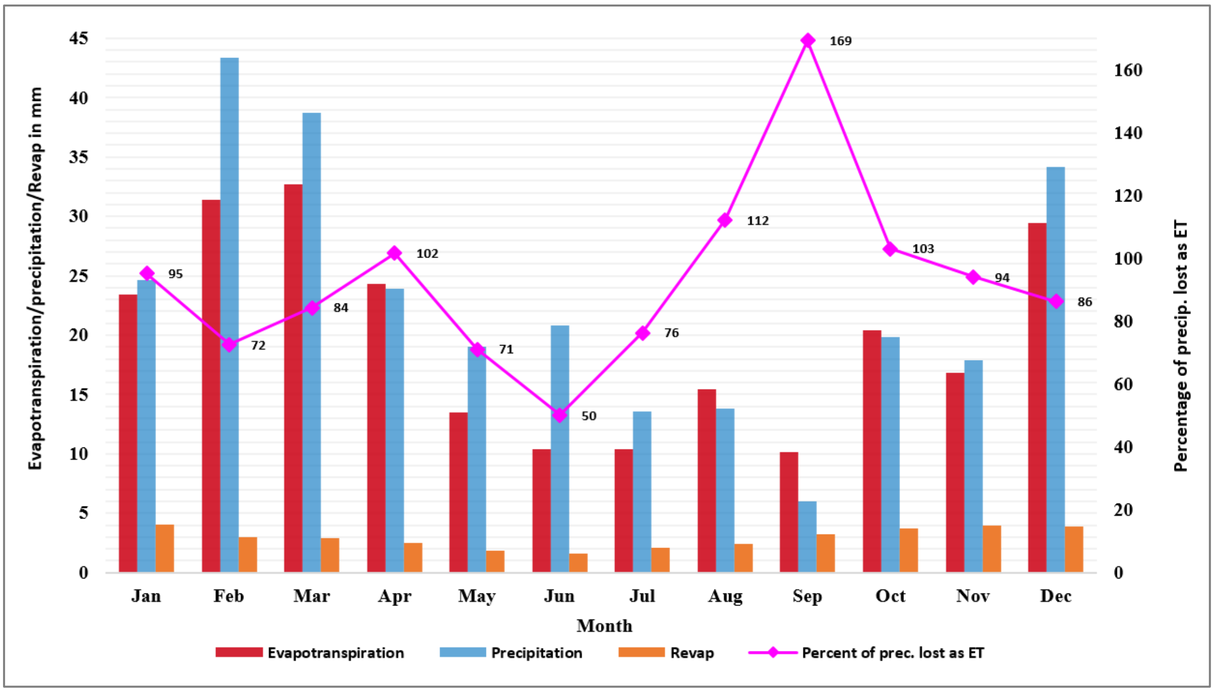

Figure 6.3: Long-term monthly mean evapotranspiration variation and comparison with the corresponding precipitation in Soutloop Catchment.

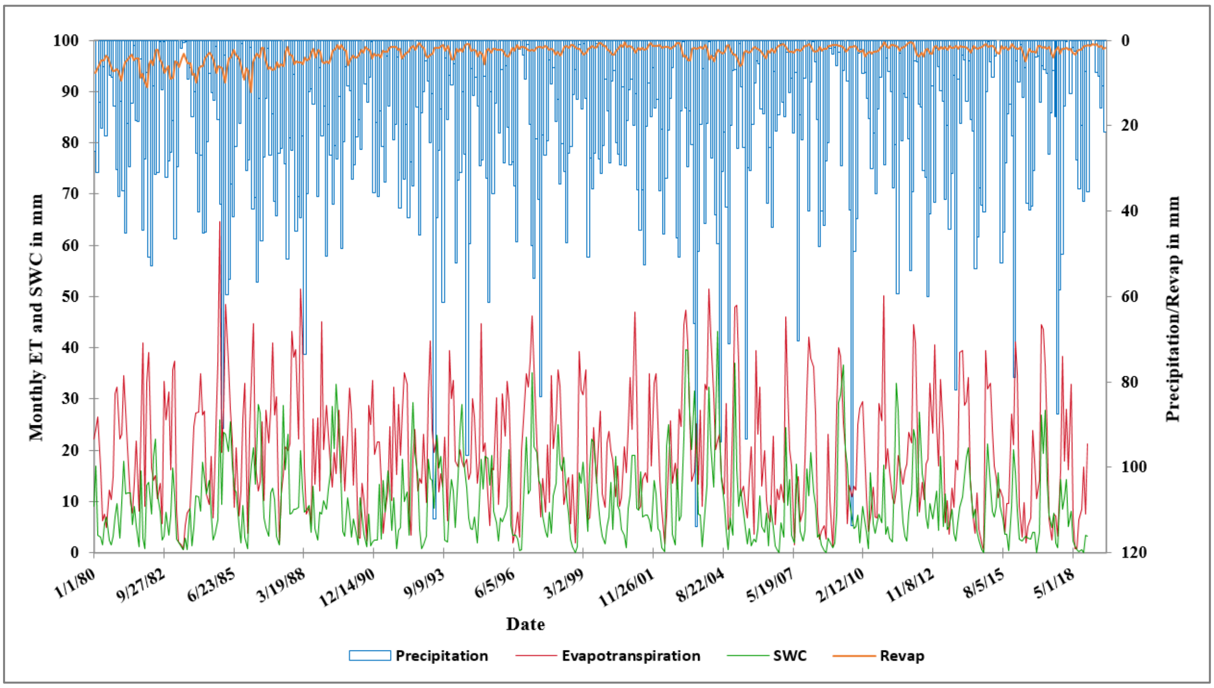

Figure 6.4: Trends of monthly evapotranspiration as compared with other water balance components in Soutloop Catchment.

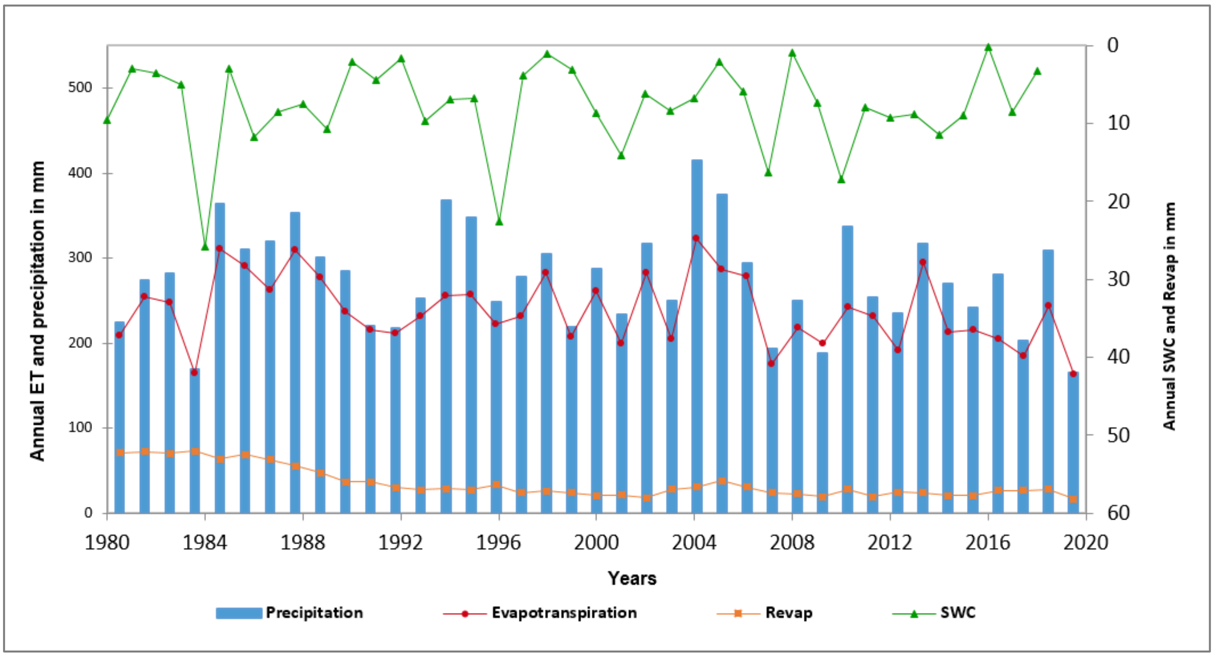

Figure 6.5: Trends of annual evapotranspiration and comparison with precipitation and soil water content in Soutloop Catchment.

Table 6.2: Statistics of the Mann-Kendall trend test for the mean annual and monthly evapotranspiration

Parameters	Annual values		Monthly values	
	ET	PET	ET	PET
Kendall's tau	-0.228	0.0877193	-0.073	0.014696
S stat	-169	65	-7957	1606
Var(S)	6834	6834	11425598	11425622
p-value	0.042	0.439	0.019	0.635
Sen's slope	-1.25	1.553	-0.01	0.011

Regarding the mean daily variation (Figure 6.2 above), the evapotranspiration follows the patterns of daily precipitation and soil water content. Hence, the mean evapotranspiration increased as the precipitation and soil water content increased, and vice versa. Unlike the potential evapotranspiration, the magnitude of estimated evapotranspiration is highly dependent on the precipitation. It also shows that there was a very high precipitation deficit, since there was a large gap between the long-term values of precipitation and potential evapotranspiration. The comparison between the actual evapotranspiration and precipitation shows that on some days of the year, particularly in the drier seasons, the rate of evapotranspiration was above the precipitation. This condition could be attributable to the influence of the revap water from the shallow groundwater (Figure 6.3 above). Generally, as precipitation increases, both soil water content (up to the field capacity) and evapotranspiration (up to the potential evapotranspiration) increase.

Most of the long-term mean monthly parameters (Figure 6.3 above) show approximately similar trends as observed for evapotranspiration, i.e. evapotranspiration increased with precipitation, and vice versa. However, the contribution from the revap water is contrary to this trend. In this case, the revap water increases as the precipitation decreases, as seen in the winter and early spring seasons. Figure 6.3 above also shows the amount of precipitation lost through evapotranspiration. The amount of precipitation lost through evapotranspiration varies from 50% in winter (e.g., June) to 169% during spring (e.g., September). Some months in the late winter and late spring seasons experienced more than 100% of precipitation losses.

Furthermore, the long-term trends of the time series analysis are depicted in Figures 6.4 and 6.5 above for the mean monthly and annual actual and potential evapotranspiration, respectively. Based on this, both the annual and monthly time series for actual evapotranspiration showed a significant, decreasing trend. However, no significant trend was detected for both the annual and monthly potential evapotranspirations. The annual time series mean evapotranspiration was decreased by 1.25 mm per annum, while the monthly time series evapotranspiration decreased by 0.01 mm per month, on average, as shown by the Sen's slope values. It is also important to note from the previous chapters that the precipitation (Chapter 4, Subsection 4.3.2) and the revap water (Chapter 5, Subsection 5.3.2) also showed decreases of 0.011 and 0.007 mm per month, respectively.

6.3.3 Spatial variation of evapotranspiration

This section explains the spatial variation of evapotranspiration and the contribution of the revap water to evapotranspiration during times of soil water deficit from shallow aquifers. Figures 6.6 and 6.7 below show the long-term mean annual evapotranspiration and the revap water, respectively. Similarly, Figures 6.8 and 6.9 below show the long-term mean seasonal variations in evapotranspiration and the revap water, respectively.

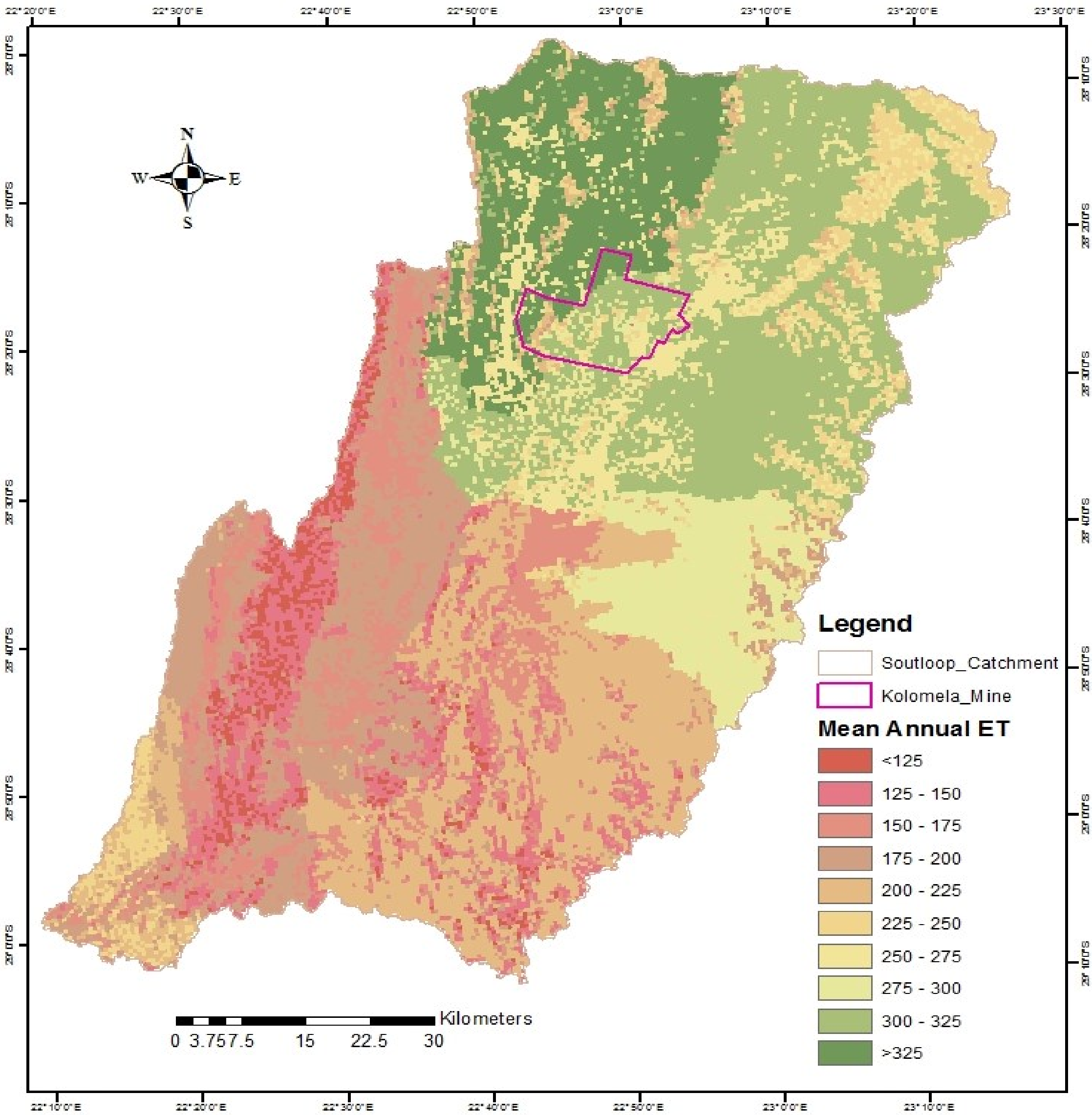

Figure 6.6: Spatial variations of the long-term mean annual evapotranspiration in Soutloop Catchment.

The long-term mean annual evapotranspiration (Figure 6.6) divides the catchment into two, i.e. the northern part that has a relatively higher evapotranspiration (> 250 mm per annum) and the southern part that has a relatively lower amount of evapotranspiration (<250 mm per annum). This spatial pattern of evapotranspiration follows the same trend as the long-term annual precipitation in the catchment (as explained in Chapter 4, Subsection 4.3.3). In the case of the revap water, Figure 6.7 below shows that areas with low altitudes with flat slopes had a higher contribution of revap water to evapotranspiration. Areas that are dominated by deep-rooted vegetation also experience a better contribution. Hence, those areas where the stream network passes throughout the catchment, the south-western lowlands, and small patches of land with deep-rooted vegetation throughout the catchment, had a higher contribution to revap water in the Soutloop Catchment. The land cover and slope classes in the catchment are explained in Chapter 3, Section 3.2.1.4.

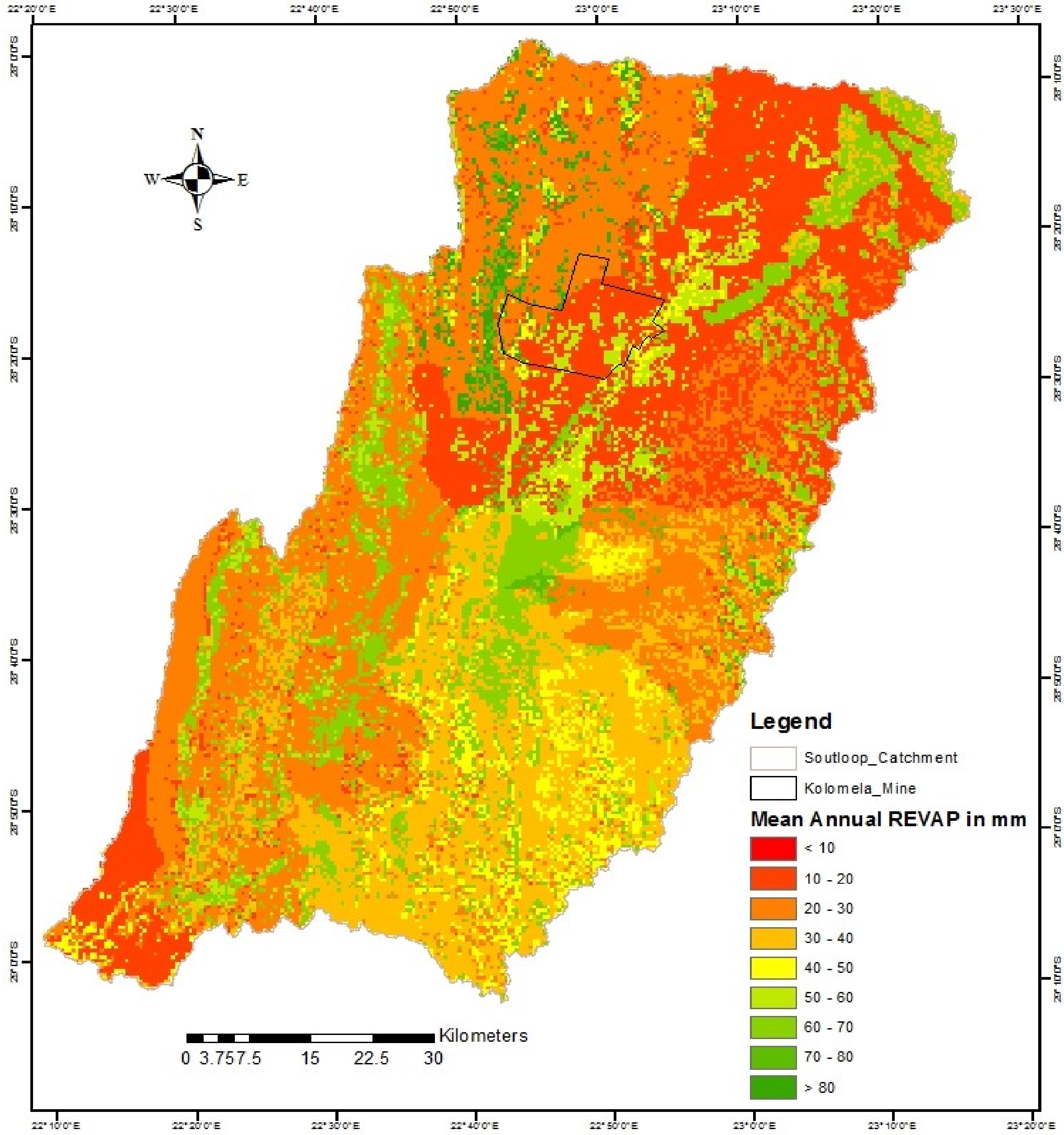

Figure 6.7: Spatial variations of the long-term mean annual revap in Soutloop Catchment.

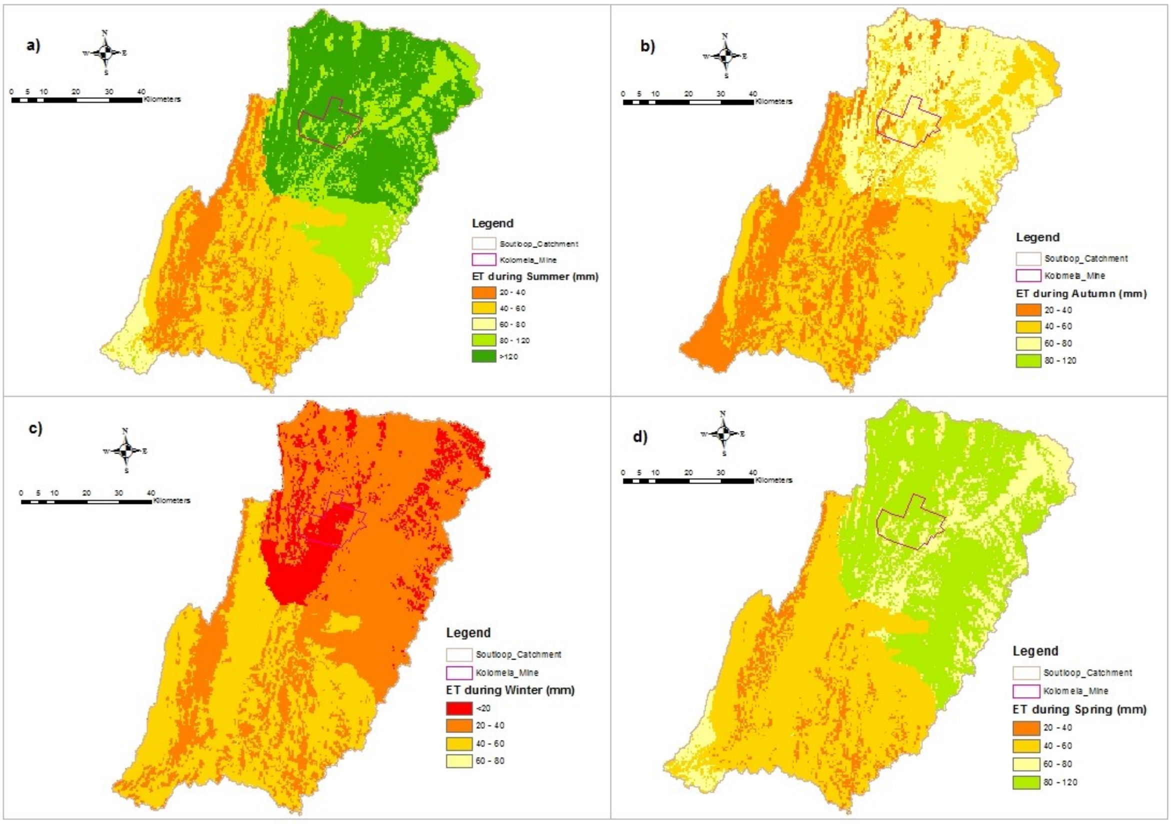

Figure 6.8: Spatial variations of the long-term mean seasonal evapotranspiration in Soutloop Catchment.

Notes: a) in summer season, b) in Autumn season, c) in winter season, and d) in Spring season.

The spatial variation of evapotranspiration and the revap water varied seasonally, as shown in Figures 6.8 above and 6.9 below, respectively. In the summer season, the evapotranspiration follows the trend of the precipitation, i.e. evapotranspiration decreases as one goes from north to south. In autumn, evapotranspiration also decreases, but with narrow ranges, as compared with the summer season, from north to south directions. On the other hand, in the winter season, the reverse for summer is true, i.e. evapotranspiration decreases as one moves from south to north, which is similar to the trends of precipitation. Finally, during spring, evapotranspiration decreases from north to south, but still with the same trends as those for precipitation. However, the case of the revap water was different. Autumn was the season with lowest revap water, while spring was the season with the highest contribution of evapotranspiration from revap water. This trend is also opposite to the spatial trends of the soil water content, as explained in Chapter 5, Subsection 5.3.3. Therefore, the spatial distribution of the revap water was dependent primarily on the precipitation distribution (which also affects the spatial distribution of soil water content that would be mostly lost as evapotranspiration), altitude and slope (as the altitude and the slope decreased, there would be higher contribution to revap water), and variation in LULC, where deep-rooted vegetation had higher revap contribution to evapotranspiration.

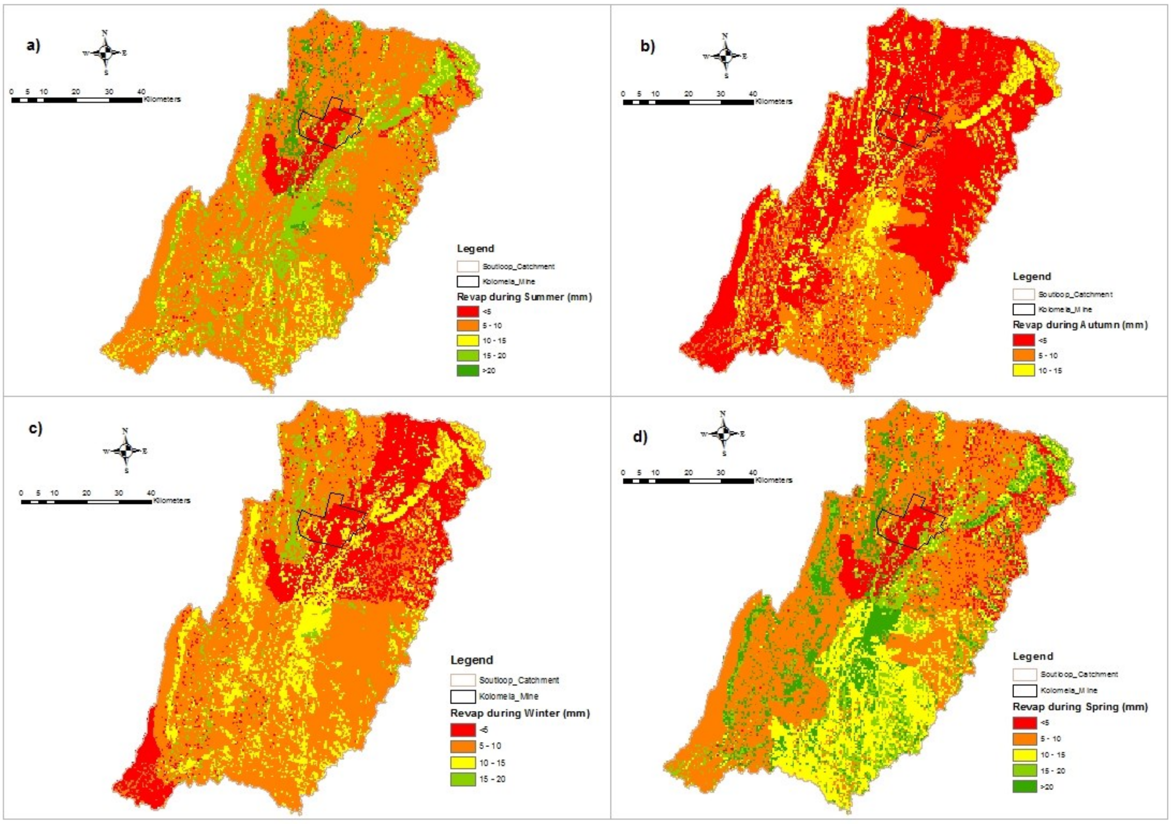

Figure 6.9: Spatial variations of the long-term mean seasonal revap in Soutloop Catchment

Notes: a) in summer season, b) in autumn season, c) in winter season, and d) in spring season.

6.3.4 Indicators of vegetation water deficit

In water-limited areas, much of the available water can be lost as evapotranspiration, which is also true for the Soutloop Catchment (see Section 6.3.2 of this chapter). Since evapotranspiration shows the productivity and health of ecosystems (Lu *et al.*, 2011; Tian *et al.*, 2010), its spatial and temporal variation can indicate important information regarding water availability or deficit. Therefore, in this section, the evaporative stress index (ESI) and the normalized difference vegetation index (NDVI) are explained to evaluate water deficit by using vegetation water stress as a major indicator in the study area.

6.3.4.1 Evaporative stress index (ESI)

The time series of annual and monthly variation of the evapotranspiration stress index (ESI) is given in Figure 6.10 below. The comparison of the long-term mean values of daily, monthly and annual values of the evapotranspiration stress index is shown in Figure 6.11 below. Generally, the magnitude of the ESI values shows that the area was subjected to a high vegetation water stress condition throughout the study period. Based on the monthly ESI (Figure 6.10 below), the lowest stress record (better availability of water) in the catchment was experienced in April 1986 (with an ESI value of 0.55), and the worst stress periods were experienced in July 1983, December 2008, and November 2014 (with ESI values of closer to 1). Regarding annual stress, 1987 and 2003 were relatively the lowest stressed years (with an ESI of 0.83), whereas 1983, 2006 and 2015 were the years with the worst evaporative stress in the catchment. The long-term mean daily, monthly and annual trends of ESI values (Figure 6.11 below) follow more or less a similar pattern of change, and vary around the annual value for the different seasons throughout the year. It also shows that late summers and the early spring seasons were the relatively lowest and highest stress periods, respectively.

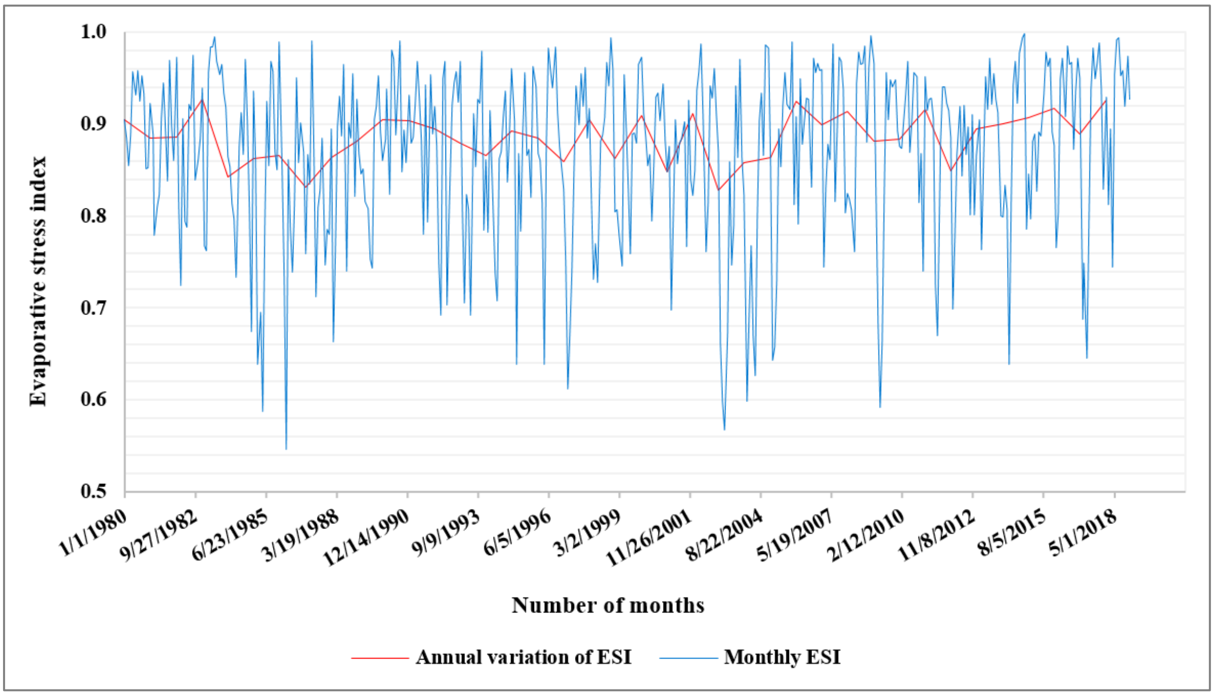

Figure 6.10: Comparison of the monthly and annual values of the evaporative stress index in the catchment.

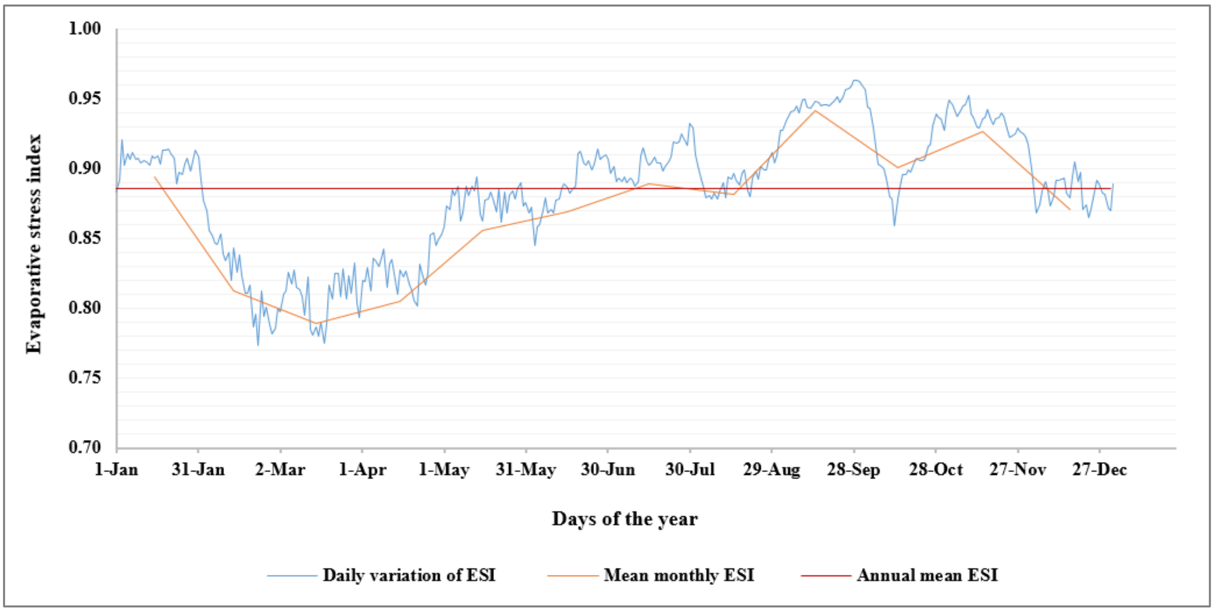

Figure 6.11: Daily variation of the evaporative stress index and comparison of its monthly and annual mean values in the catchment.

6.3.4.2 Normalized difference vegetation index (NDVI)

The other indicator of water deficit, which is based on remote sensing data, is the normalized difference vegetation index (NDVI). The time series NDVI anomaly, which shows the deviation of each NDVI value from the normal value (the average of all NDVI values in the analysis period, 2000–2018), is reflected in Figure 6.12 below. The analysis of the 8-day NDVI anomaly in the 19 consecutive years (2000–2018) shows that the driest vegetation seasons, with more than 25 consecutive weeks, include: 17/1/2002–13/8/2002 (27 weeks), 1/1/2003–10/2/2004 (52 weeks), 26/2/2004–15/10/2004 (30 weeks), 2/6/2005–9/1/2006 (29 weeks), 1/5/2009–27/12/2009 (31 weeks), 1/1/2015–13/8/2015 (29 weeks), and 6/9/2015–29/3/2016 (27 weeks). Similarly, the relatively wet seasons with better green vegetation, which has more than 25 consecutive wet weeks, include: 26/2/2000–5/9/2000 (25 weeks), 7/4/2001–9/1/2002 (36 weeks), 17/1/2006–17/11/2006 (39 weeks), 1/1/2011–12/11/2011 (44 weeks), 14/4/2012–25/1/2013 (37 weeks), and 9/1/2017–6/9/2017.

Figure 6.13 below shows a comparison of annual NDVI values at different seasons of the year. Five years were selected for comparison, at five-year intervals from 2000 to 2018, where the last year was taken as a fifth NDVI dataset. Accordingly, 2000, 2005, 2010, 2015 and 2018 were selected for comparison. Generally, NDVI values were higher in the early autumn season and lowest in the spring season. In comparing the years, the year 2000 had relatively better green vegetation (higher NDVI value) than the others did, whereas the year 2015 had the lowest green vegetation (lower NDVI value) in the study catchment. The lowest NDVI value in 2015 is also consistent with the occurrence of drought, as discussed in Chapter 4, Subsection 4.3.4.

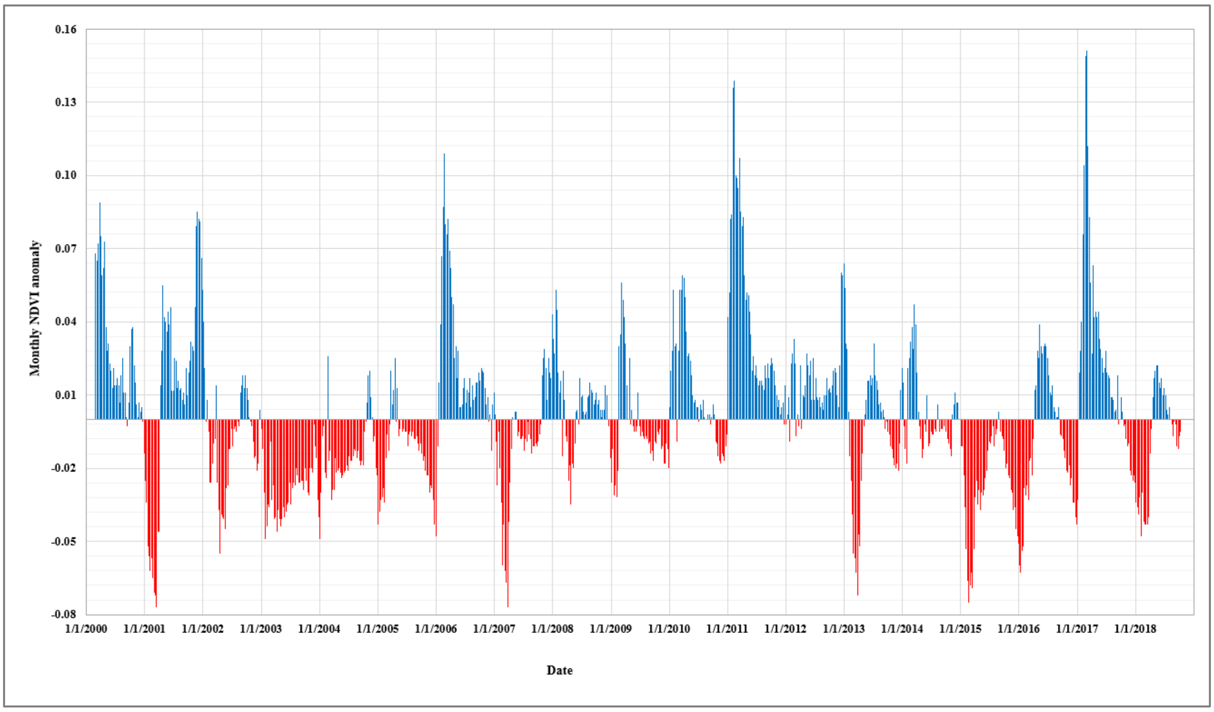

Figure 6.12: Anomaly of the time series NDVI from 2000 to 2018 in the catchment.

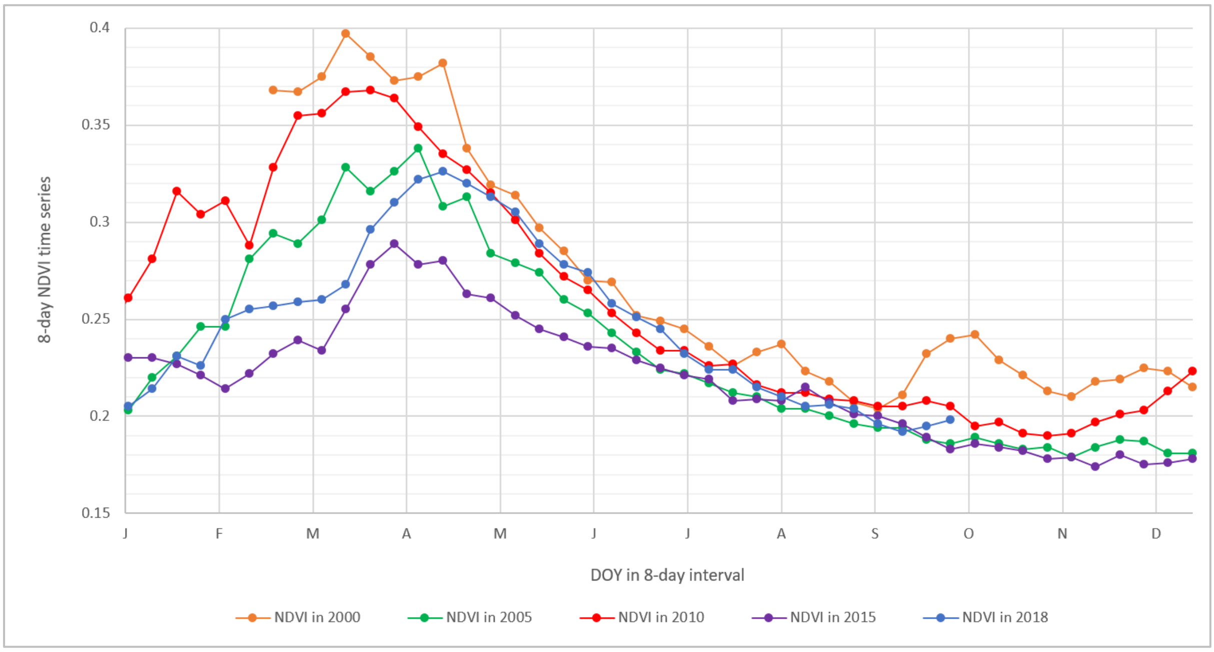

Figure 6.13: Temporal variation of an 8-day MODIS NDVI in the catchment.

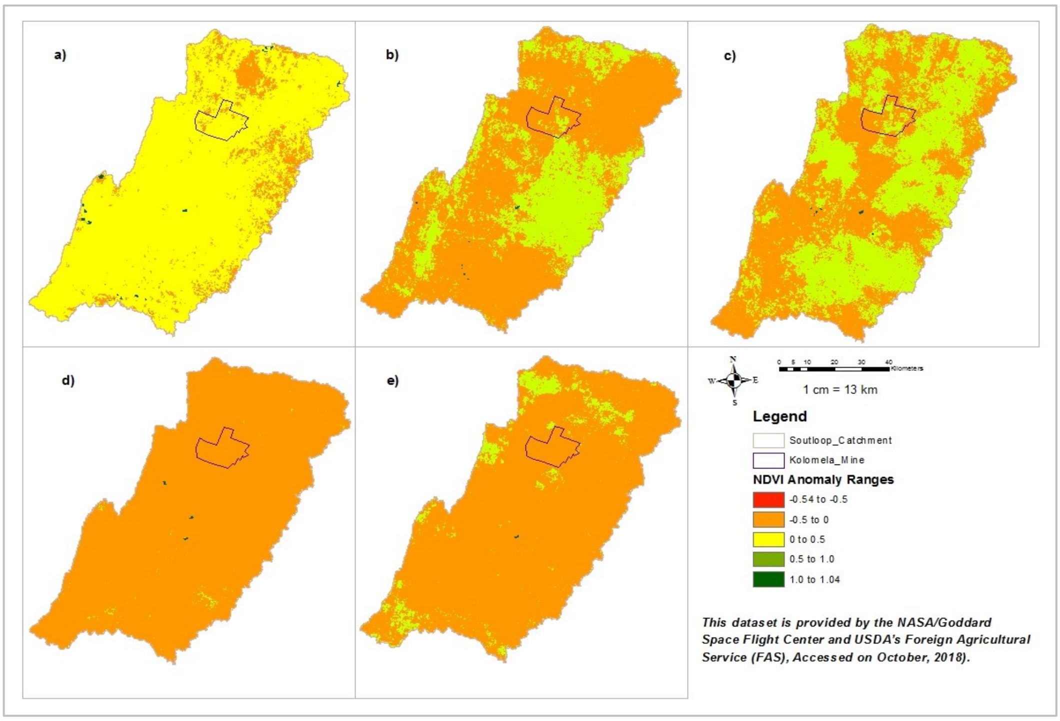

Figure 6.14: Spatial variation of an 8-day NDVI anomaly in Soutloop Catchment (February).

Notes: a) February, 2000, b) February, 2005, c) February, 2010, d) February, 2015, and e) February, 2018.

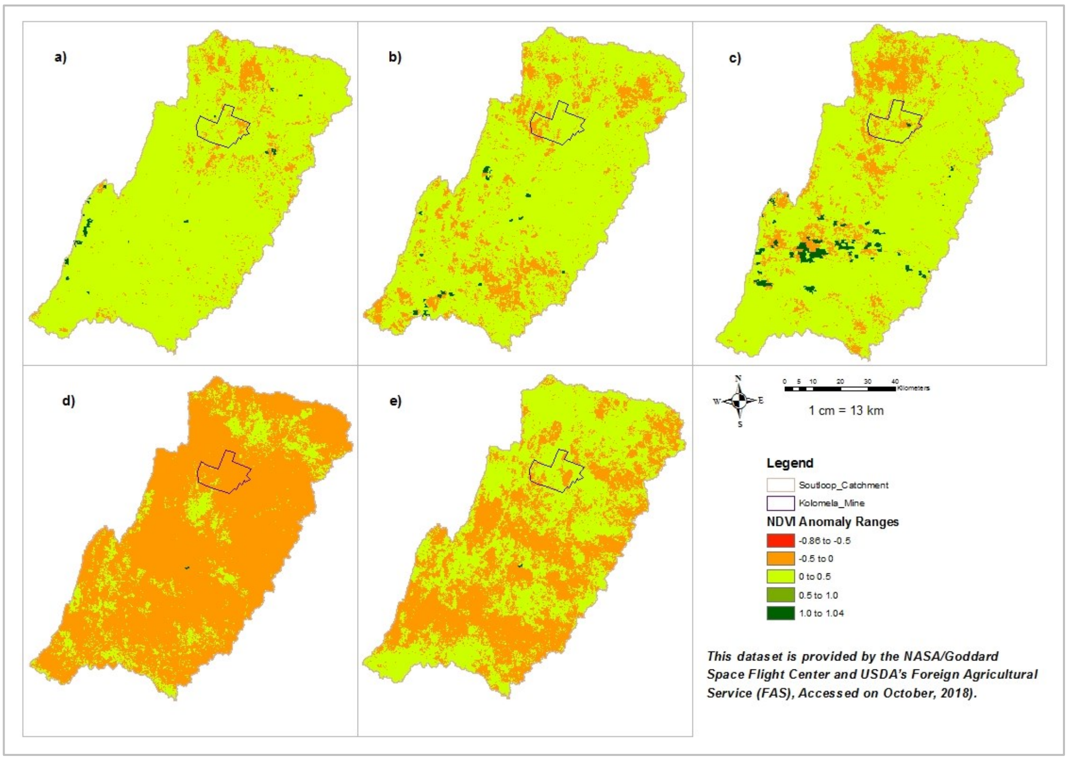

Figure 6.15: Spatial variation of an 8-day NDVI anomaly in Soutloop Catchment (April).

Notes: a) April, 2000, b) April, 2005, c) April, 2010, d) April, 2015, and e) April, 2018.

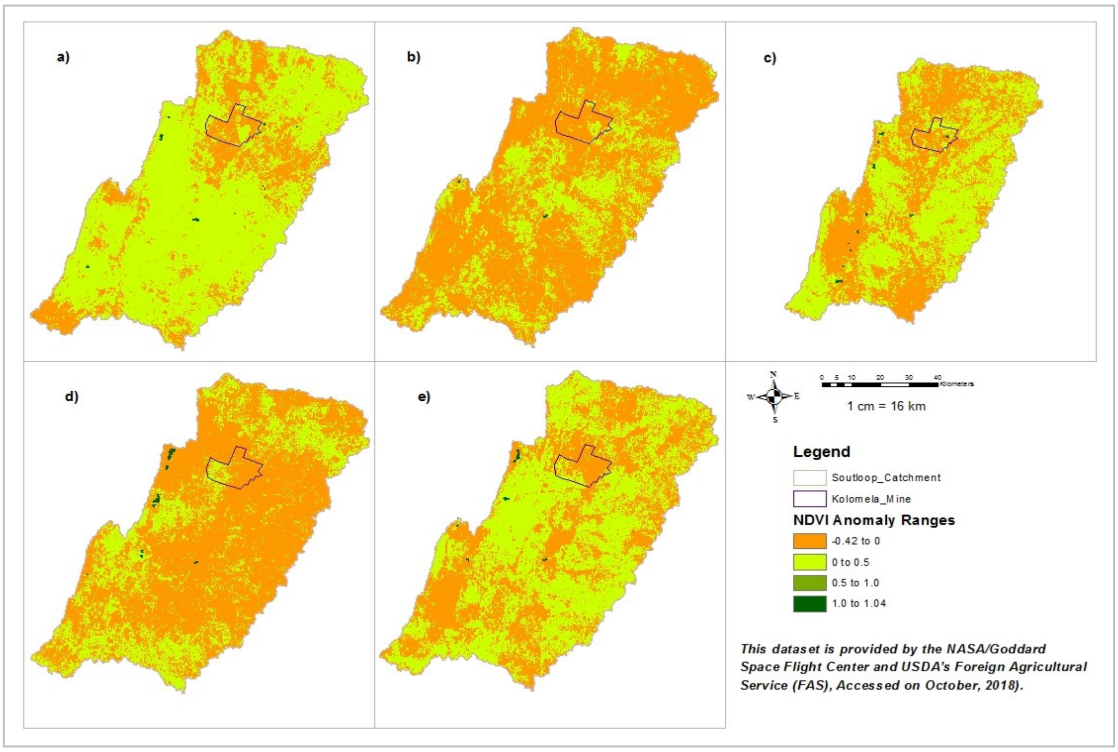

Figure 6.16: Spatial variation of an 8-day NDVI anomaly in Soutloop Catchment (July).

Notes: a) July, 2000, b) July, 2005, c) July, 2010, d) July, 2015, and e) July, 2018.

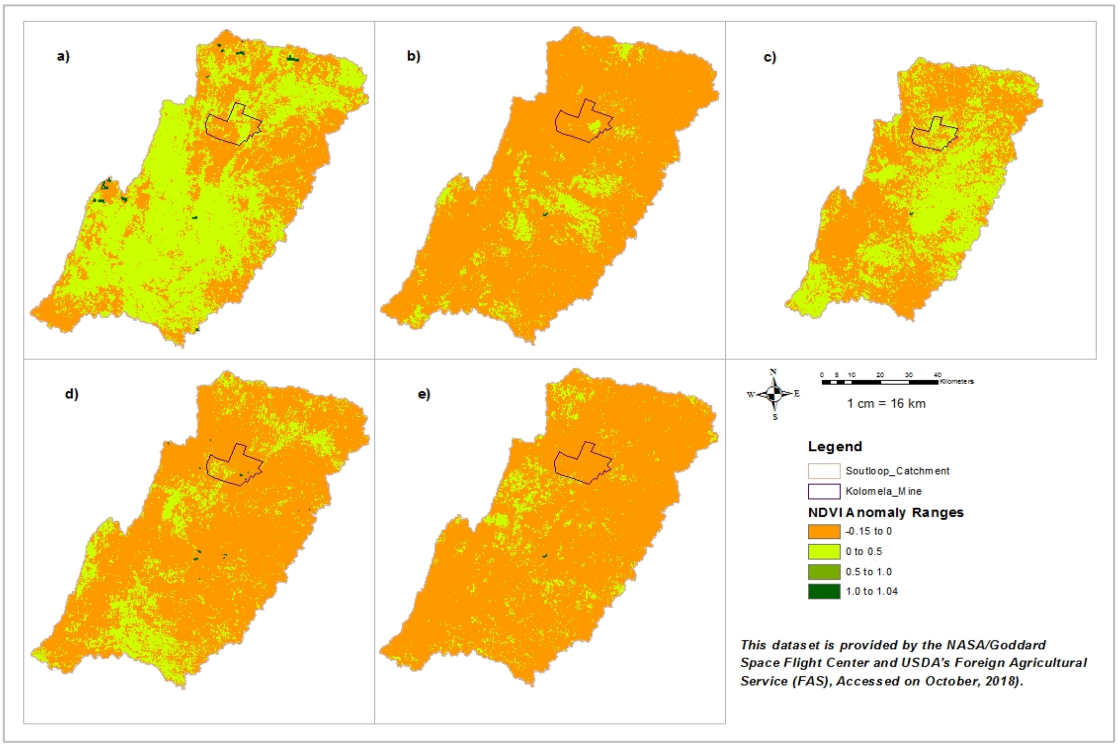

Figure 6.17: Spatial variation of an 8-day NDVI anomaly in Soutloop Catchment (September).

Notes: a) September, 2000, b) September, 2005, c) September, 2010, d) September, 2015, and e) September, 2018.

The spatial variations of NDVI values within the study catchment were also compared. For this comparison, four dates were selected randomly from the four seasons of the year. Hence, the following days of the year (DOY) were selected: DOY 049 was assumed to represent the summer season, DOY 105 was assumed to represent autumn season, DOY 193 was assumed to represent the winter season, and DOY 265 was assumed to represent the spring season in the study catchment. The results for the comparisons are depicted in Figures 6.14, 6.15, 6.16 and 6.17 above for the summer, autumn, winter, and spring seasons, respectively. The spatial maps show that the NDVI anomaly varied both spatially and temporally within the selected years and seasons. In the first selected season (summer as shown in Figure 6.14 above), the NDVI anomaly was above-normal ranges (0-0.5) for most areas of the catchment in 2000, whereas almost all areas were below normal (<0) during 2015, which is consistent with the 2015 drought. Most areas in 2018 were also below the normal value. The summer seasons of 2005 and 2010 had a mix of below-normal (<0) and above-normal (>0) NDVI anomalies. The comparison of the autumn seasons for the selected years (Figure 6.15 above) indicates that in 2000, 2005 and 2010 years, most of the catchment area had above normal rainfall; however, the 2015 drought had also been reflected in autumn. Figure 6.16 above also shows the NDVI anomaly in the winter season. Hence, 2000 was the best year for green vegetation in the catchment, followed by 2018. The impact of the 2015 drought was still visible in winter season. Finally, the NDVI anomaly for spring (Figure 6.17 above) shows that 2000 was the better year for green vegetation, followed by 2010, whereas the analysis of the NDVI anomaly shows that the spring seasons during 2005, 2015 and 2018 had dry vegetation in most of the catchment area.

6.4 Discussion

6.4.1 Spatio-temporal variability of evapotranspiration

The temporal variations of evapotranspiration in the Soutloop Catchment were analysed in two ways. The first is the analysis of long-term averages, such as the daily (Figure 6.2 above) and monthly averages (Figure 6.3 above). The other way of analysis is the detection of trends on the time series values, such as trends in annual time series (Figure 6.5 above) and monthly time series (Figure 6.4 above). The spatial analysis, on the other hand, is based on the long-term average of the annual evapotranspiration, as given in Figure 6.6 above, with revap being shown in Figure 6.7 above, seasonal evapotranspiration in Figure 6.8 above, and seasonal revap in Figure 6.9 above.

The rate of mean daily evapotranspiration follows the patterns of daily precipitation and soil water content. Accordingly, it increases as the precipitation and soil water content increases, and vice versa. It also shows that there was a very high gap between the actual and the potential evapotranspiration, indicating that the catchment is under severe deficit of precipitation, which was discussed in Chapter 4. On the other hand, the daily mean comparison shows that the actual evapotranspiration was greater than precipitation in some seasons of the year, particularly in drier seasons. Jovanovic *et al*. (2009) has also reported greater evapotranspiration than the precipitation on alien vegetation in Western Cape, South Africa. This condition could be attributed to the influence of the revap water from the shallow aquifers (See Figure 6.3 above). As the soil water deficit increased due to lower precipitation and higher evaporation demand by the atmosphere, the revap water would be increased (Neitsch *et al*., 2011; Arnold *et al*., 2012; Winchell *et al*., 2013). Similarly, the percentage of precipitation lost through evapotranspiration varied from 50% in early spring to 169% in early winter. This result is consistent with the previous result on the contribution of the revap water to soil water and evapotranspiration (up to 32%), as discussed in Chapter 5, Subsection 5.3.2. From the annual precipitation, an average of 85% of the precipitation was lost as evapotranspiration in Soutloop Catchment. Reports show that the total mean annual losses of precipitation through evapotranspiration in South Africa has been estimated to vary from 65%, as reported by Bennie and Hensley (2001), to 67% as reported by Jovanovic *et al*. (2015). Therefore, it indicates that the shallow aquifer has a significant influence on the water balance of the Soutloop Catchment. As similarly reported by Yeh and Famiglietti (2009), Adrià Barbeta and Peñuelas (2017), and Evaristo and McDonnell (2017), the aridity of the catchment and the presence of perennial vegetation could have accounted for the significant contribution of the revap water in Soutloop Catchment. Particularly, in areas covered with natural and perennial vegetation, the revap contribution will be very high, since perennial vegetation is deep rooted in nature and easily extracts water from a shallow aquifer (Yeh and Famiglietti, 2009; Balugani *et al*. (2017; Adrià Barbeta and Peñuelas, 2017).

Regarding the trends of the time series of annual (Figure 6.5 above) and monthly (Figure 6.4 above) evapotranspiration, both the annual and monthly time series evapotranspiration showed a significant, decreasing trend. The annual time series mean evapotranspiration showed an average decrease of 1.25 mm per annum, while the monthly time series evapotranspiration decreased by 0.01 mm per month. One possible reason for the decrease in the trend of evapotranspiration might be the decrease in monthly precipitation, as discussed in Chapter 4, Subsection 4.3.2. The decrease of the revap contribution (as discussed in Chapter 5, Subsection 5.3.2) could also be another reason. Moreover, there was no significant trend in the potential evapotranspiration at both monthly and annual time scales. Therefore, the variations of climate, other than precipitation, (i.e. air temperature, humidity, solar radiation and wind speed) could not be the cause for the decrease in evapotranspiration. The other possible cause could be (although this is not yet tested) the change in LULC. Therefore, the change in LULC in the study catchment should be investigated in future studies.

There was also a higher spatial variation of evapotranspiration and contribution from the revap water in the study catchment, as shown in Figures 6.6 and 6.7 above, respectively. Generally, the long-term mean annual evapotranspiration divided the catchment into two, i.e. the northern part that has a higher evapotranspiration (> 250 mm per annum) and the southern part that has a lower amount of evapotranspiration (<250 mm per annum). This spatial pattern of evapotranspiration follows the same trend for the long-term annual precipitation in the catchment (explained in Subsection 4.3.3). In the case of the revap water (Figure 6.7 above), it is shown that areas with low altitudes, and with flat slopes, had a higher contribution of revap water to evapotranspiration. Areas that are dominated by deep-rooted vegetation also have a better contribution. Hence, those areas where the stream network passes throughout the catchment, the south-western lowlands, and small patches of land with deep-rooted vegetation throughout the catchment, had a higher contribution to revap water in the Soutloop Catchment. The land cover and slope classes in the catchment are explained in Chapter 3, Subsection 3.2.1.4. The distribution of evapotranspiration and its revap contribution were highly variable according to the seasons, as seen in Figures 6.8 and 6.9 above, respectively. The seasonal variation was primarily caused by the seasonal distribution of the precipitation. Generally, the distribution of precipitation, variation in the potential evapotranspiration, LULC, topographic features, altitudinal difference and soil types play a vital role in the seasonal and annual spatial variation of evapotranspiration and revap contribution in the catchment (Yeh and Famiglietti, 2009; Evaristo and McDonnell, 2017; Balugani *et al.*, 2017; Adrià Barbeta and Peñuelas, 2017).

6.4.2 Evaluation of vegetation water deficit

The evaluation of water stress in the study catchment was also conducted by the analysis of the fraction of evapotranspiration as compared with the potential evapotranspiration, and by the direct analysis of the relative differences of the different land cover classes to light reflectance, at different electromagnetic spectra (Huete *et al*., 1999; Didan *et al*., 2015). The first method of analysis is called the evaporative stress index (ESI) and the latter is called the normalized difference vegetation index (NDVI). Hence, the time series variation of monthly and annual ESI is given in Figure 6.10 above, and the comparison of long-term values of the daily, monthly and annual ESI is given in Figure 6.11 above. Similarly, the time series (every 8 days) variation of mean NDVI anomaly is given in Figure 6.12 above, and a comparison of selected years for their time series variation in NDVI values is shown in Figure 6.13 above for the catchment. The spatial variation of NDVI for the selected years and one representative measure per month per season is shown in Figures 6.14 to 6.17 above.

The value of ESI varied, based on the time scale: for example, the monthly values vary from the lowest stress record of 0.55 in April, 1986, to the worst record, which is closer to 1, in July, 1983, December, 2008, and November, 2014. Regarding the annual stress values, 1987 and 2003 were the relatively lowest-stressed years (with an ESI of 0.83) and 1983, 2006 and 2015 were the worst evaporative stress years in the catchment. Most of these stress values (for example, the worst stress years of 1983 and 2015, and the relatively less stressed years of 1986 and 2003) are consistent with the SPI values that are discussed in Chapter 4, Subsection 4.3.4. The long-term mean daily and monthly ESI values (Figure 6.11 above) follow more or less a similar pattern of variability, and vary around the annual value for the different seasons throughout the year. It also shows that late summers and early spring seasons were relatively the lowest and the highest stress periods, respectively, which is consistent with other results and discussions in Chapters 4 and 5 of this thesis.

The evaluation of water stress was conducted with the help of the MODIS (Moderate Resolution Imaging Spectro-radiometer) NDVI products, with a spatial resolution of 250 metres and an 8-day temporal resolution. The time series anomaly (Figure 6.12 above) clearly showed the condition of water stress, with the higher temporal scale (every 8 days) from 2000 to 2018 in the catchment. The years which had longer drier seasons were 2014, 2015, 2016 and 2018, which is consistent with SPI results that indicate that these consecutive years comprised the longest drought occurrence for the catchment since 1980. A comparison of annual time series NDVI values was also conducted at every 5-year interval from 2000 (2000, 2005, 2010, 2015 and 2018), as reflected in Figure 6.13 above. Generally, the NDVI values were higher (having much green vegetation) in the early autumn season, and lowest in the spring season, which follows the seasonal precipitation distribution. In comparing the years, the year 2000 had relatively better green vegetation (higher NDVI value) than others did, whereas the year

2015 had the lowest green vegetation (lower NDVI value) in the catchment. The lowest NDVI value in 2015 is also consistent with the occurrence of the drought, as discussed in Chapter 4, Subsection 4.3.4.

Finally, the spatial variations of the NDVI anomaly for the five years were compared. For this comparison, four days of the year (DOYs) were selected randomly from the four seasons of the year (DOY 49 represents summer, 105 represents autumn, 193 represents winter, and 265 represents spring seasons), as shown in Figures 6.14, 6.15, 6.16 and 6.17 above for summer, autumn, winter and spring, respectively.

The spatial maps show that the NDVI anomaly varied both spatially and temporally within the selected years and seasons. In the summer season, the NDVI anomaly was slightly above normal (0-0.5 ranges) for most areas of the catchment in 2000, whereas almost all areas were below normal (<0) during 2015 and 2018, which is consistent with the 2015–2018 drought. The summer seasons of 2005 and 2010 had a mix of below-normal (<0) and above-normal (>0) NDVI anomalies. The comparison of the autumn seasons for the selected years shows that in 2000, 2005 and 2010, most of the catchment area experienced above-normal NDVI anomaly; however, the 2015 drought had been also reflected in autumn. Regarding winter, 2000 was the best year for green vegetation in the catchment, followed by 2018. The impact of the 2015 drought was still visible in winter season. Finally, the NDVI anomaly for spring shows that 2000 was the better year for green vegetation in spring, followed by 2010, whereas the spring seasons during 2005, 2015 and 2018 experienced dry vegetation in most of the catchment area. Generally, as the precipitation increased, there was a better chance of seeing green vegetation in the catchment.

6.5 Conclusion

The main objectives of this chapter were to analyse the spatial and temporal variability of evapotranspiration and to evaluate the extent of vegetation stress in the Soutloop Catchment, based on the long-term simulated outputs of the SWAT model and satellite products. The analysis of evapotranspiration in the Soutloop Catchment indicated that it had experienced higher spatial and temporal variations during the study period. The long-term trend shows that the rate of actual evapotranspiration was far below the rate of the potential evapotranspiration, this showing a severe precipitation deficit in the catchment. In some seasons of the year, the actual evapotranspiration was higher than the precipitation because of the movement of water from the shallow groundwater upwards to the root zone, and extraction by deep-rooted vegetation. The monthly and annual time series ET also showed a decreasing trend due to the decrease of precipitation and the revap water. This study also showed alternative indices for evaluating water deficit in catchments. Hence, the evapotranspiration-based ESI and the satellite-based NDVI methods are good indicators to describe the extent of water deficit, and as an alternative index for monitoring agricultural drought, other than the usual precipitation-based SPI. However, some results of the ESI and NDVI were not consistent with the precipitation-based SPI, probably due to its differences in time scale and nature of the indices. The outcomes of this study suggest that NDVI has good potential for monitoring agricultural drought in arid areas. Further analysis of the NDVI, including the drought impact and assessment regarding other climatic variables and land uses/land covers, is needed to fully evaluate its potential applications. Overall, the results presented in this study provide information for the management of climate change impacts, as well as for devising appropriate mitigation measures at a local scale.

6.6 References

Allen, R. G., Pereira, L. S., Raes, D. and Smith, M., 1998. *Crop evapotranspiration - guidelines for computing crop water requirements.* FAO Irrigation and drainage paper 56. Rome, Italy.

Anderson, M.C., Norman, J.M., Mecikalski, J.R., Otkin, J.A. and Kustas, W.P., 2007. A climatological study of evapotranspiration and moisture stress across the continental United States based on thermal remote sensing: 1. model formulation. *Journal of Geophysical Research: Atmospheres,* 112(D10).

Arnold, J.G., Moriasi, D.N., Gassman, P.W., Abbaspour, K.C., White, M.J., Srinivasan, R., Santhi, C., Harmel, R.D., van Griensven, A., Van Liew, M.W. and Kannan, N., 2012. SWAT: model use, calibration, and validation. *Transactions of the ASABE,* 55(4), pp. 1491-1508.

Babkin, V., 2009. Evaporation from the surface of the globe. *In: Hydrological Cycle Volume II.* Encyclopedia of Life Support Systems (EOLSS), p. 48, Paris, France.

Badgley, G., Fisher, J.B., Jiménez, C., Tu, K.P. and Vinukollu, R., 2015. On uncertainty in global terrestrial evapotranspiration estimates from choice of input forcing datasets. *Journal of Hydrometeorology*, 16(4), pp.1449-1455.

Balugani, E., Lubczynski, M.W., Reyes-Acosta, L., van Der Tol, C., Francés, A.P. and Metselaar, K., 2017. Groundwater and unsaturated zone evaporation and transpiration in a semi-arid open woodland. *Journal of hydrology*, 547, pp.54-66.

Banimahd, S., Khalili, D., Kamgar-Haghighi, A. and Zand-Parsa, S., 2015. Evapotranspiration model selection for estimation of actual evaporation from bare soil, as required in annual potential groundwater recharge studies of a semi-arid foothill region. *Archives of Agronomy and Soil Science*, 61(10), pp. 1455-1472.

Barbeta, A. and Peñuelas, J., 2017. Relative contribution of groundwater to plant transpiration estimated with stable isotopes. *Scientific Reports*, 7(1), p.10580.

Bennie, A. T. P. and Hensley, M., 2001. Maximizing precipitation utilization in dryland agriculture in South Africa-a review. *Journal of Hydrology*, 241 (1), 124-139.

Christensen, L., Tague, C.L. and Baron, J.S., 2008. Spatial patterns of simulated transpiration response to climate variability in a snow dominated mountain ecosystem. *Hydrological Processes*, 22(18), pp.3576-3588.

Davies, C.L., Timm Hoffman, M. and Roberts, W., 2016. Recent trends in the climate of Namaqualand, a megadiverse arid region of South Africa. *South African Journal of Science*, 112(3-4), pp.1-9.

Didan, K., Munoz, A.B., Solano, R. and Huete, A., 2015. *MODIS vegetation index user's guide (MOD13 series)*. Vegetation Index and Phenology Lab, The University of Arizona, pp. 1-38.

Dzikiti, S., Jovanovic, N.Z., Bugan, R., Israel, S. and Le Maitre, D.C., 2014. Measurement and modelling of evapotranspiration in three fynbos vegetation types. *Water SA*, 40(2), pp.189-198.

Emanuel, R.E., Epstein, H.E., McGlynn, B.L., Welsch, D.L., Muth, D.J. and D'Odorico, P., 2010. Spatial and temporal controls on catchment ecohydrology in the northern Rocky Mountains. *Water Resources Research*, 46(11), pp. 1-14.

Evaristo, J. and McDonnell, J.J., 2017. Prevalence and magnitude of groundwater use by vegetation: a global stable isotope meta-analysis. *Scientific reports*, 7, p.44110.

Ferraz, T.M., Netto, A.T., Reis, F.D.O., Peçanha, A.L., De Sousa, E.F., Machado Filho, J.A., Rodrigues, W.P., Glenn, D.M. and Campostrini, E., 2015. Relationships between sap-flow measurements, whole-canopy transpiration and reference evapotranspiration in field-grown papaya (Carica papaya L.). *Theoretical and Experimental Plant Physiology*, 27(3-4), pp.251-262.

Gibson, L.A., Jarmain, C., Su, Z. and Eckardt, F.E., 2013. Estimating evapotranspiration using remote sensing and the Surface Energy Balance System–A South African perspective. *Water SA*, 39(4), pp.477-484.

Hatfield, J.L. and Prueger, J.H., 2011. Agroecology: implications for plant response to climate change. *Crop Adaptation to Climate Change*, pp.27-43.

Huete, A., Justice, C. and van Leeuwen, W., 1999. *MODIS vegetation index (MOD13) algorithm theoretical basis document*. NASA Goddard Space Flight Centre, Greenbelt, Maryland, USA.

Jarmain, C. and Meijninger, W.L., 2010. Assessing the impact of invasive alien plants on South African water resources using remote sensing techniques. *In Proceedings of a Symposium organized by the International Commission on Remote sensing of IAHS*, pp. 27-30. Jackson Hole, Wyoming, USA.

Jarmain, C., Mengitsu, M., Jewitt, G.P.W., Kongo, V. and Bastiaanssen, W., 2009. *A methodology for near-real time spatial estimation of evaporation*. Water Research Commission, Pretoria, South Africa.

Jovanovic, N. and Israel, S., 2012. Critical review of methods for the estimation of actual evapotranspiration in hydrological models. *In Irmak, D.A., ed. Evapotranspiration - remote sensing and modelling.* InTech Open, pp. 329-350.

Jovanovic, N., Mu, Q., Bugan, R.D. and Zhao, M., 2015. Dynamics of MODIS evapotranspiration in South Africa. *Water SA*, 41(1), pp.79-90.

Jovanovic, N.Z., Israel, S., Tredoux, G., Soltau, L., Le Maitre, D., Rusinga, F., Rozanov, A. and van der Merwe, N., 2009. Nitrogen dynamics in land cleared of alien vegetation (Acacia saligna) and impacts on groundwater at River Lands Nature Reserve (Western Cape, South Africa). *Water SA*, 35(1).

Jung, M., Reichstein, M., Ciais, P., Seneviratne, S.I., Sheffield, J., Goulden, M.L., Bonan, G., Cescatti, A., Chen, J., De Jeu, R. and Dolman, A.J., 2010. Recent decline in the global land evapotranspiration trend due to limited moisture supply. *Nature,* 467(7318), p.951.

Kramer, R.J., Bounoua, L., Zhang, P., Wolfe, R.E., Huntington, T.G., Imhoff, M.L., Thome, K. and Noyce, G.L., 2015. Evapotranspiration trends over the eastern United States during the 20th century. *Hydrology*, 2(2), pp.93-111.

Li, H., Chen, Z., Jiang, Z., Sun, L., Liu, K. and Liu, B., 2015. Temporal-spatial variation of evapotranspiration in the Yellow River Delta based on an integrated remote sensing model. *Journal of Applied Remote Sensing*, 9(1), p.096047.

Li, H., Zhang, Y. and Zhou, X., 2015. Predicting surface runoff from catchment to large region. *Advances in Meteorology*, 2015, p. 13.

Lu, N., Chen, S., Wilske, B., Sun, G. and Chen, J., 2011. Evapotranspiration and soil water relationships in a range of disturbed and undisturbed ecosystems in the semi-arid Inner Mongolia, China. *Journal of Plant Ecology*, 4(1-2), pp. 49-60.

Majozi, N.P., Mannaerts, C.M., Ramoelo, A., Mathieu, R., Mudau, A.E. and Verhoef, W., 2017. An intercomparison of satellite-based daily evapotranspiration estimates under different eco-climatic regions in South Africa. *Remote sensing*, 9(4), p.307.

Meijninger, W.M.L. and Jarmain, C., 2014. Satellite-based annual evaporation estimates of invasive alien plant species and native vegetation in South Africa. *Water SA*, 40(1), pp.95-108.

Neitsch, S.L., Arnold, J.G., Kiniry, J.R. and Williams, J.R., 2011. *Soil and water assessment tool: theoretical documentation, Version 2009.* Texas Water Resources Institute Technical Report No. 406. Texas A&M University, Texas, USA.

Nistor, M.M., Ronchetti, F., Corsini, A., Cheval, S., Dumitrescu, A., Rai, P.K., Petrea, D. and Dezsi, Ş., 2017. Crop evapotranspiration variation under climate change in South East Europe during 1991-2050. *Carpathian Journal of Earth and Environmental Sciences*, 12(2), pp. 571-582.

Nouri, H., Beecham, S., Kazemi, F. and Hassanli, A.M., 2013. A review of ET measurement techniques for estimating the water requirements of urban landscape vegetation. *Urban Water Journal*, 10(4), pp.247-259.

Schaffrath, D. and Bernhofer, C., 2013. Variability and distribution of spatial evapotranspiration in semi-arid Inner Mongolian grasslands from 2002 to 2011. *SpringerPlus*, 2(1), p. 547.

Senay, G.B., Velpuri, N.M., Bohms, S., Budde, M., Young, C., Rowland, J. and Verdin, J.P., 2015. Drought monitoring and assessment: remote sensing and modelling approaches for the famine early warning systems network. *In Paron, P., ed. Hydro-meteorological hazards, risks and disasters*. Elsevier, pp. 233-262.

Tian, H., Chen, G., Liu, M., Zhang, C., Sun, G., Lu, C., Xu, X., Ren, W., Pan, S. and Chappelka, A., 2010. Model estimates of net primary productivity, evapotranspiration, and water use efficiency in the terrestrial ecosystems of the southern United States during 1895–2007. *Forest Ecology and Management*, 259(7), pp.1311-1327.

Vinukollu, R.K., Wood, E.F., Ferguson, C.R. and Fisher, J.B., 2011. Global estimates of evapotranspiration for climate studies using multi-sensor remote sensing data: evaluation of three process-based approaches. *Remote Sensing of Environment*, 115(3), pp.801-823.

Wang, K. and Dickinson, R.E., 2012. A review of global terrestrial evapotranspiration: observation, modelling, climatology, and climatic variability. *Reviews of Geophysics*, 50(2).

Wang, S., Yang, Y., Luo, Y. and Rivera, A., 2013. Spatial and seasonal variations in evapotranspiration over Canada's landmass. *Hydrology and Earth System Sciences*, 17(9), pp. 3561-3575.

Western, A.W., Zhou, S.L., Grayson, R.B., McMahon, T.A., Blöschl, G. and Wilson, D.J., 2004. Spatial correlation of soil moisture in small catchments and its relationship to dominant spatial hydrological processes. *Journal of Hydrology*, 286(1), pp. 113-134.

Winchell, M., Srinivasan, R., Di Luzio, M. and Arnold, J., 2013. *ArcSWAT interface for SWAT2012: user's guide*. Texas A&M AgriLife Blackland Research and Extension Centre, Blackland, Texas, USA.

Yeh, P.J. and Famiglietti, J.S., 2009. Regional groundwater evapotranspiration in Illinois. *Journal of Hydrometeorology*, 10(2), pp.464-478.

Zhang, K., Kimball, J.S. and Running, S.W., 2016a. A review of remote sensing based actual evapotranspiration estimation. *Wiley Interdisciplinary Reviews: Water*, 3(6), pp.834-853.

Zhang, Y., Peña-Arancibia, J.L., McVicar, T.R., Chiew, F.H., Vaze, J., Liu, C., Lu, X., Zheng, H., Wang, Y., Liu, Y.Y. and Miralles, D.G., 2016b. Multi-decadal trends in global terrestrial evapotranspiration and its components. *Scientific Reports*, 6, p.19124.

Zhang, Z., Tian, F., Hu, H. and Yang, P., 2014. A comparison of methods for determining field evapotranspiration: photosynthesis system, sap flow, and eddy covariance. *Hydrology and Earth System Sciences*, 18(3), pp. 1053-1072.

Zhao, L., Xia, J., Xu, C.Y., Wang, Z., Sobkowiak, L. and Long, C., 2013. Evapotranspiration estimation methods in hydrological models. *Journal of Geographical Sciences*, 23(2), pp.359-369.

Zhao, W. and Ji, X., 2016. Spatio-temporal variation in transpiration responses of maize plants to vapour pressure deficit under an arid climatic condition. *Journal of Arid Land*, 8(3), pp.409-421.

Zhao, W., Li, A. and Deng, W., 2014. Spatial and temporal variation of evapotranspiration estimated by MODIS data over South Asia. *In 2014 IEEE International Geoscience and Remote Sensing Symposium (IGARSS 2014).* Institute of Electrical and Electronics Engineers (IEEE), pp. 3049-3052), Quebec City, Quebec, Canada.

CHAPTER 7
THE SPATIO-TEMPORAL VARIATIONS OF RUNOFF IN THE CATCHMENT

7.1 Introduction

Runoff is a natural phenomenon of the downward flow of water into a stream or a reservoir within a specific time period, under the influence of gravitational force. It is formed when the intensity of precipitation exceeds the rate of surface infiltration, and it is an important and indispensable element of the hydrological cycle (Tarboton, 2003; Vinogradov, 2009). The prediction of the spatial and temporal variation of runoff in catchments has many practical applications. It is important for the design of drainage and flood defence structures (Blöschl *et al*., 2013). Runoff is also important in many areas of hydrological research regarding stream flow estimation, irrigation, flood estimation and management (Mdee, 2015). More especially, significant variations of hydrological characteristics in time and space demand the need to predict seasonal runoff fluctuations (Mdee, 2015; Rejani *et al*., 2015). The precise estimation of runoff is also essential in catchment development interventions, such as designing water harvesting (Bothma *et al*., 2012) and *in situ* water conservation structures (Zelelew, 2012; van Rensburg *et al*., 2012; Rejani *et al*., 2015). During periods of the over-exploitation of groundwater, particularly in dry areas, the precise estimation of runoff is essential for planning intervention strategies (Ramakrishnan *et al*., 2009; Zelelew, 2012; Rejani *et al*., 2015).

The runoff process differs from place to place and time to time, depending on a number of factors. The spatial and temporal characteristics of the runoff process are very complex since they are influenced by many factors (Mzezewa and van Rensburg, 2011). The spatial patterns of catchment characteristics provide important information to link runoff generation and its controlling factors within catchments (Zelelew, 2012). Firstly, the characteristics of the land surface, such as topography, LULC, and presence of surface sealing, are the primary influential factors (Tarboton, 2003; Ramakrishnan *et al.*, 2009; Rejani *et al.*, 2015). Secondly, soil behaviours, such as the initial soil water content, soil type, lithology and hydraulic properties of the soils, also have key influences (Tarboton, 2003; Ramakrishnan *et al.*, 2009; Rejani *et al.*, 2015). Finally, climatic factors, particularly the rainfall properties (intensity, duration and frequency), are the most important factors for runoff formation, magnitude and its spatio-temporal variation (Tarboton, 2003; Ramakrishnan *et al.*, 2009 and Rejani *et al.*, 2015).

Several methods are available in the literature for determining runoff at different scales of study (catchment, regional, or global scales). The methods vary from direct measurements taken at gauging stations constructed at the outlet of the area of interest, to the use of rainfall simulators, as explained by Kinner and Moody (2008), Sangüesa *et al*. (2010) and Mzezewa and van Rensburg (2011), to the Upwelling Bernoulli Tube (UBeTube), which is a simple apparatus for measuring runoff (Stewart *et al*., 2015), as well as other prediction methods. The measurement methods mentioned above apply to smaller scales of study and give better values, but only point data. Hence, these categories of equipment do not show the spatial distribution of the runoff. Therefore, prediction methods (hydrological models) constitute a first priority for efficiently analysing spatial variations of runoff.

Hydrological models are simplified representations of the complex nature of the hydrologic cycle in an area (Sorooshian *et al*., 2009). Hence, hydrological modelling is a valuable tool for researchers that enables them to investigate complex processes. Such complex processes include those regarding the impacts of climate change on water resources (Kundzewicz *et al*., 2008; Montenegro and Ragab, 2012; Candela *et al*., 2012; Schwank *et al*., 2014), the impacts of land use change on hydrology (Montenegro and Ragab, 2012; Dos Santos *et al*., 2014), and other related environmental impacts.

Numerous studies have been conducted on the spatial and temporal distribution of runoff at different scales of study. The global studies show contrasting results for the trends of stream flow. For example, Alkama *et al*. (2013) showed that no significant changes had occurred in the trends of stream flow from 1958 to 2004, globally, although they predicted a significant variation from 2016 to 2040. On the other hand, Dai *et al*. (2009), Labat *et al*. (2004), Milly *et al*. (2005), and Stahl *et al*. (2010) showed significant variations in runoff, globally, during the last century. Different factors are suggested as being the main drivers causing the spatio-temporal variations and trends in stream flow. Many researchers have shown the presence of a strong link between global warming and the global hydrological cycles. More particularly, variations in precipitation and the El Niño–Southern Oscillation (ENSO) are suggested by Güntner *et al*. (2007), Krakauer and Fung (2008), and Dai *et al*. (2009). Piao *et al*. (2007) demonstrated the higher impact of LULC as causing changes in runoff variations, particularly in the tropics.

Runoff studies have also been conducted in South Africa. Grenfell and Ellery (2009) showed a general decreasing trend in stream flow due to climate change. Lakhraj-Govender (2010) also found a decreasing stream flow trend in Vaal River, Mgeni River, Tugela River and Breed River basins from 1951 to 2008; however, she found an increasing trend in the Orange River

Basin. An investigation by Bugan *et al*. (2012) in the Sandspruit catchment showed that only 6.5% of the precipitation was converted to stream flow for the period 1990 to 2010. Hence, most of the studies in South Africa rely on point data analysis that shows only the trend of total runoff for a particular catchment. They do not show the variation of runoff in the study area. Therefore, the aim of this study was to analyse the spatial and temporal variation of runoff in a selected catchment in the Northern Cape Province, South Africa.

7.2 Materials and methods

7.2.1 Description of the study area

The study catchment is located in the Northern Cape Province, South Africa with a geographic location of between 22°11’00” and 23°28”00” E longitudes, and 28°03’00” and 29°06’00” S latitudes. The details for the location and description of the study catchment can be seen in Chapter 3, Subsection 3.2.1.

7.2.2 Testing normality of time series data

As already explained in previous sections (e.g. those in Chapter 4), the tests of normality were analysed by a graphical method (probability-probability (P-P plot) and quantile-quantile (Q-Q plot)) and by a statistical method (Shapiro-Wilk test).

7.2.3 Trend analysis of direct runoff

The trend analysis in the long-term runoff (1980–2018) data was investigated by the non-parametric Mann-Kendall test. For details, see Chapter 4, Subsection 4.2.3.

7.2.4 The spatial variation of runoff

SWAT estimates the spatial and temporal values of runoff at HRU and sub-basin scales, as discussed in Chapter 3. In this section, therefore, the mean value of the long-term monthly and yearly variations of runoff are analysed with the help of ArcGIS 10.4.

7.3 Results

7.3.1 Normality of runoff data

The tests of the normality of the time series annual and monthly total runoff, which includes the surface runoff, lateral flow and contribution from the shallow aquifer (return flow or base flow), were conducted both graphically with a visual assessment, and numerically with statistical tests. The graphical assessment is depicted in Figure 7.1 below, panels a–d, and the numerical tests are given in Table 7.1 below. Both the graphical assessment and the numerical test show that the runoff data do not meet the requirements of the normal distribution. Therefore, non-parametric tests are recommended for further data analysis.

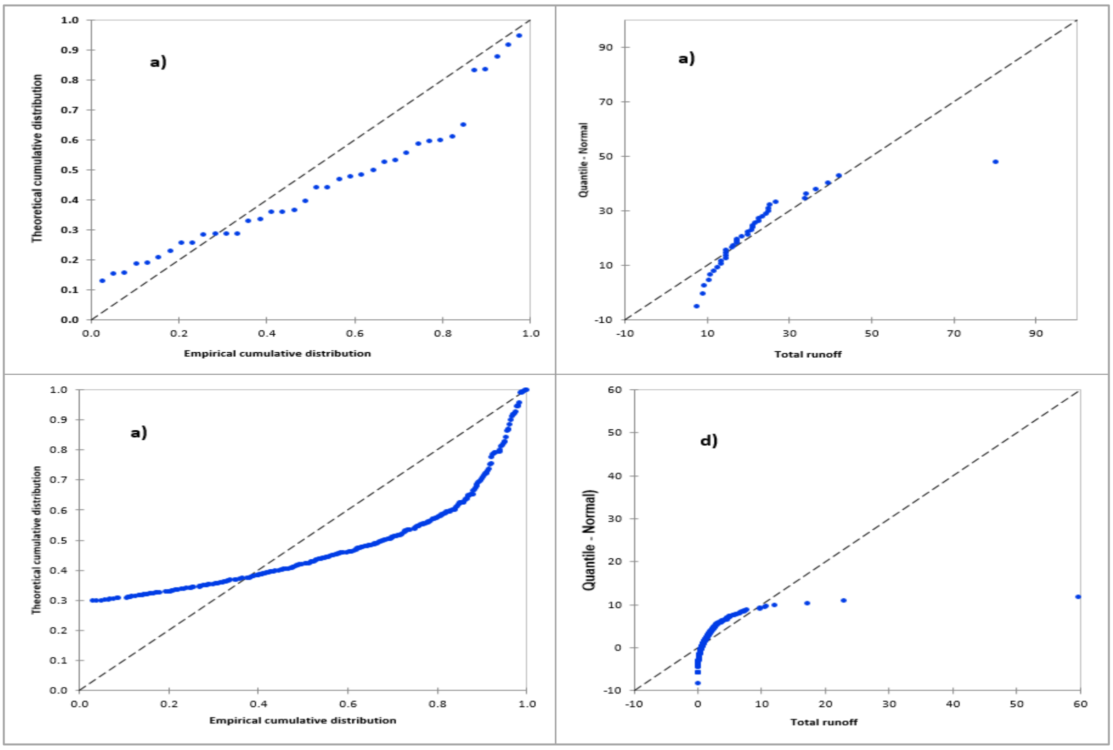

Figure 7.1: Graphical sketches showing the normality of the runoff data.

Notes: (a) probability-probability (P-P plot) for the mean annual runoff, (b) quantile-quantile (Q-Q plot) for mean annual runoff, (c) probability-probability (P-P plot) for the mean monthly runoff, and (d) quantile-quantile (Q-Q plot) for the mean monthly runoff.

Table 7.1: Tests of normality for the time series of total runoff data

Variable	Observations	Minimum	Maximum	Mean	Std. dev	Shapiro-Wilk test	
						W	p-value
Annual runoff	39	7.5	80.2	21.6	12.76	0.751	< 0.01
Monthly runoff	468	0	59.7	1.8	3.41	0.363	< 0.01

7.3.2 Trends of the runoff components

The long-term mean daily values of the three components of runoff (surface runoff, lateral flow, and base flow) and their comparison with daily precipitation throughout the year are shown in Figure 7.2 below. The long-term mean monthly records of each of the runoff components are shown in Figure 7.3 below.

The daily mean values show that the amount of precipitation converted to runoff was very small. It also shows that most of the runoff occurs as lateral flow, and only very little amounts were contributed from surface runoff and the shallow aquifer as return flow. Hence, the mean total daily runoff varied from 0 mm (in the early spring season) to 1.43 mm (in the autumn season). The peak runoff has a similar trend with the precipitation, i.e. runoff was at maximum when the precipitation was at maximum, and vice versa. The monthly means (Figure 7.3 below) also show similar results. It indicated that the runoff conversion varied from 3.32% in October to 16.5% of precipitation in May. The water yield also varied from 0.44 mm in early spring to a maximum of 3.37 mm in the late summer season, approaching the value of total runoff. Water yield differs from total runoff in that total runoff does not include the water stored in the soil profile and all the transmission losses.

The trends of the time series annual and monthly total runoff were also analysed by the Mann-Kendall trend analysis, as depicted in Figures 7.4 and 7.5 below for annual and monthly total runoffs, respectively. The parameters for the statistics of Mann-Kendall trend tests are given in Table 7.2 below. Accordingly, it is shown that there is no significant trend in the annual time series data. However, a significant negative (decreasing) trend has been found in the monthly time series data. As a result, there was a mean decrease of 0.002 mm runoff per month in the Soutloop Catchment within the study period.

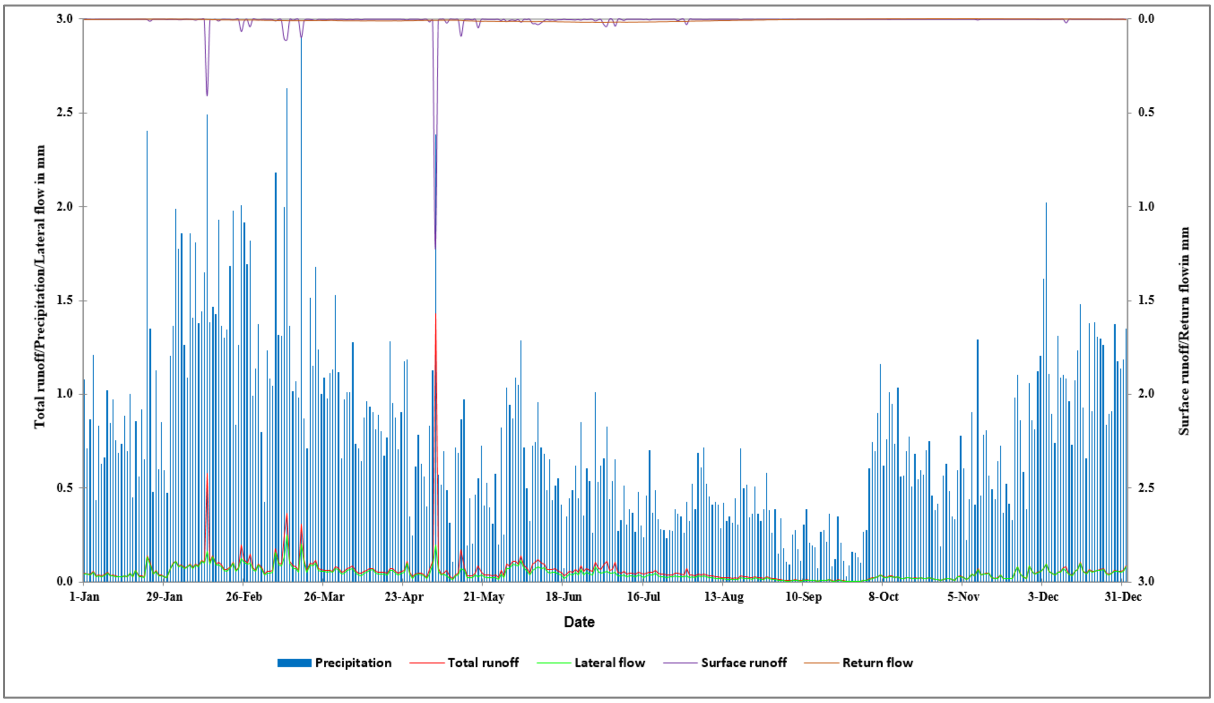

Figure 7.2: Comparison of the long-term mean daily runoff and precipitation in the catchment.

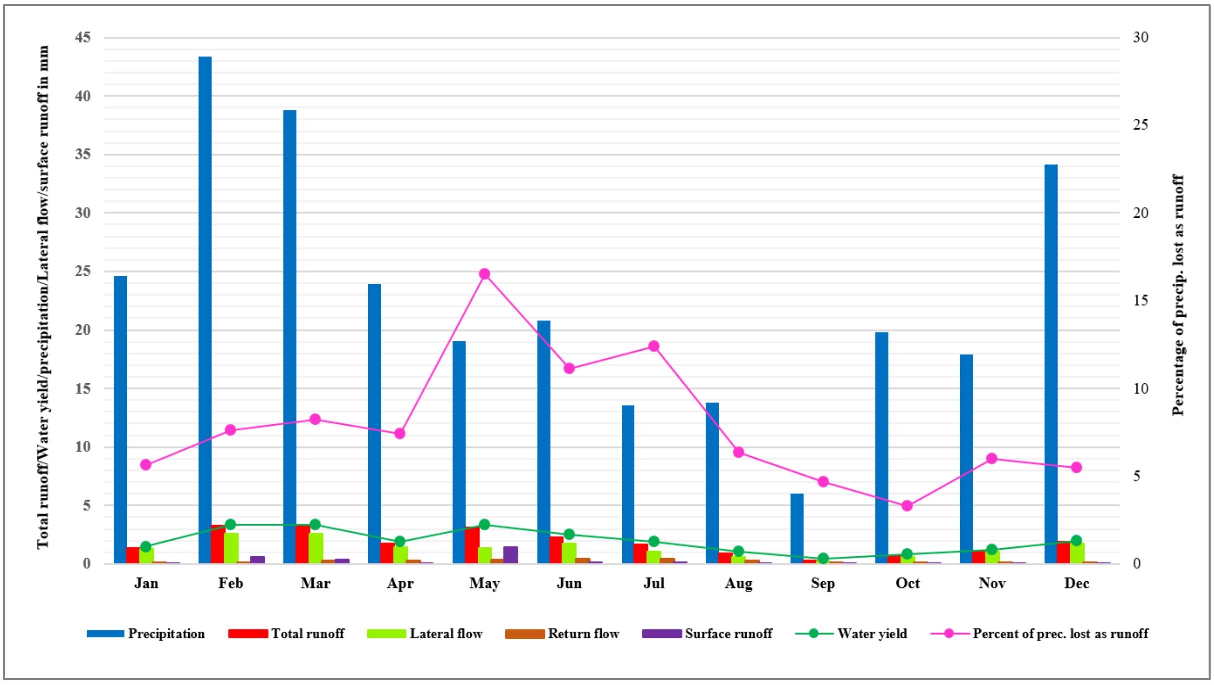

Figure 7.3: Long-term monthly mean runoff variations and comparison with the corresponding precipitation in Soutloop Catchment.

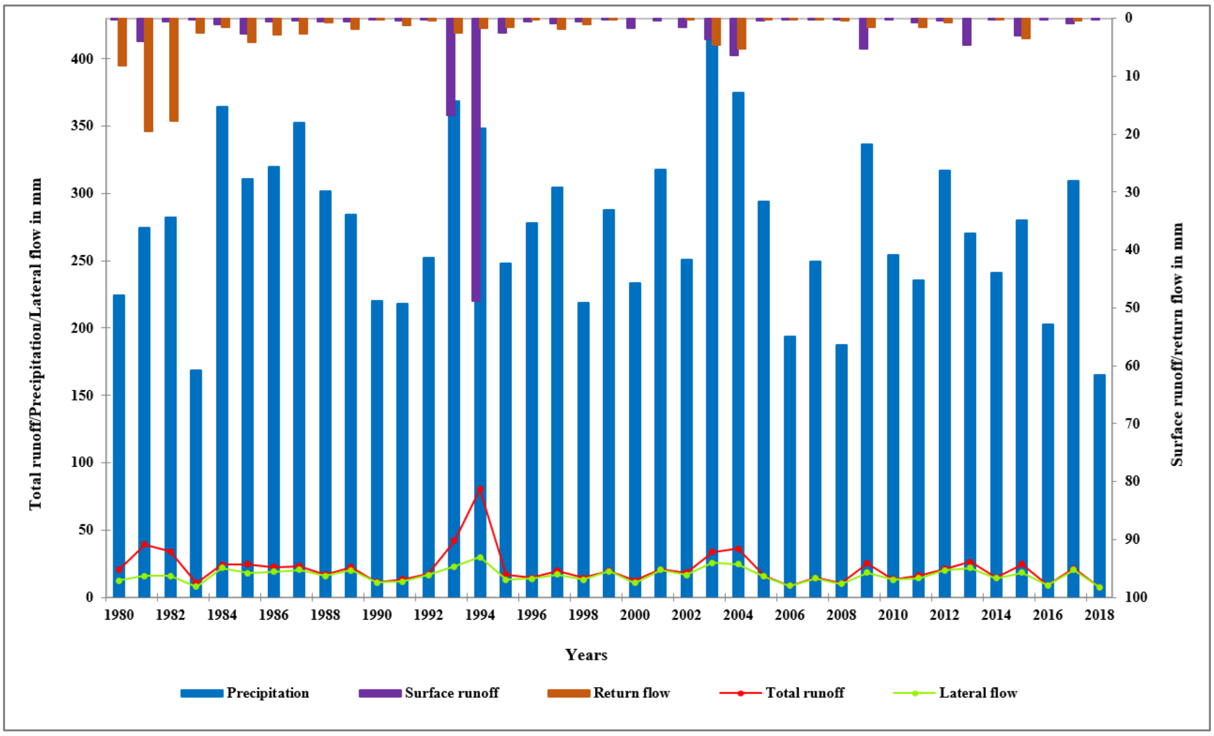

Figure 7.4: Trends of annual runoff and comparison with precipitation in Soutloop Catchment.

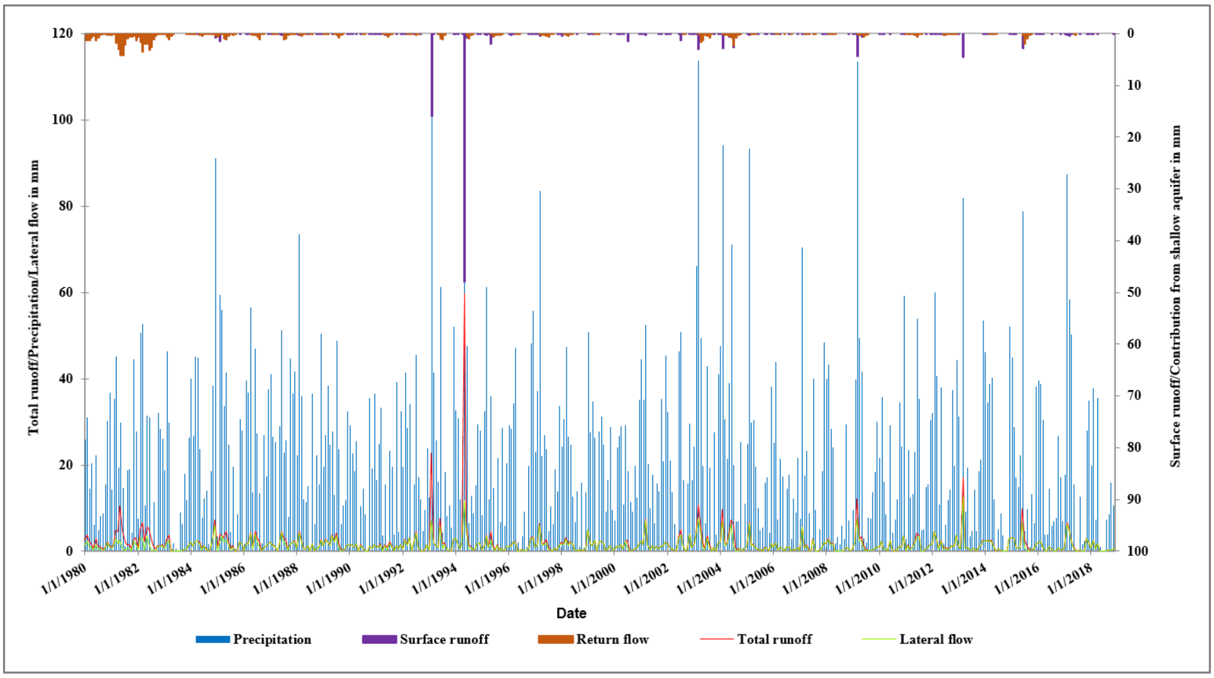

Figure 7.5: Trends of monthly runoff components as compared with precipitation in Soutloop Catchment.

Table 7.2: Statistics of the Mann-Kendall trend test for the mean annual and monthly runoff

Parameters	Annual runoff	Monthly runoff
Kendall's tau	-0.196	-0.140
S stat	-145	-15289
Var(S)	6834	11424794
p-value	0.082	< 0.01
Sen's slope	-0.246	-0.002

7.3.3 Spatial variation of runoff and water yield

In this section, the spatial variations of the long-term mean total annual and seasonal runoff and the total water yield are presented. The total runoff (which includes surface runoff, lateral flow, and return flow) is displayed in Figure 7.6 below, panel a, and in Figure 7.7 below, panels a–d, for annual and seasonal time scales, respectively. The water yield is depicted in Figure 7.6 below, panel b, for the annual time scale. Both the runoff and water yield showed a higher spatial and temporal variation. It is worthy to note that the runoff and water yield are more or less similar, both in their patterns of spatial distribution and in their magnitudes. The two parameters differ significantly when the magnitudes of the transmission losses and the change in soil water content vary significantly. Therefore, both runoff and water yield varies spatially, from 0 to 214 mm per annum. Generally, most of the Kolomela Mine area, the central part below the Kolomela Mine, and the north-eastern and south-western tips of the study catchment had the lowest annual runoff volume and water yield. On the other hand, smaller and sparsely distributed patches of land on the north-western and south-eastern tips of the catchment had relatively higher runoff and water yield.

Regarding the distribution of runoff on seasonal time scales (Figure 7.7 below, panels a–d), the seasonal runoff in the catchment varies from a very small fraction close to zero, to about 95 mm, with the maximum value being recorded in the summer season. Generally, autumn was the better season for runoff formation, since a significant area of the catchment produced runoff in this season, whereas spring showed the least runoff formation. There is no clear pattern in terms of spatial distribution in the four seasons; however, smaller and sparsely distributed patches of lands in the catchment, including the north-western, the southern and the south-eastern parts, as well as the mountainous and rocky area of the western part, had a better chance for runoff formation.

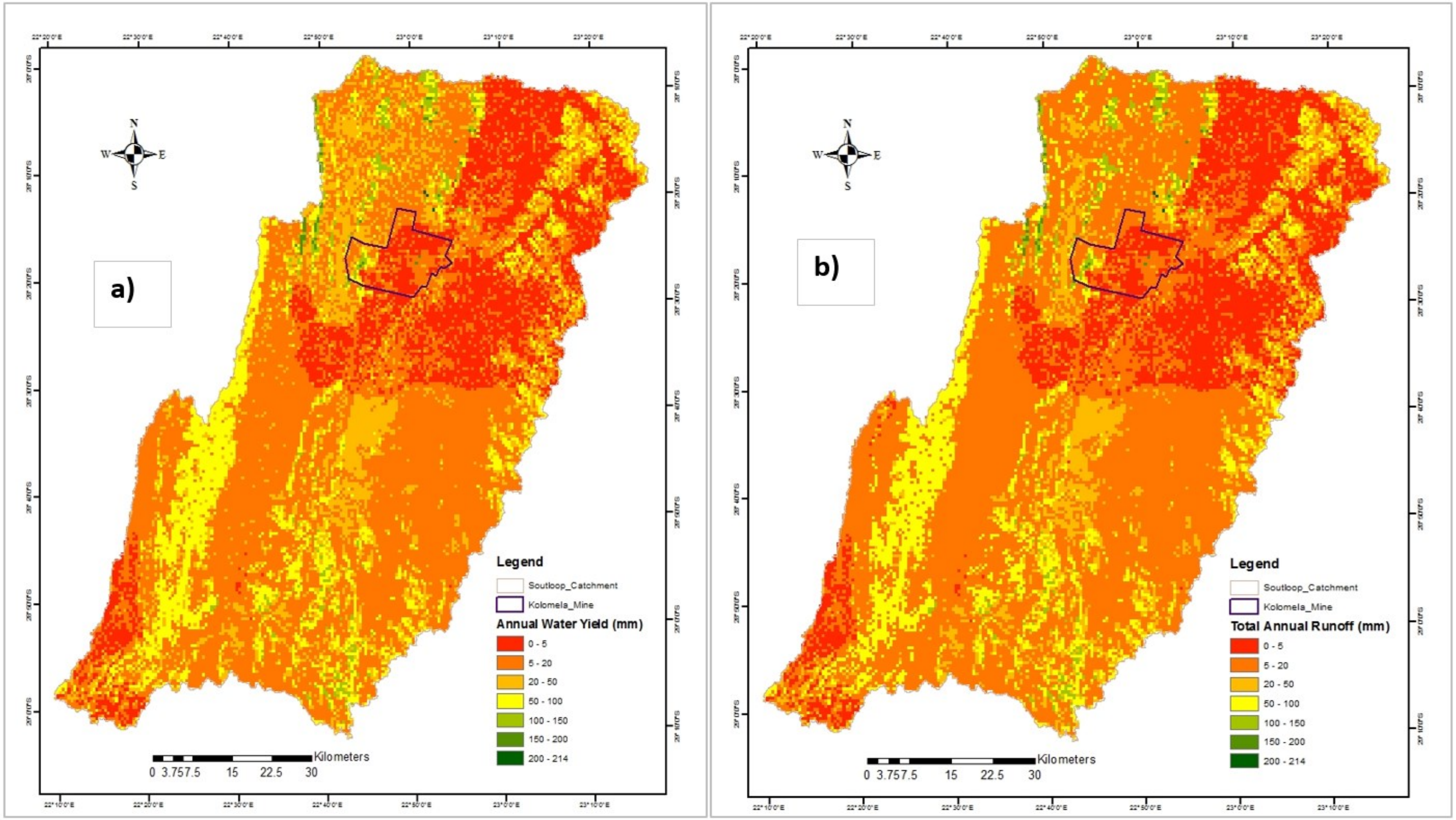

Figure 7.6: Spatial variation of the long-term mean a) total annual runoff (surface runoff, return flow, and contribution from shallow aquifer), and (b) water yield.

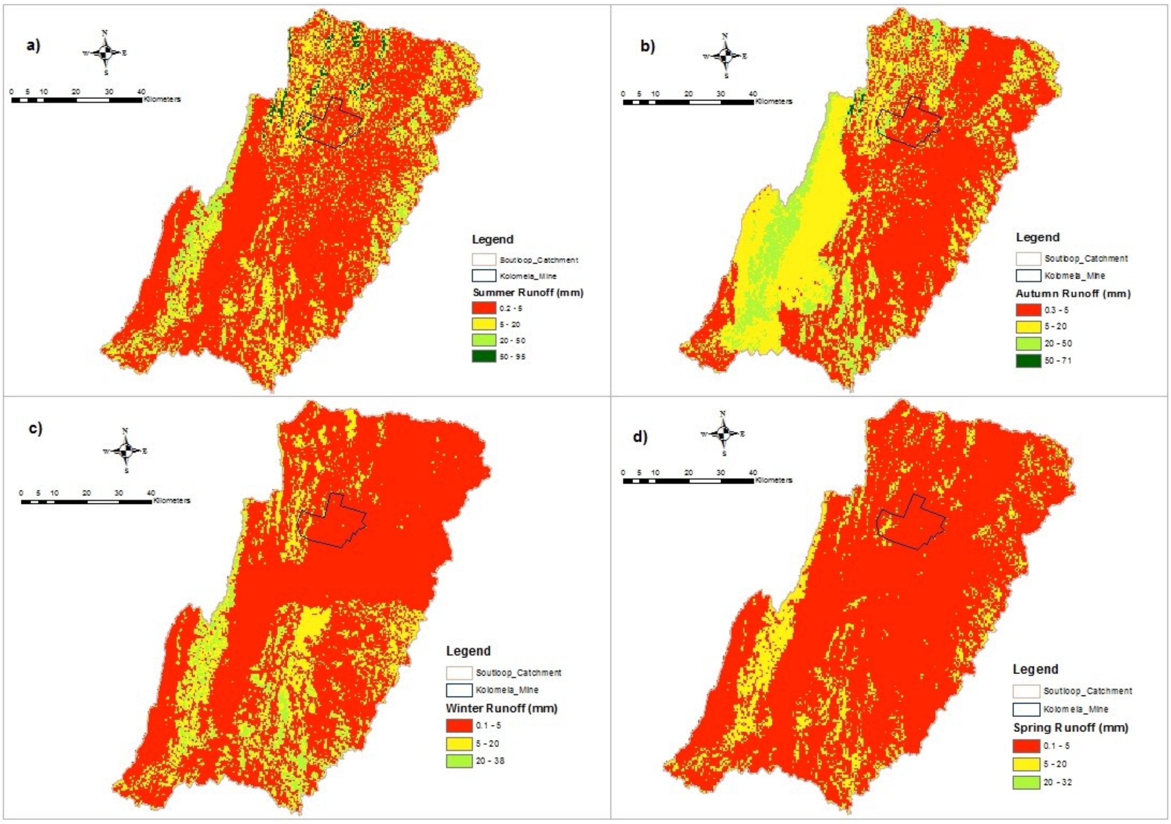

Figure 7.7: Spatial variations of the long-term total mean seasonal runoff in Soutloop Catchment.

Notes: a) summer season, b) autumn season, c) winter season, and d) spring season.

7.4 Discussions

Total runoff is one of the major determinants of the catchment water balance in arid areas, and its three components are investigated in this study. The surface runoff is the component created when the rate of precipitation exceeds the rate of soil surface infiltration. The lateral flow component occurs when the root zone is saturated and an impermeable soil layer is encountered below the root zone, which impedes percolation. Lastly, the return flow or base flow component is the contribution of the shallow aquifer to runoff volume. The combination of these three types are referred here as total runoff.

This study shows that the Soutloop Catchment had a very low amount of runoff coefficient throughout the study period, where the long-term annual average was estimated to be 0.077. As a result, the mean total daily runoff (Figure 7.2 above) varied from 0 mm (in early spring season) to 1.43 mm per day (in autumn season). The monthly means (Figure 7.3 above) also indicate that the runoff conversion varied from 3.32% in October to 16.5% in May. The total mean annual runoff was also estimated as being up to 21.6 mm per annum. The comparison of these results with previous research studies seems difficult to achieve, and depends on the detail of the study, length of study period, method of study, and so on. However, the result is generally within the reported ranges. For example, the Permanent Water Commission (PWC) (2005) found a figure of 5.3 mm for Lower Orange Catchment; DWAF (2009) estimated 7.08 mm for the D73B quaternary catchment; Schulze *et al*. (2007) estimated 10–50 mm for both D73A and D73B quaternary catchments; and Kleynhans *et al*. (2005) estimated 5–20 mm for the catchment under study, in which all figures are for annual runoff. The comparison between the three components in this study shows that most of the runoff (i.e. 76% of the annual runoff) was contributed by the lateral flow. This might be attributable to the soil type (light textured soil on the top horizon, with the presence of impermeable subsoil, such as lime, higher clay content soil, or rocks) and the presence of a lower slope class (more than 68% of the catchment area has <5%, which induces infiltration rather than surface runoff). The details of soil type and topography are described in Chapter 3, Subsection 3.2.1.4. Generally, the catchment can be considered as one of the driest catchments in South Africa, where no stream flow is recorded at its outlet for long time periods. The only local runoff experienced is the usual that occurs during heavy storms. However, most of the runoff would infiltrate to the shallow aquifer along the alluvial ephemeral stream beds or in the main river beds, which is similar to what has been reported by Morin *et al*. (2009) and Hashemi *et al*. (2013). Farmers in close proximity to the junction area between Soutloop and the Orange River have stated that it usually takes between 15 and 30 years to experience one runoff occasion that would contribute to the Orange River. However, this catchment has not contributed any runoff to the Orange River over the last 30 years. The reason for this could be the low amount of precipitation distribution in the catchment. Moreover, the runoff formation during heavy storms would be converted to transmission losses and percolate to the shallow aquifer while flowing through dry stream beds. Therefore, Soutloop can be classified as an episodic river.

Table 7.3: Correlation of the runoff with land use, slope and soil characteristics

	LULC	AWC	Slope class	SOL_ZMX	Total_Q
LULC	1				
AWC	0.02	1			
Slope class	0.01	-0.09	1		
SOL_ZMX	0.03	0.92	-0.11	1	
Total_Q	0.002	-0.52	0.71	-0.58	1

N.B: LULC-land use and land cover class AWC-available water capacity SOL_ZMX-maximum soil depth Total_Q-total runoff

Table 7.4: Correlation of the runoff with other components of water balance

	Prec	Surf_Q	Lat_Q	GW_Q	Perc	SW	Total_Q
Prec	1						
Surf_Q	0.34	1					
Lat_Q	0.91	0.44	1				
GW_Q	0.01	0.01	0.07	1			
Percolate	0.73	0.49	0.87	0.10	1		
SW	0.66	0.15	0.70	0.22	0.64	1	
Total_Q	0.65	0.90	0.77	0.19	0.75	0.45	1

N.B.: Prec-precipitation Surf_Q-surface runoff Lat_Q-lateral flow GW_Q-return flow Perc-percolation SW-soil water content Total_Q-total runoff

Regarding the presence of trends in the time series total runoff, the Mann-Kendall trend analysis (see Figures 7.4 and 7.5 above for annual and monthly total runoff, respectively) shows that there is no significant trend in the annual time series data. However, a significant negative (decreasing) trend has been identified in the monthly time series data. As a result, there was a mean decrease of 0.002 mm runoff per month in the Soutloop Catchment during the study period. DWAF (2013) and Midgley *et al*. (2016) have reported that climate change is a measureable reality that causes stress to water resources in South Africa. The increase in mean temperature was particularly significant in the study area. This study also shows a significant, decreasing trend in monthly precipitation. Therefore, climate change could be the primary cause of the decrease in runoff. The correlation analysis between total runoff and other components of catchment water balance (Table 7.4 above) also shows that precipitation is strongly correlated to runoff, indicating that decreasing precipitation could be a major cause for the decrease in runoff. Surface runoff, lateral flow, percolation and soil water content are also highly correlated. However, the correlation between the total runoff and base flow/groundwater flow is very weak, as compared with the others. This could also indicate that the contribution from ground water to runoff was very low.

The rainfall–runoff process shows high spatial variability throughout the catchment (Figures 7.6 above for annual variation and Figure 7.7 above for seasonal variation). Both the runoff and water yield showed a higher spatial and temporal variation. Hence, both runoff and water yields vary spatially from 0 mm to 214 mm per annum, while 21.6 mm was the catchment average value measured, as seen above. Generally, most of the Kolomela Mine area, the central part below Kolomela Mine, the north-eastern and the south-western tips of the study catchment had the lowest annual runoff volume/water yield. On the other hand, smaller and sparsely distributed patches of land on the north-western and south-eastern tip parts of the catchment had relatively higher runoff/water yield. Regarding the seasonal distribution (Figure 7.7 above, panels a–d), the seasonal runoff in the catchment varies from a very small fraction close to zero to 95 mm in the summer season. Generally, the autumn season was the better season for runoff formation, whereas the spring season showed the lowest runoff formation. There is no clear pattern discernible in terms of spatial distribution across the four seasons. As is true for temporal variability, the spatial variation of runoff followed the spatial distribution of precipitation in the catchment. The spatial variation of runoff across the four seasons is also highly affected by the rainfall distribution. Similar results have been reported by Bugan *et al*. (2012), Schulze *et al*. (2007), and Midgley *et al*. (2016). As is true for the other components of the catchment water balance, the spatial variation of the runoff process was also highly dependent on the complex interaction of soil type, LULC, and topographic features (Pilgrim *et al*., 1988; Schulze *et al*., 2007; Mahmoud and Alazba, 2015). Table 7.3 above shows the correlation between total runoff and soil type (profile depth and available water capacity), topography (percentage slope) and land cover class. The soil characteristics (depth and AWC) were negatively correlated, whereas the slope was positively correlated to runoff. However, there was a weak correlation between runoff and land cover, which is inconsistent with other reports (e.g. Pilgrim *et al*., 1988; Schulze *et al*., 2007; Mahmoud and Alazba, 2015). Therefore, the impact of LULC on the spatial variability of the total runoff was very low, as compared with the precipitation, soil characteristics and topographic features. The most probable cause for this could be the presence of lower variations of land cover in the area, i.e. the land cover map shows that more than 80% of the catchment is covered by similar vegetation (shrub land), as described in Chapter 3, Subsection 3.2.1.4.

7.5 Conclusion

The aims of this section were to analyse the spatio-temporal variability of runoff in an arid catchment in the Northern Cape Province, South Africa, based on the outputs of a SWAT model. It is expected that there might be considerable uncertainty in the modelling process, which could be attributed to the unavailability of flow data for calibration, uncertainty and validation of the model. However, it is also possible to note that the regionalization approach had been applied successfully, since the statistical results of the validation of the model with *in situ* soil water content were acceptable, and the comparison of the simulated results was consistent with previous studies in the catchment.

The Soutloop Catchment can be considered as one of the dry catchments in South Africa, where no runoff yield has been recorded over the last 30 years at the outlet or the junction with Orange River. However, local surface runoff and sub-surface runoff have been observed, although such runoff infiltrates along the way to the downstream river beds. Generally, the rainfall–runoff process exhibited higher spatial and temporal variations in the study catchment. It is worthy to note that most of the temporal variation of runoff was attributed to the variation of rainfall and the climate as a whole. The spatial variability of the runoff coefficient was also influenced by the variation in soil characteristics and topographic features, other than the rainfall distribution. It is also indicated that the impact of LULC was minimal, as the variation of LULC was minimal in the catchment.

This study showed some interesting trends, with the majority of the data indicating that water resources in the study catchment are actually under threat, and that some of the water balance components, such as runoff and others discussed in Chapters 4, 5, 6 and 8, have significantly declined, which places additional stress on the already existing water deficit in the catchment. The additional water stress attributable to the indicated decreasing trends will constitute a huge disaster for the natural ecosystem. This indicates that future water resource planning is critical for ensuring a sufficient supply of water for the area. Further research is also recommended on the application of hydrological models on event-based rainfall–runoff relationships for comparison with continuous models like the SWAT model. This could constitute one way to decrease the uncertainty and to improve the reliability of model outputs.

7.6 References

Alkama, R., Marchand, L., Ribes, A. and Decharme, B., 2013. Detection of global runoff changes: results from observations and CMIP5 experiments. *Hydrology and Earth System Sciences*, *17*(7), pp.2967-2979.

Blöschl, G., Sivapalan, M., Savenije, H., Wagener, T. and Viglione, A. eds., 2013. *Runoff prediction in ungauged basins: synthesis across processes, places and scales.* Cambridge University Press.

Bothma, C.B., Van Rensburg, L.D. and Le Roux, P.A.L., 2012. Rainfall intensity and soil physical properties influence on infiltration and runoff under in-field rainwater harvesting conditions. *Irrigation and Drainage*, 61, pp.41-49.

Bugan, R., Jovanovic, N. and De Clercq, W., 2012. The water balance of a seasonal stream in the semi-arid Western Cape (South Africa). *Water SA,* 38(2), pp. 201-212.

Candela, L., Tamoh, K., Olivares, G. and Gomez, M., 2012. Modelling impacts of climate change on water resources in ungauged and data-scarce catchments. Application to the Siurana catchment (NE Spain). *Science of The Total Environment*, *440*, pp.253-260.

D. H. Pilgrim, T. G. Chapman and D. G. Doran, 1988. Problems of rainfall-runoff modelling in arid and semiarid regions, *Hydrological Sciences Journal*, 33:4, 379-400, DOI: 10.1080/02626668809491261.

Dai, A., Qian, T., Trenberth, K.E. and Milliman, J.D., 2009. Changes in continental freshwater discharge from 1948 to 2004. *Journal of Climate*, *22*(10), pp.2773-2792.

Department of Water Affairs and Forestry (DWAF), 2009. *Development of an integrated water quality management strategy for the Upper and Lower Orange Water Management Areas: Desktop Catchment Assessment Study: Lower Orange Water Management Area (WMA 14).* Department of Water Affairs and Forestry Report: No: 2.2 (P RSA D000/00/7909/3), Pretoria, South Africa.

Department of Water Affairs, 2013. *National Water Resource Strategy*. Accessed 18 December 2018 at: http:// www.dwa.gov.za/documents/Other/Strategic%20Plan/NWRS2-Final-email-version.pdf.

Dos Santos, J.Y.G., Da Silva, R.M., Carvalho Neto, J.G., Montenegro, S.M.G., Santos, C.A.G. and Silva, A.M., 2014. Assessment of land-use change on streamflow using GIS, remote sensing and a physically-based model, SWAT. *Proceedings of the International Association of Hydrological Sciences*, 364, pp.38-43.

Grenfell, S.E. and Ellery, W.N., 2009. Hydrology, sediment transport dynamics and geomorphology of a variable flow river: The Mfolozi River, South Africa. *Water SA*, *35*(3).

Güntner, A., Stuck, J., Werth, S., Döll, P., Verzano, K. and Merz, B., 2007. A global analysis of temporal and spatial variations in continental water storage. *Water Resources Research*, *43*(5).

Hashemi, H., Berndtsson, R., Kompani-Zare, M. and Persson, M., 2013. Natural vs. artificial groundwater recharge, quantification through inverse modelling. *Hydrology and Earth System Sciences*, 17(2), pp.637-650.

Hughes, D.A., 2008. Modelling semi-arid and arid hydrology and water resources: the southern Africa experience. *In Weater, H., Sorooshian, S. and Sharma, KD (eds.) Hydrological modelling in arid and semi-arid areas*, Cambridge University Press, pp.29-40.

Kinner, D.A. and Moody, J.A., 2008. *Infiltration and runoff measurements on steep burned hillslopes using a rainfall simulator with variable rain intensities*. U. S. Geological Survey.

Kleynhans, C.J., Thirion, C. and Moolman, J., 2005. *A level I river ecoregion classification system for South Africa, Lesotho and Swaziland*. Department of Water Affairs and Forestry Pretoria, South Africa.

Krakauer, N.Y. and Fung, I., 2008. Mapping and attribution of change in streamflow in the coterminous United States. *Hydrology and Earth System Sciences*, *12*(4), pp.1111-1120.

Kundzewicz, Z.W., Mata, L.J., Arnell, N.W., Döll, P., Jimenez, B., Miller, K., Oki, T., Şen, Z. and Shiklomanov, I., 2008. The implications of projected climate change for freshwater resources and their management. *Hydrological Sciences Journal*, 53(1), pp.3-10.

Labat, D., Goddéris, Y., Probst, J.L. and Guyot, J.L., 2004. Evidence for global runoff increase related to climate warming. *Advances in Water Resources*, *27*(6), pp.631-642.

Lakhraj-Govender, R., 2010. *Assessing the potential impact of rainfall change on southern African river flows* (Master's dissertation). University of Witwatersrand, Johannesburg, South Africa.

Mahmoud S.H., Alazba A.A., 2015. Hydrological response to land cover changes and human activities in arid regions using a geographic information system and remote sensing. *PLoS ONE* 10(4): e0125805. DOI: 10.1371/journal.pone.0125805.

Mdee, O. J., 2015. Spatial distribution of runoff in ungauged catchments in Tanzania. *Water Utility Journal,* Volume 9, pp. 61-70.

Midgley G, Makholele, T. and Mantlana, B., 2016. Climate change trends risks, impacts and vulnerabilities. Department of Environmental Affairs, Pretoria South Africa, https://www.environment.gov.za/sites/default/files/reports/themeC_vulnerabilities_risks.pdf.

Milly, P.C., Dunne, K.A. and Vecchia, A.V., 2005. Global pattern of trends in streamflow and water availability in a changing climate. *Nature*, *438*(7066), p.347.

Montenegro, S. and Ragab, R., 2012. Impact of possible climate and land use changes in the semi-arid regions: A case study from North Eastern Brazil. *Journal of Hydrology*, *434*, pp.55-68.

Morin, E., Grodek, T., Dahan, O., Benito, G., Kulls, C., Jacoby, Y., Van Langenhove, G., Seely, M. and Enzel, Y., 2009. Flood routing and alluvial aquifer recharge along the ephemeral arid Kuiseb River, Namibia. *Journal of Hydrology*, 368(1-4), pp.262-275.

Mzezewa, J. and van Rensburg, L.D., 2011. The effects of tillage and rain intensity on runoff generation and infiltration rate on bare clayey Oxisol in Limpopo Province (South Africa). *Water SA*, 37(1), pp.165-172.

Permanent Water Commission (PWC), 2005. Hydrology, water quality and system analysis. *Pre-feasibility study into measures to improve the management of the lower Orange River and to provide for future developments along the border between Namibia and*

South Africa. Department of Water Affairs of South Africa and Namibia, Report No: 400/8/1/P, 13.a

Piao, S., Friedlingstein, P., Ciais, P., de Noblet-Ducoudré, N., Labat, D. and Zaehle, S., 2007. Changes in climate and land use have a larger direct impact than rising CO2 on global river runoff trends. *Proceedings of the National Academy of Sciences*, *104*(39), pp.15242-15247.

Ramakrishnan, D., Bandyopadhyay, A. and Kusuma, K., 2009. SCS-CN and GIS-based approach for identifying potential water harvesting sites in the Kali Catchment, Mahi River Basin, India. *Journal of Earth System Science,* 118(4), pp. 355-368.

Rejani, R., Rao, K.V., Osman, M., Chary, G.R., Reddy, K.S. and Rao, C.S., 2015. Spatial and temporal estimation of runoff in a semi-arid microcatchment of Southern India. *Environmental Monitoring and Assessment,* 187(8), pp. 1-16.

Sangüesa, C., Arumí, J., Pizarro, R. and Link, O., 2010. A rainfall simulator for the in situ study of superficial runoff and soil erosion. *Chilean Journal of Agricultural Research*, *70*(1), pp.178-182.

Schulze, R.E., Horan, M.J.C., Lumsden, T.G. and Warburton, M.L. 2007. Runoff and streamflow and their variability. *In Schulze, R.E. (ed). South African atlas of climatology and agro hydrology*. Water Research Commission, WRC Report 1489/1/06, Section 21.4, Pretoria, South Africa.

Schwank, J., Escobar, R., Girón, G.H. and Morán-Tejeda, E., 2014. Modelling of the Mendoza River catchment as a tool to study climate change impacts on water availability. *Environmental Science & Policy*, 43, pp.91-97.

Sorooshian, S., Hsu, K.L., Coppola, E., Tomassetti, B., Verdecchia, M. and Visconti, G. (eds.), 2009. *Hydrological modelling and the water cycle: coupling the atmospheric and hydrological models (Vol. 63)*. Springer Science & Business Media.

Stahl, K., Hisdal, H., Hannaford, J., Tallaksen, L., Van Lanen, H., Sauquet, E., Demuth, S., Fendekova, M. and Jordar, J., 2010. Streamflow trends in Europe: evidence from a dataset of near-natural catchments. *Hydrology and Earth System Sciences*, *14*, pp.-2367.

Stewart, R.D., Liu, Z., Rupp, D.E., Higgins, C.W. and Selker, J.S., 2015. A new instrument to measure plot-scale runoff. *Geoscientific Instrumentation, Methods and Data Systems*, 4(1), pp.57-64.

Tarboton, D.G., 2003. Rainfall-runoff processes. *Utah State University*.

Van Rensburg, L.D., Botha, J.J., Anderson, J.J. and Hensley, M., 2012. The nature and function of the in-field rainwater harvesting system to improve agronomic sustainability. *Irrigation and Drainage*, 61, pp.34-40.

Vinogradov, Y., 2009. Surface water runoff. *In Hydrological cycle*, Encyclopaedia of Life Support Systems (EOLSS).

Zelelew, M., 2012. *Improving Runoff Estimation at Ungauged Catchments (Doctoral dissertation),* Norwegian University of Science and Technology, Trondheim, Norway.

CHAPTER 8
THE SPATIO-TEMPORAL VARIATION OF GROUNDWATER RECHARGE IN THE CATCHMENT

8.1 Introduction

Groundwater is a major source of fresh water, and about two billion people and 40% of irrigation depend on it, globally (Jasechko *et al*., 2014). Hence, gaining an understanding of the spatio-temporal variation of recharge will help us to understand the linkages between groundwater and ecosystems that enable human adaptation in a changing climate (Taylor *et al*., 2013; Jasechko *et al*., 2014). Moreover, the accurate estimation of groundwater recharge is extremely important for the proper management of groundwater systems, particularly in arid and semi-arid areas (Healy and Cook, 2002; Healy, 2010; Gates *et al.,* 2014). Researchers (Kumar, 2003; Ochoa *et al.*, 2012) have suggested that a balance should be implemented between ground water depletion and recharge in order to secure the long-term sustainability of ground water resources. Accordingly, the determination of the spatial and temporal rates of recharge helps to evaluate this balance in an area of interest for the better management of water resources.

Groundwater recharge develops after the water content of the root zone exceeds its water holding capacity and the need for evapotranspiration and lateral flows are satisfied (Gates *et al.*, 2014). Groundwater recharge varies both in spatial and temporal manner where many factors contribute for these variations. These factors can be seen in three categories, (i) due to variation in the sources of water (precipitation or irrigation), (ii) due to the characteristics of the infiltrating soil and (iii) characteristics of the land surface. Literature shows all the three categories significantly affect the recharge processes (e.g. Kumar, 2003; Ochoa *et al.*, 2012; Gates *et al.*, 2014). The first category, affects drainage by the intensity and duration of the precipitation and irrigation. The second category includes the hydraulic properties (hydraulic conductivity and capillary pressure) of the soil horizon and the unsaturated zone as a whole. Lastly, the land surface characteristics include topography, land use, land cover and management which plays a vital role.

The determination of groundwater recharge is difficult to accomplish because of the high variability of recharge with respect to time and space (Gieske, 1992; Stone *et al*., 2001; Sibanda *et al.*, 2009). However, it can be estimated by different methods. (i) The water table fluctuation method, which can be applied to derive local recharge data by assuming the change in water level in the groundwater is attributable to the recharge arriving at the water table. (ii) Stream flow methods, which include the use of seepage meters, streamflow gain/loss measurements (seepage run) and recession-curve displacement methods. (iii) Hydrologic methods, including the use of hydrologic models like the Soil and Water Assessment Tool (SWAT) developed by Arnold *et al.* (1998), the Precipitation Runoff Modeling System (PRMS) (Leavesley *et al.*, 1983), and others. (iv) Tracer methods, which include using chloride, chlorofluorocarbons, temperature and tritium as tracers to estimate the ground water recharge by a mass balance equation. Detailed descriptions can be referred to in Adams *et al.* (2004), Risser *et al.* (2005), Sibanda *et al.* (2009), Wang *et al.* (2010), Crosbie *et al*., 2010; Upreti *et al.* (2015) and Chung *et al.* (2016).

Numerous studies have been conducted on the spatio-temporal distribution of groundwater recharge, at global and continental scales. Döll and Fiedler (2008) presented a daily global dataset (0.5° by 0.5° spatial resolution) from 1961 to 1990, and found an average global groundwater recharge of 12666 km^3 $year^{-1}$. Jasechko *et al*. (2014) showed that winters are the highest periods of groundwater recharges for arid and temperate zones, while summers are the highest recharges in the tropics. Crosbie *et al*. (2010) showed that vegetation covers and soil types were the major determinants for groundwater recharges in Australia. Naylor *et al*. (2016) showed that 35% of the precipitation was converted to groundwater recharge in the mid-western U.S.A. and that soil type was the major factor for recharge. Nasta *et al*. (2016) also found a decreasing trend for recharge in Africa.

Similarly, some studies are available in a South African context, which include Conrad *et al*. (2004) in the Sandveld, Western Cape, and Wu (2005) in Table Mountains Group, who found that 0.2–3.4% and 1.65–3.30% of precipitation was converted to recharge, respectively. Another study by the Department of Water Affairs and Forestry (DWAF, 2006) estimated that most of the country experienced less than 100 mm $year^{-1}$ except for some areas in the north-eastern, eastern and south-eastern parts of the country. Albhaisi *et al*. (2013) found that an 8% annual increase in recharge was attributable to the clearance of alien vegetation in the upper Berg Catchment, Western Cape. Adams *et al*. (2004) also found recharge rates between 0.1 and 10 mm $year^{-1}$ in the Namaqualand region. The study of groundwater recharge in the South African context is relatively better covered, as compared with other components of the water balance. However, there are still limitations in clearly showing the spatio-temporal variations. Therefore, the aim of this study was to investigate the spatial and temporal variation of groundwater recharge, in a catchment-scale study, in the Northern Cape Province, South Africa, by applying the SWAT model.

8.2 Materials and methods

8.2.1 Description of the study area

The study catchment is located in the Northern Cape Province, South Africa, with a geographic location of between 22°11’00” and 23°28”00” E longitudes, and 28°03’00” to 29°06’00” S latitudes. The details for the location and description of the study catchment can be seen in Chapter 3, Subsection 3.2.1.

8.2.2 Testing normality of data

As already explained in previous Sections (e.g. Chapter 4, Subsection 4.2.2), the tests of normality were analysed by a graphical method (probability-probability (P-P plot) and quantile-quantile (Q-Q plot)) and by a statistical method (Shapiro-Wilk test).

8.2.3 Trend analysis of groundwater recharge

The trend analysis in the long-term (1980–2018) groundwater recharge data was investigated by the non-parametric Mann-Kendall test. For details, see Chapter 4, Subsection 4.2.3.

8.2.4 The spatial variation of groundwater recharge

SWAT was used to estimate the spatial and temporal values of the groundwater recharge and the associated flow in the catchment, at HRU and Sub-basin scales, as discussed in Chapter 3. In this section, therefore, the mean value of the long-term monthly and yearly variations are analysed with the help of ArcGIS ver.10.4.

8.3 Results

8.3.1 Normality test

The tests of the normality of the time series for groundwater (both mean annual and monthly total groundwater recharge, which includes the sum of shallow and deep groundwater recharges) were conducted by visual assessment and statistical tests. The visual assessment is depicted in Figure 8.1 below, panels a–d, and the results of the numerical tests are given in Table 8.1 below. Based on the visual assessment (Figure 8.1 below, panels a–d), the annual groundwater recharge data can be assumed to meet the requirements of a normal distribution, whereas the monthly time series do not show a normal distribution. The simple visual assessment is supported by the statistical test (Shapiro-Wilk test). Therefore, non-parametric tests are appropriate for use to further analyse the monthly groundwater recharge.

Table 8.1: Tests of normality for the time series of groundwater recharge data

Variable	Observations	Mini.	Max.	Mean	Std. dev.	Shapiro-Wilk test	
						W	p-value
Annual recharge	39	3.900	64.918	26.501	15.058	0.952	0.094
Monthly recharge	468	0.015	19.311	2.208	2.789	0.698	< 0.01

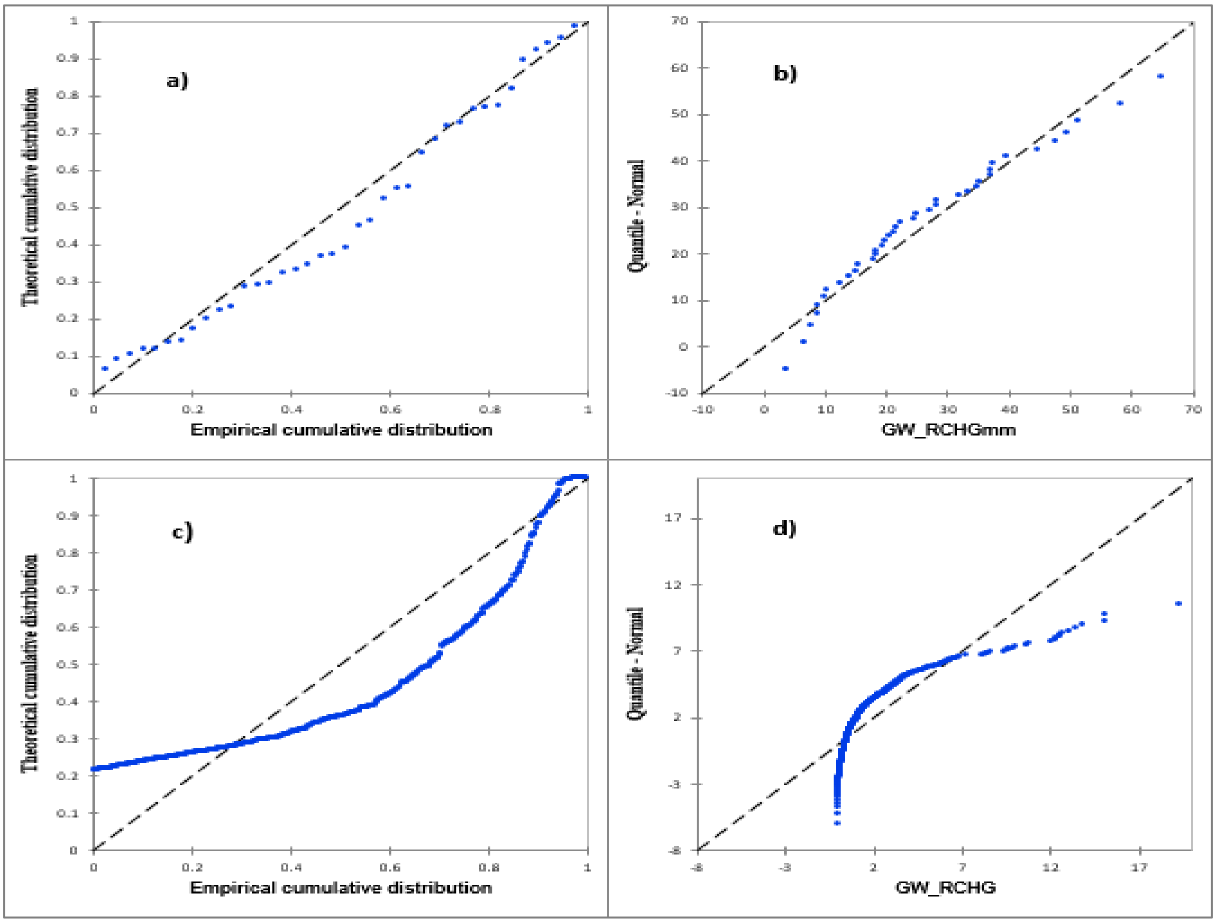

Figure 8.1: Graphical sketches showing the normality of the groundwater recharge data.

Notes: (a) probability-probability (P-P plot) for the mean annual groundwater recharge, (b) quantile-quantile (Q-Q plot) for mean annual groundwater recharge, (c) probability-probability (P-P plot) for the mean monthly groundwater recharge, and (d) quantile-quantile (Q-Q plot) for the mean monthly groundwater recharge.

8.3.2 Trends of the groundwater recharge

The time series means for monthly total, shallow and deep groundwater recharges, and their comparison with the corresponding trends of precipitation and percolation water in the catchment are given in Figure 8.2 below. It shows that the total groundwater recharge and the shallow groundwater recharge values nearly coincide, which shows that most of the percolated water from the base of the root zone was converted to shallow groundwater recharge. Hence, the shallow groundwater recharge varied from 0 to a maximum of 17.92 mm per month, while the deep groundwater recharge only attained a maximum of 1.32 mm per month in the 39-year monthly time series data. However, the trends of the fraction of precipitation that was converted to percolation show a very small amount. Figure 8.3 below shows the fraction of precipitation that was converted to percolation, as well as the fraction of percolation water converted to groundwater recharge (particularly shallow groundwater since most of the recharge water is stored in the shallow groundwater). It also shows the long-term monthly mean values of percolated water, the three recharges components (shallow, deep and their sum) and the corresponding mean precipitation in the catchment. Generally, the amount of percolated water varied from a minimum value 1% of the precipitation in October to a maximum of 26% in June. Similarly, the amount of shallow groundwater recharge, as a percentage of the percolated water, varied from a minimum of 48% in February to a maximum value of 96% of the percolated water in the month of May.

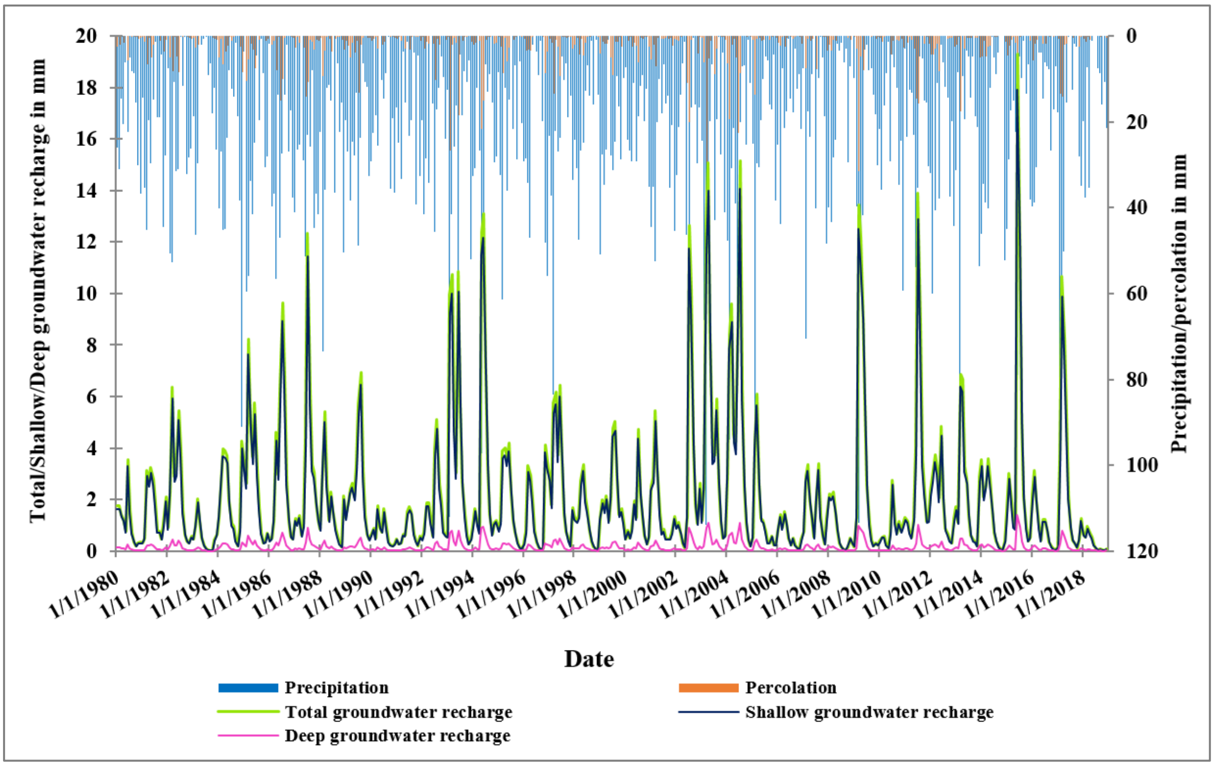

Figure 8.2: Trends of monthly recharges and comparison with precipitation and percolation in Soutloop Catchment

The time series annual trends for the different groundwater recharges (total, shallow and deep), percolated water, and precipitation was also compared (Figure 8.4 below). It shows that the amounts of total groundwater recharge and percolated water nearly coincide. The amount of total groundwater recharge varied from a minimum of 3.9 mm per annum in 2018 to a maximum value of 64.92 mm per annum in 2004. Generally, the amount of percolated water and groundwater recharge follows similar trends as the precipitation does, i.e. as the precipitation increased, the percolation and hence the groundwater recharge increased, and vice versa.

The Mann-Kendall trend analysis was also conducted to test for the presence of significant trends in both annual and monthly time series data of the total groundwater recharge in Soutloop Catchment. The results of the statistical analysis are given in Table 8.2 below. It shows that there is no significant trend in either the annual or monthly groundwater recharges ($P<0.05$).

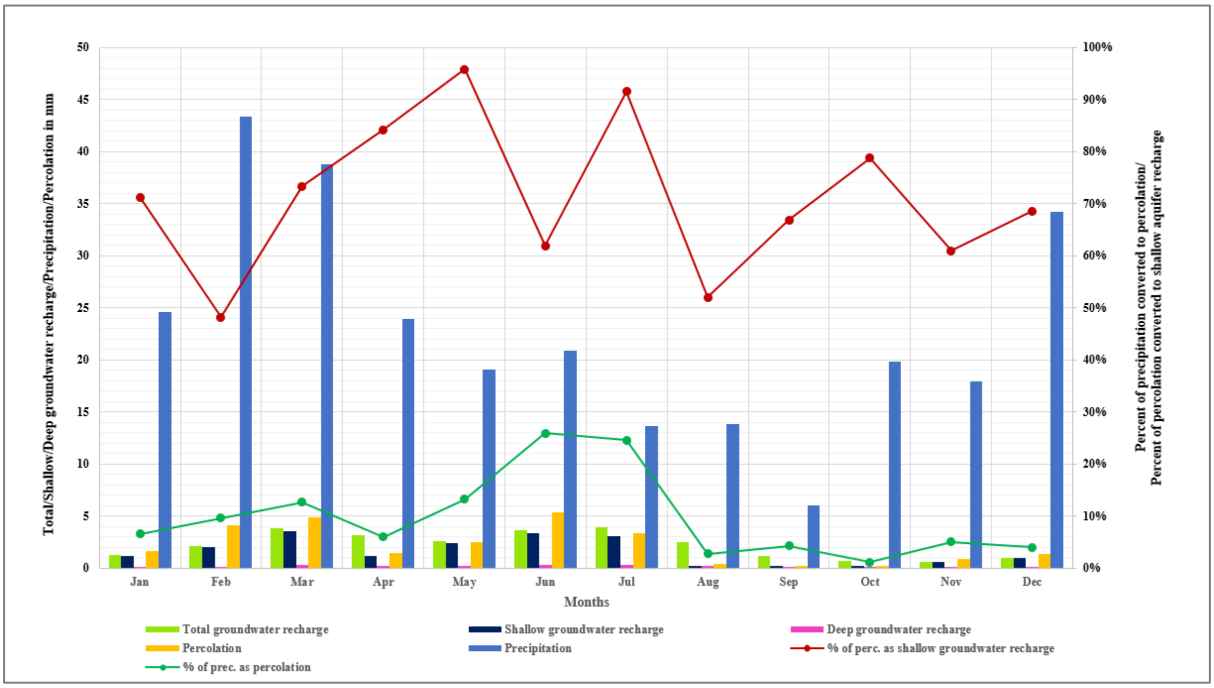

Figure 8.3: Comparison of the long-term mean monthly recharges, percolation, precipitation and percent of precipitation converted to recharges in the catchment.

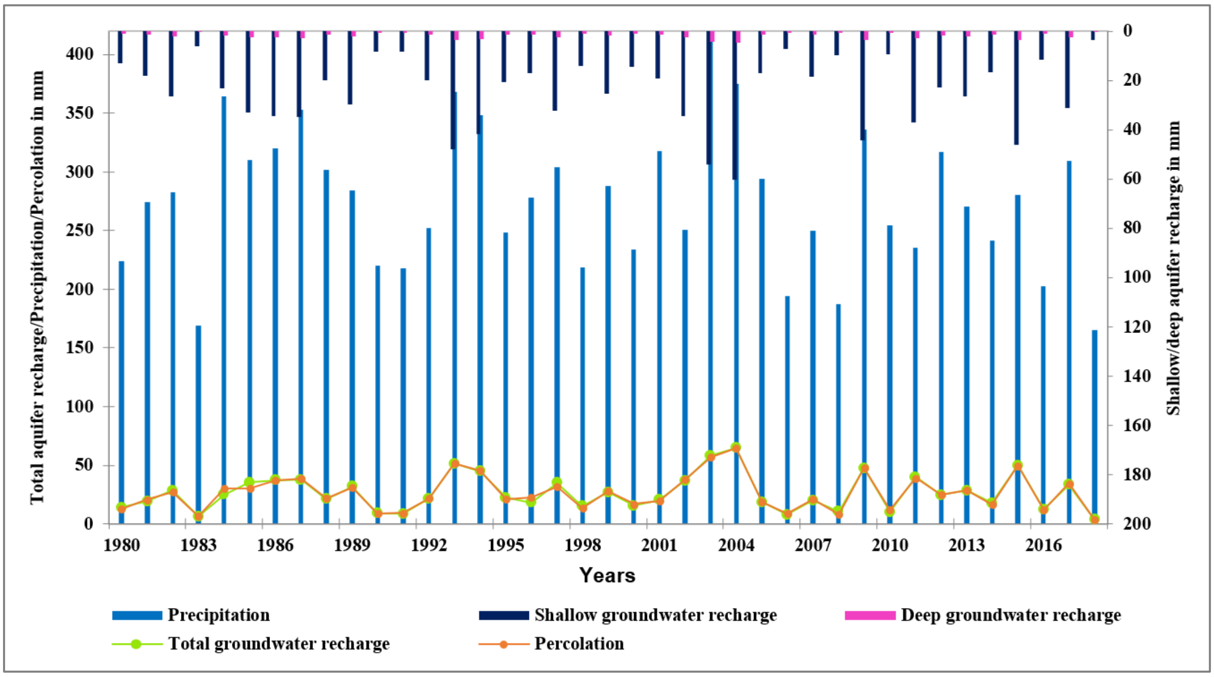

Figure 8.4: Comparison of the long-term mean annual total groundwater recharge, shallow and deep groundwater recharges, percolation and precipitation.

Table 8.2: Statistics of the Mann-Kendall trend test for the mean annual and monthly groundwater recharge in Soutloop Catchment

Parameters	Annual recharge	Monthly recharge
Kendall's tau	-0.0013	-0.0573
S stat	-1	-6266
Var(S)	6834	11425622
p-value	1	0.064
Sen's slope	-0.0040	-0.0007

8.3.3 Spatial variation of groundwater recharge

The spatial variation of the long-term mean annual total groundwater recharge and percolated water in the catchment is given in Figure 8.5 below. The magnitude of both the mean total groundwater recharge and percolated water is very similar, and only varies in some parts of the catchment. Therefore, both recharge and percolated water varied spatially from 0 to 128 mm in the catchment. As can be seen in Figure 8.5 below, the lower records of groundwater recharge have been found in large areas of the north-eastern (including Kolomela Mine area), western, and south-western parts of the catchment. On the other hand, relatively higher amounts of groundwater recharge have been recorded in large areas of the north-western and south-eastern parts of the catchment.

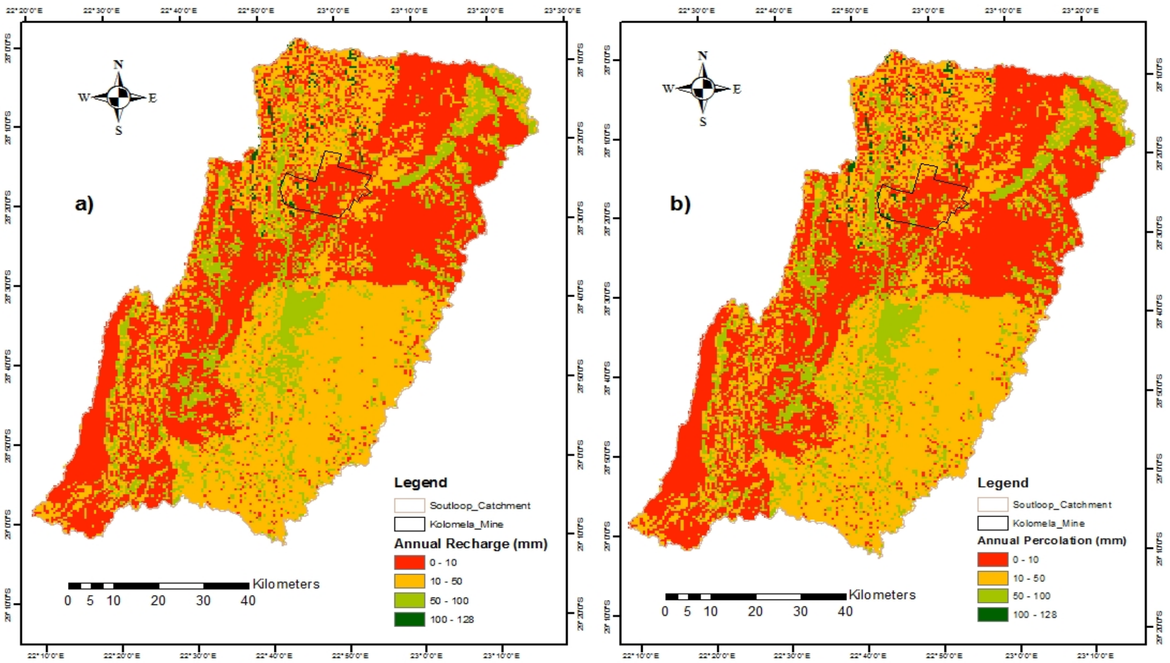

Figure 8.5: Spatial variations of the long-term mean annual a) total groundwater recharge and b) percolated water in Soutloop Catchment.

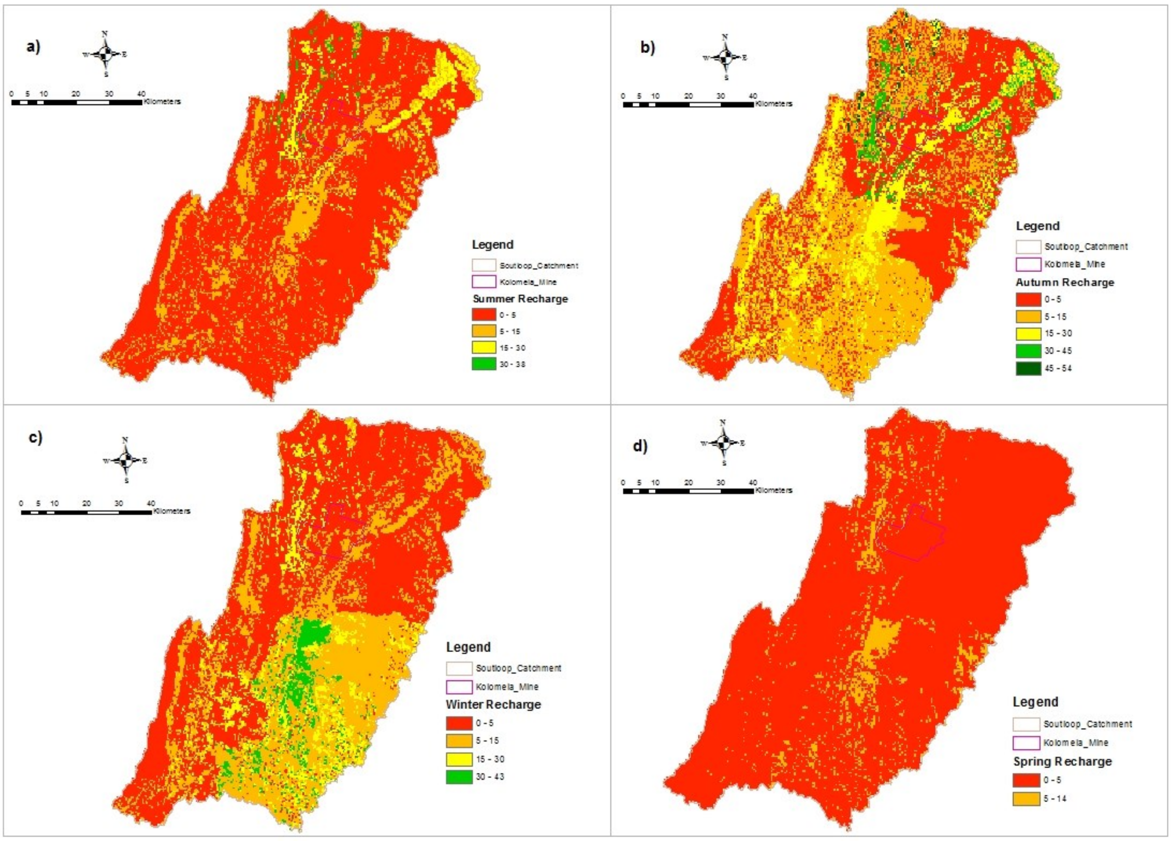

Figure 8.6: Spatial variations of the long-term mean seasonal groundwater recharge in Soutloop Catchment.

Notes: a) in summer season, b) in autumn season, c) in winter season, and d) in Spring season.

The spatial variation of the groundwater recharge was also analysed on seasonal time scales, as depicted in Figure 8.6 above. As shown, the groundwater recharge varied from 0 to 38 mm in summer, from 0 to 54 mm in autumn, from 0 to 43 mm in winter, and from 0 to 14 in spring. The long-term seasonal mean values show that most parts of the catchment during summer and spring had a groundwater recharge of less than 5 mm. Similarly, the larger part of the catchment had received more than 5 mm of groundwater recharge during autumn. The distribution in the winter season requires special attention, in that the groundwater recharge is relatively higher in the south-eastern part, having greater than 5 mm, whereas most of the other parts of the catchment remain lower than 5 mm. Generally, autumn was found to be the better season for a higher groundwater recharge in the study catchment, whereas spring was the season with the lowest magnitude of total groundwater recharge.

8.4 Discussions

Gaining an understanding of the groundwater recharge is a key step to take in achieving the sustainable management and monitoring of groundwater resources. Generally, there are two major classes of recharge: natural and artificial/managed groundwater recharges. The natural recharge might be derived from precipitation, lakes, ponds, and rivers (including perennial, seasonal, and ephemeral flows) and from other groundwater sources (Sophocleous, 2004; Hashemi *et al*., 2013). Sophocleous (2004) and Hashemi *et al*. (2013) also indicated that in arid catchments, groundwater recharge by direct percolation is not common, and that instead recharge from other sources, such as temporary ponds, lakes and river beds, play key roles. The latter type of recharge could be the most important groundwater recharge in the Soutloop Catchment, since no flow had been recorded for the last 30 years, as discussed in Chapter 7, Section 7.4. On the other hand, managed groundwater recharge and groundwater abstraction has been practiced around the Kolomela Mine area since the inception of the mine in 2010. However, the managed groundwater recharge and the groundwater abstraction are not considered in this analysis. The conceptualized groundwater modelling and major processes involved in the catchment are depicted in Figure 8.7 below.

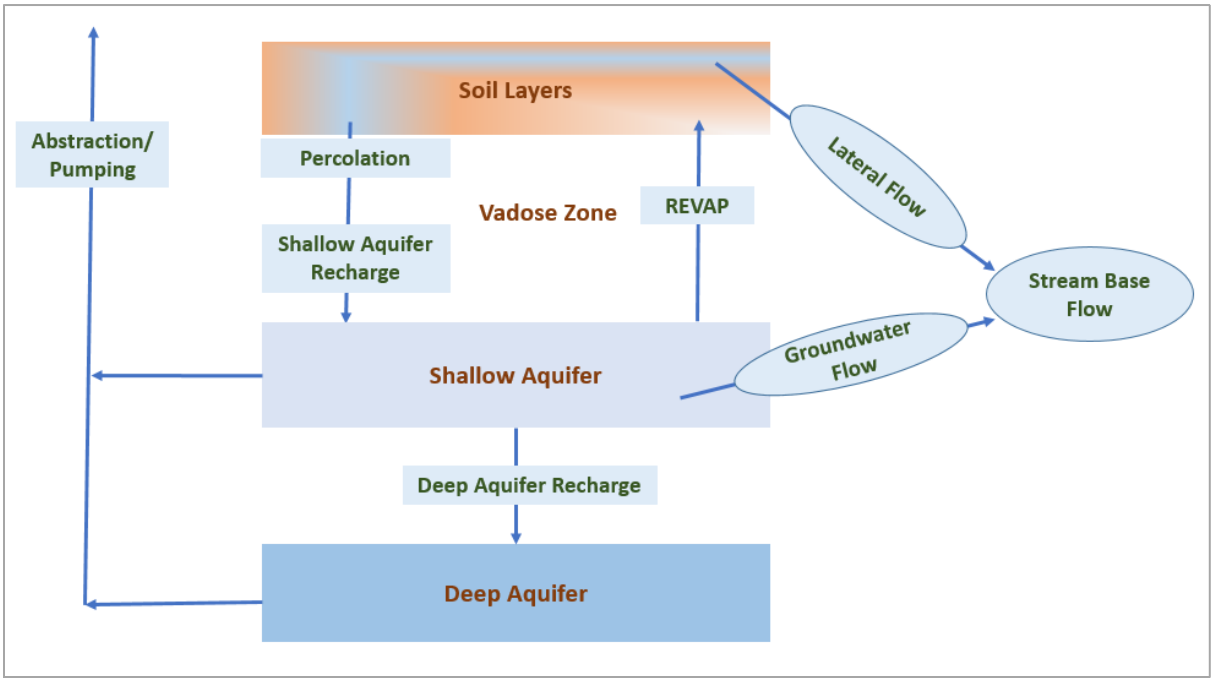

Figure 8.7: Conceptual groundwater processes and modelling in SWAT.

The results of the groundwater recharge showed a higher spatial and temporal variation in Soutloop Catchment. The long-term mean values (Figure 8.3 above) show that the groundwater recharge varied from a minimum value of 1% of the precipitation in October, to a maximum of 26% in June. It is also indicated that most of the percolated water was converted to shallow groundwater recharge. Hence, a mean value of 7.7% of the precipitation was converted annually to shallow groundwater recharge, whereas only 0.6% of the annual precipitation was used to replenish the deep groundwater in the catchment. This result is more or less consistent with previous studies, such as those of Colvin *et al*. (2016), who estimated the national average for South Africa to be 4%; Nakwafila (2015), who reported 1–5% in the Namaqualand area, and Van Dyk *et al*. (2008), who estimated between 0 and 10% of precipitation for Lower Vaal and Lower Orange water management areas. Similarly, the time series analysis (Figures 8.2 above for monthly and 8.4 above for annual) shows that the amount of total groundwater recharge varied from a minimum of 3.9 mm per annum in 2018 to a maximum value of 64.92 mm per annum in 2004. The lowest recorded value coincides with the longer drought conditions in the catchment that started in 2014 and which have continued to the current date. Similarly, the maximum value of the groundwater recharge is also consistent with the relatively wet year of 2004, as discussed in Chapter 4, Subsection 4.3.4. Moreover, the Mann-Kendall trend analysis identified no significant trend in either the annual or monthly time series values of groundwater recharge. Generally, the amounts of percolated water and groundwater recharge follow similar trends, with the trends for the precipitation showing that the impact of precipitation was higher. The most probable reason for the temporal variation could be weather parameters, particularly precipitation, that play a vital role, as shown in the correlation analysis in Table 8.3 below.

Regarding the spatial variations (Figure 8.5 above for annual and Figure 8.6 above for seasonal variations), the total recharges varied spatially from 0 to 128 mm and from 0 to 54 mm for the annual and seasonal time scales, respectively. The long-term seasonal mean values show that most parts of the catchment during summer and spring had groundwater recharges of less than 5 mm, whereas during autumn, the larger part of the catchment had a groundwater recharge of greater than 5 mm. Generally, autumn was found to be the better season for a higher groundwater recharge in the study catchment, whereas spring was the season with the lowest total groundwater recharge, in terms of the magnitude. As is true for the spatial variability of other components of the catchment water balance, topography, and soil type played a significant role in the spatial variation of groundwater recharge. The correlation analysis (Table 8.3 below) also shows that recharge negatively correlated with the available water capacity, slope class, soil depth and bulk density. This indicates that the groundwater recharge decreased as the available water capacity, slope class, soil depth and bulk density increased, and vice versa. It was also indicated that the embankments of the stream network, throughout the catchment, had recorded the highest recharge values. This confirms the reports of Sophocleous (2004), Hashemi *et al*. (2013), and Şen (2015) which explained that recharge in arid catchments is primarily derived from temporary ponds, lakes and river beds. The impact of LULC was very low, as was also true for total runoff, due to similar possible reasons (most of the catchment area has a similar land use/cover class, e.g. 80% is shrub land).

Table 8.3: Correlation of groundwater recharge with other components of water balance, soil, topography and LULC

Variable	Prec	Perc	LULC	AWC	SLOPE	SOL_ZMX	SOL_BD
Groundwater recharge	0.40	0.67	0.03	-0.61	-0.38	-0.65	-0.36

N.B: Prec-precipitation Perc-percolation LULC-land use and land cover class AWC-available water capacity SOL_ZMX-maximum soil depth SOL_BD-soil bulk density

8.5 Conclusion

This study was aimed at assessing the spatio-temporal variation of groundwater recharge in Soutloop River Catchment. The groundwater recharge was estimated by the application of a SWAT model. Although considerable uncertainty is expected due to the scarcity of data for the calibration, uncertainty and validation procedures, the comparison of similar reports indicated that the SWAT model successfully simulated the groundwater recharge.

The study area is one of the driest catchments in South Africa that experience very low levels of natural groundwater recharge. The study indicated that the natural groundwater recharge exhibited a higher spatial and temporal variation in the catchment. Groundwater is the only source of freshwater that is available for developmental and environmental requirements. Besides the natural stress (low amounts of precipitation and higher evaporative demands), the impact of human activity is prominent in the area. Although the impact of land use change, from natural and open vegetation to an area with mining activity, is a common experience, the impacts of the human-induced LULC change were not considered in this study. Accordingly, a further study on the impacts of this manmade LULC change should be undertaken. The influence of artificial groundwater recharge on the soil quality and environment should also be studied with a better spatial and temporal scale. Further studies are also recommended on the application of other groundwater models to evaluate their performances and adopt the best ones that are suited to arid catchments, as compared with SWAT.

8.6 References

Adams, S., Titus, R. and Xu, Y., 2004. *Groundwater recharge assessment of the basement aquifers of central Namaqualand,* Bellville, South Africa: South African Water Research Commission.

Albhaisi, M., Brendonck, L. and Batelaan, O., 2013. Predicted impacts of land use change on groundwater recharge of the upper Berg catchment, South Africa. *Water SA*, 39(2), pp.211-220.

Arnold, J., Srinivasan, R., Muttiah, R. and Williams, J., 1998. Large area hydrologic modeling and assessment part I: Model development. *Journal of the American Water Resources Association,* 34(1), pp. 73-89.

Chung, I., Sophocleous, M., Mitiku, D. and Kim, N., 2016. Estimating groundwater recharge in the humid and semi-arid African regions: review. *Geosciences Journal,* 20(5), pp. 731-744.

Colvin, C., Muruven, D., Lindley, D., Gordon, H. and Schachtschneider, K., 2016. *Water facts and futures: rethinking South Africa's water future*. WWF-SA 2016 Water Facts and Futures, pp.2-96.

Conrad, J., Nel, J. and Wentzel, J., 2004. The challenges and implications of assessing groundwater recharge: a case study–northern Sandveld, Western Cape, South Africa. *Water SA,* 30(5), pp.75-81.

Crosbie, R., Jolly, I., Leaney, F., Petheram, C. and Wohling, D., 2010. *Review of Australian groundwater recharge studies.* The Commonwealth Scientific and Industrial Research Organisation (CSIRO), Canberra, Australia.

Department of Water Affairs and Forestry (DWAF), 2006. *Groundwater resource assessment II –Task 3ae-recharge*. Department of Water Affairs and Forestry*,* Pretoria, South Africa.

Döll, P. and Fiedler, K., 2007. Global-scale modeling of groundwater recharge. *Hydrology and Earth System Sciences Discussions*, 4(6), pp.4069-4124.

Gates, J., Steele, G., Nasta, P. and Szilagyi, J., 2014. Lithologic influences on groundwater recharge through incised glacial till from profile to regional scales: Evidence from glaciated Eastern Nebraska. *Water Resources Research,* 50(1), pp. 466-481.

Gieske, A.S.M., 1992. *Dynamics of groundwater recharge: a case study in semi-arid eastern Botswana (a PhD Thesis)*. University of Twente, Enschede, Netherlands.

Hashemi, H., Berndtsson, R., Kompani-Zare, M. and Persson, M., 2013. Natural vs. artificial groundwater recharge, quantification through inverse modelling. *Hydrology and Earth System Sciences*, 17(2), pp.637-650.

Healy, R., 2010. *Estimating groundwater recharge.* Cambridge University Press, Cambridge, UK.

Healy, R.W. and Cook, P.G., 2002. Using groundwater levels to estimate recharge. *Hydrogeology Journal*, 10(1), pp.91-109.

Jasechko, S., Birks, S.J., Gleeson, T., Wada, Y., Fawcett, P.J., Sharp, Z.D., McDonnell, J.J. and Welker, J.M., 2014. The pronounced seasonality of global groundwater recharge. *Water Resources Research*, 50(11), pp.8845-8867.

Kumar, C., 2003. Estimation of groundwater recharge using soil moisture balance approach. *Journal of Soil and Water Conservation,* 2(1-2), pp. 53-58.

Kumba Iron Ore Limited, 2014. *Kolomela Mine socio-economic assessment tool (SEAT) report 2014*. AngloAmerican, Kolomela Mine, Postmasburg, South Africa.

Leavesley, G., Lichty, R., Thoutman, B. and Saindon, L., 1983. *Precipitation-runoff modeling system: user's manual.* US Geological Survey, Washington, DC, USA.

Nakwafila, A.N., 2015. *Salinisation source (s) and mechanism (s) in shallow alluvial aquifers along the Buffels River, Northern Cape Province, South Africa (PhD Thesis).* Stellenbosch University, Stellenbosch, South Africa.

Nasta, P., Gates, J.B. and Wada, Y., 2016. Impact of climate indicators on continental-scale potential groundwater recharge in Africa. *Hydrological Processes*, 30(19), pp.3420-3433.

Naylor, S., Letsinger, S.L., Ficklin, D.L., Ellett, K.M. and Olyphant, G.A., 2016. A hydro-pedological approach to quantifying groundwater recharge in various glacial settings of the mid-continental USA. *Hydrological Processes*, 30(10), pp.1594-1608.

Njamnsi, Y.N. and Mbue, I.N., 2009. Estimation for groundwater balance based on recharge and discharge: a tool for sustainable groundwater management, Zhongmu County Alluvial Plain Aquifer, Henan Province. China. *Journal of American Science*, 5(2), pp.83-90.

Ochoa, C.G., Fernald, A.G., Guldan, S.J., Tidwell, V.C. and Shukla, M.K., 2012. Shallow aquifer recharge from irrigation in a semiarid agricultural valley in New Mexico. *Journal of Hydrologic Engineering,* 18(10), pp. 1219-1230.

Peek, C., Barrow, D., and Conrad, J., 2015. *Geo-hydrological impact assessment relating to the proposed new Waste Water Treatment Works at Postmasburg, Northern Cape*. GEOSS–Geo-hydrological and Spatial Solutions International (Pty) Ltd, Stellenbosch, South Africa.

Risser, D., Gburek, W. and Folmar, G., 2005. *Comparison of methods for estimating ground-water recharge and base flow at a small catchment underlain by fractured bedrock in the eastern United States.* US Geological Survey, Reston, Virginia, USA.

Şen, Z., 2015. Applied drought modelling, prediction, and mitigation. Elsevier.

Sibanda, T., Nonner, J. and Uhlenbrook, S., 2009. Comparison of groundwater recharge estimation methods for the semi-arid Nyamandhlovu area, Zimbabwe. *Hydrogeology Journal,* 17(6), pp. 1427-1441.

Sophocleous M., 2004. groundwater recharge. *In Luis Silveira, Stefan Wohnlich, and Eduardo J. Usunoff (eds): Groundwater.* Encyclopedia of Life Support Systems (EOLSS).

Sophocleous, M., 2005. Groundwater recharge and sustainability in the High Plains Aquifer in Kansas, USA. *Hydrogeology Journal*, 13(2), pp.351-365.

Stone, D.B., Moomaw, C.L. and Davis, A., 2001. Estimating recharge distribution by incorporating runoff from mountainous areas in an alluvial basin in the Great Basin Region of the south-western United States. *Groundwater*, 39(6), pp.807-818.

Synergistics Environmental Services, 2013. *Artificial recharge of aquifers on farms Leeufontein 488 and Kappies Kareeboom 540 at the Sishen Iron Ore Company's Kolomela Mine, near Postmasburg, environmental management programme report*. Sishen Iron Ore Company Ltd, Kolomela Mine, South Africa.

Synergistics Environmental Services, 2015. *Scoping report for the proposed Kolomela Mine Expansion Project*. Sishen Iron Ore Company Ltd – Kolomela Mine, South Africa.

Taylor, R.G., Scanlon, B., Döll, P., Rodell, M., Van Beek, R., Wada, Y., Longuevergne, L., Leblanc, M., Famiglietti, J.S., Edmunds, M. and Konikow, L., 2013. Ground water and climate change. *Nature Climate Change*, 3(4), p.322.

Upreti, H., Ojha, C.S.P. and Hari Prasad, K.S., 2015. Estimation of Deep Percolation in Sandy-Loam Soil using Water-balance Approach. *Irrigation & Drainage Systems Engineering,* pp. doi:10.4172/2168-9768.S1-002.

Van Dyk, G.S., Makhetha J., Potgieter D., Zikali T., Leeme V., Moletsane F., Vonya T. 2008. *Groundwater resources in the Northern Cape Province 2008 (a combined report).* Department of Water Affairs and Forestry, Kimberley, South Africa.

Wang, L., Dochartaigh, B. O. and Macdonald, D., 2010. *A literature review of recharge estimation and groundwater resource assessment in Africa.* British Geological Survey, Groundwater Resources Programme. Nottingham, UK.

Wu, Y., 2005. Groundwater recharge estimation in Table Mountain Group aquifer systems with a case study of Kammanassie area (Doctoral dissertation, University of the Western Cape).

CHAPTER 9
GENERAL CONCLUSIONS AND RECOMMENDATIONS

9.1 General conclusions

It is obvious nowadays that freshwater is a scarce resource on our planet earth, and this precious resource is considerably scarce in the South African context. More particularly, the study area (the Soutloop Catchment) is one of the driest catchments in South Africa, which is characterized by very low rainfall, but high evaporative demand, leading to the unavailability of surface water. As a result of this, any demands for water (whether economic, social or environmental) are entirely dependent on the groundwater resources of the area. This lead to increasingly destructive competition between the different entities of water demands, unless a proper management plan is urgently devised and implemented.

Therefore, the general objectives of this thesis were to assess, quantify, and evaluate the spatio-temporal variability of the different components of water balance at Soutloop Catchment. It was also aimed to identify the most probable causes of the spatio-temporal variability and evaluate the intensity of water stress in the catchment. This will assist researchers, educators, policymakers and resource managers in the water sector to suggest, develop and implement proper water management programmes. The study was further aimed at evaluating the application of hydrologic models, i.e. the Soil and Water Assessment Tool (SWAT), in arid and semi-arid catchments in a case with limited input data for model calibration, validation and uncertainty procedures, in a South African context.

Regarding the modelling procedure, it is possible to generalize that the Soil and Water Assessment Tool (SWAT) model was applied successfully through the regionalization procedure using a physical similarity approach. This is indicated by the acceptable model calibration, uncertainty and validation statistics (although conducted in the donor catchment), consistency of the results with previous studies of the area, and by the *in situ* validation of the time series soil water content at selected sites in the Kolomela Mine area. However, it was also expected that there would be a considerable uncertainty of the modelling process, which would be primarily attributable to unavailability of flow data for *in situ* calibration, uncertainty and validation of the model.

It was also observed that all the components of the catchment water balance exhibited a higher spatial and temporal variability in the catchment, primarily because of the variation of climatic variables, soil factors, topographic features, and LULC variation. The climatic variations (except precipitation) were responsible primarily for the temporal/time series variability, whereas the soil type, topographic features and LULC variations were attributed mainly to the spatial variability of the components of water balance in the catchment. However, the influence of precipitation was significant for both spatial and temporal variations. On the other hand, the impact of the variation in LULC was found to be relatively small because most of the area was covered by similar LULC classes, which was classified as low shrub land, based on the national LULC classification of South Africa for the 2013/2014 year.

Regarding the evaluation of water stress by using hydro-meteorological indicators, this study concluded that the application of the most-commonly used indicator, the SPI-standardized precipitation index, alone could lead to wrong conclusions being drawn, particularly for arid catchments. Hence, it should be interpreted together with other additional indicators, such as the aridity index (AI), soil water anomaly (SWA), evapotranspiration stress index (ESI), normalized difference vegetation index (NDVI), and others. More particularly, the application of the satellite-based indicator, NDVI, was found to be an important alternative for arid catchments, since it can show the timely time series relative variations of water stress on vegetation for an area with a better spatial and temporal coverage. The study also showed that the use of model-derived simulations for evaluating water stress and drought is an alternative data source and an encouraging approach that could be applied at local, national or regional scales in environmental monitoring programmes.

9.2 Recommendations

Arising from the analysis conducted so far in the catchment, the following tasks are recommended for further investigation and for attention to be given in order to obtain important and full information needed for the management of water resources, for the sake of the social, economic and environmental benefits of the area considered in this study.

It is recommended that a hydro-census (inventory of water resources) should be carried out, particularly on groundwater abstraction. As the area is totally dependent on groundwater resources, the spatial distribution and the time series volumes of water abstracted should be recorded. One of the points of data in the area that is difficult to get relates to the volume of water abstracted from boreholes on private farms. Therefore, a procedure should be developed to record and gather this data on regular timescales (daily, monthly, annually) for the ease of future hydrological investigations.

As has already been made clear in many reports, climate change is inevitable and this is true for South Africa as well. One of the primary influences of climate change is experienced in water resources. Therefore, the assessment of climate change (e.g. precipitation and air temperature) could also help in planning a good strategy for managing water resources.

As the study area is dominated by shrub land (which includes deep-rooted vegetation), any deleterious impacts suffered by groundwater resources will be immediately reflected in the vegetation status. Therefore, analysis of the impact of groundwater on vegetation in the area is expected to be straightforward. Hence, LULC change is a good indicator of the health of groundwater in such arid areas. Therefore, time series change detection with respect to the vegetation condition is recommended for further study.

Various indices are available nowadays to evaluate or monitor the intensity of water stress of an area. Together with the land use change, other indicators are important, such as the standardized precipitation index (SPI), soil water anomaly (SWA), and the normalized difference vegetation index (NDVI. Therefore, analyses of these indices should be conducted regularly, with higher spatial and temporal scales for better environmental monitoring.

It has been reported that a considerable amount of water is being released around the Kolomela Mine area into the environment (including the artificial aquifer recharge). The impacts of this on the quality and quantity of groundwater, soil quality, vegetation, and the environment as a whole should be investigated.

The soil and water assessment tool (SWAT) is a continuous simulation model. In order to compare it with event-based models, further research is recommended to compare and contrast the two types of models as one way to decrease model uncertainty.

Finally, this study considers only the variability of the natural hydrological processes, both in space and time. However, this area, particularly the northern part of the catchment, is well known for the intervention of human activity on the environment. More particularly, large-scale mining activities, like iron ore mining, are common practice these days. Following on from the mining activity, other related practices that influence the water resource significantly, such as LULC changes and groundwater abstraction, become common. Therefore, the impacts of these human-induced economic activities should be studied further to better understand the hydro-climatological behaviours of the area.

APPENDICES

Appendix 1: General characteristics of the catchment

Name of the study catchment	Soutloop Catchment
No. of Sub-catchments	27
No. of HRUs	1490
Catchment area (ha)	676971.26

Appendix 2: Soil characteristics

SOIL	No. Layers	SOL_ZMX	SOL_Z1	SOL_BD1	SOL_Z2	SOL_BD2	AWC mm	WP (mm)	FC (mm)	Saturation (mm)
Calcic	2	350	150	1.52	200	1.57	24.50	9.50	24.50	74.90
Cumulic	2	1550	450	1.38	1100	1.43	89.50	117.80	89.50	397.10
Duplex	2	787	150	1.85	637	1.53	65.60	59.90	65.60	191.20
Gleyic	2	1300	450	1.54	850	1.44	184.05	84.40	184.10	286.80
Lithic	1	129	129	1.31	0	0.00	19.41	7.50	19.40	58.00
Oxidic	2	876	150	1.32	726	1.44	87.36	52.80	87.40	285.50

Appendix 3: Comparison of LULC classes in South African classification and SWAT databases classes

LULC in SA classification	LULC in SWAT	SWAT Code	Area (ha)	Percent of catchment
Cultivated comm fields/pivots med or low	Agricultural Land-Generic	AGRL	184.88	0.0273
Cultivated comm pivots (high)	Agricultural Land-Row	AGRR	29.56	0.0044
Bare land	Barren	BARR	13029.03	1.9246
Plantations / Woodlots young or mature	Forest-Evergreen	FRSE	9.07	0.0013
Thicket/woodland/urban informal/urban sports and golf dense bush or trees	Forest-Mixed	FRST	45386.10	6.7043
Low shrub land	Range-Brush	RNGB	540944.11	79.9065
Grassland	Range-Grasses	RNGE	76385.78	11.2835
Urban commercial	Commercial	UCOM	70.97	0.0105
Urban school and sports ground	Institutional	UINS	44.56	0.0066
Urban residential/township/built up dense trees or bush	Residential-High density	URHD	87.77	0.0130
Urban informal/residential/sports and golf/township/village/built up-low vegetation or grass	Residential-Low density	URLD	543.14	0.0802
Urban residential/sports and golf/township/village/built up open trees or bush)	Residential-Medium density	URMD	61.36	0.0091
Water seasonal	Wetlands-Non-Forested	WETN	23.18	0.0034
Cultivated comm fields (high)	Agricultural Land-close-grown	AGRC	13.65	0.0020
Urban industrial and Mine buildings	Industrial	UIDU	139.15	0.0206
Water	Water	WATR	15.81	0.0023
Cultivated vines	Vineyard	GRAP	3.14	0.0005

Appendix 4: Monthly minimum temperature (°C)

Year	Jan	Feb	Mar	Apr	May	Jun	Jul	Aug	Sep	Oct	Nov	Dec
1980	16.16	12.39	12.87	9.46	6.80	1.82	3.45	6.44	9.03	9.11	12.75	16.39
1981	14.66	14.84	15.05	11.57	7.36	2.99	4.24	5.97	10.32	9.57	15.28	14.61
1982	18.33	14.82	13.60	6.82	4.95	1.07	2.62	7.01	8.90	13.62	11.34	17.03
1983	14.26	16.94	14.79	7.18	7.90	3.20	2.15	6.17	7.22	11.35	13.65	19.57
1984	16.07	18.23	13.50	10.94	7.05	2.94	3.69	6.54	8.41	9.27	13.10	17.02
1985	15.79	18.29	15.12	8.19	5.07	3.87	3.21	3.80	5.83	13.36	13.04	14.65
1986	17.68	14.91	12.33	11.41	7.09	1.70	2.41	6.78	9.05	10.97	13.19	14.97
1987	17.35	14.51	14.85	9.50	4.96	1.49	8.05	3.64	10.74	15.25	13.97	14.85
1988	17.10	17.58	15.39	7.89	6.47	1.52	4.07	6.20	8.18	10.53	14.79	15.58
1989	15.22	18.81	12.91	8.65	7.21	4.40	2.05	1.65	4.37	12.99	12.97	15.25
1990	15.99	12.06	13.05	7.42	4.23	3.20	6.77	9.16	10.99	10.20	15.84	16.90
1991	18.04	15.56	15.88	8.23	4.74	2.46	-0.42	3.97	8.37	8.70	13.37	16.18
1992	14.37	17.06	15.61	7.26	5.69	3.68	1.68	4.63	9.19	10.31	14.55	15.93
1993	16.95	17.16	15.06	9.28	6.70	4.91	6.67	1.17	8.44	12.63	13.94	18.17
1994	16.16	18.82	14.10	7.86	6.17	0.76	3.78	7.22	6.88	14.73	13.45	18.16
1995	18.58	15.12	15.41	11.77	5.58	1.19	-0.04	5.07	11.60	10.23	14.04	14.55
1996	17.85	14.46	12.91	10.66	5.84	0.67	1.03	3.10	9.63	11.13	15.46	15.09
1997	16.29	17.94	14.03	11.61	4.36	2.73	4.33	5.37	8.65	15.17	13.22	15.18
1998	17.78	16.71	14.19	11.45	6.34	4.64	6.07	6.28	7.37	10.52	13.23	14.61
1999	18.13	14.54	16.06	10.18	7.91	4.11	3.57	5.44	8.29	10.13	14.47	16.74
2000	18.27	14.98	14.34	8.95	9.16	3.36	2.53	3.93	7.41	12.92	13.42	16.65
2001	16.69	15.23	15.86	11.70	7.78	2.46	3.60	5.65	9.96	11.02	13.29	16.45
2002	15.20	16.78	15.56	10.33	4.59	2.63	5.95	7.06	9.66	12.73	15.66	15.18
2003	15.50	16.29	14.63	9.74	8.26	3.02	5.28	4.21	6.19	9.40	14.37	17.32
2004	14.74	16.06	13.81	6.75	2.58	3.93	1.95	5.26	6.56	11.65	12.77	14.19
2005	17.77	16.17	14.48	10.96	5.18	1.87	3.62	5.94	11.83	11.97	12.79	14.02
2006	16.59	18.77	15.54	10.74	9.31	0.53	2.84	7.36	6.23	11.38	14.82	18.45
2007	17.49	19.26	14.35	10.22	9.30	3.47	2.84	6.12	9.48	10.23	17.04	12.73
2008	16.17	16.90	17.34	9.59	5.54	6.08	0.49	5.83	9.45	12.61	12.97	15.56
2009	17.75	14.29	15.00	8.88	5.57	3.60	4.28	5.25	6.59	10.12	13.79	15.96
2010	19.00	17.31	16.12	7.36	6.88	3.70	5.86	6.87	10.11	9.99	14.30	17.26
2011	17.71	18.53	14.76	11.64	4.68	1.16	1.82	2.90	11.02	14.38	14.66	17.11
2012	14.52	15.51	13.09	10.59	6.24	4.47	6.45	3.28	10.74	13.70	11.56	16.25
2013	16.03	15.90	14.65	10.36	5.84	6.16	4.08	6.97	7.71	12.03	12.63	15.48
2014	18.11	18.77	12.68	10.32	4.00	5.16	3.28	6.83	10.76	11.60	14.84	15.26
2015	16.17	17.71	13.97	11.53	4.49	2.72	1.66	4.84	7.64	12.72	14.63	12.88
2016	14.67	16.08	15.11	8.34	8.13	2.49	1.09	5.37	14.73	12.31	15.83	16.52
2017	15.19	17.96	13.73	9.06	7.45	2.93	5.23	5.63	7.37	10.12	13.49	14.86
2018	15.82	14.39	15.50	11.52	8.62	1.45	4.02	0.64	8.32	12.67	10.85	15.46

Appendix 5: Monthly maximum temperature (°C)

Year	Jan	Feb	Mar	Apr	May	Jun	Jul	Aug	Sep	Oct	Nov	Dec
1980	33.07	30.38	29.26	25.10	22.90	18.19	19.16	24.67	28.08	26.85	31.28	32.02
1981	34.49	31.30	29.34	27.92	23.29	18.03	21.64	21.52	25.11	30.44	32.97	33.82
1982	38.00	32.53	27.22	24.71	17.14	15.50	19.62	24.88	30.47	29.86	27.17	33.86
1983	33.85	31.59	29.25	26.73	24.01	17.44	19.31	24.79	23.20	30.91	30.87	38.62
1984	32.89	32.47	29.34	26.01	21.52	18.53	18.23	24.16	29.39	26.07	29.53	33.29
1985	35.25	33.14	28.90	23.34	17.18	18.34	19.53	23.36	27.31	33.00	30.07	30.60
1986	38.21	28.74	27.08	23.93	23.55	13.55	14.65	24.07	27.43	26.67	30.81	31.05
1987	29.89	32.58	30.75	27.20	18.65	12.90	20.39	20.13	27.76	30.00	28.91	29.57
1988	32.00	31.76	30.00	25.95	22.84	16.83	23.39	20.81	23.97	28.71	33.75	32.78
1989	33.39	33.59	28.10	23.78	18.86	19.79	15.84	19.85	20.42	32.70	31.02	31.96
1990	32.82	32.03	30.41	24.50	23.37	17.86	23.13	27.43	30.75	26.69	31.48	32.42
1991	35.23	30.76	30.35	25.86	22.41	17.39	16.06	21.52	24.78	23.83	35.69	33.57
1992	31.79	33.32	28.92	22.44	24.99	18.90	15.41	21.51	26.10	29.17	34.54	35.44
1993	35.90	31.24	28.51	24.21	20.25	18.91	22.36	17.93	25.98	31.51	34.24	31.21
1994	31.39	30.82	32.47	21.88	18.66	14.31	20.02	23.68	22.82	31.38	28.84	33.88
1995	37.87	31.77	28.32	25.99	20.87	17.55	17.44	21.87	23.25	26.44	31.93	33.06
1996	33.57	29.77	28.58	21.60	23.11	17.41	18.14	21.71	28.31	28.91	31.17	32.88
1997	31.49	33.10	27.52	24.98	18.52	17.94	20.24	24.03	26.35	31.82	31.04	34.79
1998	34.91	31.09	27.42	26.47	18.37	17.97	20.22	24.13	26.42	30.14	34.18	33.92
1999	33.73	29.34	28.99	26.31	25.31	16.71	16.51	20.70	21.22	27.66	30.87	36.22
2000	37.03	32.42	30.55	25.35	24.47	15.08	19.11	21.33	25.38	32.02	32.90	31.75
2001	33.63	32.73	29.62	27.46	22.12	14.39	18.48	22.65	24.09	25.47	30.28	32.55
2002	31.88	31.31	31.62	27.92	22.68	16.32	17.54	24.11	29.08	30.26	33.81	34.89
2003	31.32	29.44	27.02	23.75	21.57	18.57	18.29	21.46	26.66	25.39	35.41	34.43
2004	30.22	29.07	28.33	23.48	17.11	14.77	18.81	24.69	24.08	27.77	33.60	34.97
2005	31.49	28.47	29.30	26.48	20.89	16.82	18.89	22.85	28.20	29.48	32.96	30.72
2006	32.01	30.38	33.16	27.88	21.34	17.73	17.45	23.40	26.47	30.75	34.56	35.97
2007	33.97	34.62	29.78	27.70	25.37	20.35	17.20	22.52	26.97	30.74	35.46	28.42
2008	32.49	34.03	31.39	24.26	24.72	21.69	17.53	24.27	27.39	28.46	31.49	36.09
2009	37.13	30.22	27.81	22.59	18.96	21.24	19.92	23.59	26.09	27.03	32.48	32.62
2010	34.48	33.65	31.03	24.78	23.37	14.44	22.88	25.07	25.48	24.64	29.65	30.82
2011	36.94	35.37	31.67	26.66	20.01	12.32	14.71	20.38	30.15	32.55	30.88	34.59
2012	30.66	30.08	28.33	26.32	19.14	17.90	22.11	20.79	27.79	27.27	29.88	30.76
2013	31.77	31.79	28.44	27.48	21.24	21.60	21.18	25.23	28.66	30.86	30.41	31.44
2014	33.14	32.97	26.18	22.23	17.26	21.36	19.08	24.70	29.40	32.95	35.29	30.98
2015	31.79	31.21	31.35	26.29	19.43	18.41	17.38	24.29	26.75	29.63	34.78	31.25
2016	29.71	32.06	30.70	27.49	24.15	17.90	20.02	25.33	32.20	30.01	33.70	36.74
2017	34.34	32.38	28.38	23.28	24.25	19.99	22.94	23.12	26.45	30.58	32.78	30.84
2018	32.86	29.75	28.88	26.42	24.36	18.59	19.75	21.60	27.10	29.52	32.74	33.79

Appendix 6: Monthly average temperature (°C)

Year	Jan	Feb	Mar	Apr	May	Jun	Jul	Aug	Sep	Oct	Nov	Dec
1980	24.62	21.38	21.06	17.28	14.85	10.00	11.30	15.55	18.55	17.98	22.02	24.21
1981	24.57	23.07	22.19	19.74	15.32	10.51	12.94	13.75	17.72	20.01	24.13	24.22
1982	28.17	23.68	20.41	15.77	11.04	8.29	11.12	15.94	19.68	21.74	19.26	25.45
1983	24.05	24.26	22.02	16.96	15.96	10.32	10.73	15.48	15.21	21.13	22.26	29.10
1984	24.48	25.35	21.42	18.47	14.29	10.73	10.96	15.35	18.90	17.67	21.32	25.16
1985	25.52	25.71	22.01	15.77	11.12	11.10	11.37	13.58	16.57	23.18	21.55	22.62
1986	27.94	21.82	19.71	17.67	15.32	7.62	8.53	15.43	18.24	18.82	22.00	23.01
1987	23.62	23.54	22.80	18.35	11.81	7.20	14.22	11.89	19.25	22.62	21.44	22.21
1988	24.55	24.67	22.70	16.92	14.66	9.17	13.73	13.51	16.07	19.62	24.27	24.18
1989	24.30	26.20	20.51	16.22	13.03	12.09	8.95	10.75	12.40	22.85	21.99	23.60
1990	24.40	22.04	21.73	15.96	13.80	10.53	14.95	18.30	20.87	18.44	23.66	24.66
1991	26.64	23.16	23.11	17.05	13.57	9.93	7.82	12.75	16.58	16.26	24.53	24.88
1992	23.08	25.19	22.27	14.85	15.34	11.29	8.55	13.07	17.64	19.74	24.55	25.68
1993	26.43	24.20	21.78	16.75	13.48	11.91	14.52	9.55	17.21	22.07	24.09	24.69
1994	23.77	24.82	23.29	14.87	12.41	7.53	11.90	15.45	14.85	23.06	21.15	26.02
1995	28.22	23.44	21.87	18.88	13.22	9.37	8.70	13.47	17.43	18.34	22.98	23.80
1996	25.71	22.11	20.75	16.13	14.47	9.04	9.58	12.40	18.97	20.02	23.31	23.99
1997	23.89	25.52	20.77	18.29	11.44	10.33	12.28	14.70	17.50	23.50	22.13	24.98
1998	26.34	23.90	20.81	18.96	12.35	11.31	13.14	15.21	16.89	20.33	23.70	24.26
1999	25.93	21.94	22.53	18.24	16.61	10.41	10.04	13.07	14.75	18.89	22.67	26.48
2000	27.65	23.70	22.44	17.15	16.81	9.22	10.82	12.63	16.39	22.47	23.16	24.20
2001	25.16	23.98	22.74	19.58	14.95	8.43	11.04	14.15	17.02	18.25	21.79	24.50
2002	23.54	24.04	23.59	19.13	13.64	9.47	11.74	15.58	19.37	21.50	24.74	25.03
2003	23.41	22.87	20.82	16.75	14.92	10.79	11.78	12.83	16.43	17.39	24.89	25.87
2004	22.48	22.57	21.07	15.11	9.85	9.35	10.38	14.98	15.32	19.71	23.19	24.58
2005	24.63	22.32	21.89	18.72	13.04	9.35	11.26	14.39	20.02	20.72	22.88	22.37
2006	24.30	24.58	24.35	19.31	15.33	9.13	10.14	15.38	16.35	21.07	24.69	27.21
2007	25.73	26.94	22.07	18.96	17.33	11.91	10.02	14.32	18.23	20.49	26.25	20.58
2008	24.33	25.47	24.36	16.93	15.13	13.89	9.01	15.05	18.42	20.54	22.23	25.83
2009	27.44	22.25	21.40	15.74	12.26	12.42	12.10	14.42	16.34	18.58	23.13	24.29
2010	26.74	25.48	23.58	16.07	15.12	9.07	14.37	15.97	17.79	17.32	21.98	24.04
2011	27.33	26.95	23.22	19.15	12.34	6.74	8.27	11.64	20.59	23.46	22.77	25.85
2012	22.59	22.80	20.71	18.45	12.69	11.18	14.28	12.03	19.27	20.49	20.72	23.51
2013	23.90	23.84	21.55	18.92	13.54	13.88	12.63	16.10	18.19	21.44	21.52	23.46
2014	25.62	25.87	19.43	16.27	10.63	13.26	11.18	15.77	20.08	22.28	25.07	23.12
2015	23.98	24.46	22.66	18.91	11.96	10.56	9.52	14.56	17.19	21.18	24.71	22.07
2016	22.19	24.07	22.90	17.92	16.14	10.20	10.56	15.35	23.46	21.16	24.76	26.63
2017	24.77	25.17	21.06	16.17	15.85	11.46	14.08	14.37	16.91	20.35	23.14	22.85
2018	24.34	22.07	22.19	18.97	16.49	10.02	11.88	11.12	17.71	21.09	21.80	24.63

Appendix 7: Annual and monthly potential evapotranspiration

Year	Jan	Feb	Mar	Apr	May	Jun	Jul	Aug	Sep	Oct	Nov	Dec	Annual
1980	233.58	209.57	183.11	145.90	145.53	110.80	120.59	163.10	223.36	223.37	209.03	220.22	2188.16
1981	289.35	207.22	157.10	145.66	115.31	106.07	142.71	129.14	134.93	266.60	242.46	292.54	2229.10
1982	339.88	175.49	142.30	176.44	68.63	70.93	136.22	159.79	232.40	208.33	187.10	274.08	2171.61
1983	270.10	154.43	157.78	190.48	132.51	95.00	128.96	165.33	167.53	249.33	243.78	302.65	2257.87
1984	203.11	188.02	188.24	133.01	104.01	92.02	108.09	142.12	234.50	185.20	193.25	198.20	1969.77
1985	306.27	200.64	134.05	121.61	68.04	102.07	118.46	141.39	224.70	280.04	203.03	221.83	2122.13
1986	371.68	156.85	127.86	98.30	125.05	55.96	53.33	136.72	207.95	195.97	218.37	216.44	1964.47
1987	170.42	202.19	184.46	196.30	89.24	52.22	108.73	116.13	184.51	170.42	177.72	180.34	1832.68
1988	211.64	153.02	178.55	161.16	109.60	78.76	154.43	100.69	135.36	229.01	273.09	252.54	2037.86
1989	277.78	218.54	149.08	119.93	69.64	101.69	62.19	108.48	145.60	284.37	256.03	214.06	2007.38
1990	231.23	232.33	213.45	137.66	158.28	98.95	120.84	165.34	260.22	189.93	234.88	236.75	2279.87
1991	281.59	180.88	190.50	182.02	123.73	109.65	100.88	111.66	178.13	157.18	331.85	262.71	2210.78
1992	236.48	222.34	139.90	106.85	165.69	109.22	61.99	120.28	153.17	265.84	320.43	303.84	2206.02
1993	312.49	157.93	140.69	135.17	101.21	72.55	133.84	105.91	176.97	293.71	297.87	183.56	2111.90
1994	216.43	155.04	211.69	107.58	76.80	61.44	122.49	141.09	156.27	243.41	185.50	242.49	1920.25
1995	344.49	181.89	123.65	150.41	98.58	101.93	120.92	123.48	126.65	168.17	253.46	283.86	2077.48
1996	235.80	163.12	179.71	81.41	135.75	108.70	110.54	130.00	192.12	229.26	206.06	237.37	2009.85
1997	189.43	149.67	119.16	109.53	81.57	92.59	119.36	145.12	178.47	261.84	254.34	300.92	2002.00
1998	243.84	144.28	132.96	142.07	77.98	79.97	116.02	158.07	173.99	261.65	342.81	309.51	2183.15
1999	201.35	163.99	140.03	140.42	139.92	65.07	72.38	101.14	123.09	190.41	230.82	327.32	1895.92
2000	323.64	243.78	209.65	137.73	136.76	53.13	118.56	129.27	161.53	215.46	280.26	205.43	2215.21
2001	225.76	194.16	155.62	152.87	90.38	63.48	117.63	135.13	141.42	150.06	230.40	205.98	1862.90
2002	196.60	165.84	227.89	195.09	148.50	83.25	69.10	138.29	232.01	244.22	316.22	317.00	2334.01
2003	190.01	131.66	118.10	94.45	83.76	99.45	62.61	119.00	228.77	205.12	306.69	241.02	1880.65
2004	180.91	128.47	136.25	133.23	60.92	58.23	114.06	155.21	172.72	217.25	336.36	337.06	2030.69
2005	186.99	134.31	141.14	136.53	105.81	89.26	119.99	156.85	182.26	247.86	332.52	210.26	2043.77
2006	250.79	154.68	259.32	164.10	107.04	98.59	83.65	135.20	199.58	281.82	304.91	320.86	2360.51
2007	241.09	180.42	188.44	164.46	123.05	128.64	71.05	136.50	219.78	267.51	298.10	160.82	2179.86
2008	239.50	208.48	187.66	113.89	139.26	126.90	117.17	159.63	190.88	192.52	264.56	372.08	2312.54
2009	319.11	159.26	126.48	93.69	74.98	116.02	127.77	138.49	212.32	221.51	234.21	234.58	2058.44
2010	226.68	235.14	211.24	162.66	128.58	53.12	132.89	159.60	142.11	157.18	196.48	193.30	1998.98
2011	339.51	239.63	219.74	150.61	102.07	45.25	57.46	140.53	225.08	271.39	225.01	279.25	2295.53
2012	188.55	147.60	182.78	173.58	99.19	87.61	129.84	130.88	177.92	166.86	260.23	204.25	1949.27
2013	188.77	179.84	143.27	163.08	121.85	122.15	127.79	161.25	198.75	247.07	185.70	195.53	2035.06
2014	196.15	173.89	152.33	94.59	77.87	123.94	121.26	151.00	200.23	320.06	369.53	184.20	2165.04
2015	207.36	163.32	203.18	152.44	84.47	99.05	110.52	159.71	175.17	258.63	343.70	248.75	2206.30
2016	171.64	175.77	177.27	180.75	113.05	107.18	126.70	146.80	206.65	187.27	281.69	371.21	2245.99
2017	283.83	142.43	174.04	102.96	117.04	107.62	149.67	150.18	212.53	282.73	262.14	224.57	2209.75
2018	252.63	149.38	153.82	128.91	153.22	105.45	140.61	136.41	205.14	207.42	293.59	292.67	2219.25

Appendix 8: Components of the long-term mean annual water balance

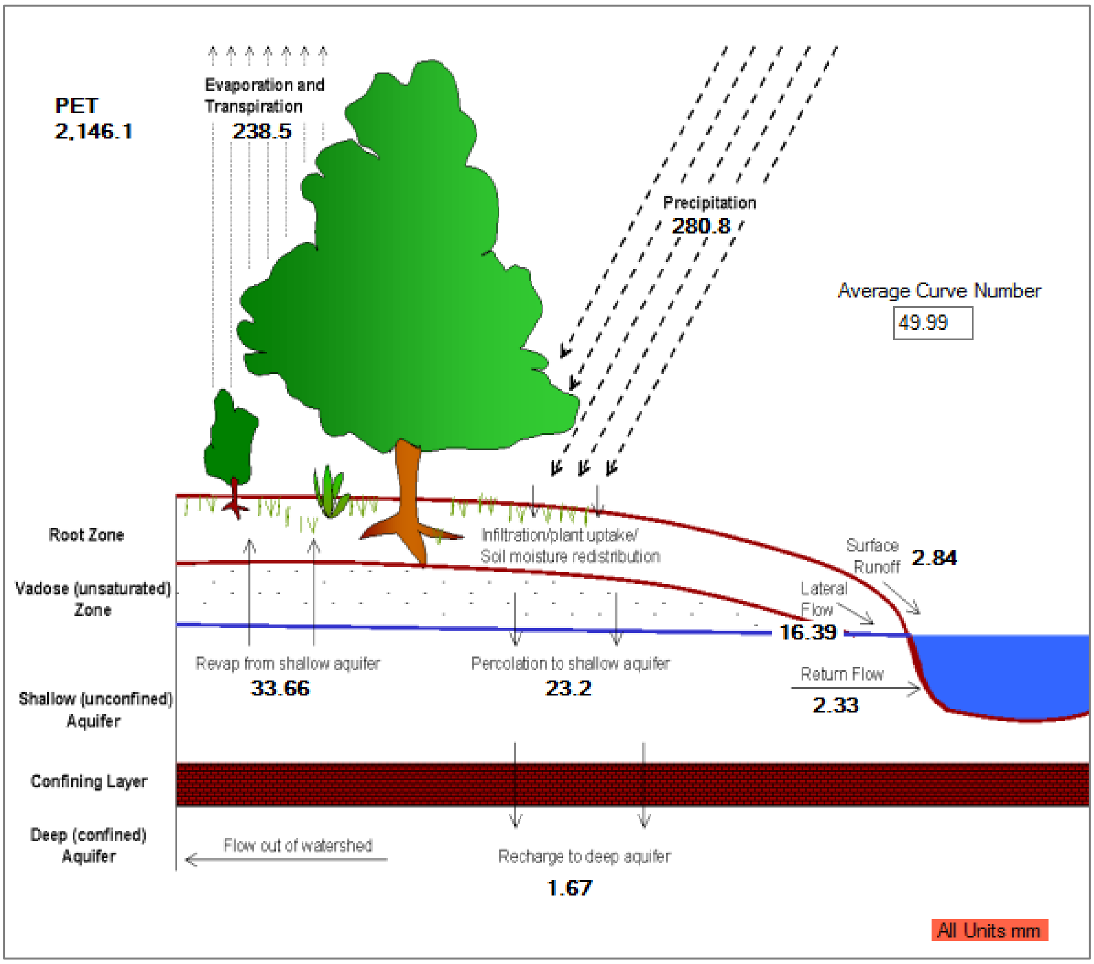

Appendix 9: DFM soil water measurement sensor

Appendix 10: Different soil profiles opened during field survey

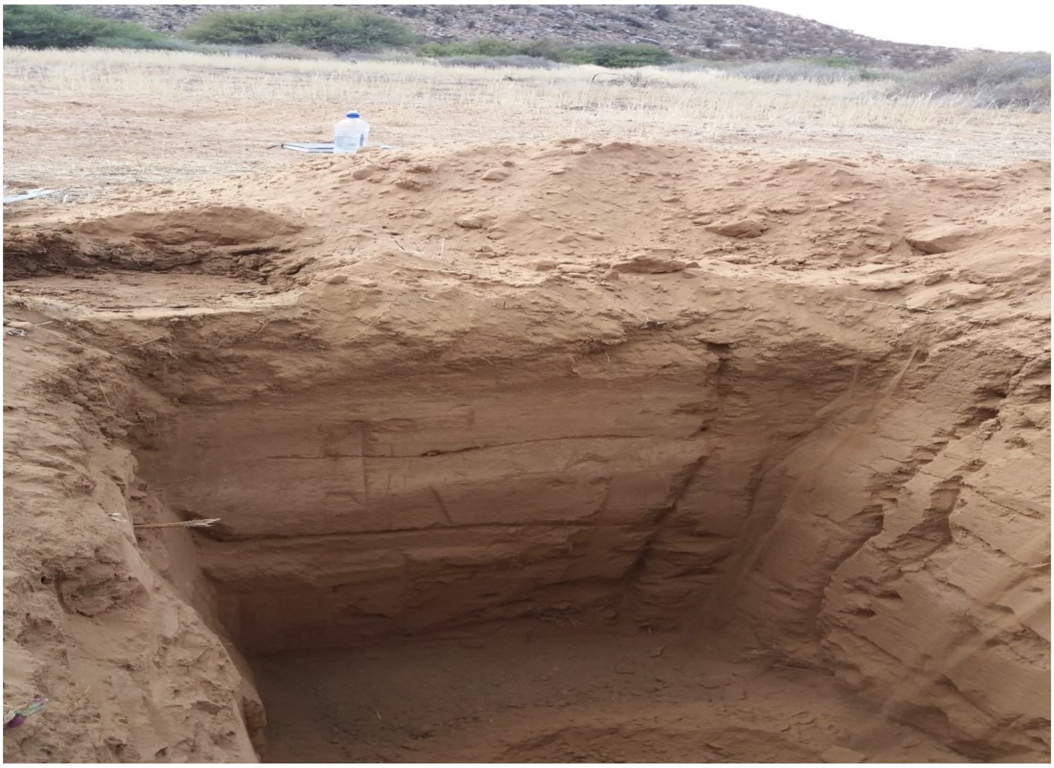

(a) Cumulic group (e.g. Dundee soil form)

(b) Oxydic group (e.g. Hutton soil form)

(c) Plinthic group (e.g. Bainsvlei soil form)

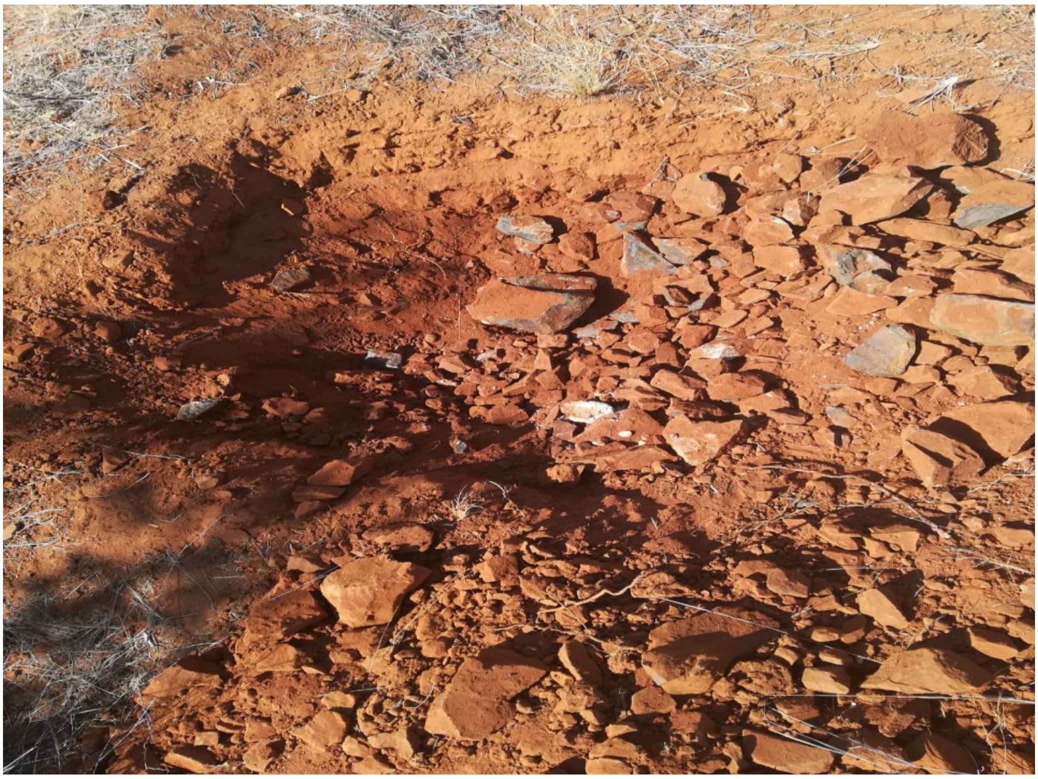

(d) Lithic group (e.g. Mispa soil form)

(e) Calcic group (e.g. Coega soil form)